



## RESEARCH ARTICLE

## Nutritive Elemental Status in Mulberry (*Morus* sp.) Foliage under Jassids (*Empoasca flavescens* F.) Infestation

Mahadeva.A

Residential Coaching Academy, Babasaheb Bhimrao Ambedkar University, Vidya Vihar, Raebarely Road, Lucknow – 226 025, India.

Received: 7 May 2016

Revised: 10 June 2016

Accepted: 02 July 2016

### Address for correspondence

Mahadeva. A  
Residential Coaching Academy,  
Babasaheb Bhimrao Ambedkar University,  
Vidya Vihar, Raebarely Road,  
Lucknow – 226 025, India.  
Email: amdeva2007@gmail.com



This is an Open Access Journal / article distributed under the terms of the **Creative Commons Attribution License (CC BY-NC-ND 3.0)** which permits unrestricted use, distribution, and reproduction in any medium, provided the original work is properly cited. All rights reserved.

### ABSTRACT

Silkworm (*Bombyx mori* L.) is economically important monophagous insect for the production of a natural fiber 'Silk'. Mulberry (*Morus* sp.) leaves is the only source for its entire requirement for good growth and development followed by quality and quantity silk production. So, the nutritive status of mulberry is having a pivotal role in the success of silkworm rearing. Mulberry foliage nutrition levels have been influenced by many factors including agricultural practices and variety. Even after following optimum agricultural practices, mulberry is susceptible to various pests and pathogens. Jassids is one important sap sucking pest and information about the nutritional level in mulberry under this pest attack is very scanty. So, an attempt have been made to know the influence of jassids infestation on the six macro (nitrogen, phosphorus, potassium, calcium, magnesium and sulphur) and seven micro nutrients (zinc, iron, manganese, copper, boron, molybdenum and chloride) level in mulberry foliage. It was found that there was a wide variation in macro and micro nutritive elements in jassids infested mulberry leaves compare to healthy ones. These variations the mineral nutrients results in nutritional inferiority of mulberry leaves, which is detrimental to growth and development of silkworm.

**Keywords :** Mulberry, macro element, micro element, nutrition, pest.



**Mahadeva****INTRODUCTION**

Mulberry (*Morus* sp.) is a fast growing deciduous woody perennial tree grown under varied climatic conditions ranging from temperate to tropics. It produces very large amount of renewable bio-mass in the form of branches, shoots, leaves and fruits. The mulberry foliage is a major economic component is sericulture as it is the sole feed of mulberry silkworm, *Bombyx mori*. The quality and quantity of leaf produced per unit area has direct impact on cocoon harvest. Like other agricultural crop plants, mulberry is also prone to attack by various insect and non-insect pests. It reduces the leaf yield and quality which reflects adversely on quantum of silkworm rearing and silk productivity. Jassid, *Empoasca flavescens* F. (Homoptera: Cicadellidae) commonly called leaf hoppers is the major sucking pest of mulberry (Reddy and Kotikal, 1988). Both adult and nymphs of little greenish hoppers sucks the sap on the underside of the leaf, at the time of sap sucking from the veins and causing characteristic non-contagious symptoms known as "hopper burn". Initially symptoms appear as triangular brown spots at the tip of the leaf. Similar triangles appear at the end of veins and the entire margin may roll upward and turn down at one time, as though scorched by fire or drought (Sengupta *et al.*, 1990). Gradually, the affected leaves become brick red or brown, crinkled and curled, and ultimately the plant shows stunted growth. The characteristic symptom is a result of dynamic interaction of complex insect feeding stimuli and plant responses triggered by a unique type of stylet movement (Backus *et al.*, 2005). It is well known truth that the yield and quality of mulberry is varied due to pests and pathogens. There are good amount of information is available regarding the variation in mulberry nutritive under microbial and pest attack. But, it is scanty or meager information is available about mulberry under jassids infestation. Therefore, an attempt has been made to know the impact of jassids infestation on the nutritive elemental levels in mulberry foliage.

**MATERIALS AND METHODS**

The jassids infested and healthy mulberry (6 varieties viz., M<sub>5</sub>, MR<sub>2</sub>, Mysore local, S<sub>36</sub>, S<sub>54</sub> and V<sub>1</sub>) were collected from plantations in and around Tumkur district and Kanakapura taluk, Ramanagara district (Karnataka state, India). They were washed thoroughly with distilled water and blotted to dry. The leaves were dried in hot air oven at 60–65°C for 48 hrs. The dried leaf materials were grinded to fine powder and used for analysing micro and macro mineral elements. The Micro-Kjeldahl flask method was followed to estimate total nitrogen content Piper (1966). To analyse the mineral elements level, one gram of dried mulberry was digested over sand bath until clear solution, by using 15 mL of nitric acid followed by addition of 10 mL of perchloric acid. It was cooled and by using a de-ionised water the volume was made up to 100 mL. It was filtered through Whatman's No. 1 filter paper (GE Healthcare, Little Chalfont, UK). 25 mL aliquots were used to estimate mineral nutrients of phosphorus and potassium by using Elico CL 360 Flame Photometer. Atomic Absorption Spectrophotometer was used to analyse the quantity of calcium, magnesium, sulphur, zinc, iron, manganese, copper, boron, molybdenum and chloride (Martin *et al.*, 1987). The obtained data were subjected to Student's t – test (Dixon and Massey, 1957). Significant differences were expressed at  $p < 0.05$  and  $p < 0.01$  levels. The results were also compared by change by percentage (decrease/increase) in the infested and healthy leaves.

**RESULTS AND DISCUSSION**

The six macro nutrients (Nitrogen, phosphorus, potassium, calcium, magnesium and sulphur) and seven micro nutrients (zinc, iron, manganese, copper, boron, molybdenum and chloride) were varied in jassids infested leaves of popular six indigenous mulberry varieties (M<sub>5</sub>, MR<sub>2</sub>, Mysore local, S<sub>36</sub>, S<sub>54</sub> and V<sub>1</sub>) compared to healthy ones.

**Macro nutrients (Table – 1)**

The macro nutrients were varied in the mulberry varieties due to jassids infestation. Nitrogen is a critical limiting element for mulberry growth and production. It is a major component of chlorophyll, the most important pigment



**Mahadeva**

needed for photosynthesis, as well as amino acids, the key building blocks of proteins. It is also found in other important biomolecules, such as ATP and nucleic acids. The N content of the mulberry determines the quality of the foliage (Shankar, 1997). In this study, the nitrogen content was reduced in all the varieties considered except MR<sub>2</sub> (0.71 %) where it was increased. It was significant in the Mysore local and S<sub>54</sub> varieties. The maximum (2.38 %) and minimum (0.22 %) was observed in Mysore local and V<sub>1</sub> varieties respectively. It was observed that there was a decreased N content in thrips infested tender and medium leaves of K<sub>2</sub>, S<sub>13</sub>, S<sub>34</sub> and S<sub>36</sub> mulberry varieties (Satya Prasad et al., 2002). Similar decreased trend of N content was noticed by Narayanaswamy et al., (1999) due to spiralling whitefly attack on mulberry leaves (M<sub>5</sub> var.). The damage caused by insect pest through sucking of the leaf sap may lead to altered metabolic activity in turns results in declined protein synthesis or else failure in mobilization of protein to the infected tissues to develop resistant to insect bite (Satya Prasad et al., 2002). Since, N is a biologically important macro-nutrient, its reduced level leads to stunted growth of shoot and root, reduced leaf area, prolonged bud dormancy and delayed flowering in mulberry (Manuel Sanchez, 2006). The limited leaf protein hinder the biosynthesis of silk which comprises two proteins i.e., fibroin and sericin (Rangaswami et al., 1976). Subbarayappa and Bongale (1997) noticed a highly significant correlation between N content of mulberry leaf and silkworm body weight, cocoon and shell. Therefore, reduced N level due to pest injury in mulberry obviously causes reduction in availability of amino acids and protein for the silkworms, which adversely affects their growth and development.

Phosphorus (P) is an important major nutrient in mulberry plant. It is a component of the complex nucleic acid structure of plants, which regulates protein synthesis. Therefore, it is very important in cell division and development of new tissue. Phosphorus is also associated with complex energy transformations like ATP. In the present work, the phosphorus content was decreased in leaves of M<sub>5</sub>, Mysore local, S<sub>36</sub> (15.79 %), S<sub>54</sub> (3.70 %) and V<sub>1</sub> varieties. However, in MR<sub>2</sub> it remained unaltered. The decrease was significant in S<sub>36</sub> and V<sub>1</sub> hopper burnt varieties. Narayanaswamy et al., (1999) noticed a reduced (26.53 %) in the P content in mulberry (M<sub>5</sub> var.) due to spiralling whitefly infestation. Similarly, it was decreased (43.14 %) in the leaf roller infested mulberry foliage (Naryanaswamy, 2003). Inadequate amount of P level affects the uptake of other nutritive elements in mulberry leaves for various other physiological activities, it in turn hampered the growth, and economic characters of silkworm, which is very essential for monophagous insect, Silkworm (Ito and Nimura, 1966; Chakrabarti et al., 1997).

Potassium (K) does not become a part of the biochemical structure in plants, but plays important regulatory roles. K moves into the guard cells around the stomata's, the cells accumulate water and swell, causing the pores to open and exchange carbon dioxide (CO<sub>2</sub>), water vapor, and oxygen (O<sub>2</sub>) with the atmosphere. The potassium was reduced in the leaves of M<sub>5</sub>, MR<sub>2</sub> (2.26 %) and Mysore local (0.48 %) and increased in the S<sub>36</sub>, S<sub>54</sub> (0.55 %) and V<sub>1</sub> (13.81 %) varieties. the decrease was significant in the M<sub>5</sub>, MR<sub>2</sub> and V<sub>1</sub> varieties. The K content in spiralling whitefly infested mulberry (M<sub>5</sub> var.) leaves was increased by 19.41 % over healthy ones (Narayanaswamy et al., 1999). On contrast, K was reduced by 5.61 % in leaf roller infested mulberry (M<sub>5</sub> var.) foliage (Narayanaswamy, 2003). The enzyme responsible for synthesis of starch (starch synthetase) is activated by K. Thus, with inadequate K, the level of starch declines while soluble carbohydrates and N compounds accumulate. Therefore, it also plays a significant role in high yield (productivity) and quality of leaf (Shree et al., 2005). It also involved in translocation of carbohydrates, protein metabolism, fungal pathogen tolerance in mulberry. The deficiency leads to accumulation of hydrogen peroxide in plants which is toxic and results in abnormal respiration and catalase activity (Manuel Sanchez, 2006). In the silkworm body, strong alkalinity of the gastric juice originates from potassium and sodium compounds present in the hemolymph. The high alkaline condition of digestive fluid has a strong germicidal power against pathogens. K is a unique element which contributes for the growth of silkworms to maximum extent. In addition, K has a stimulating effect on protein synthesis including silk protein in the silk glands and on the function of ovary (Shankar et al., 1990).

Calcium (Ca), in the form of calcium pectate, is responsible for holding the cell walls together in plant. Its deficiency causes incomplete cell division or mitosis, without formation of new cell wall resulting in multi-nucleatic cells (Bidwell, 1979). Calcium is also important in activating certain enzymes and to acts as second messengers in cell





### Mahadeva

signaling that coordinate certain cellular activities. Calcium acts as detoxifying agent by neutralizing organic acids such as oxalic acid which helps in membrane stability and maintenance of chromosome structure, activity of enzymes and translocation of carbohydrates. It is also involved in the differential permeability of membranes (Shankar, 1997). In the present investigation, the calcium content was decreased in all the varieties considered except in the V<sub>1</sub> (1.08 %), where it was increased. The maximum (2.22 %) and minimum (0.97 %) decrease was observed in the M<sub>5</sub> and Mysore local varieties respectively. Narayanaswamy et al., (1999) noticed a decrease (35.31 %) in the Ca content in spiralling whitefly infested mulberry (M<sub>5</sub> var.) leaves. There was decrease of Ca content (39.52 %) in leaf roller infested mulberry (M<sub>5</sub> var.) foliage over healthy (Narayanaswamy, 2003).

Magnesium (Mg), the central atom of chlorophyll, with its specific electron resonance properties to which the organic components of chlorophyll is responsible for photo-reduction and photochemical breakdown of water are attuned, is vital for the process of photosynthesis (Bergmann, 1992). Apart from this, Mg is of importance mainly as a co-factor and activator for many enzymes and substrate transfer reactions (Gunther, 1981). In the present investigation, the magnesium content was also reduced in all the varieties except in S<sub>54</sub> (2.63 %) variety. The decrease was in the range of 2.38 % to 5.19 % in MR<sub>2</sub> and Mysore local varieties respectively. The Mg content was reduced (23.59 %) in the spiralling whitefly infested mulberry (M<sub>5</sub> var.) leaves (Narayanaswamy et al., 1999). Narayanaswamy (2003) observed reduced (27.11 %) Mg content in the leaf roller infested mulberry (M<sub>5</sub> var.) foliage. Thangavelu and Bania (1990) noticed an accelerated growth and increases in oviposition rate of silkworm due to the Magnesium content. Ca and Mg accelerated the growth of silkworms and reduced the larval duration; decrease in the intake of these elements reduced the body weight of silkworms (Chakrabarti et al., 1997).

Sulphur (S) is known to have an important role in the synthesis of proteins, oils and vitamins (Epstein, 1972). It plays a vital role in the N metabolism and proper development of mulberry plant tissues (Munirathnam Reddy et al., 1990). It is a constituent of amino acids, cysteine (contains 27 % of S) and methionine (contains 21 % of S). In the present study, the sulphur content was decreased in the leaves of M<sub>5</sub> (15.79 %), Mysore local (6.12 %), S<sub>54</sub> and V<sub>1</sub>; increased in the S<sub>36</sub> (11.76 %) and no changes were observed in the MR<sub>2</sub> variety due to hopper burn. The S content was increased (11.11 %) in the spiralling whitefly infested mulberry (M<sub>5</sub> var.) leaves (Narayanaswamy et al., 1999) and it decreased (47.76 %) in the leaf roller - infested mulberry (M<sub>5</sub> var.) leaves (Narayanaswamy, 2003). This is because of the association of sulphur - amino acid *viz.*, methionine and cystine, methionine forms one of the ten essential amino acids for silk formation in silkworms. Cystine and cysteine are among the non-essential amino acids, the quantitative presence of which influences the formation of fibroin over sericin (Mahadevappa et al., 2001). Deficiency of S level leads to low level of S - containing amino acids, thus reducing protein synthesis. As a result, amino acids without S and amides of nitrate ions accumulate in the plant tissue and lead to decrease in sugar as well as insoluble N (protein) in plants (Munirathnam Reddy, 1990).

#### Micro - nutrients (Table – 2)

Mulberry needs micronutrients like zinc, iron, manganese, copper, boron, molybdenum and chloride in very small quantities. They play a pivotal role in the enzymatic reactions in turn govern the growth, development and yield of mulberry, wherein they participates in enzymatic reactions. The metal activators in enzymes are nothing but micronutrients (Shankar, 1997).

Similar to macro nutrients, the micro nutrients also shown a variation in jassids infested leaves mulberry varieties compare to healthy ones. The micro nutrients like zinc was reduced in all the six varieties *viz.*, M<sub>5</sub>, MR<sub>2</sub>, Mysore local, S<sub>36</sub>, S<sub>54</sub> and V<sub>1</sub> due to jassids infestation. The reduction was in the range of 0.40 % to 2.04 % in S<sub>36</sub> and S<sub>54</sub> varieties respectively. A significant increase was observed in the Zn content in tender and medium leaves and decrease in coarse leaves in mulberry plants infested by giant African snails (Shree and Ravi Kumar, 2002). Among all other micro nutrients, 50 % of Zn assimilation at later larval stage passed to silkworm seed. It also increases the silk



**Mahadeva**

filament length and pupal weight (Chakrabarti et al., 1997). The excess in Zn content in mulberry leaves leads to reduction in cocoon yield (Lokanath et al., 1986).

The iron (Fe) is present in the chloroplast proteins and several enzymes. It plays a dominant role in protein metabolism and N fixation (Shankar, 1997). In the present study, the iron was decreased in the leaves of M<sub>5</sub>, MR<sub>2</sub> (0.55 %), S<sub>54</sub> (1.69 %) and V<sub>1</sub>; increased in S<sub>36</sub> (0.64 %) and no changes were observed in the Mysore local variety. In contrasting these, Shree and Ravi Kumar (2002) noticed a decrease in the Fe content of mulberry (M<sub>5</sub> var.) leaves of all the three maturity levels (tender, medium and coarse) due to giant African snails attack. The increase may be due to failure in its translocation to the physiologically active site (Nagaraja, 1987). The altered Fe content in mulberry foliage resulted in the reduced larval weight, cocoon weight and silk filament length (Shankar, 1997).

Manganese (Mn) is essential for the synthesis of chlorophyll. It is immobile and its principal function is to activate some of the enzyme systems in plant physiology and to some extent regulation of Fe metabolism. In addition, it has a close relation with N metabolism (protein), assimilation of carbohydrates and formation of vitamin C. It is involved in oxidation - reduction processes and electron transport system (Shankar, 1997). In the current study, the manganese content was reduced in the infested leaves of M<sub>5</sub>, MR<sub>2</sub>, Mysore local (0.76 %) and S<sub>54</sub> (3.10 %) varieties. However, there was no changes were noticed in the leaves of S<sub>36</sub> and V<sub>1</sub> variety. Shree and Ravi Kumar (2002) noticed a contrasting results that Mn content was increased as well as decreased in the giant African snails infested mulberry (M<sub>5</sub> var.) leaves. The increase was significant in medium and coarse leaves, the significant decrease in tender leaves. Fe and Mn have potentiality to enhance the larval (silkworm) development, filament length of single cocoon, cocoon weight and yield (Lokanath et al., 1986).

A number of enzymes with diverse properties and functions are dependent on copper (Cu) and the metal ion is found in many proteins especially chloroplast proteins (Shankar, 1997). In the present investigation, the copper content was decreased in the hopper burnt leaves of M<sub>5</sub> (0.17 %), S<sub>36</sub>, S<sub>54</sub> and V<sub>1</sub> (0.45 %) but, increase in the Mysore local (0.16 %) and remained unaltered in the MR<sub>2</sub> variety. Shree and Ravi Kumar (2002) noticed a decrease in the copper content of tender, medium and coarse leaves of giant African snails infested leaves of M<sub>5</sub> mulberry cultivar. The boron (B) was reduced in the leaves of all varieties assayed except in V<sub>1</sub>, where it shows no alterations due to jassids infestation in this study. The maximum (13.33 %) and minimum (6.90 %) reduction was observed in the Mysore local and MR<sub>2</sub> varieties respectively. Boron plays an essential role in the growth and development of new cells in plant meristem. This element bears close relation with the translocation of carbohydrates and protein synthesis. In addition, the phenol metabolism and auxin activity is also regulated by boron. It also associated with the uptake of Ca and its utilization and regulates K and Ca ratio in plants (Shankar, 1997).

Molybdenum (Mo) has a close association with N utilization and metabolism in plants by regulating two important enzymes viz., nitrate reductase and nitrogenase. In addition, it also reduces protein metabolism in combination with other micronutrients especially Fe (Shankar, 1997). The molybdenum content was reduced in jassids infested mulberry leaves of all the varieties except M<sub>5</sub>, where it remained unaltered. The decrease was in the range of 1.92 % to 10.81 % in S<sub>36</sub> and V<sub>1</sub> varieties respectively. The chloride content was reduced in the leaves of MR<sub>2</sub> (1.09 %), Mysore local (3.67 %), S<sub>54</sub> and V<sub>1</sub>; increased in the M<sub>5</sub> (4.44 %) and no changes in the S<sub>36</sub> variety due to jassids infestation. Chloride is involved in photosynthesis, synthesis of starch, cellulose and lignin. It influences water holding capacity of plant tissues. It stimulates the activities of some enzymes. It is not readily mobile in plants (Shankar, 1997).

In the present investigation, it has been proved that mineral nutrition of the host is imbalanced due to pest - infestation. Similar variation in mineral nutrition were observed when mulberry leaves were infested by other sap sucking pests like jassids (Mahadeva et al., 2006), spiralling whitefly (Mahadeva and Nagaveni, 2012), thrips (Mahadeva and Shree, 2014) and mealy bugs (Mahadeva and Shree, 2006; Mahadeva and Shree, 2015). The spiralling whitefly is a phloem sap feeder and its direct consumption of transportable carbohydrate and other nutrients carried in phloem reduces productivity of host plants by competing for available nutrients and causing premature leaf





### Mahadeva

shedding (Bryne et al., 1990). This may be due to direct plundering by the pest or indirect effects of the pest on absorption, mobilization, etc., (Vamseedhar, 1999). Most sap sucking insects use a specialized mouth part, the stylet, to locate, penetrate and drain sap from the phloem sieve elements of the plants vascular tissue. Heavy infestation by sap sucking insects cause chronic shortages of photosynthates and thus severely reduces the growth potential of the plant (Kim Hammond-Kosack et al., 2000).

If the mineral content is increased due to infestation/infection, it induces toxicity symptoms not only in mulberry plants, but also in silkworms. Likewise, if a macro and micro elements are deficient in mulberry leaves due to infestation/infection a physiological disorder will occur. This makes leaves to be nutritionally inferior. Obviously, the increase or decrease in the mineral content(s), affects the growth and development of silkworms, which consequently alters the quality of silk produced (Ito and Nimura, 1966; Shree et al., 2005). Horie et al., (1985) observed that higher Ca, Mg and Fe content in mulberry stimulates the metabolic activity of silkworm and results in variation of economic characters i.e. shorter larval duration and increased pupation rate. Since, silkworm is a monophagous insect, mulberry leaves is the only source of nutrition. Growth and development of silkworms depend on the nutritive status of leaves. Therefore, mineral nutrition of mulberry foliage has a decisive role in the production of good quality cocoons. If there is an imbalance in elemental contents (mineral nutrition), the leaf quality is severely deteriorated, it may affect adversely on quality and quantity production of silk (Mahadeva and Shree, 2005). Therefore, the sericulturist's must avoid the feeding silkworm infested with pests and diseases. They should also follow eco-friendly Integrated Pest Management (IPM) as preventive measures to avoid poor outcome of silkworm rearing and economic loss caused by pests.

## REFERENCES

1. Backus A Elaine, Miguel S Serrano, Christopher M Ranger. Mechanisms of hopperburn: An overview of insect taxonomy, behavior, and physiology. *Annu. Rev. Entomol.* 2005;50, 125–151.
2. Bergmann W. *Nutritional Disorders of Plants – Development, Visual and Analytical Diagnosis*. Gustav Fischer, New York. 1992.
3. Bidwell RGS. *Plant Physiology*. Mc Millan Publishing Co. Inc., New York. 1979.
4. Bryne DN, Bellows TS, Parella MP. Whiteflies in agricultural system In: Whiteflies - their bionomics, pest status and management. (Eds. Gerling, D and Wimborne) U.K. Intercept. 1990;227-261.
5. Chakrabarti S, Subramanyam MR, Singhal BK, and Datta RK. Nutrient deficiency management in mulberry. Central Sericultural Research and Training Institute, Mysore. 1997;5-15.
6. Dixon W, Massey FJ. *Introduction of Statistical Analysis*. New York: McGraw Hill Book Co. 1957.
7. Epstein E. *Mineral Nutrition of Plants: Principles and Perspectives*. John Willey and Sons. Inc. New York. 1972.
8. Gunther T. Biochemistry and pathobiochemistry of magnesium. *Magnesium Bull* 1981;3,91-101.
9. Horie Y, Nakasone S, Watanabe K, Nakamura M, Suda H. Daily ingestion and utilization of various kinds of nutrients by the silkworm *Bombyx mori*. *Appl. Ent. Zool.* 1985;20(2), 159-172.
10. Ito T, Nimura M. Nutrition of the silkworm *Bombyx mori* L., its specific nutrient requirements and its nutrition in relation to the mineral nutrition of its host plant mulberry, *Morus indica* L. *Indian J Exptl Biol.* 1966; 4, 31-36.
11. Kim Hammond-Kosack, Jonathan DC, Jones. Responses to Plant Pathogens. *Biochemistry and Molecular Biology of Plants*. (Eds; Buchanan, B., Gruissem, W. and Jones, R.) *American Society of Plant Physiology*. 2000;1102-1155.
12. Lokanath R, Shivashankar K, Kasiviswanathan K. Effect of foliar application of magnesium and micronutrients to mulberry on the quality and production of cocoons. *Indian J Seric.*, 1986;24(1), 40-45.
13. Mahadeva A, Nagaveni V. Evaluation of nutritional quality in spiralling whitefly (*Aleurodicus dispersus* Russell) infested mulberry (*Morus* sp.) foliage. *International Journal of Environmental Sciences*. 2012;3(3), 1065-1071.
14. Mahadeva A, Shree MP. Effect of feeding spiralling whitefly (*Aleurodicus dispersus* Russell) infested mulberry (*Morus* spp.) leaves on silkworm (*Bombyx mori* L.). *Geobios*. 2005;32(4), 241-244





### Mahadeva

15. Mahadeva A, Shree MP. An Investigation on the changes in biochemical constituents and photosynthetic pigments in pink mealy bugs (*Maconellicoccus hirsutus* Green) infested mulberry (*Morus* sp.) foliage. 93<sup>rd</sup> Indian Science Congress, 3<sup>rd</sup> to 7<sup>th</sup> January, N.G. Ranga Agriculture University, Hyderabad, India. 6-7. 2006.
16. Mahadeva A, Shree MP, Nagaveni V, Srilakshmi N. Mineral nutrition in mulberry (*Morus* sp.) foliage under pest (Jassids – *Empoasca* sp.) attack. *International Conference on "Life Through Chemistry"*. 25<sup>th</sup> and 26<sup>th</sup> February, Ponnaiyah Ramajayam College, Thanjavur, Tamil Nadu. Abstract No. OP – 11. 7-8. 2006.
17. Mahadeva A, Shree MP. Post infestational changes in the nutritive elements of thrips (*Pseudodendrothrips mori*) attacked mulberry (*Morus* sp.) foliage. *Int. J. Bioassays*. 2014;3(07), 3171-3175
18. Mahadeva A, Shree MP. Evaluation of macro and micro nutritive elemental levels in the mealy-bug (*Maconellicoccus hirsutus*) - infested leaves of mulberry (*Morus* sp.) *Journal of Plant Nutrition*, 2015;38, 96–107.
19. Mahadevappa L, Magadi SP, Prabhuraj DK, Thimmareddy H, Bongale U D. Available sulphur in some mulberry growing soils of Karnataka. *Nutritional Management and Quality Improvement in Sericulture. Proceedings of the National Seminar on "Mulberry Sericulture Research in India"*, 26<sup>th</sup> to 28<sup>th</sup> November, Karnataka State Sericulture Research and Development Institute, Bangalore. 161-165. 2001.
20. Manuel D Sanchez. Mulberry: an exceptional forage available almost worldwide. <http://www.fao.org/ag/aga/AGAP>. 2006;15-30.
21. Martin PR, Gagnard J, Gautier P. *Plant analysis*. SBA Publications. Calcutta. 1987.
22. Munirathnam Reddy M, Subbaswamy MR, Sinha AK. Sulphur nutrition in mulberry plants. *Indian Silk*. 1990;29(7), 45-46.
23. Nagaraja TG. Cytological development and pathophysiological studies of some Indian fungi. Ph.D. (Agric.) thesis. Shivaji University, Kolhapur, Maharashtra state. India. 1987.
24. Narayanaswamy KC. Biochemical composition of leaf roller infested mulberry leaf. *Insect Environment*. 2003;8(4), 166-167.
25. Narayanaswamy KC, Ramegowda T, Raghuraman R, Manjunath MS. Biochemical changes in spiralling whitefly (*Aleurodicus dispersus* Russell) infested mulberry leaf and their influence on some economic parameters of silkworm (*Bombyx mori* L.). *Entomon*. 1999;24(3), 215-220.
26. Piper CS. *Soil and Plant Analysis*. Inter. Sci. Pub. Inc., New York. United States of America. (1966)
27. Rangaswami G, Narasimhanna MN, Kasiviswanathan K, Sastry CR. *Sericulture Manual - 1: Mulberry Cultivation*. Food and Agriculture Organisation. Agricultural Services Bulletin. United Nations Organization, Rome. 1976;1-97.
28. Reddy DNR, Kotikal YK. Pest of mulberry and their management. *Indian Silk*. 1988;26(11), 9-15.
29. Satya Prasad K, Sreedhar S, Singhvi NR, Kodandaramaiah J, Sen A.K. Post - thrips infestation biochemical changes in leaves of mulberry (*Morus* spp.). *Plant Archives* 2002;2(1): 85-88.
30. Shankar MA. *Handbook of Mulberry Nutrition*. Published by Shetty, G.P., Multiplex, Karnataka Agro Chemicals. Bangalore. 1997;19-75.
31. Shankar MA, Puttaswamy B, Puttaraju TB, Ravi KN, Devaiah MC. Role of potassium in mulberry. *Indian Silk*. 1990;29(2): 27-30.
32. Shree MP, Anuradha R, Nagaveni V. Impact of rust disease on the mineral nutrition of mulberry plants. *Sericologia*. 2005;45(1),115-121.
33. Shree MP, Ravi Kumar K. Effect of giant African snail *Achatina fulica* Bowdich infestation on the nutritional quality of mulberry (*Morus* sp.) leaves. *Bull Ind Acad Seri*. 2002;6(1),50-55.
34. Subbarayappa C T, Bongale UD, Nitrogen nutrition of mulberry – A review. *Indian J Seric*. 1997;36(2), 92-98.
35. Thangavelu K, Bania HR. Preliminary investigation on the effects of mineral in the rain water on the growth and development of silkworm, *Bombyx mori* L. *Indian J Seric*. 1990;29, 37-43.
36. Vamseedhar P, Shree MP, Subramanyam MVV. Impact of mealy bug infestation on bio-chemical constituents of mulberry leaves and their acceptability as silkworm feed. *National Seminar on "Tropical Sericulture"*, 28<sup>th</sup> to 30<sup>th</sup> December, University of Agricultural Sciences. Bangalore. 34. 1999.





**Mahadeva**

**Table. 1: Changes in the macro nutrients in the jassids infested mulberry foliage.**

Mulberry Varieties	Nitrogen (%)		Phosphorous (%)		Potassium (%)		Calcium (%)		Magnesium (%)		Sulphur (%)	
	H	I	H	I	H	I	H	I	H	I	H	I
M <sub>5</sub>	3.70	3.68	0.28	0.26	2.72	2.69**	1.35	1.32	0.64	0.62	0.19	0.16
	(-0.54)		(-7.14)		(-1.10)		(-2.22)		(-3.13)		(-15.79)	
MR <sub>2</sub>	2.80	2.82	0.25	0.25	3.99	3.90**	1.90	1.86	0.77	0.73	0.26	0.26
	(+0.71)		(----)		(-2.26)		(-2.10)		(-5.19)		(----)	
Mysore local	4.20	4.10**	0.26	0.28	4.17	4.15	3.09	3.06	0.84	0.82	0.49	0.46
	(-2.38)		(-7.69)		(-0.48)		(-0.97)		(-2.38)		(-6.12)	
S <sub>36</sub>	2.21	2.19	0.19	0.16**	3.34	3.36	3.01	2.96	0.46	0.44	0.17	0.19
	(-0.90)		(-15.79)		(+0.60)		(-1.66)		(-4.35)		(+11.76)	
S <sub>54</sub>	3.59	3.55*	0.27	0.26	1.82	1.83	2.36	2.31	0.38	0.39	0.36	0.32
	(-1.11)		(-3.70)		(+0.55)		(-2.11)		(+2.63)		(-11.11)	
V <sub>1</sub>	4.53	4.52	0.23	0.20*	4.20	4.28**	2.77	2.80	0.51	0.49	0.22	0.19
	(-0.22)		(-13.04)		(+13.81)		(+1.08)		(-3.92)		(-13.64)	

H = Helathy, I = Infested, \*\* - Highly significant at 1%; \* - Highly significant at 5 %; Values in brackets ( ) indicate % difference over healthy (+ = more than; - = less than; ---- = not altered).

**Table – 2 : Changes in the micro nutrients in the jassids infested mulberry foliage.**

Mulberry Varieties	Zinc (ppm)		Iron (ppm)		Manganese (ppm)		Copper (ppm)		Boron (ppm)		Molybdenum (ppm)		Chloride (%)	
	H	I	H	I	H	I	H	I	H	I	H	I	H	I
M <sub>5</sub>	176	174	320	317	226	222	12.12	12.10	21	19	0.59	0.59	0.90	0.86
	(-1.14)		(-0.94)		(-1.77)		(0.17)		(-9.52)		(----)		(+4.44)	
MR <sub>2</sub>	131	129	362	360	240	238	11.10	11.10	29	27	0.62	0.60	0.92	0.91
	(-1.53)		(-0.55)		(-0.83)		(----)		(-6.90)		(-3.23)		(-1.09)	
Mysore local	126	124	284	284	262	260	12.26	12.28	30	26	0.48	0.46	1.36	1.31
	(-1.59)		(----)		(-0.76)		(+0.16)		(-13.33)		(-4.17)		(-3.67)	
S <sub>36</sub>	251	250	312	314	212	212	10.09	10.06	24	21	0.52	0.51	1.21	1.21
	(-0.40)		(+0.64)		(----)		(-0.30)		(-12.50)		(-1.92)		(----)	
S <sub>54</sub>	196	192	296	291	290	281	10.31	10.27	22	20	0.32	0.31	0.99	0.96
	(-2.04)		(-1.69)		(-3.10)		(-0.39)		(-9.09)		(-3.13)		(-3.03)	
V <sub>1</sub>	183	180	270	268	230	230	8.90	8.86	18	18	0.37	0.33	1.14	1.12
	(-1.64)		(-0.74)		(----)		(-0.45)		(----)		(-10.81)		(-1.75)	

H = Helathy, I = Infested, \*\* - Highly significant at 1%; \* - Highly significant at 5 %; Values in brackets ( ) indicate % difference over healthy (+ = more than; - = less than; ---- = not altered).







## Decolorisation of Reactive Red-11 by *Klebsiella* CMGS-3

Madhuri R.Basutkar , Channappa T. Shivannavar\* and Subhaschandra M.Gaddad

Department of P.G. Studies and Research in Microbiology, Gulbarga University,  
Kalaburagi-585106, Karnataka, India.

Received: 2 June 2016

Revised: 7 July 2016

Accepted: 10 Aug 2016

### Address for correspondence

Channappa T. Shivannavar  
Professor, Department of P.G. Studies and  
Research in Microbiology, Gulbarga University,  
Kalaburagi-585106,  
Karnataka, India.  
Email: ctshiv@gmail.com



This is an Open Access Journal / article distributed under the terms of the **Creative Commons Attribution License (CC BY-NC-ND 3.0)** which permits unrestricted use, distribution, and reproduction in any medium, provided the original work is properly cited. All rights reserved.

### ABSTRACT

Recent changes in climate conservation of water reuse and recycling became essentiality; hence treatment of waste water is elemental. Synthetic dyes are used in textile industries became major source of contaminants of water. Without treatment of these effluents into natural water bodies may leads to long lasting harmful effects due to half life of dyes and their intermediates. Recently Biological treatment gain importance, by the usage of microbes one can completely decolorize and degrade these dyes in the effluent and water can be reused. By the application of concept isolated dye decolorizing novel bacterial strain *Klebsiella* sps- CMGS-3, from the soil collected from the textile industrial area solapur. Isolate could decolorize initially added 82.3% of reactive red-11(100mg/L) in mineral salt of medium without any additional nutritional source within 72 hours of incubation. The decolorisation efficiency was increased drastically around 95% of initially added RR-11 within 16 hours of incubation, when decolorisation was performed under optimized conditions with 0.1% of yeast extract and dye concentration of 200mg/L. It also decolorize structurally different dyes Reactive orange -16 94.5%, Reactive violet -1 93.5% and Reactive navy blue 59- it was 94.1% Reactive blue MR- 56.3%, Reactive yellow -86 67.4%, Through these data results it concludes that the isolate CMGS-3 was the better candidate for the decolorisation of wide range of reactive azo dye.

**Keywords :** Decolorisation, reactive dyes, *Klebsiella* sps.



**Channappa T.Shivannavar et al.**

## INTRODUCTION

Among the environment problems water pollution became major issues. Synthetic dyes are extensively used in various industries, after china, India is the second largest dye manufacturer and exporter (Sriram *et al.*, 2013). It is estimated that more than 10,000 varieties of synthetic dyes are available and being used commercially, and also studied that in textile effluent waters dye concentration range is from 10-200 mg/ L( Kadam *et al.*, 2011). Out of all synthetic dyes reactive azo dyes are used maximum (Saratale *et al.*, 2010). Reactive dyes having binding capacity with fabric is only 50 to 70% so effluent containing high concentration of reactive dyes thus alter COD, TOC, BOD causes a drastic effect on ecosystem. The recalcitrant nature, of dye causes toxic effect on living systems and earth structure (Jadhav *et al.*, 2010 ;Kalyanee *et al.*, 2007).Azo dye containing azo bonds between nitrogen -nitrogen these bonds acts as the coloring agents and having simple application procedures, less cost and uses less energy (Othman *et al.*, 2011). Microbial degradation achieved promising role in the degradation of dyes. And the biodegradation process well established and powerful can be used in industrial and domestic purpose, having the genetic level capacity to degrade to degrade aromatic organic compounds (Manogari *et al.*, 2008; Jayarajan *et al.*, 2011). Moreover biological treatment is ecofriendly, require less cost, can be reutilized for the industrial and agriculture purpose (Mondal *et al.*, 2009). Several microorganisms can able to degrade dye which includes fungi, bacteria, yeasts, algae can be using but compare to all bacterial degradation is fast and effective , it cleaves azo bonds, completely neutralize the dye. Hence tentatively identified *Klebsiella* sps CMGS-3, isolated from surrounding soil of textile area, having capacity to degrade reactive red -11, and wide range of dyes. So could helps in the resolving of environmental problems.

## MATERIALS AND METHODS

### Dyes

The dyes used in this study are azo reactive dyes namely Reactive orange -16, Reactive blue-4 ,Reactive yellow – 84, Reactive red -11, Reactive violet-1 and were procured from Colorise and Heena Textiles Industries, Ahmadabad (Gujarat) and sigma Aldrich U.S.A. Out of these reactive red-11 was selected for the decolorisation study, it is a polycyclic aromatic with single azo bonded chromopheric group having Chlorine, SO<sub>3</sub>OH, NO<sub>2</sub>. as reactive group attached with benzene rings. It is having molecular weight—681.33 with a  $\lambda_{max}$ 540nm, and water soluble in nature and widely used in the dyeing of cotton, viscose fabrics and silk.

### Mineral Salt Medium (MSM)

The chemicals used for the media, reagents, stains preparations were analytical graded. The mineral salt medium (MSM) composition broth was prepared by adding Na<sub>2</sub>HPO<sub>4</sub>.2H<sub>2</sub>O -12.00 g, KH<sub>2</sub>PO<sub>4</sub>-2.00 g, NH<sub>4</sub>NO<sub>3</sub> -0.50 g, MgCl<sub>2</sub>. 6H<sub>2</sub>O -0.10 g, Ca(NO<sub>3</sub>)<sub>2</sub>. 4H<sub>2</sub>O - 50.00 mg, FeCl<sub>2</sub>.4H<sub>2</sub>O - 7.50 mg to 1000 ml of distilled water and to this 10 ml of trace elements solution was added before adjusted the pH to 7.0. Trace elements solution was prepared by adding FeSO<sub>4</sub>.7H<sub>2</sub>O -10 mg, ZnSO<sub>4</sub>. 7H<sub>2</sub>O- 10 mg, CuSO<sub>4</sub>.5H<sub>2</sub>O- 1 mg, CaCl<sub>2</sub>.6H<sub>2</sub>O - 1 mg, MnSO<sub>4</sub>.H<sub>2</sub>O -1.7 mg to 1000 ml of distilled water. MS agar medium was prepared by adding 1.8 % agar to MS broth. All media were sterilized at 121° C for 15min before use (Brilon *et al.*, 1981). The MSM blended with required amount of testing dyes was used as decolorizing medium (DM) for isolation of dye decolorization experiments.

### Collection and Preparation of samples for isolation of dye degrading bacteria

The soil samples were collected from different sites of dye industry and textile treatment unit solapur, in sterile containers and brought to laboratory. The samples were prepared by adding 10 gm of soil sample and 10 ml of water sample added 100 ml of sterile saline (0.9%) and mixed, flask kept on the orbital shaker for 1hour at 120 rpm. The flasks were allowed to stand at room temperature settle down the soil and supernatant was collected and used for the isolation of dye degrading bacteria by inoculating 10-20 ml to 100 ml dye degrading MS broth. Routine observation were made to check decolorisation ability and flasks showing decolorisation more than 50% were selected and



**Channappa T.Shivannavar et al.**

transferred to again fresh DM broth. Flasks showing decolorisation in freshly added medium were selected, for the isolation of decolorizing bacteria streaking on mineral salt agar with 100mg/l RR-11, the bacterial colony showing zones were selected and used for the decolorisation experiments.

**Preparation of bacterial pre-inoculum**

Single isolated colony of isolate CMGS-3 on the mineral salt agar medium containing RR-11 (100 mg/L) was aseptically added to 10 ml of nutrient broth and incubated at 35° C for overnight. After checking the purity of the culture transfer all (10ml) to 100ml of MSB containing 100 mg/L of reactive red-11 and 0.1% of yeast extract and incubated under static conditions at 35°C. The complete decolorized dye culture was once again checked for its purity and was used as pre-inoculums for further studies.

**Decolorization assay**

Dye decolorisation in MS broth supplemented with yeast extract (0.1% w/v) and reactive red-11 (200mg/L) complete decolorisation of dye occurred within 24 hours of duration. Dye decolorization was confirmed by the checking optical density of supernatant at 540 nm for different intervals of time during incubation period. The percentage of decolorisation was calculated by following equation (R. Dave and H. Dave., 2009).

**Calculation of % decolorization**

$$\text{Percentage of decolorization} = \frac{\text{initial O.D} - \text{final O.D}}{\text{initial O.D}} \times 100$$

**Optimization of various factors for maximum decolorisation of RR-11 by isolate CMGS-3**

For optimization of each biotic and abiotic parameter used the decolorisation assay protocol by varying one parameter and keeping all other parameter constant. The parameter tested to optimizations were pH, temperature, aeration, salt concentration and inoculum size using determined optimum value of each parameter for the effect addition of carbon and nitrogen sources on the decolorization efficiency was checked by 1% various carbon and nitrogen sources (Jain *et al.*, 2012; Moosvi *et al.*, 2007; Bheemaraddi *et al.*, 2014; Rajeshwari *et al.*, 2014;).

**Determination of reactive red-11 decolorization efficiency of isolate CMGS-3**

To determine the reactive red-11 decolorization efficiency of isolate CMGS-3 was performed adding 200 mg/L reactive red-11 to 100 ml of decolorization medium with all optimized conditions then added 10 % of bacterial inoculums and incubated at 35° C. To determine rate of % RR-11 decolorization at different intervals of incubation period, decolorized sample was drawn from flask aseptically and centrifuged at 10,000 rpm for 10 min then supernatant was used for scanning from 190 to 900 nm in a UV-Vis spectrophotometer. A decrease in the optical density at  $\lambda_{\text{max}}$  540 nm and no peaks at different wave length during the scanning and compared to control indicates decolorization of dye is due to degradation.

**RESULTS AND DISCUSSION****Isolation and Characterization of reactive red -11 decolorizing bacteria**

The colonies showing clear zone on the MS agar plate containing 100mg/l RR-11 were selected for the further characteristic observation by studying their cultural, morphological, and biochemical characters, growth characteristic on the differential and selective media and other characteristics are given in table-1. Compared the results of all conventional methods with the results in the standard taxonomical book up to genus level with the characters described in the slandered taxonomy books, (Bergey's manual of systematic bacteriology edition-2) isolate tentatively identified as *Klebsiella* sps and the name given to isolate as *Klebsiella* CMGS-3. Based on the results isolate tentatively identified as *klebsiella* sps and designated as *klebsiella* CMGS-3.





Channappa T.Shivannavar *et al.*

## Optimization of RR-11 decolorizing isolates CMGS -3 for the enhancement decolorisation activity

### Decolorisation of RR-11 with and without yeast extract by isolate CMGS-3

In the decolorisation of RR-11 (100mg/l) without yeast extract, isolate *Klebsiella* sps CMGS-3 could utilize RR-11 as sole source of carbon and decolorizes 82.3% of initially added RR-11 within 72 hours of incubation period. However further incubation period does not effect on the decolorisation (fig-2). On the other hand addition of 0.1% yeast extract to decolorizing medium (DM) around 95% of decolorisation of initially added RR-11 was occurred within 16 hours of incubation period and was same even the initial dye concentration was increased to 200mg/l(fig-3). Many of the earlier reports on decolorisation of azo dyes by bacteria under static conditions suggested that even it does not favors the growth of bacteria but enhances the decolorisation process by regenerating NADH which acts as electron donors in azo bond reduction (Kadpan *et al.*, 2000; Jain *et al.*, 2012).

### Optimization of pH

CMGS-3 shown effective RR-11 decolorisation in wide range of pH ranges from 4 to 14 and present decolorisation was around 60% and above, highest decolorisation was at pH-8(95%) however it was more than 70% in the pH through 7 to 11. Other reports on the degradation of reactive black 5, a bacterium *Pseudomonas entomophila* BS1 by (khan *et al.*, 2015) shown good decolorisation between 5 to 9 pH (Imran *et al.*, 2014) showed that *Shewanella* sps IFN4 decolorized mixed azo dyes in the pH range of 5-9.

### Optimization of temperature

Temperature plays a important role in the decolorisation of dyes, isolate CMGS-3 shown degradation ranging from the 20 to 50°C and was around 80% and above from 25 to 45°C with highest decolorisation at 35°C(96%) was the optimum for isolate. Reports on *Staphylococcus hominis* RMLRT03 strain showed decolorisation, in temperature from 20–35°C in the degradation of acid orange (Singh *et al.*, 2012). Some isolate shown decolorisation in lesser temperatures, *Alcaligenes* sp. Aa09 shown complete Decolorisation, at 25°C temperatures, in the degradation of Reactive Red BL (Pandey *et al.*, 2012).

### Optimization of salt concentration

This isolate is tolerate 1% salt concentration without change in its decolorizing efficiency above this activity is reduced and was 50% at 5% of NaCl. CMGS-3 shows lesser degradation when salt concentration was increased. But some reports shown microbes may tolerate higher amount of salt concentration, (Mallikarjun, *et al.*, 2014) reported *Paracoccus* sps shown decolorisation up to 6% salt concentration.

### Optimization of inoculum size

Even though azo dyes decolorisation is not potentially increased with cell growth minimum bacterial inoculation required for the maximum decolorisation of RR-11 by isolate CMGS-3. It was found to be necessary for maximum decolorisation (Sahastrabdhe *et al.*, 2014). *Enterococcus faecalis* YZ66 showed 10% of inoculums size as optimum and in the degradation of red 3BN by the bacterial strain *Bacillus cereus* shown inoculums size 8% (Praveen Kumar and Sumangala, 2012).

### Optimization of Dye concentration

The percent decolorization of RR-11 at increased dye concentrations. Percent decolorization values obtained at 16h of incubation were found to be 95.30, 94.23, 85.93, 86.63 and 70.32 % respectively over a dye concentration of, 200, 400, 600, 800 and 1000 mg/l optimization of dye concentration. Highest decolorization of 95.3 % of RR -1 by the bacterial strain CMGS-3 was observed at a dye concentration of 200 mg/l (Jain *et al.*, 2012) observed dye concentration effect the decolorisation efficiency and in report of stated that higher concentration of dye may having inhibitory effect on decolorisation and also high concentration of reactive azo dye inhibits nucleic acid synthesis in microbial cell growth





### Channappa T.Shivannavar *et al.*

(Kalyani *et al.*, 2009). Bhatt *et al.*, (2005) stated increase in the dye concentration effect on the percent of decolorisation. Anjaneya *et al.*, (2011) reported decolorisation of metanil yellow by lysinibacillus sps and bacillus sps was (200 mg/L).

#### Decolorization of in different kinds of dyes Effective of individual dyes on decolorization of RR-11

The percent decolorisation was more than 50% for all Dyes tested and was more than 90% with Reactive orange-16, Reactive navy blue 059. And Reactive violet-1. Patil *et al.*, (2008) stated the decolorisation capacity of an organism mainly depends on the structure, molecular weight, various chemical substitutes, inhibitory groups like  $-NO_2$ ,  $SO_3Na$  etc.

#### Optimization of additional nutrients for maximum decolorization of isolate CMGS-3

##### Optimization of additional Carbon source and nitrogen sources

In addition of a different carbon source not shown any enhancement in the decolorizing efficiency of isolate CMGS-3 however only additional nitrogen source in the form of yeast extract was enhanced the decolorisation efficiency drastically (94.8%) within 16 hours of incubation. And the maximum decolorisation was studied in 0.1% of yeast extract and these concentration used throughout the studies (fig-10). Rajeshwari *et al.*, (2014) showed *Lysinibacillus sphaericus* RSV-1, shown degradation with the increase of 3-5%, using dextrose, starch, sucrose. (Oturkar *et al.*, 2010) showed the carbon source may increase the decolorisation and *Bacillus lantus* BI377 showed maximum decolorisation in fructose and starch but isolate CMGS-3 not shown any effective decolorisation in different carbon sources. Moonsvi *et al.*, (2007) stated carbon and nitrogen sources are the essential in the decolorisation of reactive violet -5. Jain *et al.*, (2012) showed yeast extract helps in the maximum decolorisation. Dawkar *et al.*, (2009) reported degradation of the bacillus sp. vs. Yeast extract was the best medium for faster decolorization.

## REFERENCES

1. Ajay Kumar Pandey and Vinay Dubey (2012) Biodegradation of Azo Dye Reactive Red BL by *Alcaligenes Sp.* AA09. *Int J of Eng and Sci* ISSN: 2278-4721, Vol. 1, Issue 12, PP 54-60.
2. Anjaneya O, Souche SY, Santoshkumar M, and Karegoudar TB: (2011) Decolorization of sulfonated azo dye Metanil Yellow by newly isolated bacterial strains: *Bacillus sp.* strain AK1 and *Lysinibacillus sp.* strain AK2. *J Hazard Mater*, 190:351–358.
3. Bhatt N, Patel KC, Keharia H, Madamwar D (2005): Decolorization of diazo dye Reactive blue 172 by *Pseudomonas aeruginosa* NBAR 12. *J Basic Microbiol*, 45:407–418.
4. Bheemaraddi M, Patil S, Shivannavar CT, and Gaddad SM (2014). Isolation and characterization of *Paracoccus sp.* GSM2 capable of degrading textile azo dye Reactive Violet 5. *Scientific World J.* 2014:410704. Doi:10.1155/2014/410704.
5. Brilon C, Beckmann W, Hellwig M, Knackmuss H-J (1981). Enrichment and isolation of naphthalenesulfonic acid-utilizing pseudomonads. *Applied and Environ Microb*;42(1):39–43.
6. Dave SR, Dave RH. (2009) Isolation and characterization of *Bacillus thuringiensis* for Acid red 119 dye decolorisation. *Bioresource Technol*; 100(1):249–253.
7. Dawkar, V.V., Jadhav, U. U., Ghodake, G. S., and Govindwar, S. P. (2009). Effect of inducers on the decolorization and biodegradation of textile azo dye Navy blue 2GL by *Bacillus sp.* VUS. *Biodegradation*. 20:777787.
8. Imran M, Arshad M, Asghar HN, Asghar M, Crowley DE, (2014). Potential of *Shewanella Sp.* Strain IFN4 to Decolorize Azo Dyes under optimal conditions. *Int J. agri boil*, 16: 578-64





**Channappa T.Shivannavar et al.**

9. Jadhav JP, Kalyani DC, Telke AA, Phugare SS, Govindwar SP (2010) Evaluation of the efficacy of a bacterial consortium for the removal of color, reduction of heavy metals, and toxicity from textile dye effluent. *Bioresource Technol* 101:165–173.
10. Jain K., Shah V., Chapla D. and Madamwar D.,(2012) Decolorization and degradation of azo dye--Reactive Violet 5R by an acclimatized indigenous bacterial mixed cultures SB4 isolated from anthropogenic dye contaminated soil. *J Hazard Mater*, 213–214:378–386
11. Kadpan, I.K., Kargi, F., McMullan, G., and Marchant, R., (2000). Effect of environmental conditions on biological decolorization of textile dye stuff by *C. versicolor*. *Enzyme. Microb. Technol.*, 26: 381-387.
12. Kalyanee J, Rujikan N, Jongjira N, and Boonsiri C. (2008) Decolourization and degradation of C I reactive Red 195 by Enterobacter species. *Thammasat Int J of Sci Tech.*; 12(4).
13. Jayarajan, M., R. Arunachalam, G. Annadurai, (2011). Agricultural wastes of jackfruit peel nano-porous adsorbent for removal of rhodamine dye. *Asian J. Applied Sci.*, 4: 263-270.
14. Kadam A, Telke A, Jagtap S, Govindwar P.(2011) Decolorization of adsorbed textile dyes by developed consortium of *Pseudomonas* sp. SUK1 and *Aspergillus ochraceus* NCIM-1146 under solid state fermentation. *J Hazard Mater*. 189:486–94
15. Madhuri M Sahastrabdhe, Rijuta G Saratale, Ganesh D Saratale, and Girish R Pathade (2014) Decolorization and detoxification of sulfonated toxic diazo dye C.I. Direct Red 81 by *Enterococcus faecalis* YZ. *J of Environ Health Sci& Eng*. 12:151 DOI 10.1186/s40201-014-0151-1
16. Mallikarjun C. Bheemaraddi, Channappa T. Shivannavar, Subhaschandra M. Gaddad(2014), Effect of carbon and nitrogen sources on biodegradation of textile azo dye Reactive Violet 5 by *Pseudomonas aeruginosa* GSM3. *Sch. Acad. J. Biosci.*; 2(4): 285-289.
17. S. Moosvi, X. Kher, and D. Madamwar,(2007) "Isolation, characterization and decolorization of textile dyes by a mixed bacterial consortium JW. 2," *Dyes and Pigments*, vol. 74, no. 3, pp. 723–729,
18. Manogari, R., D. Daniel and A.Krastanov, (2008). Biodegradation of rice mill effluent by immobilized *Pseudomonas* sp. cells. *Ecol. Eng. Environ. Prot.*, 1: 30-35.
19. Mondal, P. K., and Ahmad, R.(2009) "Aerobic Biodegradation and Adsorption of Industrial Sludge Containing Malachite Green by Sequential Batch Reactor." *Proceedings in Inter Conference on Energy & Environ*.
20. Othman, N., N. Mili and Y.M. Wong, (2011). Liquid-liquid extraction of black B dye from liquid waste solution using tridodecylamine. *J. Environ. Sci. Technol.*, 4: 324-331.
21. Oturkar, C.C., Nemade, H.N., Mulik, P.M., Patole, M.S., and Hawaldar, R.R. (2010). Mechanistic investigation of decolorization and degradation of Reactive Red 120 by 494 *Bacillus lentus* BI377. *Bioresour. Technol.*, 102: 758-764.
22. Praveen Kumar G.N. and Bhatt (2012) Decolorization of Azo dye Red 3BN by Bacteria (2012). *Int Research J of Bio Sci*. ISSN 2278-3202 Vol. 1(5), 46-52).
23. P. S. Patil, U. U. Shedbalkar, D. C. Kalyani, and J. P. Jadhav, (2008)"Biodegradation of Reactive Blue 59 by isolated bacterial consortium PMB11," *J of Industrial Micro and Biotech*, vol. 35, no. 10, pp. 1181–1190,
24. K. Rajeshwari, R. Subashkumar and K. Vijayaraman,(2011) Biodegradation of Mixed Textile Dyes Bacterial Strains Isolated from Dye waste Effluent: *research j of environ toxicol*5(2):97-107.
25. Rajat Pratap Singh, Pradeep Kumar Singh, and Ram Lakhan Singh (2014): Bacterial Decolorization of Textile Azo Dye Acid Orange by *Staphylococcus hominis* RMLRT03, *Toxicol Int.* 21(2): 160–166.
26. Sana Khan and Abdul Malik: (2016) Degradation of Reactive Black 5 dye by a newly isolated bacterium *Pseudomonas entomophila* BS1,) *Canadian J of Microb*, 62(3): 220-232, 10.1139/cjm-2015-0552.
27. R. G. Saratale, G. D. Saratale, J. S. Chang, and S. P. Govindwar.(2010) Decolorization and biodegradation of reactive dyes and dye wastewater by a developed bacterial consortium. *Biodegrad* 21:999–1015.
28. Sriram, D. Reetha and P. Saranraj (2013) Biological Degradation of Reactive Dyes by Using Bacteria Isolated from Dye Effluent Contaminated Soil. *Middle-East J of Scientific Research* 17 (12): 1695-1700, 2013 ISSN 1990-9233 © IDOSI Publications.





**Channappa T.Shivannavar et al.**

**Table1: Morphological and biochemical characteristics of isolate CMGS-3.**

Tests	Observation
<b>A. Colony character on MacConkey agar</b> Size Shape Color	Medium entire pink
<b>B. Morphological Characteristics of CMGS-3</b> Grams staining Motility Cell shape and arrangement of spore	Gram negative bacilli Non motile No spore former
<b>C. Carbohydrate utilization</b> Glucose Sucrose Lactose Mannitol fermentation	Acid production Acid production Acid production Non fermenter
<b>D. IMViC tests</b> Indole Methyl Red Voges Proskaur Citrate	- ve + ve + ve + ve
<b>E. Urease production</b> <b>F.catalase test</b>	-ve -ve
<b>G. Gelatin hydrolysis test</b> <b>H.Nitrate reduction test</b> <b>I. Starch hydrolysis test</b>	- ve +ve +ve

**Table 2- Effect of Carbon and Nitrogen Sources**

Carbon and Nitrogen sources	% of degradation	Duration
Mineral salt medium with dyes	82.33	72hours
Glucose+MSM	84.5	16hours
Sucrose +MSM	85.6	16hours
Lactose+MSM	78.4	16hours
Starch+MSM	65.3	16hours
Yeast extract+MSM	94.8	16hours
Beef extract+MSM	81.5	16hours





**Channappa T.Shivannavar et al.**

Peptone+MSM	88.5	16hours
Potassium nitrate+MSM	59.8	16hours
Ammonium nitrate+MSM	68.5	16hours

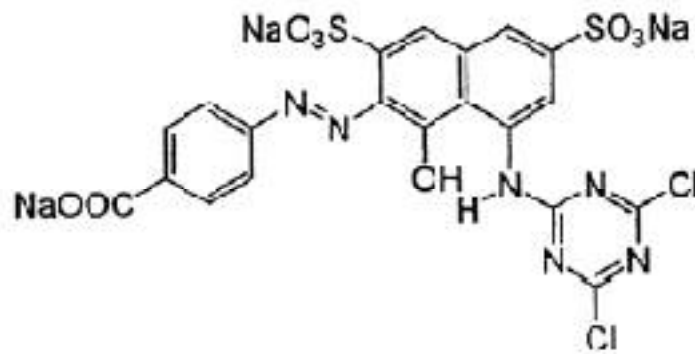


Fig-1 Structure of reactive red-11

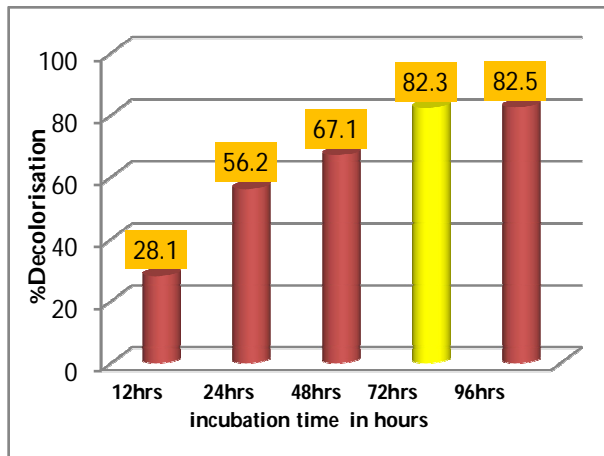


Fig -2 –Decolorisation of RR-11 without yeast extract by isolate *Klebsiella* CMGS-3

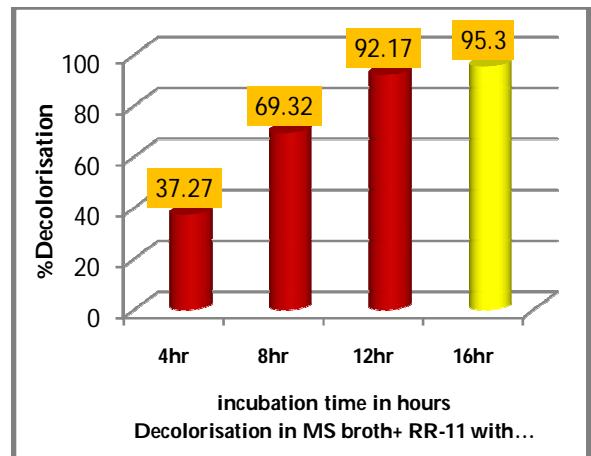


Fig -3 Decolorisation of RR-11 with 0.1% of yeast extract by isolate *Klebsiella* CMGS-3







Channappa T.Shivannavar et al.

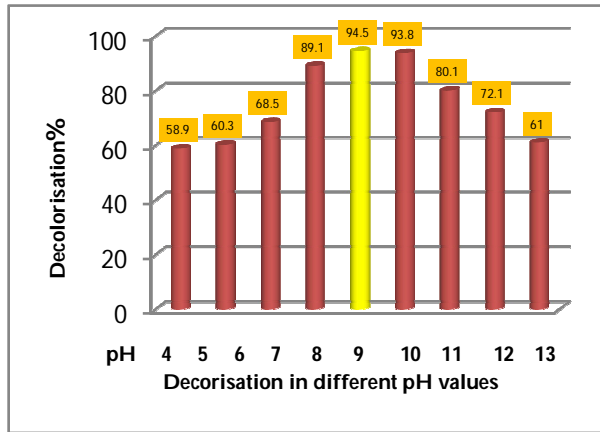


Fig 4: optimization pH on decolorization of Reactive red – 11 by isolate *Klebsiella* -CMGS-3

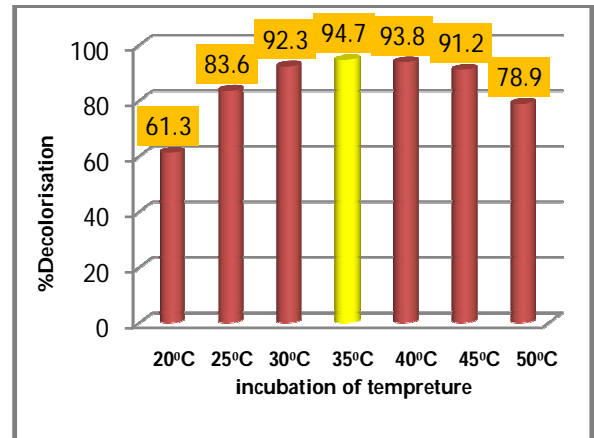


Fig 5: Optimization of temperatures on decolorization of Reactive red – 11 by *Klebsiella* CMGS-3

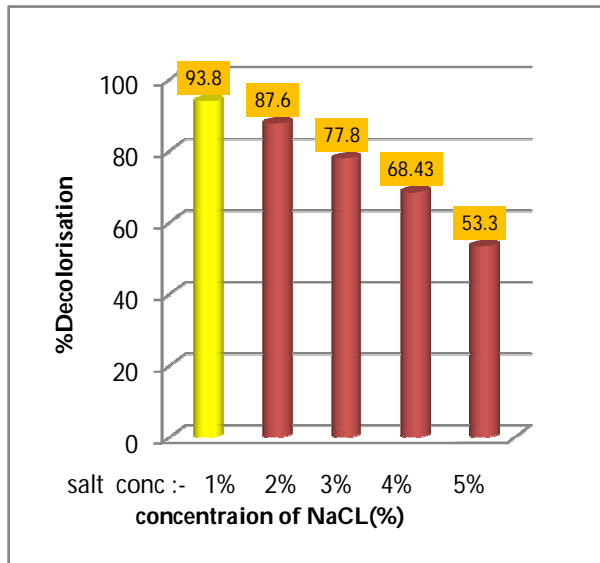


Fig 6: Effect of salt concentration on decolorization of Reactive red – 11 by isolate CMGS-3

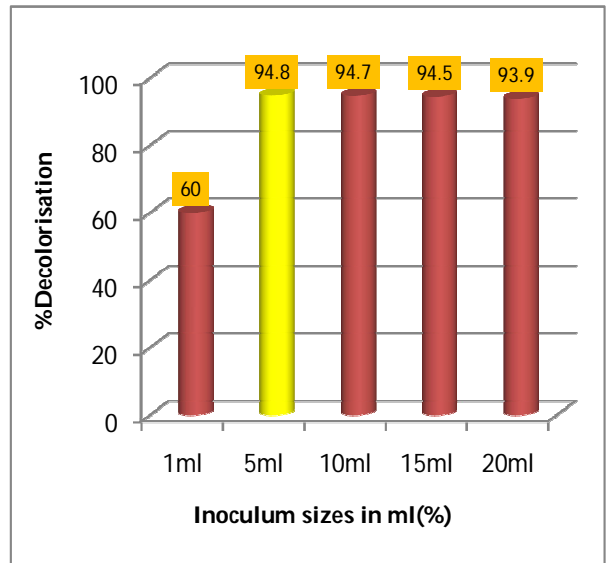


Fig 7: Effect of inoculum size on decolorization of Reactive red – 11 by *Klebsiella* CMGS-3





Channappa T.Shivannavar et al.

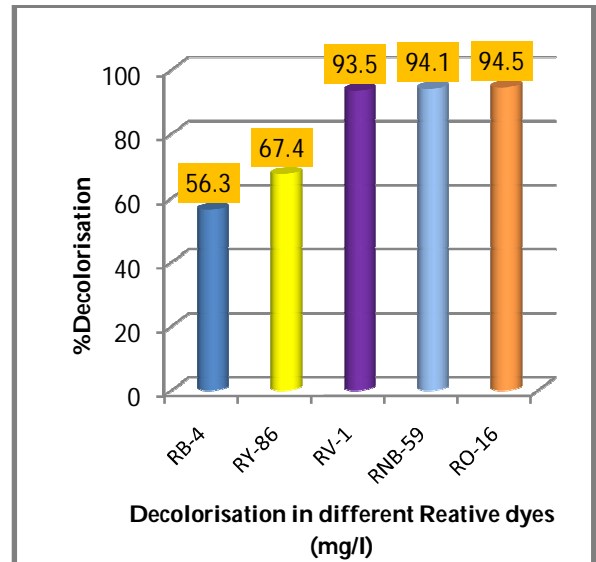
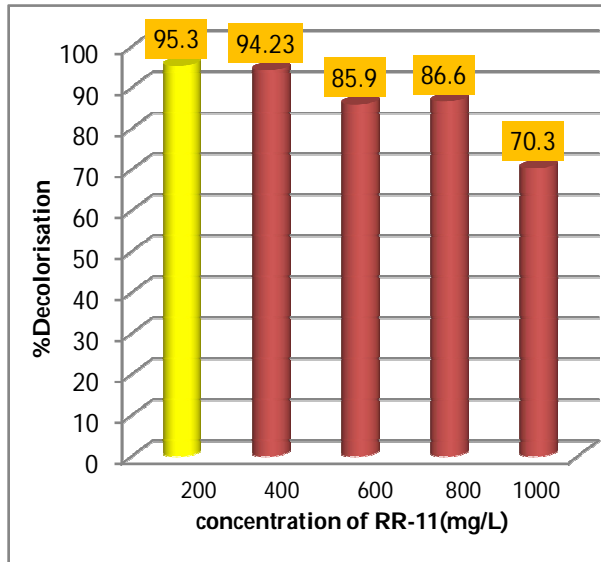


Fig 8: Effect of dye concentration on decolorization of Reactive red – 11 by isolate CMGS-3

Fig 9: Decolorization in different dye by isolate CMGS-3

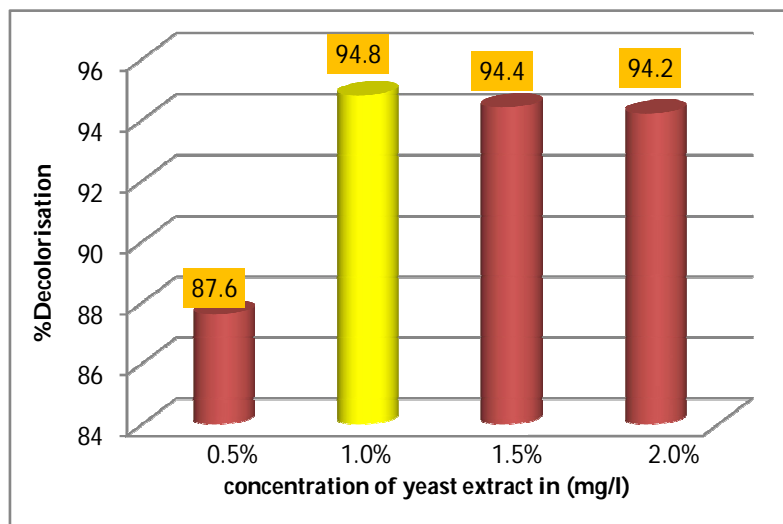


Fig 10: Effect of yeast extract on decolorization of Reactive red – 11 by *Klebsiella* CMGS-3





## RESEARCH ARTICLE

## Ultrasound Waves Employment in the Medical Diagnostic for Kidneys

Faik H. Anter and Roaa M. Hussian\*

Department of Physics, College of Science, AL- Anbar University, Iraq.

Received: 18 June 2016

Revised: 10 July 2016

Accepted: 25 Aug 2016

### Address for correspondence

Roaa M. Hussian

Department of Physics, College of Science,

AL- Anbar University, Iraq.

Email: roaa.physicist@gmail.com



This is an Open Access Journal / article distributed under the terms of the **Creative Commons Attribution License (CC BY-NC-ND 3.0)** which permits unrestricted use, distribution, and reproduction in any medium, provided the original work is properly cited. All rights reserved.

### ABSTRACT

Ultrasound imaging is nowadays a well established imaging technique for medical diagnostics. In fact, ultrasound is the fastest, least invasive and least expensive, screening modality for imaging kidneys and other organs, therefore it is commonly used in clinical practice for assessing possible abnormalities in several parts of the human body. Through the relation between physics and medicine by employing the ultrasound waves to in medical diagnostics for kidneys appear the normal *cortico* kidneys with gray color while kidneys stones appear with (*hyperechoic*) white color because attenuation artifact where this artifact is caused by partial or total reflection or absorption of the sound energy.

**Keywords :** ultrasonic, transducer of ultrasound, kidneys stone

### INTRODUCTION

Sound is a mechanical wave that travels through an elastic medium. Ultrasound (US) is sound at a frequency beyond 20000Hz, the limit of human hearing. The frequency range of diagnostic (US) is between (1-20MHz) [1,2]. Ultrasound waves are longitudinal, compressional waves, that can be periodic or pulsed, propagate at roughly 1500 m/s in water or biological tissue, can leave the medium unchanged (diagnostic ultrasound), but at higher intensities can also change it (therapeutic ultrasound) [3]. Diagnostic ultrasound is based on the pulse-echo principle and widely used in medicine [1,2]. The smallest functional units of the transducer are the piezoelectric crystals. The crystals are embedded in the probe, and each crystal has a specific frequency. Some of the energy is absorbed in the tissue and some is reflected. The reflected energy is received by the probe, which calculates the depth of the interface by measuring the time taken to return [2]. Present medical ultrasound transducers are constructed of arrays with several piezoelectric crystals. During the transmission phase, the crystals can be activated either in groups (linear transducer) or all at the same time (phased array transducer). The linear transducer normally operates at a high frequency range



**Roaa M. Hussian and Faik H. Anter**

(4-15 MHz), and the phased array transducer at a low frequency range (1-3 MHz). An ultrasound system can operate in several different imaging modes, providing both two-dimensional (2D) and three-dimensional (3D) images [4].

The human body is composed of three basic materials differing in acoustic impedance: gas with a very low impedance, bone with a very high impedance and soft tissue with an impedance somewhere in between. The large mismatch between air, bone and tissue causes 100% of the sound to be reflected at air/ tissue interfaces and almost all the sound at bone/ tissue interfaces, there is a small mismatch between different soft tissue impedances a fact that is the basis for diagnostic ultrasound [2]. The sound is generated by a transducer that first acts as a loudspeaker sending out an acoustic pulse along a narrow beam in a given direction. The transducer subsequently acts as microphone in order to record the acoustic echoes generated by the tissue along the path of the emitted pulse. These echoes thus carry information about the acoustic properties of the tissue along the path. The emission of acoustic energy and the recording of the echoes normally take place at the same transducer, in contrast to CT imaging, where the emitter ( the X-ray tube ) and recorder (the detectors ) are located on the opposite side of the patient [5].

**MATERIALS AND METHODS**

Ultrasound imaging produces gray-scale images that consist of bright points of different intensities on a dark background. Darkness in the image means absence of echoes from that area, or that the emitted ultrasound has failed to reach that specific area. Consequently, brightness in the image means that a part of the emitted ultrasound wave has echoed back. The reasons for the generation of echoes /bright areas in the image are mainly two folds. Firstly, when a sound wave is propagating through a homogenous medium no energy of the sound wave is reflected back and consequently the resulting image is dark. However, if the examined volume constitutes of several media with different acoustic impedance, some of the energy is reflected back in the transition from one medium to medium. Acoustic impedance is an important media characteristic in ultrasound imaging; it is the product of the density and the speed of sound of the media. The border between two different medium with the same acoustic impedance cannot generate a returning echo; the ultrasound wave passes through the interface without loss of energy in the form of a returning echo. It is the returning echoes from the interface between different medium that constitute the information about the examined structure in the ultrasound image. The proportion of the energy that is reflected back depends mainly on the difference in acoustic impedance and to a lesser extent by the angle of incidence.

Secondly, echoes can arise within inhomogeneous medium because of the scattering effect by very small objects in the size of the wavelength or smaller. These small objects are too small to be individually resolved in the ultrasound image. The echoes generated in this way are very weak compared to echoes from interface transitions and are undetectable. A very large number of echoes from many scatters can however be added together by constructive interference and become detectable. This phenomenon is seen in almost every tissue in the body except blood and gives rise to so-called speckles in the ultrasound image. The ultrasound image is built up from scan lines. Sound waves propagate in straight lines. If the sound waves interact with the tissue media during the propagation along the scan lines and are reflected back, an echo can be registered by the ultrasound scanner. The placement of the echo signal along a scan line depends on two factors; the time for the ultrasound to return back to the transducer and the propagation speed of the sound in the material.

The travel time can always be measured accurately by the ultrasound scanner. It is however more problematic to know the propagation speed of the sound since the human body consists of many tissue types with different properties. The speed of sound in soft tissue of the human body is ranging from about 1440 m/s in adipose tissue to 1580 m/s in muscle tissue. Therefore the manufacturers of ultrasound scanners use a fixed mean value regardless of tissue type. The mean value differs between the manufacturers, but is in the range of 1540 – 1560 m/s[6]. And the impact of structural noise on medical ultrasound images is much stronger than the influence of speckle noise, since it



**Roaa M. Hussian and Faik H. Anter**

not only effects single pixel but whole image regions. In general, structural noise occurs in the presence of *strong reflectors* in the image, e.g., bone structures or air. One canonical example of structural noise is induced by insufficient covering of the US transducer with acoustic coupling gel. This causes strong reflection right at the transducer due to the presence of air bubbles, which have significantly lower acoustic impedance. The immediate reflection of ultrasound waves leads to *dropout of signal* in the image regions beneath the air bubbles.

The most important from of structural noise within this work are so called acoustic shadowing effects. Acoustic shadowing occurs when a strong reflector (having significantly different acoustic impedance as the surrounding tissue) blocks the transmission of ultrasound waves beyond that point [7], e.g., bones or the lungs. Similar to the shape of a shadow caused by in transparent objects in a light beam, the acoustic shadow follows the transmission path of the ultrasound waves. This leads to the fact that a small reflector near the transducer can cause large shadowing effects to the image regions beyond. Typically, these regions appear dark with only little signal intensities, since almost no ultrasound echo is received from these regions. Figure(1) shows typical structural artifacts caused by shadowing effects in two situations with different extend. Due to the presence of a strong reflector in the upper part of the US B-mode images, one obtains images perturbed by acoustic shadowing (delineated by the red dashed lines). As can be seen, almost no information can be received from the shadowed regions. Furthermore, the closed contour of the connected anatomical structure in shows gaps. Another class of structural noise artifacts is caused by reverberation. Reverberation is caused by two or more highly- reflective interfaces and leads to multiple linear high- amplitude ultrasound signals projecting the structure of the reflectors repeatedly beneath the correct image position [8]. The reason for this effect is that ultrasound waves are reflected several times between the reflectors. At each reflection a part of the ultrasound waves is transmitted back to the transducer, leading to a periodic received signal [9].

**RESULTS AND DISCUSSION**

To prepare the patient for kidneys examination, the patients should be lying in the supine position. Each kidney may also need to be examined in the *decubitus* position and Raise the *ipsilateral* arm above the patient's head. For adults, use a 3.5 MHz (normal or obese patients) or 5 MHz (slim patients or children) transducer. If the transducer has variable frequency, deep structures can be adequately seen by lowering the frequency. A curvilinear transducer will usually be adequate, but a sector transducer may given better *intercostal* views. For scanning technique Place the transducer over the right upper abdomen. Set the focal depth for about the centre of the kidney, and adjust the gain to obtain the best image of the renal parenchyma. The focal depth that produces the best image varies somewhat among machines. Like other organ, the kidneys should be scanned in longitudinal and transverse planes that include the whole organ as in figures (2,3). Care should be taken to ensure that the whole of the upper and the lower poles are seen, to prevent missing an *exophytic mass* or *horseshoe kidney* (lower pole united).

*The cortical echogenicity* should be compared with that of the liver, spleen and renal pyramids. The right kidney can be seen best when the patient is supine, with the liver as an acoustic window (*anterolateral* approach). Deep inspiration can help to visualize the upper pole, but remember to let the patient breathe! A left lateral *decubitus* position may help show the lower pole. The upper pole of the left kidney can usually be seen by using the spleen as an acoustic window, but in this position, the lower pole is often obscured by bowel gas. The whole of the left kidney is often seen more easily when the patient's left side is raised, allowing a more posterior approach. Ultrasound artifacts are useful for characterizing any pathological condition; for example, simple renal cyst contains fluid and have posterior acoustic enhancement. Calcification is *echogenic* or bright and causes "clean" posterior acoustic shadowing, as in renal calculi. Gas or air will be *echogenic* but will cast a "dirty" shadow. The machine used in figure (4) from type "*sonoscape ultrasound*" consist of following parts: Transducer (probe), Central Processing Unit (CPU), Display, Transducer pulse controls, Disk storage, Printers, and Keyboard (cursor).





### Roaa M. Hussian and Faik H. Anter

Images in figure (5) refer to the medical diagnostics for kidneys. From figure (5a), the gray colors denote to liver, spleen and cortico of both kidneys where the right kidney beside the liver, and left kidney beside the spleen, the white (*hyperechoic*) colors in middle of kidneys refer to pelvises of kidneys, *sagittal* scan through both kidneys, both kidneys have normal size & texture, no dilation of PCS, no stone, no SOL and smooth out line. Figure (5b) illustrated that the gray color on the right side of this figure refers to left kidneys, also it is normal in size & position, *normal parenchymal thickness & echogenicity*, no stone, normal PCS, with small simple cystic lesion about (3.7cm x 3.9cm) appears in black color in middle of left kidney and the scan is *sagittal* through left kidney, while the figure (5c), shows that the gray color on left side of this figure denotes to right kidney where it is bedside Right liver (RL), RT kidney normal in size & texture, no dilatation of PCS, no SOL, smooth out line, but left kidney appears in gray color on the right side of this figure, it located in right *hypoconderuim* and *epigastric area*, ectopic- kidney, also the scan is *sagittal* through them. Also figure (5d) shows that the gray color denotes to Left Kidney and the scan is *sagittal* through it, Left kidney has double collecting system these works comparable to Narrotams' and Pokhrajs' works where noticed the ectopic kidney and double collecting system of kidney [10], increase in size 120mmx 40mm & normal texture, mild dilatation in PCS, no SOL, smooth out line, there is stone 3mm appears in white (*hyperechoic*) color, also Barbrina Dunmire and others determined kidney stone size[11].

## CONCLUSION

1. Kidneys better evaluated during stop breathing (in full inspiration) to avoid motion artifact.
2. Different position better than one position to achieve good image for each kidney.  
Linear probe with frequency 7.5MHz can use in examination of kidneys in thin adult patients and in pediatric for more resolution to curvilinear probe with frequency 3MHz.

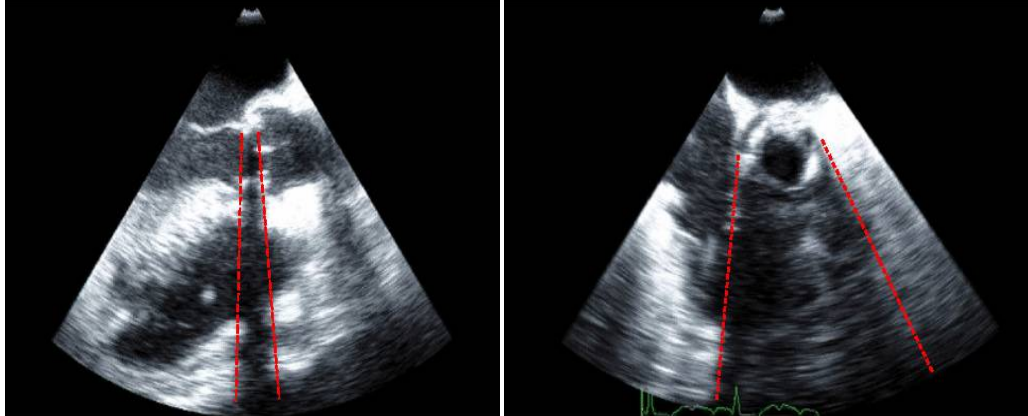
## REFERENCES

1. W. I. Zwiebel and R. Sohaey, " Introduction to ultrasound", 1997.
2. J. Bitz. "Fundamental of ultrasound", 1963.
3. B Cox, "Acoustics for Ultrasound Imaging," no. Janu.ary, 2013.
4. A. Guariento and el al, " Liver and spleen biometric in childhood- onset systemic lupus erythematosus patients", 2015.
5. C. Kasia, K. Namekawa, A. Koyano, R Omoto. Real- Time Two Dimentional Blood Flow Imaging Using an Autocorrelation Technique. IEEE Trans Sonic Ultrasonics, SU-32(3), 1985.
6. M. Martensson, " Evaluation of errors and limitations in ultrasound imaging systems", 2011.
7. C. OTTo, Texbook of Clinical Echocardiography, Saunders, 2000.
8. H. WEISS and A. WEISS, Ultraschall-Atlas 2, VCH, 1990.
9. S. BAKKER, D. SCHARSTEIN, J. LEWIS, S. ROTH, M. BLACK, AND R. SZELISKI, A Database and evaluation Methodology for Optical Flow, International journal of computer vision, 92, pp. 1-31, 2011.
10. N. A. Patel, P. P. Suthar, " Ultrasound appearance of congenital renal disease", 2014.
11. B. Dunmire, "Use of the acoustic shadow with to determine kidney stone size with ultrasound," no. January, 2016.





Roa M. Hussian and Faik H. Anter



Figure(1) : Illustration of shadowing effects of different extend due to strong reflectors in two US B- mode images[7].

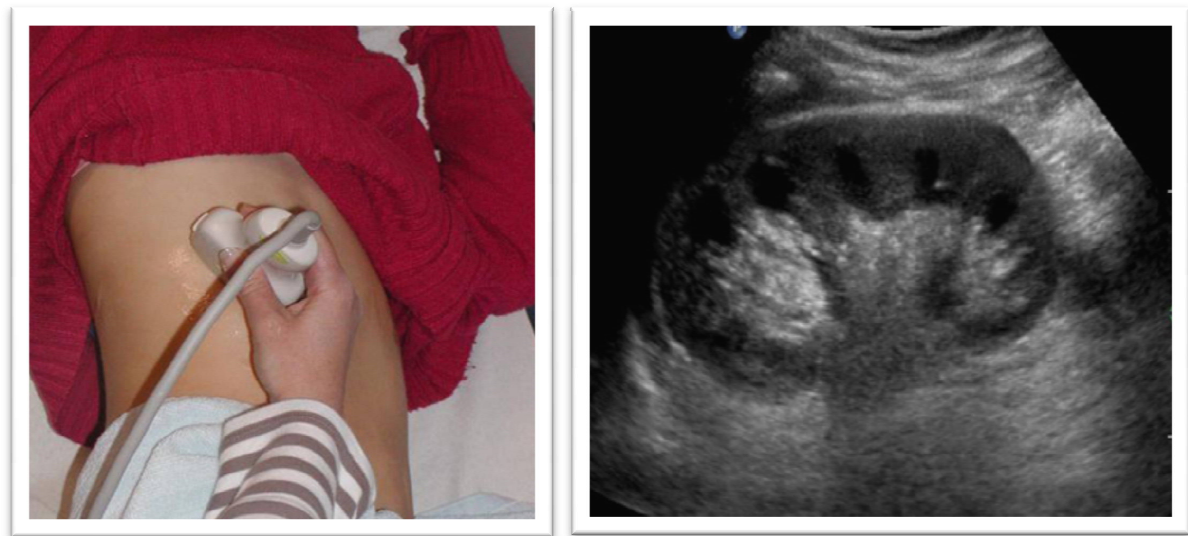


Figure (2): a) coronal scan plane for the Right Kidney

b) longitudinal: normal right kidney





**Roa M. Hussian and Faik H. Anter**

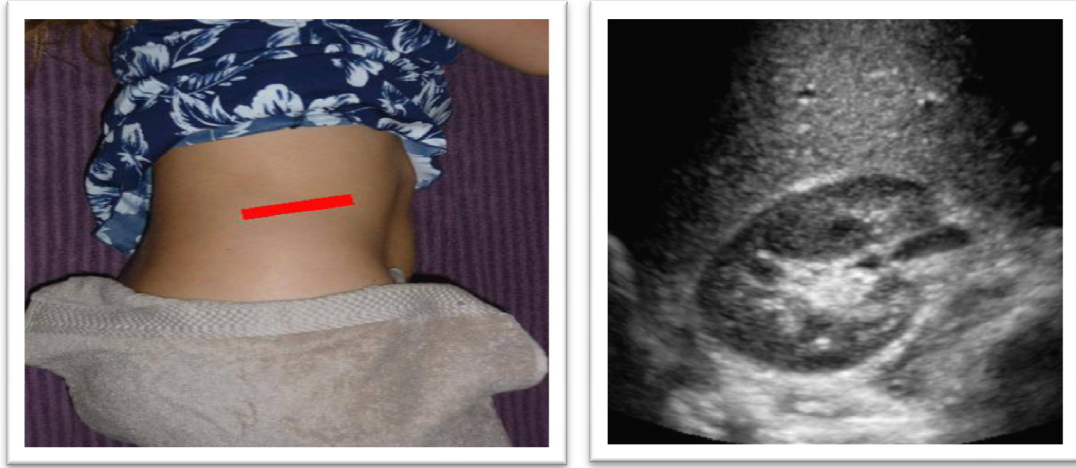


**Figure (3): a) shows scan plane transverse kidney**

**b) Transverse normal image of Right kidney.**



**Figure (4): Machine used "Type Sonoscape Ultrasound".**







**Roa M. Hussian and Faik H. Anter**

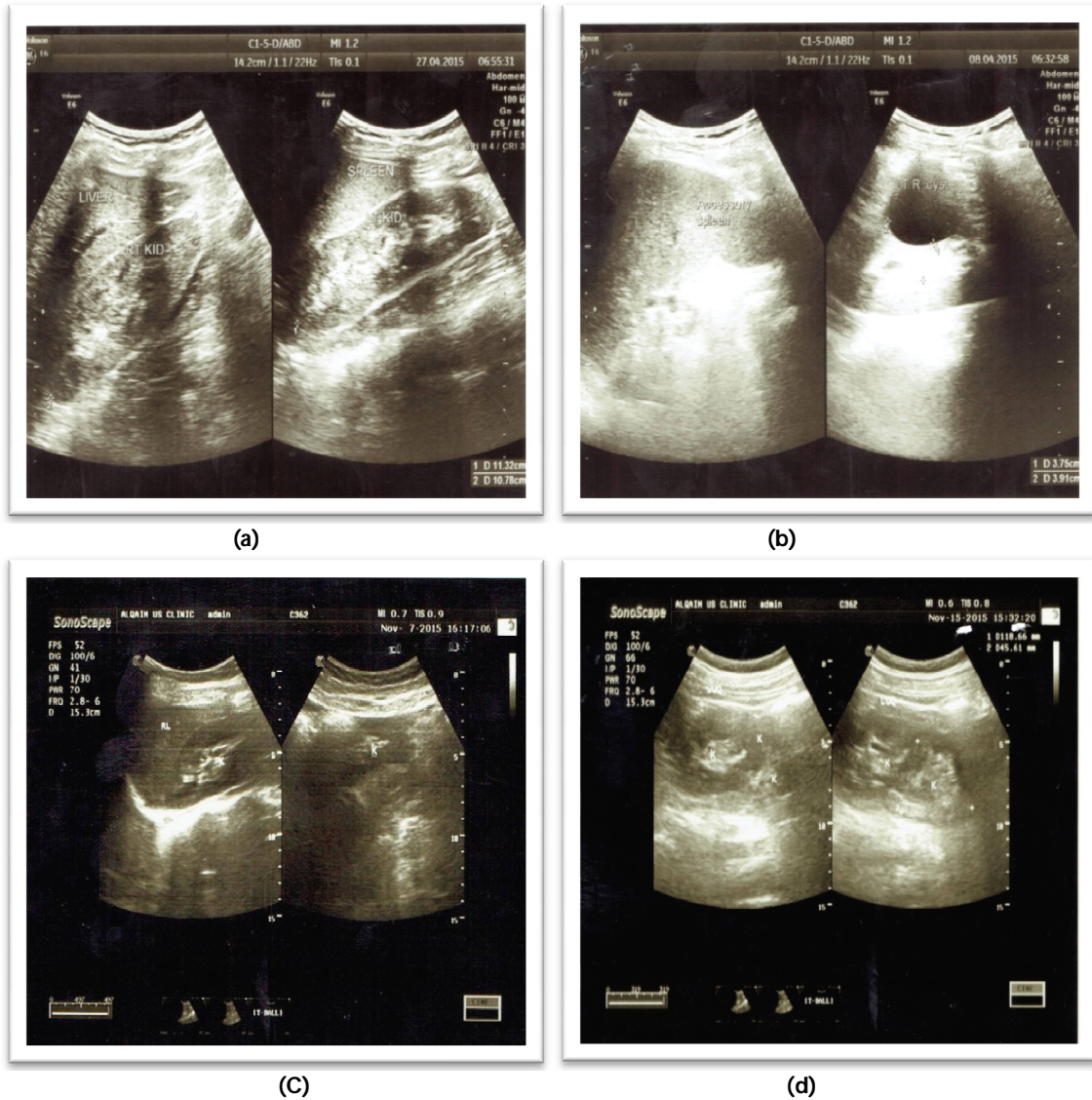


**Figure (5): Images of medical diagnostics for kidneys.**

- a) Liver, spleen and *cortico* of both kidneys.
- b) Left kidney with normal size.
- c) Right kidney on the left side of image in normal position.
- d) Left kidney is double collecting system.





## Earthworms Supplemented Poultry Feed as an Alternate to Vaccines

A.Shamasath Begam<sup>\*</sup> and Sujatha Ilangovan

P.G & Research Department of Zoology, Holy Cross College, Trichy, TamilNadu, India.

Received: 24 June 2016

Revised: 17 July 2016

Accepted: 30 Aug 2016

### Address for correspondence

A.Shamasath Begam  
Research Scholar, P.G & Research Department of Zoology,  
Holy Cross College, Trichy,  
TamilNadu, India.  
Email: shamsath1985@yahoo.com



This is an Open Access Journal / article distributed under the terms of the **Creative Commons Attribution License (CC BY-NC-ND 3.0)** which permits unrestricted use, distribution, and reproduction in any medium, provided the original work is properly cited. All rights reserved.

### ABSTRACT

Vaccines administered to poultry have become a topic of debate. An attempt to test the efficacy of 5% earthworm supplemented feed as an alternate to vaccines, in increasing the life of poultry was assessed. Native earthworms were collected from Thachankurichi village in Tiruchirappalli District were mixed with poultry feed and their effect on weight gain as well as on mortality was assessed in a group of 24 chicken. These native earthworms were identified to enhance the life span of unvaccinated broiler chickens. Statistical analysis of the results of life span using chi square analysis revealed significant effect of 5% earthworm supplemented poultry feed. Thus it could be recommended to supplement broiler chicken with 5% earthworm feed as an alternate to vaccination. No profound changes were observed on the weight gain in broiler chicken fed on normal poultry feeds as well as those fed on 5% earthworm supplemented food.

**Keywords :** Earthworms, Poultry feed, Mortality

### INTRODUCTION

Earthworms have been long recognized by farmers as beneficial to the soil (Edwards and Lofty, 1972) and therefore, rightly described to as soil engineers (Jones *et al.*, 1994; Lavelle *et al.*, 1997). Approximately 8,300 species of Oligochaetes have been described in 38 families and 811 genera (Reynolds, 2009). Vaccines are administered to poultry in order to protect them against infectious diseases and disease causing organisms like that of *E. coli* on day 1 of hatching, Marek's disease on 3 day old chick and infectious Bursal disease on 10-28 day old chicks, Coccidiosis on 9 day old chick. These vaccines help to decrease the mortality but adverse effects of vaccines on end users could not be over ruled. Vaccination in poultry is giving rise to a number of problems on its consumers. Many authors has



**Shamasath Begam and Sujatha Ilangovan**

reported that man has begun to consume hormones that are administered to conventional turkeys, chicken and cattle etc., The vaccines administered to these animals are reported to exert an adverse effect like infertility, coronary heart diseases, ovarian cancer, thyroid tumors, breast cancer, etc. (S.D.Wells march 12,2014).

Devon (2016) has suggested the raising of organic livestock to overcome the threats of antibiotic resistance. Numbers of attempts to identify an alternate to vaccines are made. Earthworm can be used as protein source in poultry. According to Partricia (1988), vermimeal contained 54% of protein when compared to imported fish meal and has reported a preference to vermimeal in birds. The Earthworm body fluid contain 9.4% of protein and 78.79 free amino acids and rich in vitamins, minerals and iron. Hence earthworm can be an excellent source of protein to supplement animal feed (Sun Zhenjun *et al.*,2010). Set of broiler chickens feed with 10% earthworm meal showed an increase in the weight of breast muscle and as well as in the protein content and recommend vermimeal based on these antimicrobial and antioxidant properties as an ideal feed supplement in broiler diets (VahidRezaeipour *et al.*, July 2014). Meal of local earthworm are taken for research and found that cumulative weight gain in groups of broiler feed with 10% to 15% worm meal. The broiler well adapted to worm meal feeding (T.C. Loh *et al.*, May 2009).

Son and Jo (2013) supplemented earthworm meal to seven day old broiler chicks. Chicks were fed diets containing 0%, 0.2%,0.4%, for six weeks. High feed intake, weight gain, and nutrient digestibility was observed in the chicks fed with 0.4% earthworm meal. According to ZivariBahadori *et al.*,(2015) the intake of 2% and 3% earthworm meal improved the feed conversion ratio of broiler chickens and the effect of experimental treatment was not significant on weight gain of broiler chickens. Therefore an attempt has been made in this work to test the efficacy of vermimeal on weight gain and decrease in the mortality rate in chickens.

**MATERIALS AND METHODS**

Native earthworms were collected from Thachankurichi village in Tiruchirappalli District. 24 broiler chicks were collected from poultry farms in Namakkal district on Day 1 of hatching. The chicks were divided into two groups. The two groups were fed with homemade feed (group 1) and 5%earthworm +homemade feed combination (group 2). The home made feed formulation comprised of Rice - 20 gm, Corn - 20 gm, Raggi - 20 gm, Sesame cake - 20 gm, Chollam - 15 gm, Onion - 5 gm: whereas that of 5% earthworm +homemade feed combination contained Rice - 15gm, Corn - 20 gm, Raggi - 20 gm, Sesame cake - 20 gm, Chollam - 15 gm, Onion - 5 g and earthworm- 5gm. All the above ingredients were finely ground into a paste with water and then pelleted into varying sizes so as to suit the age of feed for chick and dried in a shady and well aerated area.

Two groups of chicks that were not vaccinated were fed with homemade feed (C2) and homemade feed supplemented with 5% earthworm (E2) the other two groups were vaccinated and fed like the above and labeled as C1 and E1 respectively. Each group of chicks were fed with approximately 50 grams of feed and water *ad libitum*, three times a day at first week and then increasing the amount of feed gradually on second week onwards. Vaccination program was applied as recommended by District veterinary office to prevent Bronchitis and Ranikhet disease. Live Lentogenic lasota strain, i.p.(vet.) vaccine was used to serve the purpose. On the 21<sup>st</sup> day, the vaccine was administered as oral drops in the morning hours on the same day to the 2 sets of chicks (C1 & E1). Multivitamin tablets soluble in water were administered to the chicken in order to avoid the stress caused by vaccination within 24hours before and after vaccination. Chickens were not allowed to drink water 2 hours before vaccination. The weight gain and rate of mortality among the four groups was assessed and the significance of the feed and vaccination was calculated using Chi square analysis.





**Shamasath Begam and Sujatha Ilangovan**

## RESULTS AND DISCUSSION

The amendment of these worms in poultry feed formulations was further gauged in order to assess the efficacy of these worms as an alternative for vaccines, thus as essential immunogenic agents enhancing the life span so as to decrease the mortality rate in broiler chick and as important constituents in broiler feed formulations to improve weight gain in broiler chicks. The table depicting the outcomes of feed formulations on the mortality rate and weight gain in the tested populations was subjected to Chi square analysis and the significance of the feed was evaluated.

The net weight gain in poultry on consumption of the formulated diet is represented in Table 1. The table clearly shows that the two feed possessed similar effect on growth, that is weight gain in poultry remained the same with the two feed combinations. Chi-square analysis to reveal significance of feed on weight gain also depicted that feed had no significant difference on the weight gain in poultry. The above analysis clearly indicates similar effect of the two feed on the weight gain. It was interesting to note that 5% earthworm feed decreased the rate of mortality that is increased the life span in the tested populations. Its efficacy as a substitute for vaccination cannot be ruled out. Table 2 on rate of mortality in chick shows that the rate of mortality in the non-vaccinated group receiving 5% earthworm feed as diet to be reduced considerably. Further subjecting these results to Chi square analysis clearly illustrates the significant effect of 5% earthworm feed on broiler chickens.

Many authors have reported earthworm meal as best protein supplement to poultry. This work as thrown light on the decrease in the mortality of poultry fed with 5% earthworm. According to Sunzhenjun *et al.* (2010) reduction in the rate of mortality could be attributed to the presence of essential immunogenic agents in the body of earthworms thus enhancing the life span of the tested animal population. Works of Vahidrezaeipour *et al.* (2014) further support our findings, suggesting that 10% vermimeal formulations possess antimicrobial and antioxidant properties thus they established the use of the vermimeal feed as a supplement in broiler diet. T.C. Loh *et al.* (2009) depicted that worm meal could be replaced by soyabean and fish meal upto 10 – 15%. The broilers were well adapted to worm meal feeding thus in evidence to our findings. Many authors have experimented the performance of earthworm meal on broiler chicks and have documented weight gain with earthworm meal. These findings are in par with the present research suggesting the potentials of earthworm as supplementary feed for poultry against vaccines also.

## ACKNOWLEDGEMENTS

I kindly acknowledge DBT FIST, Centralised Instrumentation of Holy Cross College, Tiruchirappalli.

## REFERENCES

1. Edwards, C.A. and Lofty, J.R. (1972) Biology of Earthworms. Chapman and Hall, London, p.283.
2. Jones, C. G., Lawton, J. H., and Shachak, M. (1994). Organisms as ecosystem engineers. *Oikos* 69: 373-386.
3. L.J.Devon, staff writer. Natural News Aug 2, 2016. [http://www.naturalnews.com /054955\\_organic\\_livestock\\_antibiotic\\_resistance\\_superbugs.html](http://www.naturalnews.com /054955_organic_livestock_antibiotic_resistance_superbugs.html).
4. Lavelle, P., Bignell, D., Lepage, M., Wolters, W., Roger, P., Ineson, P., Heal, O. W., and Dhillon, S. (1997) Soil function in a changing world: the role of invertebrate ecosystem engineers. *Eur. J. Soil Biol.* 33: 159-193
5. Patricia M.Barcelo Production and Utilization of earthworms as feed for broilers in the Philippines. *TROPICULTURA*, 1986.6,1,21-24.
6. S.D.Wells ,Natural News Mar.12,2014 [http://www.naturalnews.com /044286\\_steroidal\\_hormones\\_livestock\\_human\\_consumption.html](http://www.naturalnews.com /044286_steroidal_hormones_livestock_human_consumption.html).
7. Son, J.H. Effects of feeding Earthworm Meal on the Meat Safety and Performance of Broiler Chicks (2007)(Daegu National University of Education , Daegu, Republic of Korea).
8. Sun Zhenjun, Liu Xianchun, Sun Lihui and Song Chunyang.(2010)*Ecol.Food Nutr.* 36:4..





**Shamasath Begam and Sujatha Ilangovan**

9. T.C.Loh, L.Y.Fong, H.L.Foo, N.T.Thanh and A.R. Sheik-Omar (2009).Utilisation of Earthworm meal in partial Replacement of Soyabean and Fish meal in Diets of Broiler, *J. Appl. Ani. Res.*36:1,29-32.
10. Vahid Rezaeipur,Omid Aghajan Nejad,Hadi Youseftabar Miri. (2014) *Int.J.Adv.Biol.Biom.Res*,2(8),2483-2494.
11. Zivar Bahadori, Ladan Esmaylzadeh and Mohammad Amir Karimi Torshizi (2015)The Effect of Earthworm (Eisenia fetida) and Vermihumus Meal in Diet on Broilers Chicken Efficiency and Carcass Components Biological Forum – An International Journal 7(1): 998-1005.

**Table 1 : Table of Chi-Square analysis to depict the significance of feed and vaccination on the weight gain in poultry**

Experimental Setup	Treatment		Statistical inference
	With vaccine	Without vaccine	
<b>Control</b> (Homemade feed only)	19.83	19.46	Chi –Square value = 0.153, Df=1, P value= 0.695, P>0.05, Insignificant
<b>Experimental</b> (Homemade feed supplemented with 5% earthworm)	25.18	19.78	

**Table 2 : Table of Chi-Square analysis to depict the significance of feed and vaccination on the percentage mortality in poultry**

Experimental set up	Groups of Chicks	Rate of Mortality	Statistical inference
Control	Homemade feed with vaccine	16.67	Chi –Square value =51.000, Df=3, P value= 0.00, P<0.05, Significant
	Homemade feed without vaccine	16.67	
Experimental	Earthworm feed with vaccine	5.56	
	Earthworm feed without vaccine	11.11	





## The Effect of Etching Current Density on Silicon Nanostructures Properties Fabricated by Electrochemical Etching Process

AsmietRamizy<sup>1</sup>, Isam M. Ibrahim<sup>2</sup> and Mays A. Hommadi<sup>1\*</sup>

<sup>1</sup>Department of Physics, College of Science, University of Anbar, Anbar - Iraq.

<sup>2</sup>Department of Physics, College of Science, University of Baghdad, Baghdad- Iraq.

Received: 21 June 2016

Revised: 16 July 2016

Accepted: 1 Aug 2016

### \*Address for correspondence

Mays A. Hommadi

University of Anbar, College of Science,

Department of Physics, Anbar – Iraq

Email: maisalalousi@gmail.com



This is an Open Access Journal / article distributed under the terms of the **Creative Commons Attribution License (CC BY-NC-ND 3.0)** which permits unrestricted use, distribution, and reproduction in any medium, provided the original work is properly cited. All rights reserved.

### ABSTRACT

Porous silicon (PS) was fabricated using p-type Si with <111> orientation by electrochemical etching process (ECE) at a constant etching time of 20min and different current density of 10-40mA/cm<sup>2</sup>. The surface morphology of PS studied by atomic force microscope (AFM) verifies that average diameter and nanostructure are dependent on the etching current density, when the current density increased from 10 to 40mA/cm<sup>2</sup> the average diameter also increased from 29.96 to 45.59nm. The FE-SEM image of the sample prepared at 20min and 10mA/cm<sup>2</sup> shows a homogeneous pattern and confirms the formation of uniform porous structures on the silicon wafer. From XRD pattern, the peak intensity decreased and full-width half maximum (FWHM) increased with increasing current density from 10 to 40 mA/cm<sup>2</sup> and the crystalline size also decreased from 10.8 to 2.5nm. From FTIR spectra of PS at different etching current range from 10 to 40 mA/cm<sup>2</sup>, it was found that the transmittance peaks around 997.13 cm<sup>-1</sup> and 1097.42 cm<sup>-1</sup> are from Si–O–Si asymmetric stretching modes, which are dependent on the oxidation degree of PS. The transmittance peaks at 624.94-630.68 cm<sup>-1</sup> Si-H wagging mode bending in (Si<sub>3</sub>-SiH), and 810.05-813.90 cm<sup>-1</sup> from Si-F stretching mode. Photoluminescence spectra (PL) showed that the band gap energy increased from 1.610 to 1.638eV when the current density increased from 10 to 40mA/cm<sup>2</sup>.

**Keywords:** Porous silicon, Atomic Force Microscope, Photoluminescence spectra.

### INTRODUCTION

Porous silicon (PS) is a material formed by anodic dissolution of single crystalline silicon in HF containing solutions [1]. Through anodization in HF solution, Silicon surface will be covered with a brown film. New physical properties





**Mays A. Hommadi et al.**

appear, when a structure becomes smaller than a characteristic length scale which is of great interest in basic research but also for applications. Nanoscale silicon reducing dimensionality of bulk silicon to nano-scale silicon (PS) leads to appreciable changes in optical, electrical and electronic properties. As a result of these advantages, PS has been widely used in technological applications such as in light-emitting diodes, light testing equipment, photoelectric solar batteries, gas testing devices, microdevices, and biological testing equipment [2]. Several methods are used and developed to fabricate the porous layer such as Photochemical, Electrochemical, Photo-electrochemical, Stain etching processes, and Laser Induced Etching Process [3]. One of the most important methods is electrochemical etching process (ECE). Many parameters that influence on the PS formation process with electrochemical anodization such as substrate doping, current density, HF concentration, and time etching [4,5]. This paper discusses the effect of current density on the morphological, structural, and optical properties of (111) p-type PS fabricated by electrochemical etching process.

## MATERIALS AND METHODS

PS layers formed by the electrochemical etching process (ECE) of p-type <111> oriented silicon substrate. The ECE cell was made of Teflon (or any highly acid-resistant polymer) base plate was made of aluminum. A Si wafer cut into a pieces with a square shape at area 1cm<sup>2</sup> and put on the bottom of the cell by using O-ring that allowed the Si surface to be exposed to the homogeneously mixed of HF: ethanol at 1:1 concentration. Si wafers were ultrasonically cleaned in distilled water and acetone, connected to the anode electrode and the Platinum connected to cathode electrode of the power supply as shown in Figure 1. PS samples were fabricated by changing the etching current density with a constant etching time. The prepared samples were characterized by Photoluminescence (PL), Fourier transform infrared transform spectroscopy (FTIR), X-ray diffraction (XRD) and atomic force microscopy (AFM).

## RESULTS AND DISCUSSION

Figure 2 shows the XRD spectra of the PS surfaces formed at different etching current densities. A strong peak of PS in 10mA/cm<sup>2</sup> current density shows a very sharp peak at  $2\theta = 27.6^\circ$  and another one, weaker than the former, at  $2\theta = 93.9^\circ$ . The founded values correspond to (111) and (151) c-Si orientations, respectively. Figure 2b illustrates a shift and a broadened peak for the sample of 20 mA/cm<sup>2</sup>. When the current density increased to 30 and 40 mA/cm<sup>2</sup> the intensity of peaks becomes very low and broadened peak increased tightly then, a new peaks appears located at  $2\theta = 16.2^\circ$ ,  $21.6^\circ$ ,  $34.0^\circ$  which corresponds to 001, 101, 002 orientations respectively represented SiO<sub>2</sub> as shown in Figure 2c and 2d. FWHM was increased from 0.8951 to 3.6250 when the current density increased from 10mA/cm<sup>2</sup> to 40mA/cm<sup>2</sup>, these computed results have been compared with the FWHM values of Cu-K $\alpha$  which have been published by Joint Committee on Power Diffraction Standards (JCPDS) the FWHM of bulk silicon about 0.295.

Crystalline size was calculated by using scherrer equation :

$$D = \frac{K\lambda}{\beta \cos\theta}$$

Where  $K$  is the Scherrer constant ( $1 > K > 0.89$ ),  $\lambda$  is the wavelength in nanometers,  $\beta$  is FWHM in radians, and  $\theta$  is the diffraction angle in radians. The result shows that the crystalline size decreased from 10.8nm to 2.5nm when the current density increased from 10mA/cm<sup>2</sup> to 40mA/cm<sup>2</sup>, respectively. In general, when the current density increase the peaks intensity of the PS decreases and crystal size is reduced toward nanometric scale, then a broadening of diffraction peaks is observed and the width of the peak is directly correlated to the size of the nanocrystalline domains [7]. Figure 3 illustrates 3-D images of prepared PS samples showed a sponge-like structure is produced. The change in anodization parameters such as current density cause a big difference in fabricated PS in terms of roughness, thickness, pore's diameter and other properties. Figure 4 shows the diameter values distribution chart of PS samples in which the irregular and randomly distributed nanocrystalline silicon pillars and voids over the entire surface. Pore diameter generally increases with increasing potential and current density [1]. At low current



**Mays A. Hommadi et al.**

density, a highly branched, randomly directed and highly interconnected meshwork of pores was obtained. However, increasing in current density orders the small pores to exhibit cylindrical shapes giving rise to larger pore diameter [8]. Table 1 shows the average diameter, average roughness, peak-peak and RMS parameters of the prepared PS samples. It was observed that the higher values of roughness, peak-peak and RMS belong to the sample prepared at current density 30mA/cm<sup>2</sup>. Figure 5 shows the FTIR spectra of the PS as a function of the transmission. It is clear that there are many distinct peaks with different intensities. The peaks around 997.13 cm<sup>-1</sup> and 1097.42 cm<sup>-1</sup> are from Si–O–Si asymmetric stretching modes, which are dependent on the oxidation degree of porous silicon. The transmittance peaks at 624.94-630.68 cm<sup>-1</sup> Si-H wagging mode bending in (Si<sub>3</sub>-SiH), and 810.05-813.90 cm<sup>-1</sup> from Si-F stretching mode. Among the three major surface contaminants, hydrogen is found to exist expectedly and hydrogen-related surface states lead to strong PL. The pore surface includes a high density of dangling bonds of Si for original impurities such as hydrogen and fluorine, which are residuals from the electrolyte. Additionally, if the manufactured PS layer is stored in ambient air for a few hours, the surface oxidizes spontaneously [9].

Figure 6 shows the PL spectra for PS samples. The PL peak position of PS is blue-shifted as a function of the current density as shown in Figure 4.8. According to the quantum confinement model, the peak shift is due to an increase in the energy band gap (E<sub>g</sub>) within the porous structure [10]. The result also suggests that the band gap energy increased from 1.610 to 1.638 eV when the current density increased from 10 to 40 mA/cm<sup>2</sup>. Figure 7 illustrates the E<sub>g</sub> as a function of variation of current density. Increasing in the current density is attributed to the reduction of the Si to nanosize, which favors charge carrier quantum confinement. The probability of recombination of e and h is higher in very small structures (quantum confinement effects), leading to higher emissions. High PL intensity is the result of the conversion of the material band gap conduction from indirect to quasidirect [11]. The quantum dimension of the structure in the sample favors PL shifting toward shorter wavelengths. Other researchers [12] have also found a blue shift of PL peak with increase in the etching current density. Figure 8 shows the FESEM image of sample prepared at current density 10mA/cm<sup>2</sup> with time about 20min, it is showed a homogeneous pattern and confirms the formation of uniform porous structures without any cracks on the silicon wafer.

## CONCLUSION

EC mechanism of the PS synthesis, the results of morphological, structural, and optical properties have been investigated. AFM images of PS shows an increment in average diameter with increasing of etching current density. FE-SEM image shows a homogeneous pattern uniform porous structures. XRD pattern of PS shows that increasing of etching current density leads to broadening in diffraction peaks which indicate forming of nanostructure shapes. From FTIR spectra of PS at different etching current density, the peaks appeared from bonding the hydrogen and fluorine from HF solution with the surface of Si. PL measurement indicated the shorter peak wavelength of luminescence has caused the increase in the energy band gap (E<sub>g</sub>) of the porous structure.

## REFERENCES

1. C.G.Vayenas and R. E. White, "Modern Aspects of Electrochemistry," Springer US, New York, (2005), Ed. G. X. Zhang, Canada, (2006), vol 39, pp.XXI-279.
2. P. Kumar and P. Huber, "Effect of Etching Parameter on Pore Size and Porosity of Electrochemically Formed Nanoporous Silicon," Jour. of Nanomaterials, (2007), Vol. 2007, Article ID 89718, 4 pages.
3. P. Malempati, "Surface-Enhanced Raman Spectroscopy Substrates Based on Nanoporous Silicon and Pattern Transfer," M.Sc. Thesis. Louisiana State University, USA, (2011).
4. E. X. Pérez, "Fabrication and Characterization of Porous Silicon Multilayer Optical Devices," University Rovera, (2007).
5. G. X. Zhang, "Morphology and Formation Mechanisms of Porous Silicon," Jour. of Electroch.Soci., Mississauga, Canada, (2003), Vol. 151, pp. 65-133.







**Mays A. Hommadi et al.**

6. L. Russo, F.Colangelo, R.Cioffi, I. Rea and L. D. Stefano, "A Mechanochemical Approach to Porous Silicon Nanoparticles Fabrication," *Materials* 4, (2011), pp. 1023-1033.
7. A. Lorusso, V. Nassisi, G. Congedo, N. Lovergine, L. Velardi, and *et al.*, "Pulsed Plasma Ion Source to Create Si Nanocrystals in SiO<sub>2</sub> Substrates," *Appl. Sur. Sci.*, (2009), 255(10), pp. 5401-5404.
8. U. M. Nayef and A. H. Jaafar, "Characteristics of Nanostructure Porous Silicon Prepared by Anodization Technique," *Eng. & Tech. Jour.*, (2013), 31(3), pp. 339-347.
9. I. M. Mohammed, A. H. Shnieshil "Characteristics Study of Porous Silicon Produced by Electrochemical Etching Technique," *Internat.Jour. of Applic.orInnova.in Eng. &Manag. (IJAIEM)*,(2013), 2(9), pp.77-80.
10. A. R. Abd-ALghafour, "Nanostructured Porous Si and GaN Fabricated by Electrochemical and Laser Induced Etching Techniques," *Ph.D thesis, University Sains, Malaysia*, (2011).
11. J. Jakubowicz., "Nanoporous Silicon Fabricated at Different Illumination and Electrochemical Conditions," *Superlats and Microsts*, (2007), 41(4), pp. 205-215.
12. J. Torres, F. Castillejo, and J. E. Alfonso, "Influence of the Current Density and Resistivity on the Optical Properties of p-type Porous Silicon Thin Films Fabricated by the Electrochemical Anodizing Method," *Brazilian Jour. of Phys.*, (2006), 36(3B), pp.1021-1024.

**Table 1: AFM parameters of the prepared PS samples.**

Etching current density (mA/cm <sup>2</sup> )	Averagedia meter (nm)	Average roughness (nm)	Peak-peak (nm)	RMS (nm)
10	29.96	0.747	2.99	0.863
20	40.81	0.712	3.07	0.836
30	43.08	1.16	4.75	1.35
40	45.59	0.883	3.77	1.03

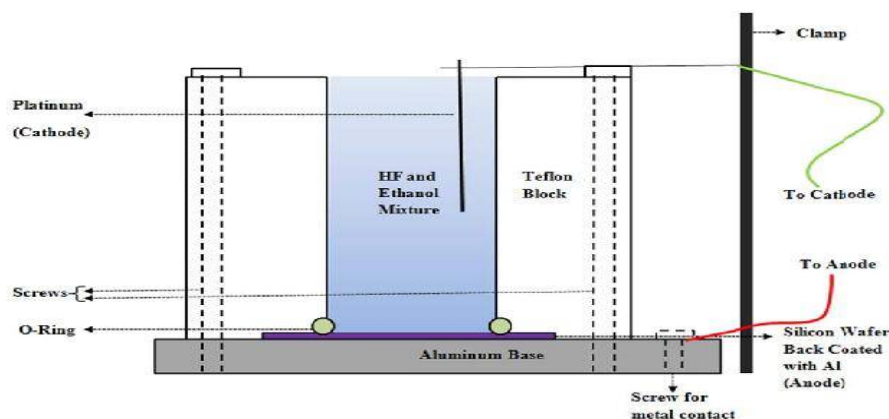


**Figure 1: Setup for the fabrication of porous silicon.**





Mays A. Hommadi *et al.*

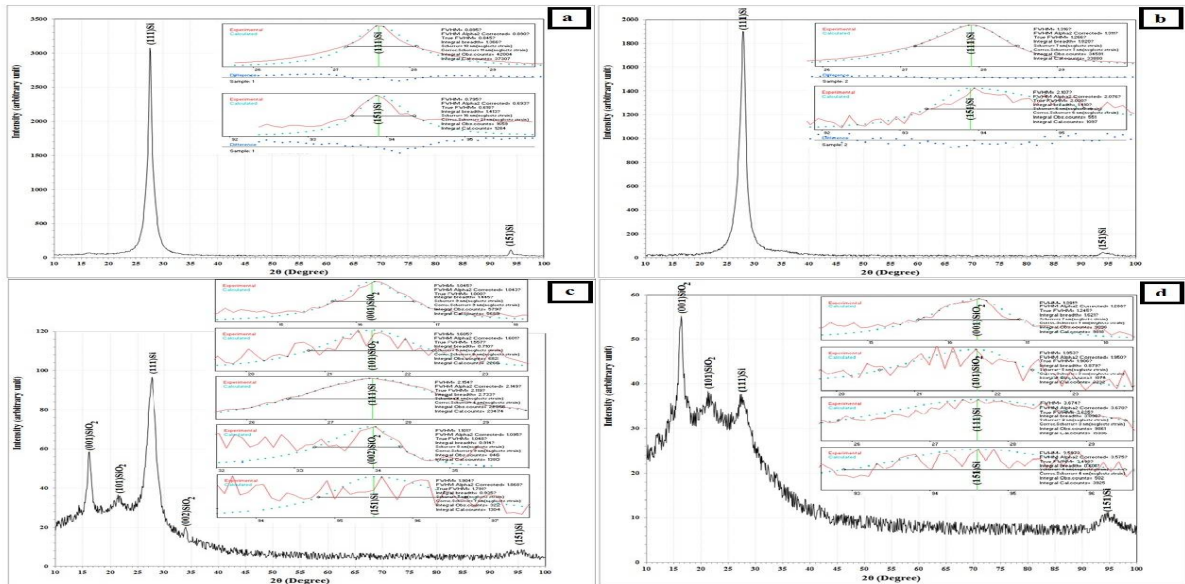


Figure 2: XRD spectra of PS samples a) at 10mA/cm<sup>2</sup> b) 20mA/cm<sup>2</sup> c) 30mA/cm<sup>2</sup> and d) 40mA/cm<sup>2</sup>.

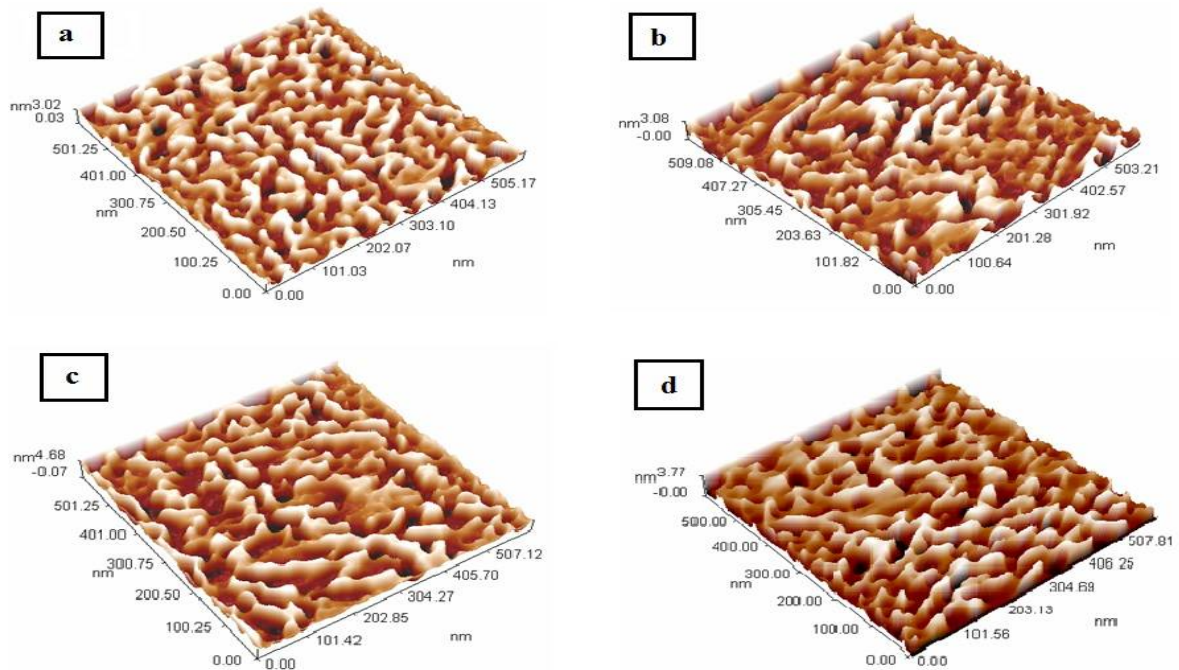


Figure 3: 3-D AFM images of PS a) at 10mA/cm<sup>2</sup> b) 20mA/cm<sup>2</sup> c) 30mA/cm<sup>2</sup> and d) 40mA/cm<sup>2</sup>.





Mays A. Hommadi et al.

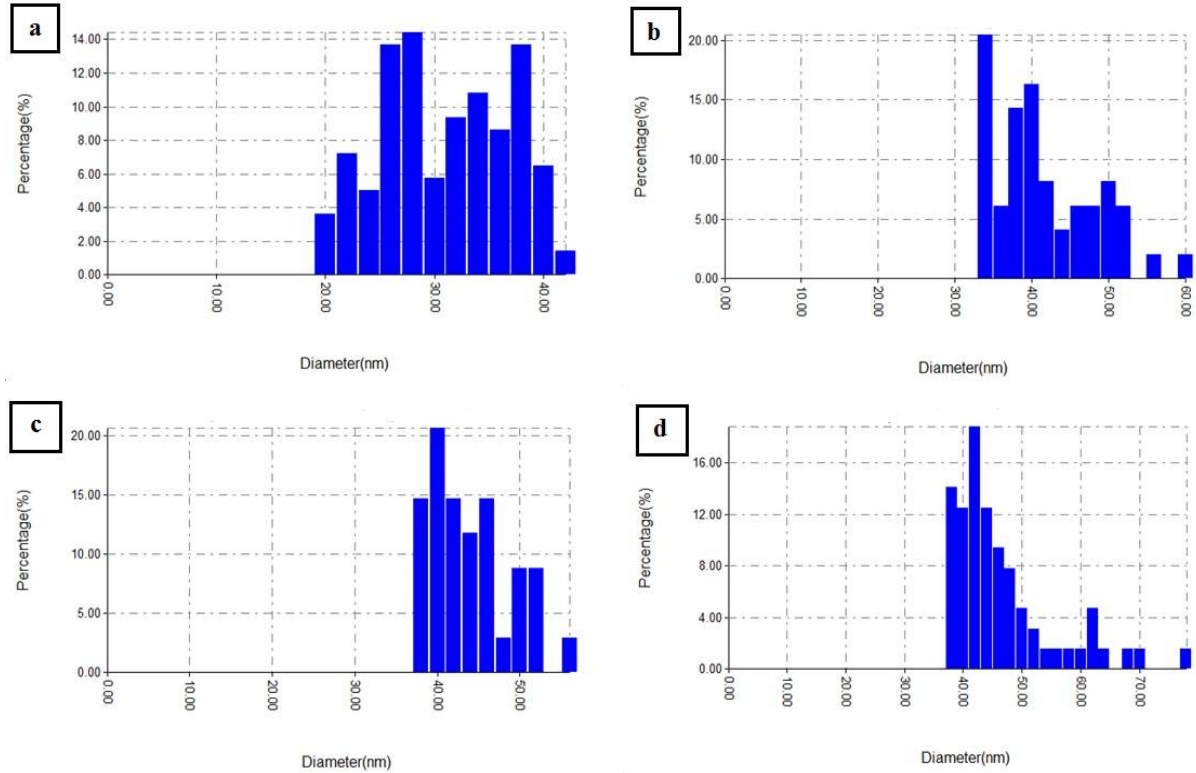


Figure 4 The diameter values distribution chart of PS samples a) at 10mA/cm<sup>2</sup> b) 20mA/cm<sup>2</sup> c) 30mA/cm<sup>2</sup> and d) 40mA/cm<sup>2</sup>

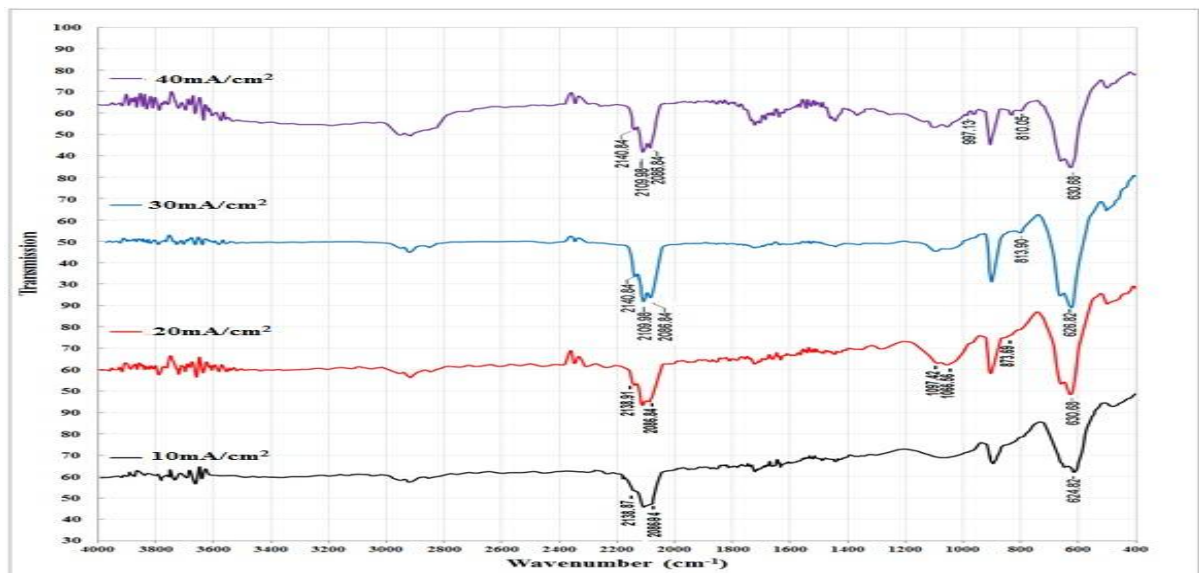


Figure 5: FTIR spectra of the samples p-type etched at a constant time 20 min and different current density.





Mays A. Hommadi et al.

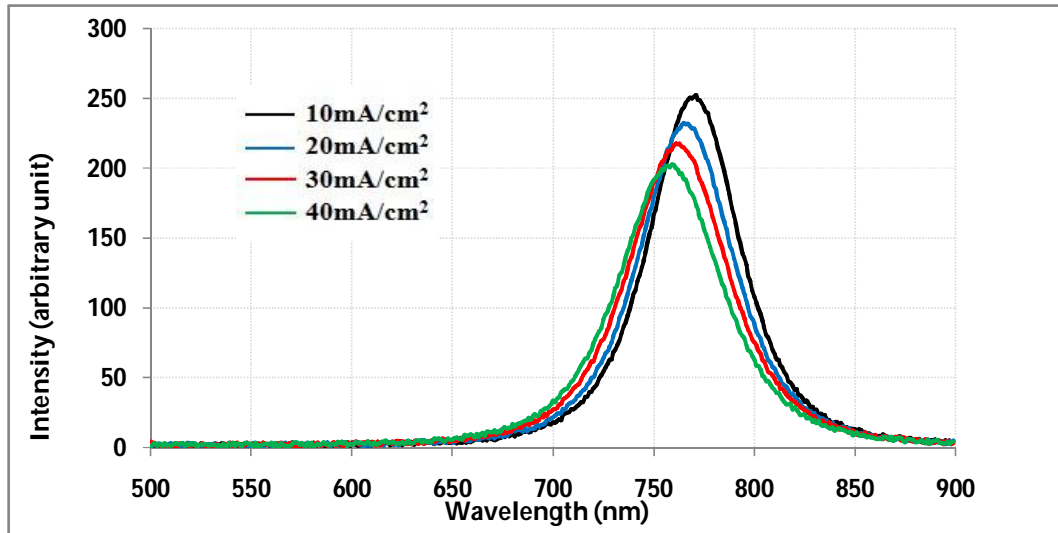


Figure 6: PL spectra of PS etched for 20 min at different current densities.

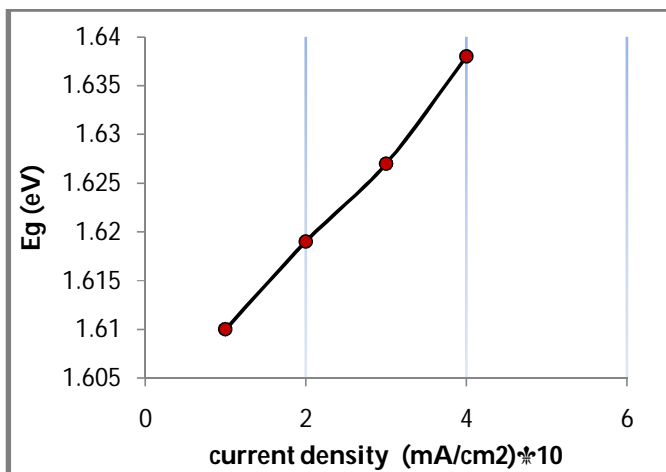


Figure 7: Energy band gap as a function of current densities.

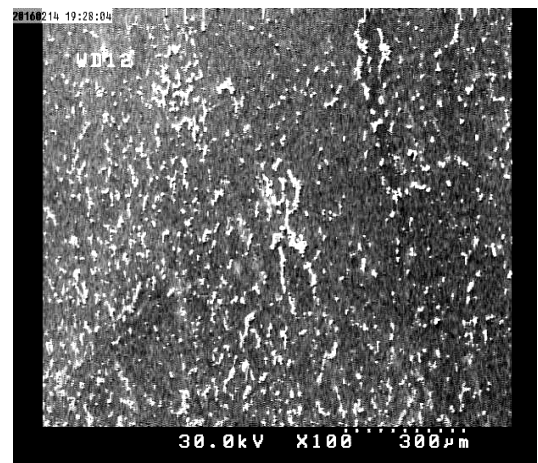


Figure 8: FESEM image of PS sample prepared at 10 mA/cm² and 20 min.





## RESEARCH ARTICLE

## Study of Beta Particles ( $\beta$ ) Effect on Hardness, Thermal conductivity and Dielectric strength for Epoxy Resin Reinforced with (Fe) Particles

Abd-Al sattarKhlilMaroof\*, FouadNajah Ali and Jassim M.Najeem

College of Science, Anbar University,Iraq.

Received: 14 July 2016

Revised: 21 Aug 2016

Accepted: 9 Sep 2016

### Address for correspondence

Abd-Al sattarKhlilMaroof

College of Science

Anbar University,Iraq.

Email: maherbiologist@gmail.com



This is an Open Access Journal / article distributed under the terms of the **Creative Commons Attribution License (CC BY-NC-ND 3.0)** which permits unrestricted use, distribution, and reproduction in any medium, provided the original work is properly cited. All rights reserved.

### ABSTRACT

In this research, composites materials samples were prepared by using Epoxy Resin (EP-Polyprime) as matrix, reinforced with (Fe) particles with weight fractions (2%), (4%) and (6%). And for irradiation periods {[4] days (174.72Gy)}, {(8) days (349.44Gy)} and {(12)days (524.16Gy)}. Composite materials samples which prepared by hand-layup method. This research studied the physical properties as Hardness, Thermal Conductivity and Dielectric strength before and after irradiation of samples by Beta particles ( $\beta^-$ ) by using the Strontium source ( $Sr^{90}$ ) with energy decay of beta particles (0.546Mev) at dose rate (1.82Gy/hr). Results showed that the reinforced blends with (Fe) better Physical properties Hardness, Thermal Conductivity and decrease of the Dielectric Strength.

**Keywords:** (Fe) particles,  $\beta$  particles, Epoxy resin.

### INTRODUCTION

The use of composite materials have overlapped a turning point in our time a major transformation due to its material from these several characteristics that led to the approach to be used widely in various fields. It is these qualities costly manufactured low-lying as well as its strength, durability and low density, high thermal and electrical isolation and resistance to chemicals, moisture and corrosion resistant and posed different shapes and sizes and high its Hardness[1]. Paying attention to the production of composite materials overlapped and development have increased access to the results and get a high material specifications for physical and mechanical properties, and low cost. This prompted many scientists and researchers to carry out studies and research focused much experience included many types of composite materials and testing physical, mechanical and chemical properties. The newly intrigued scientists irradiating composite materials with many types of radiation rays gamma, beta and

11573



**Abd-Al sattarKhlilMaroof et al.**

X-rays and ultraviolet rays and neutrons. In (2011) prepared a researcher HiderSalem study dealt with the effect of beta rays and gamma on the particle distribution of composites materials, lead and conclude that the polymers have the best protective barrier from gamma rays and show him as well as the mixture of ( PU / EP ) best stabilizing rays gamma him to beta rays[2].

In the same year conducted a researcher ( Kunal ) discussed included the study of the influence of the thermal conductivity of the composite material subsidized (Fe) particle where he noted that the thermal conductivity has been improved by( 18.5 % ) , and Article resultant can be used in various applications such as thermal paint and insulate electrical cables[3]. In the year (2013), a promising researcher ( Turgay ) and his search ate the effect of x-ray and gamma tests and neutrons on the imbricated epoxy and remnants of iron (Epoxy-Ferrochromium Slag) turned out for them increased susceptibility article overlapped on the prevention of radiation energy when increasing the remnants (Fe) particles on epoxy[4]. In ( 2015 ) conducted a researcher Abdul Hade study the mechanical properties of the epoxy resin (Fe) particles and the results showed that the hardness increased to increase the concentration of (Fe) particles after immersion in water samples , the results showed a decrease in hardness values[5]. This research aims to use beta emitted particles from the source of Strontium ( $Sr^{90}$ ) and the study of their effective on the composite materials that has been manufactured by the researcher and composed of epoxy resin reinforced by( Fe ) particles and the different effective on conductivity thermal and hardness and dielectric constant of the samples before and after irradiated and different periods of time.

## MATERIALS AND METHODS

### The Theoretical Side

#### Epoxy Resin

Epoxy is a Greek term consists of two syllables are (EP) and the mean and the (oxy) and mean oxygen and containing epoxy resin on one or more of the groups (Epoxide group) , which represents the basic unit of epoxy resin ,the simplest his formula is (Oxirane) as it represents a compound in the form of a loop consisting of an oxygen atom linked with two of carbon atoms with each other, The epoxy resin solidifies within temperatures ranging between (5-180 C°) and can be thermally stabilized to a temperature of up to (250 C°), There are no volatile materials during the hardening process , and this trait characterized by epoxy resin on the most hardened thermoplastic resins [6]. Epoxy resin is characterized by ability to adhesion and does not need high pressure a long time and also features as small shrinkage and has a high mechanical specifications to withstand high stresses inflicted it, It also features a well that is good Electrical insulation properties of epoxy resin and is one of the most common resins used as the basis of (Matrix) in the composite materials since he has the physical and mechanical properties that distinguish it from the rest of the other hardened resins [7].

#### Hardness

It called on the hardness property as resistant solid material to cut, scratching and penetration. It can also be defined as the resistance of the material bulging and itching and scratching by the number of machines more than hardness ones, which enable it to retain its surface intact together under the influence of external forces so that permanent deformation does not occur in the latter [8]. Hardness of materials depends on the type of power Association of molecules or atoms on the surface and the type of material you want to measure the hardness and temperature and other conditions affecting it [9] It is noted that the hardness of materials influenced by the type of solutions that exposed this material values [10], and the hardness of materials measured in the previous propensity to cut other materials the one who cut the other one is the most hardness .





**Abd-Al sattarKhlilMaroof et al.**

### Dielectric Strength

Called on the maximum electric field is applied to the Insulating material without collapse is resistance of the insulator and also called (Dielectric Breakdown Voltage). On this basis, the most important qualities that must be taken into account when choosing the insulator is the extent of carrying insulation voltage electric without collapsing. If polymeric material and put it in the electrostatic field it does not pass permanent current but stored energy in the form of material insulation as a result of polarization. Thus, the insulator works as a battery stored energy despite the presence of the leak of the current even in the best insulators [11]. The insulating materials in the property collapse in the strong electrostatic fields and field intensity causing the collapse called electrical insulation severity or intensity Electric ( $E_{br}$ ) which is inversely proportional to the thickness ( $d$ ) of the material, has been the collapse occurs in the lower level of the level of electrical insulation intensity of the measured result of the accumulation of energy, according to the following equation:

$$E_{br} = \frac{V_{br}}{d}$$

Where represent ( $V_{br}$ ) voltage collapse, though the intensity of the electrical insulation ( $E_{br}$ ) be significant for several polymeric insulators, The upper limit depends on the severity of the dielectric material on the ionization energy. Electrical breakdown occurs when still electrons from the atoms belonging to her, and this causes a minor collapse sooner or effect [12]. There are influential external variables on unarmed force of which the shape and size of the electrodes used in the field of application and the temperature of the model and frequency voltages and relative humidity. This should reduce these factors for the purpose of obtaining the area of the collapse of the value of accurate [13].

### Thermal Conductivity

One of the main physical characteristics would be described composite materials are thermal conductivity property, which is one of the phenomena of heat transfer. And where the heat is moving from one location to another because of the difference in temperature (the fluctuation of molecules Article). Therefore, it can define the thermal conductivity of the material as the material susceptibility to heat conduction and usually expressed by a factor of thermal conductivity ( $K$ ). The phenomenon of thermal conductivity are subject to the law of Fourier thermal connected shown in the following relationship:

$$Q = -KA \frac{dT}{dx}$$

where:

Q: amount of heat transmitted (J / Sec), K: thermal conductivity coefficient (W/m.k°)

A: sectional area perpendicular to the direction of heat transfer (m<sup>2</sup>). (dT / dx): the thermal gradient in the conduct medium (k°/ m) [14].

### Irradiation effect in Polymer properties

The high-energy nuclear radiation have a clear impact in polymeric materials due for successive operations where motivates particles and ionized and emits electrons speeds are relatively low-lying, which in turn leads to attack other molecules and generate the largest number of new ions. It gets two types of interactions, the first (Degradation) series, which in turn leads to a decrease in tensile strength and elongation and the second (Crosslinking) chains which increase the tensile strength and elongation reduce [15].

### Change of Physical Properties

To change the color of the polymer during irradiation depends on the temperature at which the irradiation and then being on the user's radiation and the amount of radiation and the irradiation type. As for the radiation effect on the thermal properties When exposing the composite materials to the effect of radiation will not affect the behavior of the thermal conductivity as a function of temperature as the thermal conductivity values continue to grow with high temperatures until the degree of access to the glass transition, which then decreases the thermal conductivity



**Abd-Al sattarKhlilMaroof et al.**

values. The reason is that the impact of radiation contributes to the increase for the process of cross-correlation and the more compromising material polymeric radiation will increase the cross-linking of the polymeric chains with each becoming more and more polymer hardness period, as the free radicals resulting from the collision of radiation with atoms overlapped will be a contributing factor in the increased values thermal conductivity [16].

**Change of Mechanical Properties**

The process of irradiation of polymers lead to a change in the physical properties have this amount of change over for any of the processes of decomposition and tangles depends (cross-linking). When the decomposition process for making polymeric chains short and weakens the internal structure of the polymeric composite materials, it becomes fragile and less tensile strength between molecules and increases its density due to increased its crystals. This leads to a decrease in Yong modules. But when you get cross-linking process of standing, branching chains and increasing composite materials hardness and less susceptibility melt and increase the tensile strength and you get an increase in Yong modules [17].

**The Practical Side****The Matrix Material**

Was used in this research epoxy resin Type (EP-Polyprime) factory by a company (Henkel) UAE as a matrix in the preparation of composite materials, and the advantage of epoxy resin being a transparent liquid and viscous with a density ( $1300 \text{ kg /m}^3$ ) turns epoxy resin to the solid state after adding Hardner the type Matavnlen Damon (MetaphenylenDiamine) (MPDA) and the factory of the same company and by (2: 1).

**Reinforcement Materials**

Was used in this research (Fe) particles as a reinforcement Material which is made from the company (BDH British) and the density of ( $7.8 \text{ gm/cm}^3$ ) and atomic weight ( $55.85 \text{ gm /mol}$ ) it has been used in reinforced the epoxy resin and characterized these particles high mechanical characteristics but more roughness of copper particles, these particles have been used in this research different weight fractures.

**Samples Preparation**

In this research method was used (Hand lay-up molding) in the preparation of polymeric complexes, one of the easiest ways and common use. Where the user has been the creation of the mold cast composite materials will then be put on thermal paper, glass base of the mold and under the strips to prevent the adhesion of glass mold base model. After that a matrix was the weight of the foundation and the additive using sensitive electronic balance type (Sartorius) and manufactured by the company (Sartorius German) who fumbles for four places ( $0.0001 \text{ gm}$ ). After that has mixing epoxy resin genitive its hardener process and by mass equivalent (1: 2) with (Fe) particles thoroughly mixed using a blender. Then pour a little of this mixture is homogenized on the block (base) glass and on a regular basis. Where Pour the mixture into the mold homogenized center and slowly seeps into the mixture to all points of the mold and evenly until it is filled template size fully to get the desired thickness (4mm). And then leave for the model (48) hours in the atmosphere of a room in order to be solidifies. Then after the expiration of the (48) hour samples are placed in a convection oven and temperature ( $50^\circ \text{C}$ ) for a period of (6) hours to complete the process of hardening and cross-linking chains. After that samples were examined thermal conductivity in a circular cutting diameter (40mm). And cutting samples examined hardness and dimensions ( $20 \text{ mm} \times 10 \text{ mm}$ ). And cutting samples examine the dielectric strength and the dimensions ( $55 \text{ mm} \times 10 \text{ mm}$ ). After that, anti-aliasing samples refrigerant iron and silicon carbide paper to get the standard dimensions.







**Abd-Al sattarKhlilMaroof et al.**

## RESULTS AND DISCUSSION

### Hardness Test Results for (Fe) Sample before and after ( $\beta$ ) Irradiation

From table (1) , which shows the hardness values of (Fe) samples for natural state (without irradiation ) and periods of irradiation (4 ,8, 12) days (Figure 1).Results show that the highest value for the hardness of a sample of (Fe) No.(1) of the weight fraction(2% Wt) was when the irradiation (12 ) days , reaching the value of hardness to (78.83N/mm<sup>2</sup>) and the lowest value for hardness appeared in normal conditions (without irradiation),where the results showed that the value of the hardness was (65.666N/mm<sup>2</sup>).But when analyzing the results of a sample of (Fe) No.(2) of the weight fraction(4% Wt) has been shown that the highest value for hardness was for a period of irradiation (12) days , reaching the value of hardness then to(78.5N/mm<sup>2</sup>),while the lowest value for hardness was when the situation natural (without irradiation ) and then the value of hardness (72 N/mm<sup>2</sup>).But when analyzing the results of a sample of (Fe) No.(3) of the weight fraction(6% Wt) it has been shown that the highest value for hardness was at a period of irradiation (12) days , reaching the value of hardness to (81N/mm<sup>2</sup>),while the lowest value for hardness was when the natural state (without irradiation ) as the value of hardness (72.666N/mm<sup>2</sup>). As shown above, to us that the hardness of the composite material reinforced by (Fe) particles is increasing with increasing periods of irradiation.

Results from the previous adopt us that hardness increases with the irradiation of samples of iron (Fe) using isotope Strontium (Sr<sup>90</sup>) radioactive particles negative beta ( $\beta^-$ ) or ( $e^-$ ) and a half-life (28.8 y).To explain this , we can say that the beta negative or electron differs from the interaction of photons ( $\gamma$ -ray UV, X-ray,) with the material, as the beta particle or electron passes a series of collisions with the material and then can be stabilized in the beam interaction the middle, during passing through the ionization process occurs in the medium to be stabilized or come out of it if the sample thickness less than (3mm).This kind of interaction with the polymer can lead to adisintegration of the polymeric chainsand re-(cross-linking) and as a result of this series of collisions in each collision will lose the electron part of the energy to be able to stability within the medium has been given enough time to form crystalline regions within this composite material has led to an increase degree of crystallization and then increase in (cross-linking) and this in turn has led to increased hardness.The increase in collisions series through which loses beta particle negative ( $e^-$ ) energy in the form of phases of (dE/dX) in the mediumthat can ionize the largest increase the time period for irradiation is happening and that means a greater number of rays negative beta and more electrons ( $e^-$ ), which settles in the material leads to disintegration the polymeric chains more and re-(cross-linking) in a greater or fences be crystalline regions within the composite material, and this leads to increase the degree of crystallization and increased cross-linking and this in turn leads to increased hardness.

And to discuss the hardness property increased weight fractionin the case of reinforced by( Fe )particle after it has been read and hardness values for each point several times and then average the readings made for the purpose of obtaining high precision results and Figure (2) below.Notes from the previous figure increased hardness of samples of (Fe)values increasedweight fraction.an reason for this is due to the volume of particles used in reinforcement the matrix was the size (100  $\mu$ m)where these particles be of high mechanical properties easy to penetrate the process inside the matrix during the manufacturing process leading to a two-way bridge voids formed during the preparation of composite material operationwhich in turn leads to increased contact area between the components of the prepared composite material thereby increasing interdependence among themselves and in an integrated manner , leading to the strong linkage at the interface between the epoxy and particles of iron (Fe),which led to better readings when checking hardness.

### Thermal Conductivity Test Results for (Fe) Samples before and after ( $\beta$ )Irradiation

From table (2), which shows the thermal conductivity of the samples (Fe) particlesnatural state values (without irradiation ) and periods of irradiation (4,8,12) days and equivalent radiation dose (174.72Gy)and(349.44Gy) and (524.16Gy) respectively under the effect of beta rays.And Figure (3). Results show that the higher the value of the thermal conductivity of a sample of (Fe) No.(1) with the weighted fraction (2% Wt) was a period when irradiation





### Abd-Al sattarKhlilMaroof et al.

(12)dayson which amounted to (0.309978w/m.k<sup>o</sup>),while the lowest value appeared in normal conditions (without irradiation ), where the results showed that the value of the thermal conductivity was (0.206491w/m.k<sup>o</sup>).But when analyzing the results of a sample of (Fe)No. (2) of the weight fraction(4% Wt) it has been shown that the highest value of the thermal conductivity was for a period of irradiation (12 ) days , reaching the value of thermal conductivity then to(0.386819w/m.k<sup>o</sup>) while less valuable when it was the natural state (without irradiation ) and the value of the thermal conductivity then (0.266034w/m.k<sup>o</sup>).But when analyzing the results of a sample of (Fe) No.(3) of the weight fraction(6% Wt) has been shown that the highest value of the thermal conductivity was at the period of irradiation (12)dayson which amounted to (0.404898w/m.k<sup>o</sup>) , while the lowest value of thermal conductivity when was the natural state (without irradiation ) where worth (0.286285w/m.k<sup>o</sup>).

As shown above, for us to thermal conductivity of the composite materialsreinforced by(Fe) particles is increasing with increasing periods of irradiation.Notes from the study of this axis containing the study of the thermal conductivity as a function to the time of irradiation with different irradiation periods.an reason for this is due to the negative interaction of beta particles ( $\beta^-$ ) or ( $e^-$ ) with composite materials.Which led to the disintegration or biodegradable polymeric chains or led to the cross-linking of molecules , which explains that the rays negative beta , which is a high-energy electrons with the electrons would lose energy in the medium as a result of a series of collisionsIn the end, these electrons will settle into the medium and that while passing in the middle, leading to the occurrence of ionization in the atoms or molecules that the mediumand the loss of energy by ( $dE/dX$ ) of any energy per unit length lossand which could lead to break ties and removing the hydrogen atoms from the totals (CH<sub>3</sub>, CH<sub>2</sub>, CH) and the formation of new chains , while retaining some of the original characteristics leads to change attributes based on polymeric chain length ( molecular weight ) due to the composition of (Cross-Linking) produces by complex combinations of these compositions is responsible for increasing the thermal conductivity of the composite materials with increasing duration of irradiation.And to discuss the thermal conductivity increased weight fraction in the case of consolidation ( Fe )particles and figure (4).

Notes from the previous figure increased thermal conductivity of samples of (Fe)increased weight fraction[18], that the reason for this is due to the heterogeneous distribution of theseparticles, and this in turn led to the parity in the number of electrons unit volume, which in turn led to the lack of difference in the density of points per sample and this in turn, led to the lack of variation of the values of the thermal conductivity of some samples per series coefficient in addition to the lack of the presence of gaps and pores in the samples and this in turn has led to increased stacking density as well as increased seam metal surfaces minutes. All these factors led to the increase of thermal conductivity coefficient of the samples increased fracture weighted.

### Dielectric Strength Test Results for (Fe) Samples before and after ( $\beta^-$ )Irradiation

From table (3), which shows the Dielectric Strength of the samples (Fe) particles natural state values (without irradiation ) and periods of irradiation (4,8,12) days and equivalent radiation dose (174.72Gy)and(349.44Gy) and (524.16Gy) respectively.And from Figure(5) . Results show that the highest value for the dielectric strength of a sample of (Fe) No.(1) of the weightfraction (2% Wt) was at the natural state (without irradiation ) which amounted to (11.481kV/mm) The lowest value appeared in the period of irradiation (12) day where the results showed that the value of the dielectric strengthwas (8.5kV/mm).But when analyzing the results of a sample of (Fe) No.(2) of the weightfraction (4% Wt) has been shown that the highest value dielectric strength was when the natural state (without irradiation ),reaching the value of the dielectric strength then to (11.2 kV/mm), while its minimum value It was at the period of irradiation(12) days and the value of the dielectric strength then(6.5kV /mm). But when analyzing the results of a sample of (Fe)No.(3) of the weighfraction(6% Wt) has been shown that the highest value was at the natural state(without irradiation) which amounted to(9.787kV/mm),while the lowest value was when the irradiation(12)days where the worth (7kV/mm).

As shown above, to us that the dielectric strength values of composite materials reinforced by (Fe) particles decreases with increasing periods of irradiation. From the above study this axis included the study of the dielectric





### Abd-Al sattarKhlilMaroof et al.

strength as a function to the time of irradiation and periods of different irradiation .The irradiation process led to a decrease in the dielectric strength and the reason is because the rays negative beta which are electrons high-energy words these electrons will lose energy in the medium,as a result of a series of collisions in the end will settle these electrons inside the medium and that while passing in the middle, leading to the occurrence of ionization in the atoms or molecules that the mediumand the loss of energy by  $dE/dX$  of any energy per unit length loss, which could lead to break the bonds or the forces that bind of composite materials, which are classified into two types:

#### a.Covalent Bond

It a vast majority in the polymers and be responsible for polymeric chains any atoms that connect the structural units with each link and these bonds broken by the high-energy beta particles , which in turn leads to generate free roots inside thecomposite materials leading to a decrease in the dielectric strength of these materials increase the period of irradiation.

#### b.Secondary forces

They are many kinds of molecules bind composite materials exist between parts per series and know the forces between the composite materials powers (VanderValls)effect on the physical properties of composite materials . This forces shattered by the high- energy beta particles , which in turn lead to a decrease in the strength of the dielectric strength.And to discuss the dielectrc strength to increase the weight fraction in the case reinforced by(Fe)particles and Figure (6).It showed results set forth in the preceding formats decreasing dielectric strength forsamples of (Fe) and all the cases and that the values of this decrease exponentially with the increase shows the weighted fracture when thecomposite materials reinforced by (Fe) particles . The reason for this is due to the strong linkage in the case of reinforced by (Fe) particles too big for that note with increased voltages article maintains composite materials reinforced by (Fe) particles on decreasing the strength of the insulation exponentially.

## CONCLUSION

After research and study on the composite materials samples prepared from epoxy resin reinforced by (Fe) was reached the following conclusions:

1-Hardness and thermal conductivity of the samples prepared in this research values increase with increasing weight fraction reaching the highest values of hardness and thermal conductivity for(Fe) particles at weight fraction (6% Wt). Also, the hardness and thermal conductivity of the samples prepared values in this research increases with increasing duration of irradiation particles beta negative ( $\beta^-$ ) or ( $e^-$ ), reaching the highest values of hardness and thermal conductivity of (Fe) particles when the irradiation (12) days that the reason for this is due to the cross-linking accidental molecules epoxy resin on the one hand and metal particles on the other shown in figure(7,8).2-The dielectric strength of the samples prepared in this research values decrease with increasing weight fraction reaching the highest values of the dielectric strength for(Fe)samples at weight fraction (2%), and that because of that those particles increased the electrical conductivity of the samples process by filling in the blanks and gaps formed during the preparation leading process to decrease the distances evidence samples prepared and thus lower the dielectric strength to those samples. While dielectric strength of samples prepared in this research values has been shown that it decreases with increasingperiod of irradiation by particles negative beta ( $\beta^-$ ) or ( $e^-$ ), reaching the highest values for dielectric strength for (Fe) particles when the natural state (without irradiation).

## REFERENCES

1. R.J. Crawford, (1987) " Plastics Engineering", 2nd Edition,Pergamon Press, New York.
2. HaiderSalimHussain (2011),"Investigation of Particles Distribution and Matrix types for  $\alpha$  and  $\beta$  Irradiated Lead PolymerComposites" Ph.D. Thesis , Collage of Science , University of Baghdad





**Abd-Al sattarKhlilMaroof et al.**

3. Kanal. K. Saraf ,(2011)."*Study on Effective Thermal Conductivity of Copper Particle Filled Polymer Composites*", Department of Mechanical Engineering, Rourkela, Roll No. 107ME008.
4. Turgay. Osman. Erol and Witold, (2013),"*X-Ray, Gamma, and Neutron Radiation Tests on Epoxy-Ferromagnetic Slag Composites by Experiments and Monte Carlo Simulations*", International Journal of Polymer Anal. Charact., 18: 224–231.
5. Abdul Hadi al- Kazim, ( 2015) , " *the study of the mechanical properties of the epoxy Iron* " Iraqi Journal of Physics , Vol. 13 , No. (26) , (p. 101-106) .
6. A.C. Gorge and Y.W Mai,(1988)."*Failure Mechanism in ToughenedEpoxy Resins-A-Review*", Composite Science and Technology,Vol.(31),No(3).
7. AL-AskareWurood Mahdi, "*Effect of Acidic Solution in Some Physical and Mechanical Properties for Epoxy Composites*"M. Sc.Thesis, University of Technology.
8. Al-Jubouri, Qusay (1998)" *the study of the mechanical properties of composite materials reinforced with wire metal*"M.Sc.Thesis, University of Technology.
9. S. M. Lee Editor, (1990), "*International Encyclopedia of Composite*", VCH publishers, Inc.
10. Al-AzzawiRaad Hussein, (2006)"*Effect of Gamma ray on physical properties(rheological , optical , electrical ) of a substance poly acrylic Amad dissolved in distilled water*",M.Sc.Mustansiriyah University.
11. J.Hearle , (1982),"*Polymer and their Properties*", vol. 1, John Wiley & Sons , INC., Canada , Limited.
12. Seqmour R. , and Bernd,E, (2001)."*Selecting and Applying Film Capacitors* ", Electronic News , Vol.47 , No.13 , pp.(3842).
13. Heinz,D. , and Bernd,E,(2001), "*Selecting and Applying Film Capacitors* " Electronic News , Vol.47 , No.13, pp.(38-42).
14. Segovia N. and Herrera R. (1980),"*Latent Track Annealing in Glass: A Comparison of thermal and Gamma Induced Annealing*", Proc. 10<sup>th</sup> Int. Conf. Solid State Nuclear Track Detectors, Lyon and Suppl. 2, Nucl. Tracks Pergamon, Oxford, (191-198).
15. Malclom B. Stevens.( 1984) "*Chemistry polymerization* " , translation Qais Abdel- Karim Ibrahim , KazemGayas al-Lami Basra University , College of Science , pp : ( 59-474 ).
16. Hamid Ibrahim Abboud, (1992)" *Study of the thermal properties of the polymer poly acrylic acid and the effects of neutrons on it*" M.Sc. Thesis, University of Basra.
17. Al-Dahshan Mohammed Izz al-Din,(2002)"*Introduction to material science and engineering*" Part(2), King Saud University.
18. Al-RawiKhaledRashad. Noor Hussain,(2015)"*Study of mechanical and thermal properties of epoxy overlay -kravaat* " Baghdad Journal of Science , Vol. (12) , No. (1).

**Table(1) Represent the hardness values of (Fe) samples before and after irradiation**

No.	Sample	Hardness $\frac{N}{mm^2}$			
		Normal Condition	Irradiation Time (day=43.68Gy)		
			0	4	8
1	Fe(2gm) + Ep(98gm)	65.666	74.333	77.5	78.83
2	Fe(4gm) + Ep(96gm)	72	74.333	78.3	78.5
3	Fe(6gm)+ Ep(94gm)	72.666	78	80	81





**Abd-Al sattarKhlilMaroof et al.**

**Table (2) Represent the thermal conductivity values of (Fe) samples before and after radiation**

S.No.	Sample	Thermal Conductivity ( w/m.k <sup>o</sup> )			
		Normal Condition	Irradiation Time (day=43.68Gy)		
		0	4	8	12
1	Fe <sub>(2gm)</sub> + Ep <sub>(98gm)</sub>	0.206491	0.276034	0.294830	0.309978
2	Fe <sub>(4gm)</sub> + Ep <sub>(96gm)</sub>	0.266034	0.353224	0.374071	0.386819
3	Fe <sub>(6gm)</sub> + Ep <sub>(94gm)</sub>	0.286285	0.376971	0.393224	0.404898

**Table (3) Represent the Dielectric Strength values of (Fe) samples before and after irradiation**

S.No.	Sample	Dielectric Strength kV/mm			
		Normal Condition	Irradiation Time (day=43.68Gy)		
		0	4	8	12
1	Fe <sub>(2gm)</sub> + Ep <sub>(98gm)</sub>	11.481	9.68	9.11	8.5
2	Fe <sub>(4gm)</sub> + Ep <sub>(96gm)</sub>	11.2	9.493	8.52	6.5
3	Fe <sub>(6gm)</sub> + Ep <sub>(94gm)</sub>	9.787	8.219	7.2	7

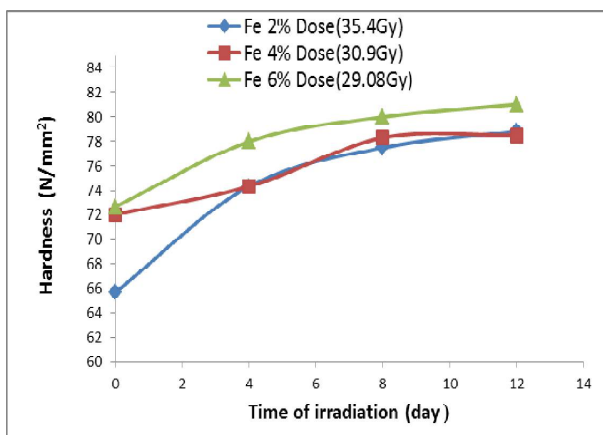


**Figure (1) Represents a Shore hardness of (Fe) samples as a function of the time of irradiation**

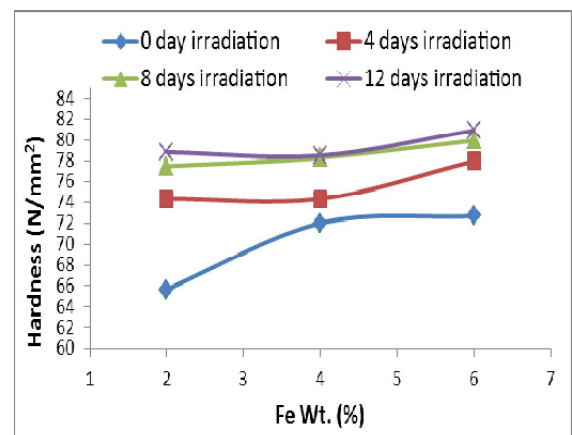


**Figure (2) Represents a Shore hardness of (Fe) samples as a function of the weight fraction**





**Abd-Al sattarKhlilMaroof et al.**

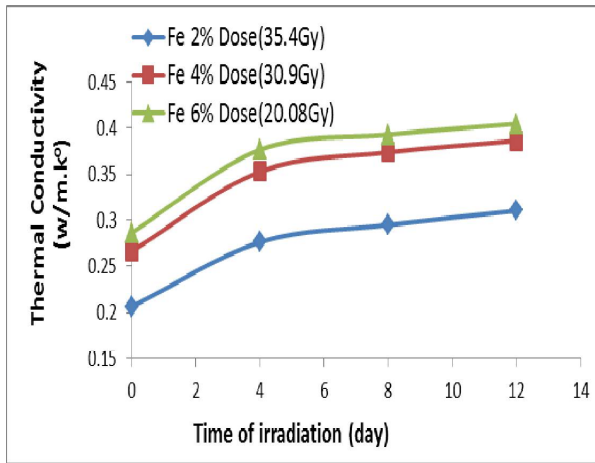


Figure (3) Represents thermal conductivity of (Fe) samples as a function of the time of irradiation

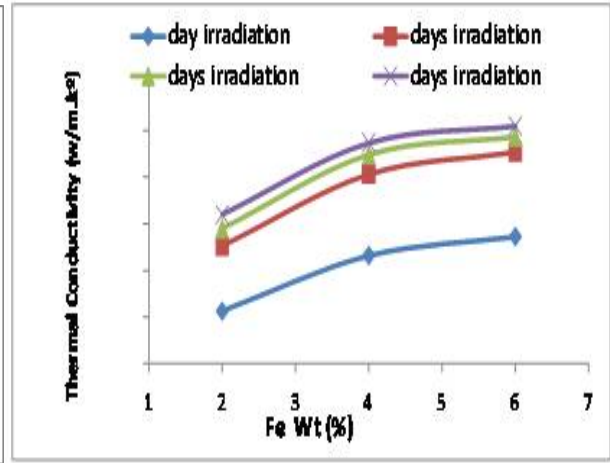


Figure (4) Represents a thermal conductivity of (Fe) samples as a function of the weight fraction

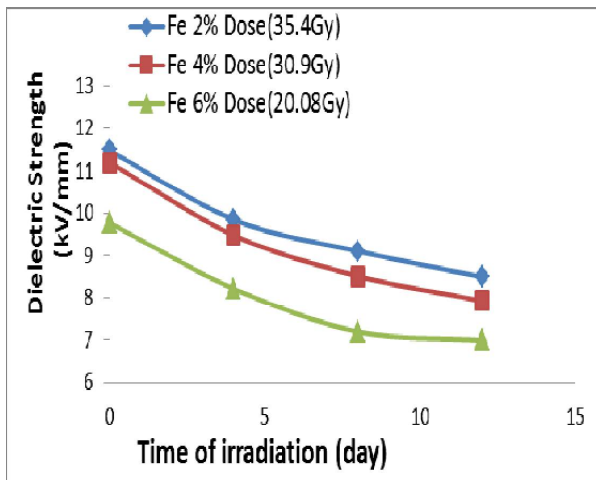


Figure (5) Represents Dielectric Strength of (Fe) samples as a function of the time of irradiation

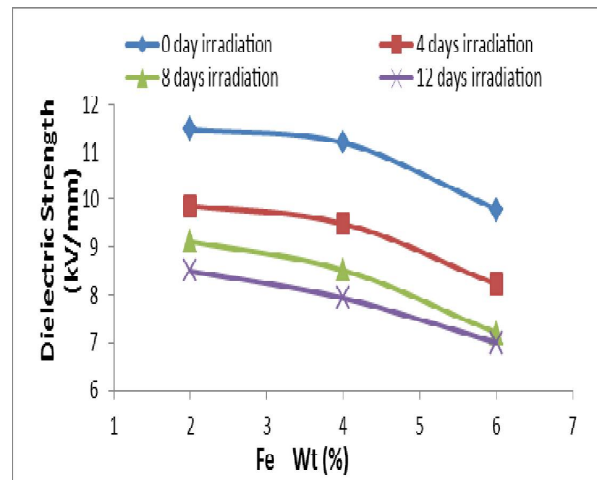


Figure (6) Represents a Dielectric Strength of (Fe) samples as a function of the weight fraction





Abd-Al sattarKhlilMaroof et al.



Figure(7) Represents Hardness test of(Fe) samples (2%, 4%, 6%) Wt



Figure(8) Represents Thermal Conductivity test of (Fe) samples (2%, 4%, 6%) Wt





## The Levels of Some Trace Elements and Correlations between them in Non-Insulin Dependent Diabetes Mellitus

Mohammed A.Hami<sup>1\*</sup>, Musher I. Salih<sup>2</sup> and Aveen A. Ibrahim<sup>1</sup>

<sup>1</sup>Dept. of Chemistry, Faculty of Science, University of Zakho, Duhok, Kurdistan region, Iraq.

<sup>2</sup>Dept. of Chemistry, Faculty of Science, University of Koya, Erbil, Kurdistan region, Iraq.

Received: 19 July 2016

Revised: 18 Aug 2016

Accepted: 9 Sep 2016

### Address for correspondence

Mohammed A. Hami

Assistant Lecturer,

Department of Chemistry, University of Zakho,

International Rd, Zakho, Duhok City, Kurdistan Region, Iraq

E. mail: mohammed.hami@uoz.edu.krd



This is an Open Access Journal / article distributed under the terms of the **Creative Commons Attribution License (CC BY-NC-ND 3.0)** which permits unrestricted use, distribution, and reproduction in any medium, provided the original work is properly cited. All rights reserved.

### ABSTRACT

Trace elements are known to play vital roles in both metabolism and growth of living cells. The aims of this study are to investigate the levels of some trace elements (copper, iron, nickel and zinc) in diabetic patients and studying the correlation between them. 50 healthy volunteers and 200 diabetic subjects were included in the study. Trace elements were measured via flame atomic absorption spectroscopy (Perkin Elmer). In addition, fasting blood sugar, serum urea and serum creatinine were measured via glucose oxidase, urease method and Jaffe method respectively. Except serum copper, all the three other trace elements were significantly lower in diabetic groups. Age and gender did not have any relationships with the levels of trace elements. All the trace elements did not correlate with each other apart from copper with both iron and nickel. These results do not confirm that low levels of trace elements causes diabetes mellitus. Further studies are needed to show the relationships.

**Keywords:** Diabetes mellitus, Trace elements, copper, iron, nickel, zinc, interactions of trace elements.

### INTRODUCTION

Type 2 Diabetes mellitus (DM) is a worldwide health problem that is caused by both genetics and environmental factors. One of the factors that is believed to cause type 2 DM is altered levels of trace elements [1]. Trace elements are present in all intact tissues and they perform vital functions in metabolism and growth in human body [2].





**Mohammed A. Hami et al.**

In human and animal experiments, trace elements have shown to be contributed in the release, storage and resistance of insulin [3]. Copper (Cu) for example, affect the reactivity and stability of many enzymes via conjugation [4]. Of these enzymes, Zn(II)-dependent superoxide dismutase, cytochrome C oxidase and others that are involved in the pathogenesis of diabetes complications [5].

In addition, Iron, which is one of the most abundant trace elements, is capable of generating reactive oxygen species. These species may affect insulin receptor resulting development of DM [6, 7]. Another trace element is nickel (Ni), whose seven neighbor elements in the periodic table are vital. This indicates that it might also be vital physiologically [2]. People can be readily exposed to nickel because of its wide distribution in the environment and its heavy use in the production of alloys, nickel-cadmium batteries, electroplating etc. [8]. Furthermore, Zinc (Zn) is believed to have an essential role in type 2 DM because of its contribution in the stimulation of the activity of insulin receptor tyrosine kinase [9]. Zn and Cu has shown to inhibit the absorption of each other [10]. This shows that it is of great important to study the interactions of various trace elements. The aims of this research study are, (1) to study the level of copper, iron, nickel and zinc in type 2 DM (2) to study the interaction of these trace elements with each other.

## MATERIALS AND METHODS

### Collection of samples

This research was conducted on 200 type 2 diabetic patients and 50 healthy volunteers, after informed written consent. All the type 2 diabetic individuals were taken from Duhok Diabetic Center in June 2015. Diagnosis of diabetes was based on the guidelines of American Diabetic Association  $\geq 126$  mg/dl (7.0 mmol/l) [11]. The recruited individuals were aged > 30 years and were from both genders. Patients who are in the following drugs; multi-vitamins, multi-minerals, diuretics, antihypertensive, or thyroid hormones, for the last three months were excluded from the study. 3-5 mL of blood was collected from peripheral venous of each subject and collected in gel tube. Afterwards, the blood was centrifuged at 3000 rpm for 10 minutes at 25 °C and stored at -20 °C until the day of analysis.

### Analysis of samples

The measurements of the trace elements were carried out after diluting the serum five-fold with de-ionized water, whereas lipemic serums were diluted ten-fold. Standard solutions of the trace elements were prepared by stepwise dilution of the stock solution Flame atomic absorption spectrometry (Perkin Elmer) was used for the determination of the levels of trace elements. For each subject the following tests were performed; fasting blood sugar via glucose oxidase method, serum urea by urease method, serum creatinine by Jaffe method.

### Statistical analysis

Date was analysed using GraphPad prism 5 and explained in the form mean  $\pm$  standard deviation. An unpaired student t- test was performed to compare the mean values between two groups. For comparing more than two groups one-way ANOVA was used. The Pearson's correlation tests were used for determining the relationships between the parameters. A probability value (p-value) of less than 0.05 was considered significance.

## RESULTS AND DISCUSSION

This research included 200 diabetic patients with type 2 and 50 healthy controls both groups were matched for age and gender. Table 1 shows the general characteristics of both groups. The mean age of diabetic groups was slightly higher than those of healthy groups ( $53.38 \pm 9.42$  vs.  $49.64 \pm 7.15$ ) (p-value > 0.05). The proportion of male was quite similar to female in both groups. There was no significant difference in the mean body mass index (BMI) for both groups (p-value > 0.05). The duration of diabetes for about half of the diabetic population was < 5 years and 30% of them 6-10 years and 18% more than 10 years.



**Mohammed A. Hami et al.**

Fasting blood sugar (FBS), serum urea and serum creatinine were assessed in both groups. There were significant statistical difference in the levels of FBS and serum urea and there was not for serum creatinine (Table 2). Table 3 among the four trace elements that were measured, all of them had significant statistical difference between the healthy and diabetic groups except serum copper. It is important to note that serum zinc had a highly significant difference. In terms of the relationships between the level of trace elements and the duration of diabetes and age, there were not any significant differences. Regarding the correlations between the trace elements, only serum Cu-Fe and Cu-Ni had strong positive correlation with each other (Table 4).

Trace elements are vital micronutrients that carry out vital functions in the living beings [12]. The purpose of this research paper is to evaluate the levels of copper, iron, nickel and zinc and the interactions between them in type 2. The most significant results on this research paper is that serum iron, nickel and zinc have lower levels in the diabetic group than healthy group ( $p$ -value  $< 0.05$ ) and copper is positively correlated with iron and nickel ( $p$ -value  $< 0.05$ ). All the researches that have been done on the levels of trace elements in DM have had various results. This might be due to the sampling methods, ethnicity, diets etc. The most diverse results in publications were for serum iron in which sometimes was higher in the healthy group and sometimes lower. In this research serum iron was significantly lower in the diabetic group than the healthy group. This is comparable to a study by Chen et al. (2012) [13]. However, in another study the levels of serum iron was significantly higher in diabetic patients [14] and in other did not show any statistical difference [15]. Our results indicate that prolonged DM might lead to anemia because of iron deficiency. This can be proved by studying the prevalence of anemia in elderly diabetic patients.

Figure 1. Like serum iron, there are contradictions in the levels of serum nickel in publications. In the present study, the level of serum nickel was significantly lower in the diabetic group. However, in a study by Aguilar et al. (2007) the level of nickel was higher in the diabetic groups. The most significant difference in the levels of trace elements in the two groups was for serum zinc ( $p$ -value  $< 0.001$ ). The lower levels of serum iron, serum nickel and serum zinc might be caused by the low intake, higher excretion via kidney. The low levels of these trace elements might cause DM or conversely, DM might be the consequences of low intake of trace elements or defect in their absorption. More researches are required to show whether DM decreases the levels of some trace elements or DM is the consequence of low levels of trace elements. This can be done by studying the levels of trace elements in pre-diabetic subjects. If in these subjects the levels of trace elements are not different from healthy control this shows that DM causes decrease in the levels of trace elements. However, if in these subjects the levels of trace elements are low, this might show that low levels of trace elements causes DM. Regarding serum Cu, in general serum Cu was higher in diabetic patients, however, it did not reach statistical significance ( $p$ -value  $> 0.05$ ).

There were not any relationships between duration of diabetes and gender with the concentrations of trace elements. Not having a relationship between trace elements and DM may indicate that DM has low effect on the lowering the levels of trace elements and it is the low levels of trace elements that cause DM. There were strong positive correlations between serum Cu with both serum iron and nickel. This indicates that these trace elements might have fairly similar functions in DM or they might participate in a similar pathway.

**CONCLUSION**

In conclusion, there are strong relationships between DM and trace elements. But further evidence are required to prove whether DM causes low levels of trace elements or low levels of trace elements cause DM. To study this for the future, research can be performed on pre-diabetic subjects and compare them with healthy control and diabetic patients.





**Mohammed A. Hami et al.**

## REFERENCES

- Zargar, A.H., et al., *Copper, zinc, and magnesium levels in non-insulin dependent diabetes mellitus*. Postgraduate medical journal, 1998. 74(877): p. 665-668.
- Reinhold, J.G., *Trace elements—a selective survey*. Clinical chemistry, 1975. 21(4): p. 476-500.
- Ekin, S., et al., *Serum sialic acid levels and selected mineral status in patients with type 2 diabetes mellitus*. Biological trace element research, 2003. 94(3): p. 193-201.
- Lin, J., *Pathophysiology of cataracts: copper ion and peroxidation in diabetics*. Japanese journal of ophthalmology, 1997. 41(3): p. 130-137.
- Khan, F.A., et al., *Comparative Study of Serum Copper, Iron, Magnesium, and Zinc in Type 2 Diabetes-Associated Proteinuria*. Biol Trace Elem Res, 2015. 168(2): p. 321-9.
- Kazi, T.G., et al., *Copper, chromium, manganese, iron, nickel, and zinc levels in biological samples of diabetes mellitus patients*. Biological trace element research, 2008. 122(1): p. 1-18.
- Aydin, E., et al., *Levels of iron, zinc, and copper in aqueous humor, lens, and serum in nondiabetic and diabetic patients*. Biological trace element research, 2005. 108(1-3): p. 33-41.
- Gang, L., et al., *Nickel exposure is associated with the prevalence of type 2 diabetes in Chinese adults*. International Journal of Epidemiology, 2014. 0(1): p. 1-9.
- Tascilar, M.E., et al., *Trace elements in obese Turkish children*. Biological trace element research, 2011. 143(1): p. 188-195.
- Thomson, A., L. Valberg, and D. Sinclair, *Competitive nature of the intestinal transport mechanism for cobalt and iron in the rat*. Journal of Clinical Investigation, 1971. 50(11): p. 2384.
- Association, A.D., *Diagnosis and classification of diabetes mellitus*. Diabetes care, 2012. 35(Supplement 1): p. S64-S71.
- Zargar, A.H., et al., *Copper, zinc and magnesium levels in type-1 diabetes mellitus*. Saudi medical journal, 2002. 23(5): p. 539-542.
- Chen, H. and C. Tan, *Prediction of type-2 diabetes based on several element levels in blood and chemometrics*. Biological trace element research, 2012. 147(1-3): p. 67-74.
- Lal, M., et al., *Influence of modified levels of plasma Magnesium, Cu, Zn and Iron levels on Thiols and protein status in diabetes mellitus and diabetic retinopathy*. International Journal of Analytical, Pharmaceutical and Biomedical Sciences, 2013. 2(1): p. 67-72.
- Forte, G., et al., *Blood metals concentration in type 1 and type 2 diabetics*. Biological trace element research, 2013. 156(1-3): p. 79-90.

**Table 1: General characteristics of the patients and the healthy control groups.**

Parameter	Non-diabetic (n=50)	Diabetic (n=200)	p-value
Mean age	49.64 ± 7.15	53.38 ± 9.42	> 0.05
Gender			
• Male	24 (48%)	94 (47%)	
• Female	26 (52%)	106 (53%)	
Mean BMI	28.32 ± 4.80	34.02 ± 6.59	> 0.05
Duration of diabetes			
• <5 years	Nil	104 (52%)	
• 6-10 year	Nil	60 (30%)	
• >10 years	Nil	36 (18%)	
Data are expressed as mean ± standard deviation			





**Mohammed A. Hami et al.**

**Table 2: The mean values of serum FBS (mg/dl), serum urea (mg/dl), creatinine (mg/dl).**

Parameter	Healthy control (n=50)	Diabetic (n=200)	p-value
Mean FBS	97.5 ± 18.2	213.7 ± 98.4	< 0.0001
Mean serum urea	30.48 ± 9.65	36.88 ± 13.79	0.0414
Mean creatinine	0.72 ± 0.22	0.89 ± 1.84	> 0.05
Data are expressed as mean ± standard deviation.			

**Table 3: Association of Cu, Fe, Ni and Zn with duration of diabetes and age. Results are expressed as mean ± standard deviation.**

Parameter	Cu	Fe	Ni	Zn
<b>Duration of diabetes</b>				
<5 years	1.802± 0.447	1.808 ± 0.606	0.426 ± 0.169	0.760 ± 0.3564
6-10 years	1.730 ± 0.363	1.725 ± 0.512	0.466 ± 0.193	0.810 ± 0.3243
>10 years	1.778 ± 0.389	1.892 ± 0.552	0.457 ± 0.190	0.716 ± 0.3625
P-value	0.873 ±	0.776	0.785	0.802
<b>Age</b>				
< or = 50 years	1.73 ± 0.073	1.73 ± 0.095	0.391 ± 0.038	0.753 ± 0.076
> 50 years	1.79 ± 0.082	1.87 ± 0.115	0.456 ± 0.035	0.773 ± 0.061
p-value	0.635	0.383	0.228	0.843
Data are expressed as mean ± standard deviation.				

**Table 4: A table showing the correlations of trace elements with each other.**

Parameters	Pearson's correlation ( r )	p-value
Cu-Fe	0.3663	0.0089
Cu-Ni	0.4879	0.0003
Cu-Zn	-0.04200	0.7721
Fe-Ni	0.1955	0.1736
Fe-Zn	-0.05738	0.6922
Ni-Zn	0.03136	0.8288





Mohammed A. Hami et al.

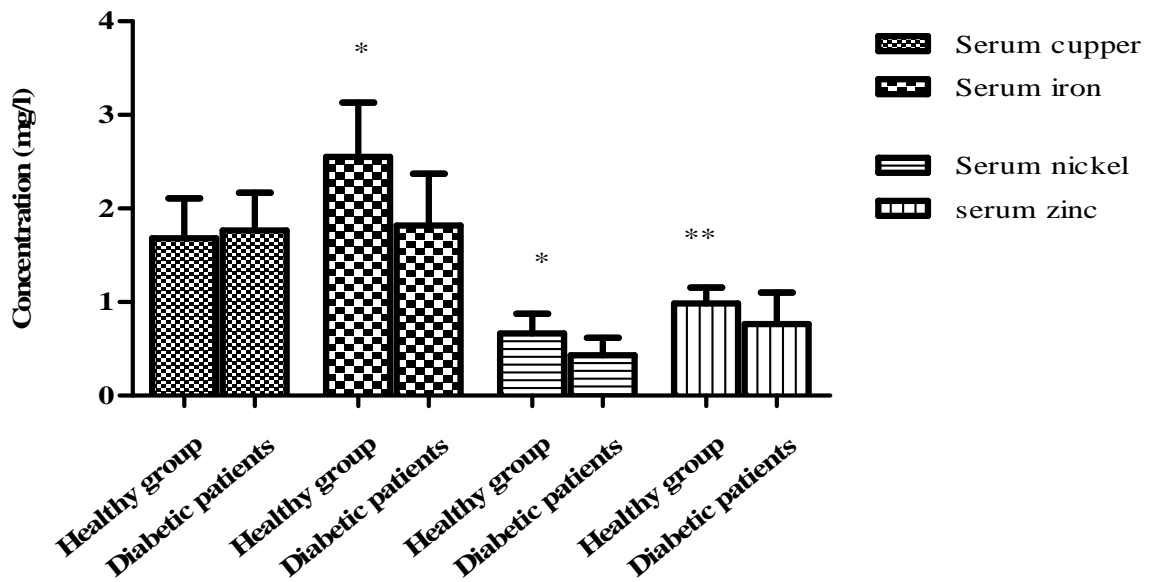


Figure 1: Figure showing the levels of trace elements in mg/L for healthy and diabetic groups. The p-value was as follow: Serum copper 0.4206, serum iron .0020, serum nickel < 0.0001, serum zinc 0.0030

\*Indicates that there is a significant difference between the two groups.

\*\*Indicates that there is a highly significant difference between the two groups (<0.0001).





## RESEARCH ARTICLE

## Techno-Economic Evaluation of Solar Tunnel Dryer

S.R.Kalbande, V.P.Khambalkar\* and Sneha Deshmukh

Department of Unconventional Energy Sources and Electrical Engineering, Dr. Panjabrao Deshmukh Krishi Vidyapeeth, Akola, Maharashtra, India.

Received: 21 June 2016

Revised: 19 July 2016

Accepted: 25 Aug 2016

### Address for correspondence

V.P.Khambalkar

Department of Unconventional Energy Sources and Electrical Engineering,

Dr. Panjabrao Deshmukh Krishi Vidyapeeth,

Akola, Maharashtra, India.

Email: vivek\_khambalkar@hotmail.com



This is an Open Access Journal / article distributed under the terms of the **Creative Commons Attribution License (CC BY-NC-ND 3.0)** which permits unrestricted use, distribution, and reproduction in any medium, provided the original work is properly cited. All rights reserved.

### ABSTRACT

Solar drying of any product is the most feasible drying method, due to retention quality of the product after drying and saving in drying time. Keeping in view these facts a study entitled, "Techno economic performance evaluation of solar tunnel dryer" was undertaken. The drying time, drying temperature in dryer, solar intensity, moisture content of the product, ambient temperature, and relative humidity were measured. The results showed that, temperature inside the solar tunnel dryer boosted up by 15-20° C more than the ambient. The overall drying efficiency of Ginger slices and Spinach leaves were found to be 39.62 per cent and 33.48 per cent, respectively. The benefit-cost ratio, net present worth and payback period for drying of Ginger slices was found to be 1.39, 1379282.13 Rs, and 3 months and 5 days, respectively. The system was found economical for drying of Ginger slices and thus the dryer can be integrated in rural system in the present energy context.

**Keywords :** solar tunnel dryer, drying efficiency, drying rate, moisture ratio

### INTRODUCTION

Drying is the most common and fundamental method for post-harvest preservation of agricultural produce because it is a simple method for the quick conservation of the agricultural produce of the plant material [1]. Ginger (*Zingiberofficinale*) is an herb in plant habit. Fresh ginger root is usually consumed as spice in the tropical countries and dried ginger is used as medicinal plant internationally. Dried ginger is produced from the mature rhizome. As the rhizome matures, the flavour and aroma become much stronger. Dried ginger can be ground and used directly as a spice or in medicinal use and also for the extraction of ginger oil and ginger oleoresin.





### Khambalkar et al.

Spinach (*Spinacia oleracea* L.) is a flowering plant in the family Amaranthacea, native to central and south western Asia. It is an important leafy vegetable, now grown throughout the temperate regions of the world. It is a rich source of iron, magnesium and potassium, and extraordinarily high in vitamins C, A, E, B6 and thiamine (Wikipedia Encyclopedia 2007). Spinach is widely used in making various foods like puree, soups and baked products [2]. Drying is one of the preservation methods that have the capability of extending the consumption period of spinach [3]. This method brings about substantial reduction in weight and volume, minimizing packaging, storage and transportation costs, and enables storability of the product under ambient temperatures [4]. The removal of moisture prevents the growth of the micro-organisms responsible for the spoilage of the foods. This can be achieved by drying or dehydration for removal of water (responsible for many deteriorative) form a product.

## MATERIALS AND METHODS

The experimentation was carried out on solar tunnel dryer installed under All India Coordinated Research Project on Energy in Agriculture and Agro based Industries, Dr. P.D.K.V., Akola installed at Chalisgaon, Varahi Agrotech, Dist-Jalgaon. Fresh Ginger and Spinach leaves were procured and used for the experimentation. The drying experiment was conducted at no load and full load condition in the solar tunnel dryer. The samples were prepared in order to undertake study of drying behavior of Ginger slices and Spinach leaves. The Ginger slices and Spinach leaves were dried in solar tunnel dryer and open sun drying having different sample codes as given in table 1. technical specification of solar tunnel dryer given in table 2.

### Performance evaluation of solar tunnel dryer

The performance of the solar tunnel dryer was evaluated for drying of ginger slices and Spinach leaves. The performance of the system was evaluated by conducting no load and full load test. The solar tunnel dryer used in experiment fig.1.

### Study of drying characteristics

The drying mechanism depends on simultaneous heat and mass transfer phenomenon and factors dominating each process determined the drying behaviour of the product. The drying rates were computed from the experimental data and drying characteristics curves i.e. moisture ratio (db) vs. time, drying rate vs. time and moisture content (db) were plotted.

### Determination of moisture content

Initial moisture content of sample was determined by the hot air oven drying method as recommended by [5]. Samples were weighed using electronic weighing balance of least count 0.01g. The Spinach leaves sample were placed in hot air oven at  $70 \pm 0.5^\circ\text{C}$  for 12.00 h and Ginger slices at  $105 \pm 0.5^\circ\text{C}$  for 24:00 h. Following formulae were used

$$M.C.(wb)\% = \frac{(W_1 - W_2)}{(W_1)} \times 100$$

$$M.C.(db)\% = \frac{(W_1 - W_2)}{(W_2)} \times 100$$

Where,

$W_1$  = Weight of sample before drying, g

$W_2$  = Weight of bone dried sample, g

### Determination of moisture ratio

The Moisture ratio of the produce was computed by following formula [6].





**Khambalkar et al.**

$$\text{Moisture Ratio (M.R.)} = \frac{(M - M_e)}{(M_0 - M_e)}$$

Where,

- M = Moisture content (db), per cent
- M<sub>e</sub> = EMC, (db), per cent
- M<sub>0</sub> = Initial MC, (db), per cent

**Determination of drying rate**

The drying rate of produce sample during drying period was determined as follows [6].

$$\text{Drying rate (D}_R\text{)} = \frac{\Delta W}{\Delta t}$$

Where,

- ΔW = Weight loss in one h interval (gm/100gm bdm min.)
- Δt = Difference in time reading (h)

**Economic analysis of the system**

The assumptions/considerations were taken for carrying out economic analysis of solar tunnel drying system. The area of the solar tunnel dryer was 18.0 m<sup>2</sup>. The capacity of the solar tunnel dryer for Spinach leaves and Ginger slices was, 40 and 100 kg batch<sup>-1</sup> respectively. The dryer produce 9 and 20Kg dried product of Spinach leaves and Ginger slices per batch respectively. The initial cost of Spinach leaves and Ginger slices Rs 20, and 80 per kg, respectively. Discounting rate was assumed to be 10 per cent as compared to bank lending rate of interest. Cost of dried product of Ginger slices and Spinach leaves were Rs. 600, and 150 Kg respectively. The annual repair and maintenance cost was Rs. 10,000 considering replacement of UV sheet after 3 years and an expenditure towards painting minor repair etc[7].

The Economic indicators were determined to access the economic viability of the system.

- 1) Net present worth (NPW)
- 2) Benefit cost ratio (B/C ratio)
- 3) Payback period

**Net present worth (NPW)**

The difference between the present value of all returns and the present money require for making an investment is the net present worth. The present value of the future returns was calculated through the use of discounting. Discounting is a technique by which future benefits and cost streams can be converted to their present worth.

$$NPW = \sum_{t=1}^{t=n} \frac{B_t - C_t}{(1+i)^t}$$

Where,

- C<sub>t</sub> = Cost in each year
- B<sub>t</sub> = Benefit in each year
- t = 1, 2, 3.....n
- i = discount rate

**Benefit cost ratio**

This is the ratio obtained when the present worth of the benefit stream is divided by the present worth of the cost stream. The mathematical benefit-cost ratio can be expressed as







**Khambalkar et al.**

$$\text{Benefit-cost ratio} = \frac{\sum_{t=1}^{t=n} \frac{B_t}{(1+i)^t}}{\sum_{t=1}^{t=n} \frac{C_t}{(1+i)^t}}$$

Where,

- C<sub>t</sub> = Cost in each year
- B<sub>t</sub> = Benefit in each year
- t = 1, 2, 3.....n (year)
- i = discount rate

**Payback period**

The payback period is the length of time from the beginning of the project until the net value of the incremental production stream reaches the total amount of the capital investment. The payback period of the project is estimated by using the straight forward formula

$$P = \frac{I}{E}$$

Where,

- P = Payback period of the project in years,
- I = Investment of the project in Rs.
- E = Annual net cash revenue in Rs.

**RESULTS AND DISCUSSION**

The variation of temperature, relative humidity of different locations inside the solar tunnel dryer with corresponding ambient temperature, relative humidity and solar insolation were recorded to evaluate the performance of solar tunnel dryer at no load condition during winter season [8].

**Full load testing of solar tunnel dryer**

The samples of the Ginger slices and spinach leaves were loaded in thin layer on trays over racks in the solar tunnel dryer. The drying of these samples was continued till the moisture content reached to EMC of the selected products on db. The drying experiments were carried out in winter season in the month of December. The results obtained from drying experiments of Ginger slices and spinach leaves, in solar tunnel dryer are compared with open sun drying are summarized as follows.

**Drying characteristics of Ginger slices and spinach leaves in open sun drying and solar tunnel dryer**

The drying characteristics of Ginger slices and Spinach leaves samples in natural convection solar tunnel dryer were studied and compared with open sun drying. The different drying characteristics in terms of moisture content per cent (db) drying rate (gm /100 gm bdm min) and moisture ratio were studied.

**Drying of Ginger slices in STD and OSD**

Fig.2 and Fig.3 revealed that the drying rate varied from 4.215 to 0.022 and 1.85 to 0.009gm/100gm bdm min for drying of Ginger slices in solar tunnel dryer and open sun drying, respectively. The average drying rate was found to be 0.382 and 0.192gm/100gm bdm min corresponding to average moisture ratio of 0.350877 and 0.311 for STD and OSD, respectively.



**Khambalkar et al.****Drying of Spinach leaves in STD and OSD**

Fig. 4 and Fig. 5 revealed that the drying rate varied from 8.715 to 0.01128gm/100gm bdm min and 6.46 to 0.01gm/100gm bdm min for drying of spinach in solar tunnel dryer and open sun drying, respectively. The average drying rate was found to be 1.068 and 0.47gm/100gm bdm min corresponding to average moisture ratio of 0.238 and 0.27 for STD and OSD, respectively.

**Overall efficiency of solar tunnel dryer**

Overall efficiency of solar tunnel dryer based on experimental data was calculated by considering the total moisture evaporated associated with heat input and heat gain by product [9]. The results obtained from overall efficiency of Ginger slices and spinach leaves dried in solar tunnel dryer is depicted in Table 3.

The economic feasibility of the solar tunnel dryer for the drying of above sample was calculated by considering the initial investment of the dryer, average repair and maintenance cost, cost of raw material and selling price of the material after drying.

**Net present worth-** Net present worth for whole Ginger Slices is presented in Table 4. The net present worth of total cash inflow and outflow for drying of Ginger Slices under solar tunnel dryer was found to be Rs.1379282.13. Based on the NPW it could be concluded that the drying of Ginger Slices in STD is an economical and there is substantial increase in the income of the above products processing.

**Benefit cost ratio-** The BC ratio of the system was calculated by dividing present worth of benefit stream and present worth of cost stream. Table 4 revealed benefits cost ratio of Ginger Slices in STD and found to be 1.39. Thus, it is concluded that investment is justified and drying of Ginger Slices in solar tunnel dryer is economically viable.

**Payback period** - Payback period for drying of Ginger Slices in solar tunnel dryer was found to be 3 month and 5 days for recovery of the initial investment of solar tunnel dryer Thus, it could be concluded that the drying of above products seems to be economical in solar tunnel dryer because solar energy is freely available throughout the year thus no additional expenditure was incurred for air heating.

**CONCLUSION**

Performance of the system was evaluated at no load and full load test by drying the Ginger slices and Spinach leaves. The quantity of the product loaded, moisture content of the product at initial and during drying period was measured. At no load test, the avg. temperature and relative humidity during daytime in the STD was 44.5°C and 15.22 per cent and in OSD was 36.23 °C and 21.44 per cent, respectively. In full load test avg. temperature and relative humidity during daytime in STD was 45.25° C and 22.44per cent in OSD was 30.91°C and 24 per cent in the month of December. Solar tunnel drying took 12h to bring down the moisture content of Ginger slices from 488.235 to 13.53 per cent (db) and 18 h under open sun drying. For Spinach leaves solar tunnel drying took 8 h to bring down the moisture content from 1050 to 13.33 per cent (db) and 13.5 h under open sun drying. The overall drying efficiency of Ginger slices and Spinach leaves were found to be 39.62 per cent and 33.48 per cent, respectively. The benefit-cost ratio, net present worth and payback period for drying of Ginger slices was found to be 1.39, 1379282.13 Rs, and 3 months and 5 days, respectively.

**REFERENCES**

1. Assefa, Ayyappan S. and Dr. K. Mayilsamy 2010. "Solar Tunnel Drier With Thermal Storage For Drying of Copra", Proceedings of the 37th National & 4th International Conference on Fluid Mechanics and Fluid Power, IIT Madras, Chennai, India.





### Khambalkar et al.

- Bala, B. K., Hussain, M. D. and Mondol (1999). "Experimental Investigation of Solar Tunnel Drier for Drying of Pineapple", Journal of the Institution of Engineers, Bangladesh, Agricultural Engineering Division, 26(4): 37-44.
- Rathore, N.S., N.L.Panwar, and B.Asnnani, 2012. Performance evaluation of solar tunnel dryer for grape drying. Int. J. Renew. Energy. Tech. 3(1.): 1–10.
- Palled, Vijaykumar, S. R. Desai, lokesh and M. Anantachar 2012. Performance evaluation of solar tunnel dryer for chilly drying Karnataka J. Agric. Sci, 25 (4): 472-474.
- Ranganna, S. 1986. Handbook of Analysis of Quality Control For Fruits and vegetable product, Chapter 1: 1-5. [6].
- Chakraverty, A. 1988. Post-harvest technology of cereals, pulses and oil Seed. New Dehli, Oxford and IBH Pub. Co. Pvt. Ltd., PP. 33-39.
- Panwar NL, Kaushik SC, Kothari S. Cost-benefit and systems analysis of passively ventilated solar greenhouses for food production in arid and semiarid regions. Environ Syst Decis DOI 10.1007/s10669–013-9438-5.
- Garg HP, Kumar R. Studies on semi-cylindrical solar tunnel dryers: year round collector performance. Int J Energy Res 1998;22: 1381–95.
- Intawee P, Janjai S. Performance evaluation of a large-scale polyethylene covered greenhouse solar dryer. Int Energy J 2011;12:39–52.

**Table 1. Sample codes used for different product**

S. No.	Different samples	Trays in Solar Tunnel Dryer			Open sun drying		
1	Ginger	IG1	IG2	IG3	OG1	OG2	OG3
2	Spinach leaves	IS1	IS2	IS3	OS1	OS 2	OS3

**Table 2. Technical specifications of solar tunnel dryer**

S. No.	Particulars	Specifications
1.	Aperture area, m <sup>2</sup>	24.25
2.	Width of dryer, m	3.00
3.	Length of dryer, m	6.00
4.	Drying tray area, m <sup>2</sup>	2.5 (1.6 m x 1.6 m)
5.	Number of trays	05 on each trolley
6.	Height of tunnel, m	2.0
7.	Plastic cover, UV stabilized	200 μm
8.	Chimney	2 Nos., Ø 0.15 m, H =0.75m
9.	Fresh air vent area, m <sup>2</sup>	0.05
10.	Exhaust Fan, single phase, 40 Wp, 1400 rpm	1Nos, Brushless AC
11.	Door	1.80 m x 0.75 m





**Khambalkar et al.**

**Table 3 Overall efficiency of solar tunnel dryer for Ginger slices and spinach leaves**

S. No.	Samples	Total drying time, (sec)	Avg. moisture removed,(kg)	Avg. Solar Radiation, (w/m <sup>2</sup> )	Efficiency, (%)
1	Ginger slices	43200	80.7	438.81	39.62
2	Spinach leaves	28800	90.93	438.81	33.48

**Table 4 Economic analysis of solar tunnel dryer for Ginger slices drying**

S. No.	Description	Ginger slices
1	Initial investment (Rs)	55000
2	Annual use no. of batches	60(100Kg)
3	Cost of raw material (Rs yr <sup>-1</sup> )	@80Kg 4,80,000
4	Cost of labour for drying (Rs yr <sup>-1</sup> )	20,000.00
5	Operation and maintenance cost (Rs yr <sup>-1</sup> )	3000.00
6	Total dried product (kg)	1200
7	Total cost of finished product	@ Rs 600/kg 720000.00
8	Net present worth, Rs	1379282.13
9	Benefit- cost ratio	1.39
10	Payback period	<b>3 month 5 days</b>



**Fig.1.Schematic view of solar tunnel dryer**





Khambalkar et al.

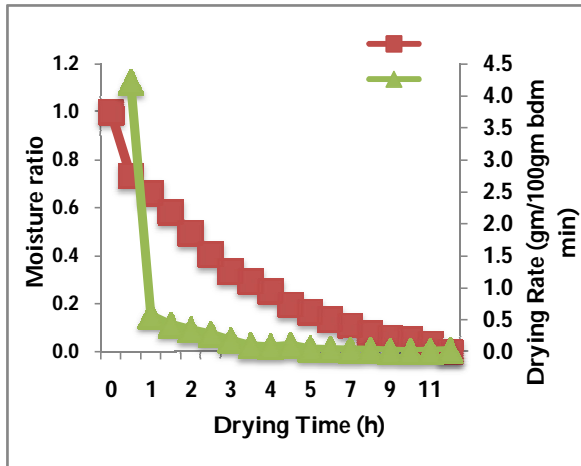


Fig. 2.Variation of moisture ratio & drying rate of Ginger slices in STD

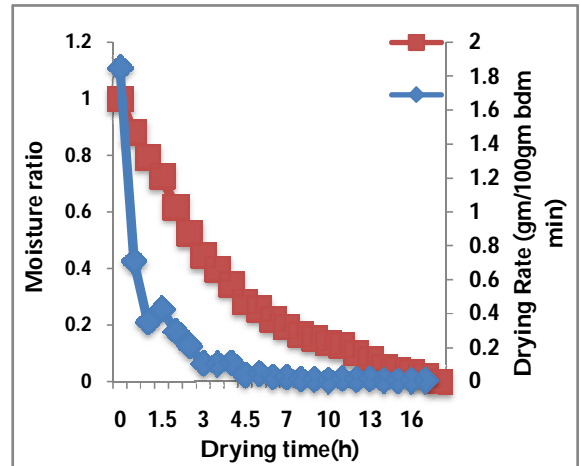


Fig. 3.Variation of moisture ratio & drying rate of Ginger slices in OSD

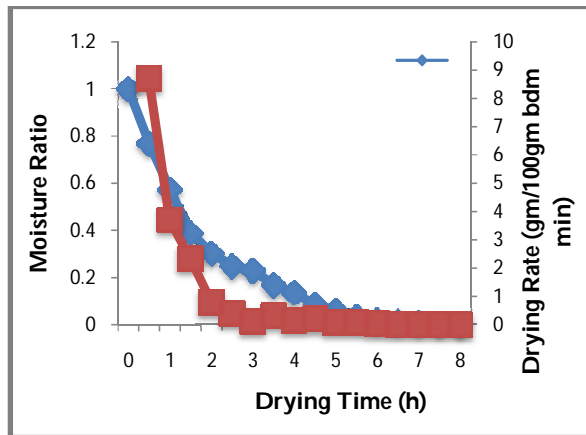


Fig. 4. Variation of moisture ratio & drying rate of Ginger slices in STD

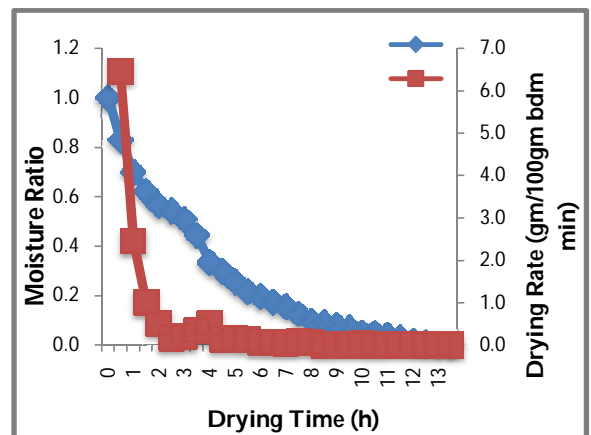


Fig. 5. Variation of moisture ratio & drying rate of Ginger slices in OSD





## Energy Conservation in Pulse Processing Industry: A Case Study

S. R.Kalbande, V.P.Khambalkar\* and Sneha Deshmukh

Department of Unconventional Energy Sources And Electrical Engineering, Dr. Panjabrao Deshmukh Krishi Vidyapeeth, Akola, Maharashtra, India.

Received: 8 June 2016

Revised: 16 July 2016

Accepted: 26 Aug 2016

### Address for correspondence

V.P.Khambalkar

Department of Unconventional Energy Sources and Electrical Engineering,

Dr. Panjabrao Deshmukh Krishi Vidyapeeth,

Akola, Maharashtra, India.

Email: vivek\_khambalkar@hotmail.com



This is an Open Access Journal / article distributed under the terms of the **Creative Commons Attribution License (CC BY-NC-ND 3.0)** which permits unrestricted use, distribution, and reproduction in any medium, provided the original work is properly cited. All rights reserved.

### ABSTRACT

Present investigation has carried out to assess the energy consumption pattern in the pulse processing industry. A survey has been carried out at M/s Radha Industries, MIDC, Akola. The pulse processing capacity of the industry is about 10 tones par day. The step wise energy consumption during the processing of the pulse for making the *dal* was worked out. The electrical energy consumption per day for the *dal* processing in a day was estimated and found to be 582 kWh which included the pre-processing operation, touching and the milling operation. The per kg of energy consumed in producing the *dal* was found to be 0.073 Kwh. The cost of energy per kg of *dal* produced was found to be Rs 0.80.

**Keywords :** Energy audit, Energy conservation, Pulse processing

### INTRODUCTION

India being the largest producer [18.5 million tons] and processor of pulses in the world also imports around 3.5 million tons annually on an average to meet its ever increasing consumption needs of around 22.0 million tons. Maharashtra is one of the major important states in growing pulses. The major pulses grown in the state are mung, urid, tur, chickpea etc. The area under major pulses i.e. mung, urid, tur and chickpea during the year 2009-10 in Maharashtra was around 12.50 lakh hectares and production was about 9.13 lakh tonnes with productivity of major pulses 730 kg/ha. However, Vidarbha contributes, 5.14 lakh hectares area under pulses and the production was about 5.43 metric tonnes with productivity of major pulses 997 kg/ha. As the production of pulses in Vidarbha region of Maharashtra state is increasing day by day, the Akola and Amravati districts of Vidarbha region are important according to pulse processing point of view. In India, pigeon pea is mostly consumed after dehulling in the form of





### Khambalkar et al.

dal (dehulled splits of pigeon pea). Pulse processing is an old practice. India produced 18.45 million tonnes of pulses in 2012-13 [1]. Pigeon pea (*Cajanas cajan*) is also known as Tur in Hindi. Production of pigeon pea to the tune 15.24 million tonnes is the 4/5th share in the world and 1/5th share in the total pulse production in the country. Maharashtra produces the maximum level of pigeon pea in India accounting to 700000 tons [2]. Dal is mostly consumed in the form of dehulled splits (dal) as it improves its appearance, texture, cooking quality, palatability and digestibility. Dehulling of pigeon pea involves two steps; pretreatment of grain for loosening the seed coat and its removal from the cotyledons. There are two approaches to remove hulls, namely wet and dry milling. Generally, the dry method of milling is used throughout the Indian subcontinent for milling of pigeon pea because the quality of splits obtained from wet milling is poor [3, 4].

Availability of power has a crucial rule in economic development of the country. In today's world energy is very precious India ranks fifth in the world in total energy. Energy conservation means reduction in energy consumption without making any sacrifice of quantity or quality. A successful energy management program begins with energy conservation; it will lead to adequate rating of equipment, using high efficiency equipment and change of habits which causes enormous wastages of energy [5].

## MATERIALS AND METHODS

### Study of locale

The operation-wise data of M/s Radha Dal/Pulse processing industry situated at MIDC, Phase III, Akola was collected and analysed. The information regarding the electric motors and other appliances has been collected during the visit. A stepwise approach has been followed in respect of energy consumption in pulse processing.

### About pulse processing industry

Processing is an important marketing function in the present day marketing of pulses. Processing converts the raw materials and brings the produce nearer to human consumption. It is concerned with value addition to the produce by changing its form. Pulses are generally converted into dal by splitting the whole seed. Hence survey of energy consumption in pulse processing industry was carried out which is situated in MIDC Akola. Capacity of processing plant is 10 tonnes /day. Details such as power consumption, various pulse processing machineries involved in processing are as given in table1.

### Assessment of energy consumption

The total energy consumption in various operations has been calculated based on the step-wise energy requirement during the process. The electrical energy consumption per day for the dal processing in a day is for the various operations which included the pre-processing operation, touching and the milling operation [6].

Energy consumption for unit operation (kWh) = Total power requirement (kW) × operation duration (h)

The annual energy consumption for the specific operation was determined by using the following relation,

Annual energy consumption = per day energy consumption (kWh) × annual working day

The total energy consumption for the whole processing of various unit operation of pulse for one day is estimated as below;

Total energy consumption (kWh)/day = Energy consumption in pre-cleaning + energy consumption in touching operation + energy consumption in main dal process operation

### Energy consumption in processed quantity of raw materials

The total energy consumption per tonne of processed raw materials has been worked out for the surveyed industry. The raw material based energy consumption is worked out by following formula; [7].





### Khambalkar et al.

Energy consumption = Total annual energy consumption in dal processing (kWh) / Total raw material processed (tonne)

#### Energy consumption per kg of dal produces

The per kg of energy consumed in producing the dal was determined on annual basis for the visited industry [8].

The details of the estimation procedure are given below;

Total dal produce during process = Total raw material process × recovery material

Total energy consumption (kWh per kg) = Total annual energy consumption (kWh) / Total raw

Material in kg Estimation of Cost of Energy:

The cost of energy for the pulse processing is evaluated based on the energy consumption and the quantity of dal produced annually. The details of the cost calculation of energy is given below;

Cost of energy per process kg of dal = Total energy consumption (kWh) × cost of energy per unit (INR) / Annual processed material (kg)

## RESULTS AND DISCUSSION

The energy consumption during the various unit operations in pulse processing was estimated. The step –wise energy consumption from pre-cleaning operation to the finished produce was evolved for determination of energy requirement to the total quantity of raw materials. The energy requirement for the per kg of the processed pulse were estimated. The cost of energy per kg of processed pulse was estimated. The estimated results obtained are presented below.

#### Pre-cleaning energy consumption

Pre-cleaning operation comprises of separation, destoning and grading of raw material used in milling operation. This operation is energy intensive and requires much energy for the pre-cleaning process. In this operation the data regarding electric motors has been collected and the total horse power requirement was found to be 20 hp (separation, destoning and grading). The details regarding energy consumption is given below

Raw material to be pre-cleaned= 10 tonnes

Power consumed during pre-cleaning (i.e. Separation/ De-stoner and elevating of material)

- 1) Total power required in pre-cleaning = 15 hp + 5 hp  
= 11.19 + 3.73  
= 14.92 kW
- 2) Energy consumption = Total power requirement × operation duration  
= 14.92 × 12  
= 179.04 kWh per day
- 3) Annual energy consumption = Per day energy consumption × annual working day  
= 179.04 × 320  
= 57292.8 kWh

The power requirement in pre-cleaning operation was observed to be 14.94 kW. This operations was continuously run over one and half shift of a day (12 h.). The annual working of the milling plant was considered as per discussion with plant managerial. The annual working days are approximately 320. The per day energy consumption in pre-cleaning operation was calculated to be 179kWh. The annual energy consumption was calculated to be 57292 kWh. It is found that pre-cleaning of raw produce in pulse processing consume more energy.







### Khambalkar et al.

#### Energy consumption in touching operation (Emery roller)

Emery rollers are the devices used for touching the seed coat for penetration of oil into the grain in order to loosening the husk/ seed coat. This operation has been followed in two passes. An electric motor of approximate 5 hp size is comfortable to drive the emery rollers. The details regarding the energy consumption during the rolling operation is narrated below.

- 1) Total power required for emery roller =  $5 \times 0.746$   
= 3.73 kW
- 2) Total energy consumption = Total power required  $\times$  working hours  
=  $3.73 \times 12$   
= 44.76 kWh per day
- 3) Annual energy consumption = Per day energy consumption  $\times$  annual working day  
=  $44.79 \times 320$   
= 14323.2 kWh

Total power required for emery roller in touching operation is observed to be 3.73 kW. Where as the total energy consumption for this operation is calculated as 45 kWh. The annual energy consumption is calculated as 14323.2 kWh.

#### Energy consumption in main dal process

The energy use pattern in the dal processing is varies according the operation involved. The main dal process involved the milling, dehusking and the splitting of dal. This process accounts the large amount of energy conservation [9]. The details calculation of the energy required for the dal process is given below;

- 1) Total power required in main dal process = 40 hp  
=  $40 \times 0.746$   
= 29.84 kW
- 2) Total energy consumption =  $29.84 \times 12$  hr  
= 358.08 kWh per day
- 3) Annual energy consumption = Per day energy consumption  $\times$  annual working day  
=  $358.08 \times 320$   
= 114585.6 kWh

It is observed that, a total of 29 kW of power is required to drive the various mechanical equipments in the process. A total of 358 kWh of electrical energy is required for the main dal process operation in a day. Per annum of 114585 kWh of energy is consumed in this operation.

#### Total energy consumption in whole dal process

The total energy consumption in various operations has been calculated based on the step-wise energy requirement during the process. The electrical energy consumption per day for the dal processing in a day was estimated and found to be 582 kWh which included the pre-processing operation, touching and the milling operation. A detail about the calculation is given below;

= (Energy consumption in pre-cleaning + energy consumption in touching operation + energy consumption in main dal process operation)

$$= (179.04 + 44.76 + 358.08)$$

$$= 582.24 \text{ kWh per day}$$

The annual energy estimate for the process is work out and the total energy consumption was found to be 186201 kWh. The details about the calculation are given below;

- Total annual energy consumption  
= Total energy consumption in whole dal process  $\times$  annual working day





### Khambalkar et al.

$$= 582.24 \times 320$$

$$= 186201.6 \text{ kWh}$$

- Total raw material processed per annual =  $320 \times 10$   
= 3200 tonne

### Energy consumption for processed quantity of raw materials

The total energy consumption per tonne of processed raw materials has been worked out for the surveyed industry. The energy consumed in processing of per tonne of raw materials was found to be 58 kWh. The detail calculation is given below;

$$= (\text{Total annual energy consumption in dal processing} / \text{Total raw material processed})$$

$$= (186201.6/3200)$$

$$= 58.18 \text{ kWh/tonne}$$

### Energy consumption per kg of dal produces

The per kg of energy consumed in producing the dal was determined on annual basis for the visited industry. It account to be 0.073 kWh/kg of produced dal. The details of the calculations are given below;

Total raw material process annual= 3200 tonne( Appro. recovery of dal = 80 %)

- Total dal produce during process = Total raw material process  $\times$  recovery material  
=  $3200 \times 0.80$   
= 2560 tonne
- Total energy consumption per kg = (Total annual energy consumption / Total raw material in kg)  
=  $(186201.6 / 2560000)$   
= 0.073 kWh/ kg

### The energy cost in the process

The cost of energy for the pulse processing is evaluated based on the energy consumption and the quantity of dal produced annually. The cost of energy per kg of dal produced is found to be Rs 0.80. The details of the cost calculation of energy are given below;

- Annual energy consumption = 186201.6 kWh
- Dal produced annually = 2560 tonne
- Annual electricity bill = Total energy consumption  $\times$  cost of energy per unit  
=  $186201.6 \times 11$   
= 2048217.6 Rs/-

Cost of energy per process kg of dal

$$= (2048217.6 / 2560000)$$

$$= 0.803 \text{ Rs/-}$$

## CONCLUSION

The survey was conducted to find the energy consumption in the pulse processing at MIDE, Akola. The details about the energy consumption in the various processes are collected to know the energy consumption. It is found that, the surveyed industry was processed the 10 tonne of raw materials per day. The annual energy consumption of the pulse processing is estimated and found to be 186201 kWh. The operation wise energy consumption showed that, the milling and spitting operation required the large amount of energy to produce the finished produce. The per kg of energy requirement for making the dal was estimated and found to be 0.073 kWh. The cost of energy (electrical) was worked out on per kg of dal produced and estimated to be Rs. 0.803.





**Khambalkar et al.**

## REFERENCES

1. "All India region wise generating installed capacity of power" Central authority ministry of power, Government of India. November 2011. [www.wikipedia.com](http://www.wikipedia.com).
2. Gard Analytics, "Energy, Economic and Environmental Research" ,[www.gard.com](http://www.gard.com).
3. Khadkikar V. Singh B. "Power Factor Correction in Electronic Ballast for Compact Fluorescent Lamps", The Institution of Engineers (I) Vol. 87, September 2006.
4. Mendis N.N.R, Perera N. "Energy Audit: A case Study" Information and automation, 2006, ICIE 2006. IEEE International Conference, page 45-50, 15- 17 Dec.2006
5. Zhang Jian, Zhang Yuchen, Chen Song, Gong Suzhou; "How to Reduce Energy Consumption by Energy Audits and Energy Management" Issue Date: July31 2011- Aug.2011 on page(s): 1 - 5 Date of Current Version: 12 September 2011
6. Shradha C. Deshmukh and Varsha Arjun Patil, Energy conservation and audit, International Journal of Scientific and Research Publications, Volume 3, Issue 8, August 2013.
7. R. Hari Baskar, Hitu Mittal, Mahesh S Narkhede and Dr. S.Chatterji, Energy Audit – A case study, International Journal of Emerging Technology and Advanced Engineering, Volume 4, Special Issue 1, February 2014.
8. Biswas, Mukherjee and Ghosh. Conservation of Energy: a Case Study on Energy Conservation in Campus Lighting in an Institution, International Journal of Modern Engineering Research, Vol.3, Issue.4, Jul - Aug. 2013 pp-1939-1941.
9. Panchal, Dwivedi and Aparnathi. The Case study of Energy Conservation & Audit in Industry Sector. International Journal of Engineering and Computer Science, Volume 3 Issue 4 April, 2014 Page No. 5298-5303.

**Table 1. Details of pulse processing industry**

Name of Agro Industry	RADHA INDUSTRIES, Phase III, MIDC Akola
Raw Material process	Green gram, Black gram
Electrical utility	Sanction load -107 hp Utilization – 50% of total Main electric motor : 50 hp (90% connections on main motor) Electrical consumption: 6000 kWh approximately
Mechanical drive	Single drive
Machineries of processing	Destoner, Pre-cleaner, elevator, , rollers, Dryer, separator, colour sorting machine, compressor





## Preparation and Characterization Cadmium Nanonickel Ferrite at Different Sintering Temperature by Sol Gel Method

Farah T.M.Noori<sup>1</sup>, Malik Jabbar<sup>2</sup>, A.Kadhim<sup>3\*</sup> and Iqbal S.Naji<sup>4</sup>

<sup>1,4</sup>College of science ,Physics department ,university of Baghdad , Baghdad , Iraq.

<sup>2,3</sup>Laser and Optoelectronic Eng.department , University of Technology, Baghdad, Iraq.

Received: 21 June 2016

Revised: 19 July 2016

Accepted: 25 Aug 2016

### Address for correspondence

A.Kadhim

Laser and Optoelectronic Eng.department,

University of Technology,

Baghdad 10066, Iraq.

Email: abdulhadikadhim5@gmail.com



This is an Open Access Journal / article distributed under the terms of the **Creative Commons Attribution License (CC BY-NC-ND 3.0)** which permits unrestricted use, distribution, and reproduction in any medium, provided the original work is properly cited. All rights reserved.

### ABSTRACT

In this paper synthesis of cadmium nickel ferrite ( $\text{Cd}_{0.9}\text{Ni}_{0.1}\text{Fe}_2\text{O}_4$ ) powder products with particles' size in nanometer range using sol gel method as well as sintering process was confirmed. X-ray diffraction measurements of the sintered trials were carried out to produce the formation of single phase materials and the lattice parameter. The lattice parameter was increased with increasing of the sintering temperature. It includes also been observed that the estimated bulk densities of the materials increase when the sintering temperature is elevated. The results of Atomic Forces Microscopy (AFM) show that the grain size increases with increase the temperature of sintering. The results of dielectric constant showed increasing at high frequencies more rapidly than that at low frequencies. The effect of different sintering temperature on the band gap and optical constants (extinction coefficient, refractive index, and dielectric constants) of these films has been investigated and the optical constants and the Urbach energy values of the films were influenced by the deposition parameters.

**Keywords :** Cadmium Nickel Ferrite , Optical properties , Sol gel method

### INTRODUCTION

Ferrites are technologically essential materials that are used in the fabrication of permanent magnetic, electronic and microwave devices. They may have gained technological importance due to their high resistivity and negligible eddy current loss [1]. Spinel ferrites have the standard molecular formula  $(\text{A}^{2+}) [\text{B}^3] \text{O}_4$ , where  $\text{A}^{2+}$  and  $\text{B}^3$  are the divalent and trivalent cation correspondingly, occupying tetrahedral (A) and octahedral (B) interstitial positions of an fcc





### A.Kadhim et al.

formed by  $O^{2-}$  ions. Nickel ferrite,  $NiFe_2O_4$ , is an inverse spinel in which the tetrahedral sites (A) are occupied by  $Fe^{2+}$  and  $Ni^{2+}$  ions [2]. This material is essentially used in electric and electronic gadgets as well as in the catalysis [3]. Substituted nickel ferrites have been the subject of extensive investigation because of their microwave applications. Solid solution of the spinel Cadmium Nickel ferrite system has cubic configuration with the unit cell consisting of eight formula units of the form  $(Cd_{1-x}Fe_x)^{2+}_A[Ni_x^{2+}Fe_{2-x}^{3+}]_B O_4$  [4], [5]. Accordingly, a normal spinel ferrites were obtained for  $x=0$ , an inverse obtained for  $x = 1$ , and intermediate for  $0 < x < 1$ . In the present work an attempt was being made to synthesis Cd-Ni ferrite with general formula  $Cd_{1-x}Ni_xFe_2O_4$  (where  $x = 0.1, 0.3, 0.5, 0.7$  and  $0.9$ ) by sol-gel method and also the influence of substitution of nickel in cadmium ferrite on structural and optical properties are investigated at different sintering temperature [6].

## MATERIALS AND METHODS

### Raw Materials

The raw materials include the following compounds:

- Nickel nitrate  $Ni(NO_3)_2$
- Iron nitrate  $Fe_2(NO_3)_2$
- cadmium nitrate  $Cd(NO_3)_2$
- Methanol and ammonia solution.

### Experimental Details

Cadmium nickel ferrite with the general formula  $Cd_{1-x}Ni_xFe_2O_4$  ( $x = 0.1, 0.2, 0.3$ ) were prepared by sol gel method. Raw materials are dissolved in distilled water. The mixture of the raw material was stirred at  $60^\circ C$  on hot plate magneto-stirrer and the ammonia is added for the purpose of access to pH 10. This process is continuously stirred to obtain uniform gel. The solution was washed by using distilled water and paper filter to get rid of ammonia and then placed in an Oven at temperature of  $150^\circ C$  for a three hours to get dry gel. Finally grinding process of dry gel to obtain fine powder and sintered at temperature range of ( $450^\circ C - 950^\circ C$ )

## RESULTS AND DISCUSSION

### X-Ray Diffraction results

Figure 1 shows the XRD Patterns of typical samples of  $(Cd_{0.9}Ni_{0.1}Fe_2O_4)$  sintering at the various temperatures. All of the characteristics peaks of spinel crystal structure were within the diffraction pattern. Critical reflections were observed from the planes of (202), (111), (313), (200), (400), (333), (404) and (531) characterizing the cubic spinel structures, demonstrating the fact that the synthesized ferrite combination of single-phase cubic spinel. Since no uncertain reflections, other than the spinel structures, were confirmed. All XRD measurements revealed match well with the typical patterns of inverse spinel ferrite. Interplant distance and planes are calculated by Bragg's diffraction law and index method using equation 1 and 2 [7]. The increasing of annealing temperature leads to that the diffraction Peaks become narrower and sharper, suggesting the increase in particle size and crystallinity. The average crystallite size has been evaluated from the full width at half maximum of the reflection and using the Scherer's formula equation 3, [8].

$$n\lambda = 2d \sin \theta \quad (1)$$

The lattice parameter 'a' was calculated using following relation

$$a = d \times \sqrt{h^2 + k^2 + l^2} \quad (2)$$

$$\text{Scherer's formula is } t = \frac{0.9\lambda}{\beta \cos \theta} \quad (3)$$

where  $t$  is the crystallite size,  $\beta$  is the full width of the diffraction line at half of the maximum intensity measured in radians, is x-ray wavelength (Cu  $k\alpha$  radiation,  $1.5405 \text{ \AA}$ ) and  $\theta$  is the Bragg angle. The crystallite sizes of the order of





### A.Kadhim et al.

nanometer dimensions were observed and are joined in the Table 1. The grain sizes increase at annealing temperature of 950 °C due to the domination of the activation energy through the grain growth process.

#### Atomic Force Microscopy (AFM) results

The atomic force microscopy of  $\text{Cd}_{0.9}\text{Ni}_{0.1}\text{Fe}_2\text{O}_4$  ferrites thin films are shown in figures 2, 3 and 4. AFM images showed that all the films have grainy nature and this confirms with the results of Dixit et al. [9]. The grain size and surface roughness increases with the sintering temperatures elevated of the films. The grain size and roughness are listed in Table 2.

#### Transmission Spectrum Results

The optical transmissions of the  $(\text{Cd}_{0.9}\text{Ni}_{0.1}\text{Fe}_2\text{O}_4)$  thin films as a function of wavelength in the range (300-1100 nm) are shown in Figure 5. All samples showed transmission less than (20%) in the wavelength of 300nm and boost to reach to (70%) at (450°C) in the wavelength of 1100nm. In general, it can be observed from Figure 5 that the transmittance decreases with increasing of sintering temperatures.

#### Absorption Coefficient

The variance of absorption coefficient with wavelength for  $(\text{Cd}_{0.9}\text{Ni}_{0.1}\text{Fe}_2\text{O}_4)$  ferrite thin films which were calculated by using equation 4 are shown in figure 6. It could be discovered that the absorption factor decreases with increasing of wave length due to increase the transmittance. The maximum value of absorption coefficient at wavelength of 335nm at UV region. The absorption coefficient begins reduced at the visible region unfaithful which is value reach to  $37118\text{cm}^{-1}$  at 1100nm and temperature of 950. Generally, it can be discovered that the absorption ratio increases when sintering temperatures increasing.

$$\alpha = 2.302A/t \quad (4)$$

Where (t) is the sample thickness.

The extinction coefficient (k) is related to the exponential decay of the wave when it passes through the medium and it is defined as:

$$k = \alpha\lambda/4\pi \quad (5)$$

Where ( $\lambda$ ) is the wavelength of the incident radiation.

Figure 7 shows the behavior of the extinction coefficient (k). Which were calculated by using equation (5). It is nearly similar to the corresponding absorption coefficient for  $(\text{Cd}_{0.9}\text{Ni}_{0.1}\text{Fe}_2\text{O}_4)$  ferrite thin films, which means that the extinction coefficient decreases with increasing of wavelength. The increasing in (k) values due to high absorption coefficient (i.e. increasing the density of localized state). In general, it may be observed that the extinction coefficient increases with increasing of sintering temperature.

#### Dielectric Properties Results

The imaginary and real parts of dielectric constant of the films were also determined by the equation (6, 7) [9]. The variation of real and imaginary part dielectric constant of all ferrite samples at different temperature with frequency is shown in figures 8 and 9 and can be observed that the real and imaginary part dielectric constant of all trials decreases rapidly when the frequency increasing. The variant of dielectric constant with frequency shows the dispersion due to Maxwell - Wagner [10, 11] type of interfacial polarization in accordance with Koops phenomenological theory [12, 13]. Among the samples  $(\text{Cd}_{0.9}\text{Ni}_{0.1}\text{Fe}_2\text{O}_4)$  exhibits the lowest dielectric constant and lowest dielectric loss tangent. The reduction in dielectric constant with accept frequency was due to the fact that polarization decreases with frequency and then remains constant. In accordance to Rabinkin and Novikova [14] the polarization mechanism is comparable to the conduction process.

$$\epsilon_1 = n^2 - k^2 \quad (6)$$

$$\epsilon_2 = 2nk \quad (7)$$

Where  $k = \alpha\lambda/4\pi$  and n are refractive index





**A.Kadhim et al.**

### Refractive index

The refractive index of the (Cd<sub>0.9</sub>Ni<sub>0.1</sub>Fe<sub>2</sub>O<sub>4</sub>) thin films as a function of wavelength in the range of 300-1100 nm are shown in Figure 10. It could be discovered that the refractive index increase with increasing the wave length but begin to reduce in the visible region. Generally, it can be discovered that the refractive index increases with increasing sintering temperatures.

### Optical Energy Gap

The optical energy gap is determined from figure (11). Which shows the variation of  $(\alpha h\nu)^2$  with photon energy ( $h\nu$ ) for direct allowed transition of (Cd<sub>0.9</sub>Ni<sub>0.1</sub>Fe<sub>2</sub>O<sub>4</sub>) films with different sintering temperature. The curve in shape is extrapolated to the energy axis to give the value of optical energy band gap which lasted in table (3). It may see from this table when that sintering temperature increase the optical energy gap decrease from 2.9 to 2.6 eV. The decrease in the optical energy gap may be due to the modification of the ferrite structure.

### Optical Conductivity

The variance of Optical Conductivity with wavelength for (Cd<sub>0.9</sub>Ni<sub>0.1</sub>Fe<sub>2</sub>O<sub>4</sub>) ferrite thin films which were calculated by using equation (8) are shown in fig (12) [16].

$$\sigma = \alpha n c / 4 \pi \quad (8)$$

Where c is speed of light.

The high magnitude of the optical conductivity ( $10^{10} \text{ sec}^{-1}$ ) confirms the very high imageresponse of the film. The increasing optic conductivity at high wave length is due to the high absorbance of Cd<sub>0.9</sub>Ni<sub>0.1</sub>Fe<sub>2</sub>O<sub>4</sub> thin film.

### Energy Urbach

The value of  $E_U$  was obtained from the reverse of the slope of  $\ln \alpha$  with  $h\nu$  as shown in figure (13).  $E_U$  values change inversely with the optical band gap. The Urbach energy is increasing with increases sintering temperature. The arise in  $E_U$  is caused by the increase of disorder of the materials occurred by doping. This kind of increase reason a redistribution of the states, from band to tail, thus allows for increased number of possible groups to tail and end to tail transitions [15]. As an end result, both a reduction in the optical gap and a broadening of the Urbach tail have taken place.

## CONCLUSION

Polycrystalline ferrites with composition (Cd<sub>0.9</sub>Ni<sub>0.1</sub>Fe<sub>2</sub>O<sub>4</sub>) have been successfully synthesized by sol gel method and it has spinel structure. The lattice parameter increases with increasing the cadmium content in ferrites. The variation of dielectric constant with frequency shows the usual dielectric dispersion in the low frequency region and almost remains regular in the high rate of recurrence region. Optical band gap decreases with the increasing of the sintering temperature from 2.9 to 2.6 eV. The Urbach energies ( $E_U$ ) values changes inversely with the optical band gap. The high extinction coefficient value ( $3 \times 10^{-2}$ ) and the high magnitude of optical conductivity ( $10^{10} \text{ s}^{-1}$ ) confirms the presence of very high photo response of the samples.

## REFERENCES

1. Gopathi Ravi Kumar, Katrapally Vijay a Kumar and Yarran Chatty Venudhar, "Synthesis, Structural and Magnetic Properties of Copper Substituted Nickel Ferrites by Sol-Gel Method", Materials Sciences and Applications, Vol 3, pp 87-91, (2012).
2. Young-Yael Song N Mo and Patton C E 2005 J. Appl. Phys. 97 093901.
3. G. Nabyouni, M. Jabari Fesharaki, M. Mozafari and J. Amighian, "Characterization and Magnetic Properties of Nickel Ferrite Nanoparticles Prepared by Ball Milling Technique", Chin. Phys. Lett. Vol. 27, pp. 12, (2010).





**A.Kadhim et al.**

4. E. Wolska, W. Wolski, J. Kaczmarek, "Defect structures in cadmium-nickel ferrites", Vol, 51, Pp.231, (1992).
5. N. A. Eissa, A. A. Bhagat and M. K. Fayek, "On the magnetic behaviour of cadmium nickel ferrites " Hyperfine Interactions, Vol.5, p.137, (1978).
6. P.B. Belavi, G.N. Chavan, L.R. Naik, R. Somashekar, R.K. Kotnala, "Structural, electrical and magnetic properties of cadmium substituted nickel-copper ferrites", Materials Chemistry and Physics, Vol.132, pp. 138–144, (2012).
7. Gopathi Ravi Kumar, Katrapally Vijaya Kumar<sup>2</sup>, Yarramchetty Venudhar<sup>1</sup> "Synthesis, Structural and Magnetic Properties of Copper Substituted Nickel Ferrites by Sol-Gel Method", Materials Sciences and Applications, Vol.3, pp.87-91, 2012.
8. G. Nabiyouni, M. Jafari Fesharaki, M. Mozafari and J. Amighian, "Characterization and Magnetic Properties of Nickel Ferrite Nanoparticles Prepared by Ball Milling Technique", Chin. Phys. Lett. Vol. 27, No. 12, pp. 6401, (2010).
9. G. Sathishkumar, C. Venkataraju and K. Sivakumar, "Magnetic and Dielectric Properties of Cadmium Substituted Nickel Cobalt Nanoferrites", J.O Mater Science: Materials in Electronics, Vol. 24, Issue 3, Pp 1057-106.2013
10. R. S. Devan, Y. D. Kolekar and B. K. Chougule, "Effect of cobalt substitution on the properties of nickel-copper ferrite" J. Phys: Condense. Matter vol.18, No.43, (2006).
11. Maxwell J. C, "Electricity and Magnetism", London Oxford University Press, 1973.
12. C. G. Koops, "On the Dispersion of Resistivity and Dielectric Constant of Some Semiconductors at Audio frequencies", Physics review. Vol. 83, pp. 121, (1951).
13. M. Abdullah. Farah T. Mohammed Noori. Amin H. Al-K, "Millimeter waves from Frequency generation and optical rectification in quantum dot structure", Optical and Quantum Electronics, 2016.
14. L. I. Rabinkin and Z. I. Novikova, "Ferrites," Doklady Akademii Nauk SSSR, Minsk, USSR, pp. 146, 1960.
15. Stephen K. O'Leary, Stefan Zukotynska and John M. Perzb, "Disorder and optical absorption in amorphous silicon and amorphous germanium", J. Non-Cryst. Solids, vol.210, No.2, pp 249-253, (1997).
16. T. Arumanayagam, P. Murugakoothan, "Optical Conductivity and Dielectric Response of an Organic Aminopyridine NLO Single Crystal", Journal of Minerals & Materials Characterization, Vol. 10, No.13, pp.1225-1231, 2011.

**Table 1: X-ray diffraction pattern data for bulk (Cd<sub>0.9</sub>Ni<sub>0.1</sub>Fe<sub>2</sub>O<sub>4</sub>) ferrites with different sintering temperatures.**

T (°C)	2θ (Deg.)	FWHM (Deg.)	d <sub>hkl</sub> Exp.(Å)	G.S (nm)	hkl	d <sub>hkl</sub> Std.(Å)	Phase	Card No.
	30.1047	0.3455	2.9661	23.8	(202)	2.9556	NiFe <sub>2</sub> O <sub>4</sub>	96-230-0296
	35.2037	0.8061	2.5473	10.3	(311)	2.5205	NiFe <sub>2</sub> O <sub>4</sub>	96-230-0296
450	38.5905	0.5758	2.3312	14.6	(200)	2.3410	CdO	96-900-6675
	44.8865	0.5758	2.0177	14.9	(111)	2.0201	Ni	96-901-1604
	65.1481	0.6910	1.4307	13.6	(531)	1.4283	CdFe <sub>2</sub> O <sub>4</sub>	96-591-0006
	30.1026	0.2576	2.9663	32.0	(202)	2.9556	NiFe <sub>2</sub> O <sub>4</sub>	96-230-0296
	33.4371	0.5151	2.6777	16.1	(111)	2.7032	CdO	96-900-6675
750	35.2016	0.6010	2.5474	13.9	(311)	2.5205	NiFe <sub>2</sub> O <sub>4</sub>	96-230-0296
	38.5884	0.4293	2.3313	19.6	(200)	2.3410	CdO	96-900-6675
	44.8844	0.4293	2.0178	20.0	(111)	2.0201	Ni	96-901-1604







**A.Kadhim et al.**

	65.1460	0.5151	1.4308	18.3	(531)	1.4283	CdFe <sub>2</sub> O <sub>4</sub>	96-591-0006
	30.1160	0.1717	2.9650	47.9	(202)	2.9556	NiFe <sub>2</sub> O <sub>4</sub>	96-230-0296
	33.4505	0.3434	2.6767	24.2	(111)	2.7032	CdO	96-900-6675
	35.2150	0.4007	2.5465	20.8	(311)	2.5205	NiFe <sub>2</sub> O <sub>4</sub>	96-230-0296
950	38.6018	0.2862	2.3305	29.4	(200)	2.3410	CdO	96-900-6675
	42.4939	0.1717	2.1256	49.7	(400)	2.0899	NiFe <sub>2</sub> O <sub>4</sub>	96-230-0296
	44.8978	0.2862	2.0172	30.0	(111)	2.0201	Ni	96-901-1604
	65.1594	0.3434	1.4305	27.5	(531)	1.4283	CdFe <sub>2</sub> O <sub>4</sub>	96-591-0006

**Table 2: Average grain size and average roughness for (Cd<sub>0.9</sub>Ni<sub>0.1</sub>Fe<sub>2</sub>O<sub>4</sub>) ferrite thin films.**

T (°C)	Ave. grain size (nm)	Ave. Roughness (nm)
450	78.20	1.06
750	89.36	1.21
950	99.83	2.7

**Table 3: Energy gap values of (Cd<sub>0.9</sub>Ni<sub>0.1</sub>Fe<sub>2</sub>O<sub>4</sub>) at different sintering temperature.**

T(°C)	Eg (eV)
450	2.9
750	2.8
950	2.6





A.Kadhim et al.

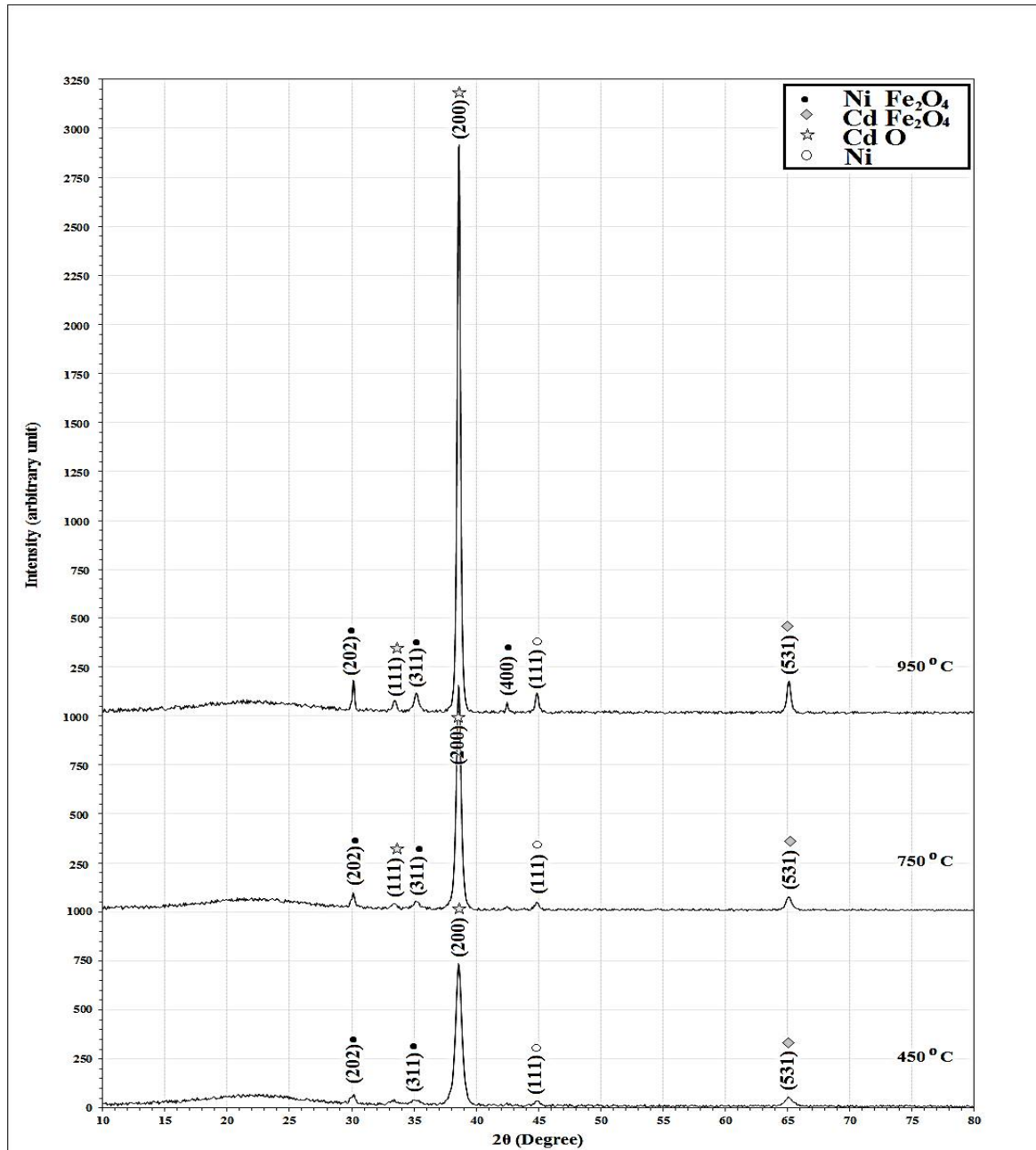
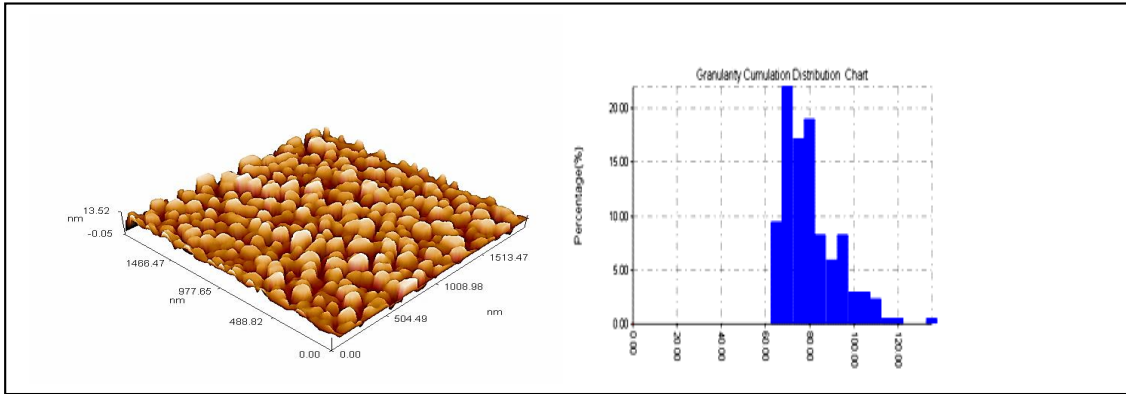


Fig. 1.X-ray diffraction pattern of a  $\text{Cd}_{0.9}\text{Ni}_{0.1}\text{Fe}_2\text{O}_4$  milled sample for 3 h at different temperatures (450°C, 750°C, 950°C).





**A.Kadhim et al.**



**Figure2: AFM micrographs for the compositionCd<sub>0.9</sub>Ni<sub>0.1</sub>Fe<sub>2</sub>O<sub>4</sub> at 450 °C**

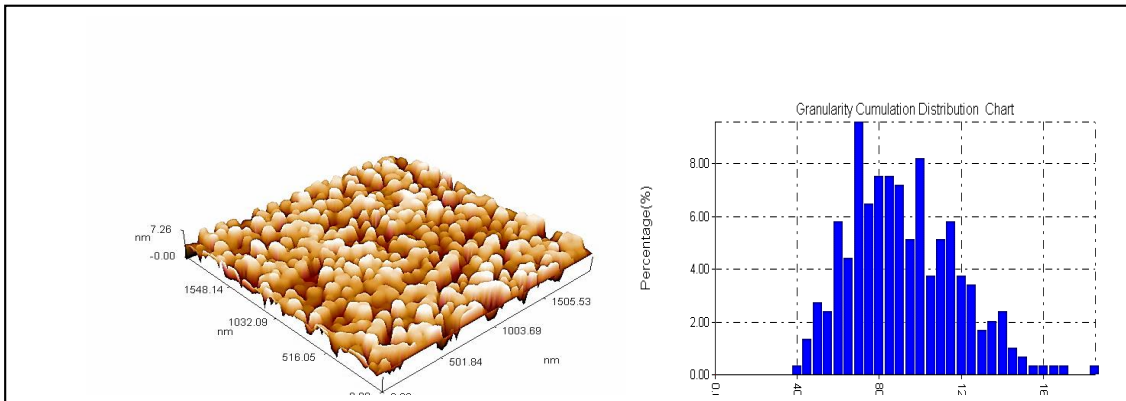


**Figure3:..AFM micrographs for the compositionCd<sub>0.9</sub>Ni<sub>0.1</sub>Fe<sub>2</sub>O<sub>4</sub> at 750°C**

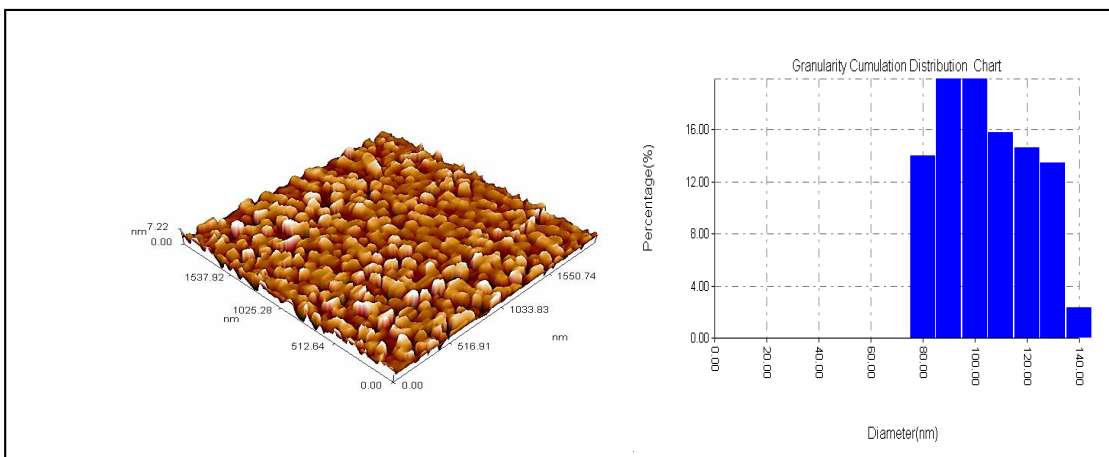


**Figure.4: AFM micrographs for the compositionCd<sub>0.9</sub>Ni<sub>0.1</sub>Fe<sub>2</sub>O<sub>4</sub> at 950°C**





A.Kadhim et al.

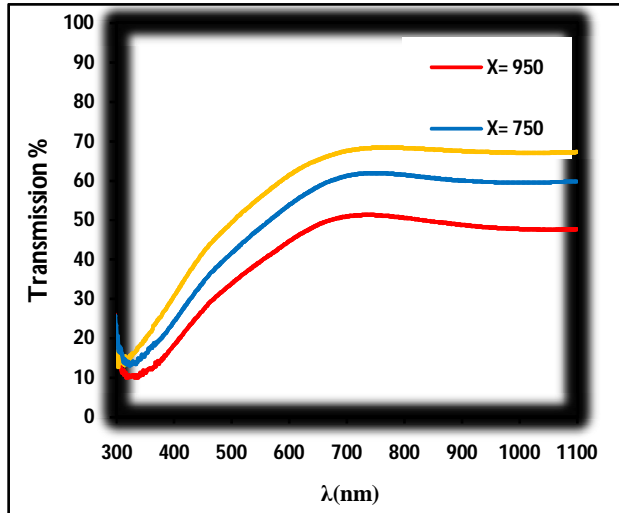


Fig .5. Transmittance versus wavelength for  $(\text{Cd}_{0.9}\text{Ni}_{0.1}\text{Fe}_2\text{O}_4)$  with different sintering temperature

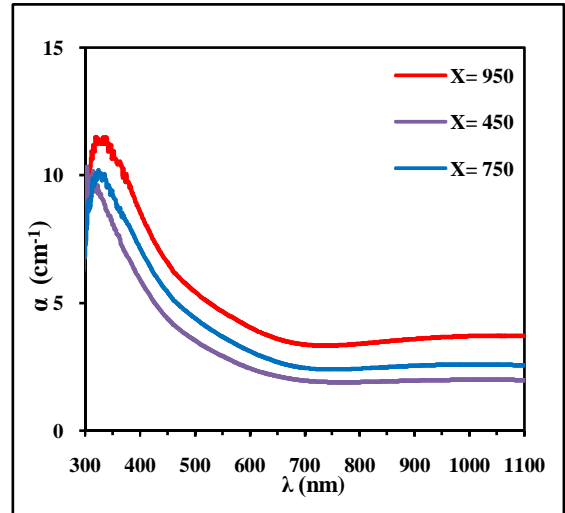


Fig .6. Absorption coefficient  $(\alpha \text{ cm}^{-1})$  versus wavelength for  $(\text{Cd}_{0.9}\text{Ni}_{0.1}\text{Fe}_2\text{O}_4)$  with different sintering temperature

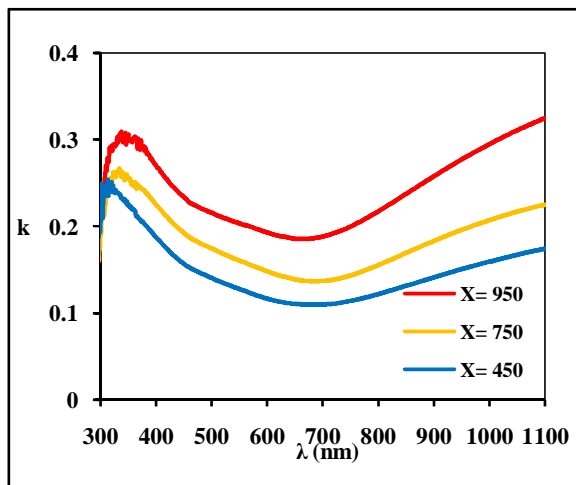


Fig .7. Extinction coefficient  $(k)$  versus wavelength for  $(\text{Cd}_{0.9}\text{Ni}_{0.1}\text{Fe}_2\text{O}_4)$  with different sintering temperature

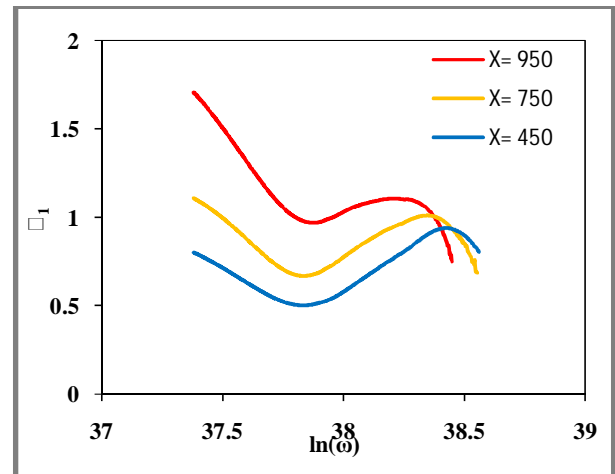


Fig .8. Real part  $(\epsilon_1)$  of dielectric constant versus frequency for  $(\text{Cd}_{0.9}\text{Ni}_{0.1}\text{Fe}_2\text{O}_4)$  with different sintering temperature





A.Kadhim et al.

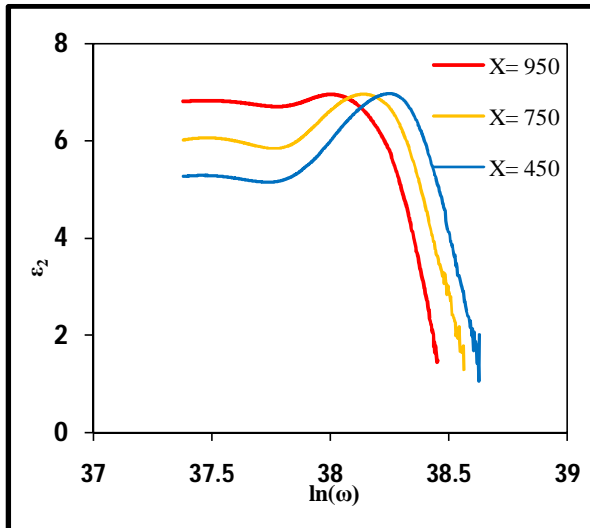


Fig .9. Changes of imaginary part ( $\epsilon_2$ ) of dielectric constant versus frequency for  $(\text{Cd}_{0.9}\text{Ni}_{0.1}\text{Fe}_2\text{O}_4)$  with different sintering temperature

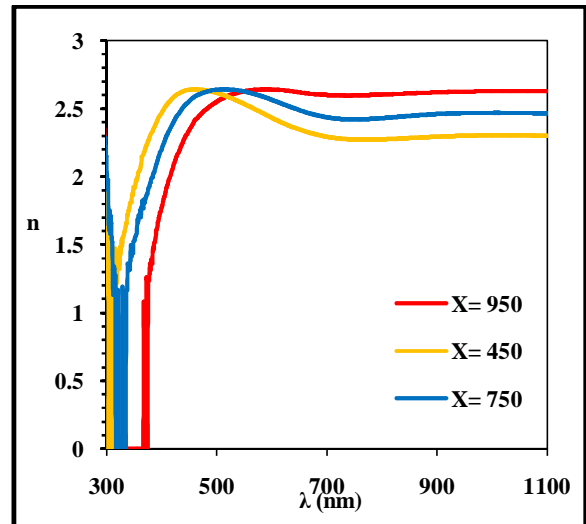


Fig .10. The refractive index versus wavelength for  $(\text{Cd}_{0.9}\text{Ni}_{0.1}\text{Fe}_2\text{O}_4)$  with different sintering temperature

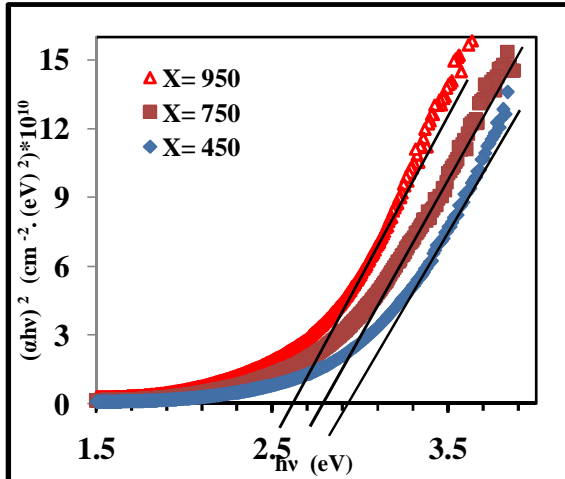


Fig .11. Energy band gap at R.T for  $(\text{Cd}_{0.9}\text{Ni}_{0.1}\text{Fe}_2\text{O}_4)$  films with different temperature

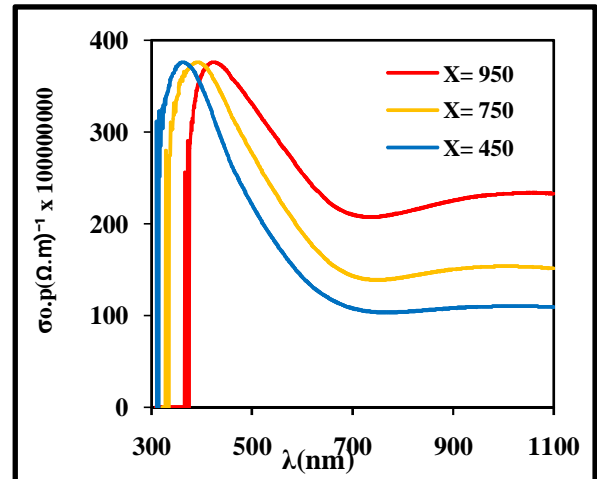


Fig .12. The optical conductivity versus wavelength for  $(\text{Cd}_{0.9}\text{Ni}_{0.1}\text{Fe}_2\text{O}_4)$  with different sintering





A.Kadhim et al.

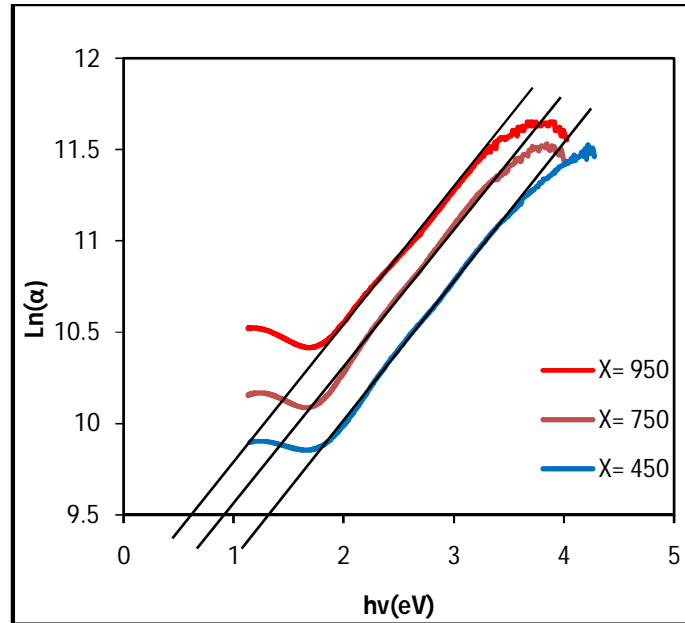


Fig (13) The Urbach energy plots for  $(\text{Cd}_{0.9}\text{Ni}_{0.1}\text{Fe}_2\text{O}_4)$  films with different sintering temperature.





## Comparative Study on Sensory Quality of Yoghurt Incorporated with Flaxseed oil and Flaxseed oil Emulsion

S.Sivakumar<sup>1\*</sup>, BV.Balasubramanyam<sup>2</sup>, K. Jayaraj Rao<sup>2</sup>, P. Heartwin Amala Dhas<sup>2</sup> and B.Surendra Nath<sup>2</sup>

<sup>1</sup>College of Dairy Science and Technology, Guru Angad Dev Veterinary and Animal Sciences University Ludhiana-141004, India.

<sup>2</sup>National Dairy Research Institute, Southern Regional Station, Bangalore, Karnataka-560030. India.

Received: 5 July 2016

Revised: 20 Aug 2016

Accepted: 9 Sep 2016

### \*Address for correspondence

Dr.S.Sivakumar

Assistant Scientist (Dairy Technology), College of Dairy Science and Technology,

Guru Angad Dev Veterinary and Animal Sciences University

Ludhiana-141004, India.

Email: drshiva2003@yahoo.com



This is an Open Access Journal / article distributed under the terms of the **Creative Commons Attribution License (CC BY-NC-ND 3.0)** which permits unrestricted use, distribution, and reproduction in any medium, provided the original work is properly cited. All rights reserved.

### ABSTRACT

The objective of the present study was to compare the sensory scores of yoghurt prepared by incorporating flaxseed oil and flaxseed oil emulsion in different varieties of milk. The results indicate that the incorporation of flaxseed oil had marginal effect on the colour and appearance of yoghurt. The mean scores indicated that the use of Toned milk(TM) for yoghurt preparation gave better body & texture compared to Double Toned milk (DTM) and Standardized milk (STM) while significant differences between control and experimental yoghurt with 2% flaxseed oil were observed. The overall acceptability scores also showed that the use of Toned Milk was more suitable for yoghurt preparation with incorporation of flaxseed oil. The results indicate that the variation in quality of milk and incorporation of flaxseed oil up to 2% had marginal effect on the flavour and overall acceptability of the product. The addition of the emulsion imparted yellow colour to the milk and the score reduced with increased incorporation of the emulsion. Though the emulsion had very bland flavour, the addition of the emulsion had imparted some external flavour similar to emulsifiers. The variation in milk quality had difference in flavour as indicated by the scores offered by the judges. The overall acceptability scores showed the similar trend of acceptability to those of flavour by judges and statistical analysis. The effect of type of milk and flaxseed oil emulsion incorporation was found to be significant at  $P \leq 0.05$  for flavour and over all acceptability.

**Keywords:** Flaxseed oil, Flaxseed oil emulsion, Double Toned milk, Standardized milk, Yoghurt.



**Sivakumar et al.**

## INTRODUCTION

There is a demand for food and beverages with health benefits and consumers are making a conscious attempt to include them in their diet. Many health conscious individuals incorporate functional foods and beverages into their daily lives, with the hopes of maintaining or enhancing quality of life. As the costs of health care and prescription drugs increase, a growing trend towards self-medication with natural food-based ingredients occurs. The idea of the incorporation of flaxseed in a milk base can provide a combination of benefits of the both the milk and flaxseed. Yoghurt is a valuable health food for both children and elderly persons. The Fat and SNF contributes to enhancement in taste of the yoghurt with improved consistency and viscosity with reduced syneresis. It improves the flavour, rheological properties and over all acceptability of yoghurt (Guirguis *et al.*, 1984). The loss of taste in yoghurt samples may be due to development of acidity, oxidation of fat or proteolysis of proteins. Spoilage of cultured dairy products is primarily caused by excessive fermentation, enzymatic breakdown or contamination with undesirable microorganisms. Present study was conducted with a systematic approach to supplement the functional yoghurt with flaxseed oil and flaxseed oil emulsion. Result obtained during trials were presented and discussed in this paper.

## MATERIALS AND METHODS

The cow milk was received from the experimental dairy of National Dairy Research Institute, Bangalore and was standardized to 1.5, 3, 4.5 % Fat and SNF content 10% was maintained in all the milk samples. Flaxseed oil emulsion obtained from Alphalite Fortifier Ensign Diets Care Pvt Ltd, Pune was used in the experimental trials. Flaxseed oil, marketed by HEALTH 1st-PranoFlax (India) Pvt Ltd, Jaipur was used for the yoghurt preparation. Yoghurt cultures maintained in the Dairy Bacteriology section of the National Dairy Research Institute, Bangalore were used in the preparation of yoghurt. The cultures were subcultured one day before their use in the experiments.

### Preparation of Yoghurt

The pure flaxseed oil/emulsion was incorporated into milk at 0%, 1% ,2 % and 0%, 2.5%, 5% 7.5% respectively. The mixture of milk and the oil/emulsion was homogenized at around 60°C before heating the milk to final heat treatment. Sugar was used at 8% levels for preparation of the all experimental yoghurt and control yoghurt. The sugar was added to milk prior to final heat treatment to eliminate the osmophilic yeasts coming from sugar, then the yoghurt was prepared as per the procedure described by Tamime and Deeth (1980) with slight modifications. The sensory evaluation of the experimental yoghurt samples were carried out with the help of 9 point hedonic scale (Shone *et al.*, 1977).

### Statistical Analysis

Sensory scores obtained during trials, were statistically analysed by Two way Anova using statistical software SPSS 15.0 for Windows Evaluation Version.

## RESULTS AND DISCUSSION

### Sensory scores of yoghurt prepared by incorporating flaxseed oil in different Varieties of milk

Sensory scores of yoghurt prepared by incorporating flaxseed oil and flaxseed oil emulsion in different Varieties of milk and the results are presented in the Table 1&2 and Table 3&4. Attempts were made to incorporate flaxseed oil at 1 and 2% levels in DTM, TM and STM to study the effect of milk quality variation on the colour & appearance and body & texture scores of yoghurt prepared with incorporation of flaxseed oil, and the results are presented in Table 1. The milk was homogenised after addition of flaxseed oil to incorporate the oil in to the milk, before it was used for yoghurt preparation. The results indicate that the incorporation of flaxseed oil had marginal effect on the colour and appearance of yoghurt. The scores for control yoghurt prepared by using DTM, TM and STM were 7.89, 7.95 and 8.00





**Sivakumar et al.**

respectively. The pleasant yellow colour resulted in increased scores with increased fat content in the milk used for the yoghurt preparation. The corresponding scores for 1% flaxseed oil incorporated yoghurt slightly reduced to 7.85, 7.83 and 7.70 due to increased yellow colour contributed by the flaxseed oil. The natural colour of flaxseed oil was yellow. The intensity of the oil also increased with increased milk fat and flaxseed oil incorporation. The milk used for the studies was cow's milk whose milk fat was yellow, also contributed to the colour of milk (Fox *et al.*, 2006). The flaxseed oil enhanced the yellow colour perception in the yoghurt beyond the acceptance level and resulted in reduced colour and appearance scores in yoghurt with STM. The results correlated with the findings of Lim *et al.*, (2010) who reported that the intensity of yellow colour of ice cream positively correlated to amount of flaxseed oil substitution.

The body and texture scores presented in the same Table indicate that the incorporation of flaxseed oil had no significant perception on the body and texture of the final product. The control yoghurt prepared by using DTM, TM, and STM recorded the body and texture score of 7.83, 7.88 and 7.90 respectively. The scores marginally reduced to 7.70, 7.90 and 7.79 respectively for the yoghurt prepared by incorporating 1% flaxseed oil in DTM, TM and STM respectively and the corresponding values for 2% oil incorporated yoghurt were 7.66, 7.85 and 7.71. The mean scores increased from 7.73 for DTM yoghurt to 7.88 for TM yoghurt and the score reduced to 7.80 for yoghurt made from STM. This could be due to the fact that the yoghurt with STM had a total fat of 5.5% i.e, 4.5% of milk fat and 1% flaxseed oil, and the higher fat content in milk made the product softer compared to the yoghurt made by using TM or DTM. The effect of type of milk and flaxseed oil incorporation was found to be significant at  $P \leq 0.05$ . The mean scores indicated that the use of TM for yoghurt preparation gave better body & texture compared to DTM and STM, while significant differences between control and experimental yoghurt with 2% flaxseed oil were observed. The results correlated with the findings of Goh *et al.*, (2006) found that higher the proportion of flaxseed oil used to replace dairy fat, the lower would be the firmness of ice cream.

The flavour scores presented in Table 2 shows that the control yoghurt made from DTM scored a score of 7.83 compared to 7.95 for the TM yoghurt, 8.00 for STM yoghurt. The gradual increase in the score could be due to the rich flavour imparted by the milk fat. The incorporation of flaxseed oil marginally reduced the flavour scores compared to that of control yoghurt samples. The flavour score for 1% flaxseed oil incorporated yoghurt made from DTM was 7.75 and score marginally increased to 7.87 for yoghurt made from TM. The score reduced to 7.80 for the yoghurt made from STM. The scores for 2% flaxseed oil incorporated yoghurt made from DTM, TM and STM were 7.60, 7.77 and 7.65 respectively. The reduction in the scores for yoghurt with increased flaxseed oil in STM could be due to increased fat level in the milk by way of incorporation of flaxseed oil which has masked the delicate milk fat flavour in the yoghurt. The two way Anova analysis of the flavour scores indicate that the use of TM along with flaxseed oil was better compared to use of DTM or STM.

The overall acceptability scores also showed that the use of TM was more suitable for yoghurt preparation with incorporation of flaxseed oil. The results indicate that the variation in quality of milk and incorporation of flaxseed oil up to 2% had marginal effect on the flavour and overall acceptability of the product. The effect of type of milk and flaxseed oil incorporation was found to be significant at  $P \leq 0.05$  for flavour and overall acceptability). Though the mean shows significant difference between the control and experimental yoghurt samples with flaxseed oil, judges liked the yoghurt made from TM with 2% oil with marginally reduced score, and was acceptable when compared to control yoghurt. Effect of milk variation on sensory quality of flaxseed oil emulsion incorporated yoghurt. The flaxseed emulsion supplied by Alphalite Fortifier Ensign Diets Care Pvt Ltd, Pune was used in place of flaxseed oil and flaxseed flour for preparation of yoghurt and analysed for sensory parameters. The colour & appearance and body & texture scores are presented in Table 3. The flaxseed oil emulsion was slightly yellowish paste like homogeneous substance with flat flavour. The addition of the emulsion imparted yellow colour to the milk and the score reduced with increased incorporation of the emulsion.



**Sivakumar et al.**

The colour and appearance for the control yoghurt prepared by using DTM, TM and STM scored 7.83, 7.88 and 7.90 respectively. The corresponding values for the yoghurt prepared by addition of 2.5% flaxseed emulsion were 7.88, 7.81 and 7.77. The scores reduced with increased level of the emulsion incorporation. The addition of 7.5% emulsion drastically reduced the score to 7.23, 7.17 and 7.13 for the yogurt prepared by using DTM, TM and STM. But statistical analysis showed significant difference between DTM and STM yoghurt, while no significant difference was observed between DTM and TM yoghurt samples. The body and texture scores for control yoghurt prepared by using DTM, TM and STM were 7.81, 7.91 and 8.00 respectively. The scores reduced with incorporation of the emulsion. As per the manufacturer's declaration, the emulsion contains alpha linolenic acid, emulsifiers and other ingredients. The presence of emulsifiers and other components of the emulsion presumably/might have resulted in increase the stickiness of yoghurt which has resulted in reduced score.

The effect of type of milk and flaxseed oil emulsion incorporation was found to be significant at  $P \leq 0.05$  for colour and appearance and body and texture. The addition of 7.5% emulsion drastically reduced the scored to 7.00, 7.22 and 6.70 for the yoghurt prepared by using DTM, TM and STM. Further statistical mean score of body and texture showed significant difference between DTM, TM and STM yoghurt. The results presented in Table 4 shows that the average flavour scores indicated by the judges were marginally varied and all the samples were accepted. The control yoghurt scored an average score of 8.09 while the flavour scores for experimental yoghurt with varied level of the emulsion varied between 7.92 and 7.28. However the flavour of the yoghurt prepared by incorporating 7.5% emulsion was very less compared to control and other experimental yoghurt samples. The mean score showed significant variation between control and experimental yoghurt and also within the experimental samples. Though the emulsion had very bland flavour, the addition of the emulsion had imparted some external flavour similar to emulsifiers.

The variation in milk quality had difference in flavour as indicated by the scores offered by the judges. But the mean scores indicate in TM yoghurt which scored 7.91 compared to 7.70 for yoghurt prepared from DTM and 7.60 for STM yoghurt. However, the yoghurts prepared by all the three variants of milk were accepted by the judges. The overall acceptability scores showed the similar trend of acceptability to those of flavour by judges and statistical analysis. The effect of type of milk and flaxseed oil emulsion incorporation was found to be significant at  $P \leq 0.05$  for flavour and over all acceptability. The flaxseed emulsion was made up of alpha linolenic acid, emulsifiers and other materials. As per the manufacturer's declaration, every 5 g of emulsion provides 750mg of alpha linolenic acid. In order to obtain 750 mg of alpha linolenic acid, 4.250 g of other components also to be consumed along with the yoghurt. Keeping in consideration of cost of flaxseed oil emulsion and easy availability of raw materials flaxseed oil, further trials on use of flaxseed emulsion in preparation not yoghurt was not taken up. Further trials were carried out with incorporation of flaxseed oil (in combination) to obtain desirable yoghurt.

## CONCLUSION

The effect of type of milk and flaxseed oil incorporation was found to be significant ( $P \leq 0.05$ ) for flavour and overall acceptability. The two way Anova analysis of the flavour scores indicate that the use of TM along with flaxseed oil was better compared to use of DTM or STM. The scores reduced with incorporation of the emulsion. The effect of type of milk and flaxseed oil emulsion incorporation was found to be significant at  $P \leq 0.05$  for flavour and over all acceptability.

## REFERENCES

1. Goh, K.T., Ye, A. and Dale, N. (2006). Characterisation of ice cream containing flaxseed oil. International Journal of Food Science and Technology, 41: 946-953.





## Sivakumar et al.

- Guirguis, N., Broome, M.C. and Hickey, M.W. (1984). The effect of partial replacement of skim milk powder with whey protein concentrate on the viscosity and syneresis of yoghurt. *Australian Journal of Dairy Technology*, 39(1): 33-35. 38.
- Fox, Patrick F., McSweeney .and Paul L. H. (2006). (Eds.) *Advanced Dairy Chemistry Volume 2: Lipids* originally published by Aspen Publishers, 3rd ed., XXV, 801 p.
- Lim C W, Norziah MH, Lu HFS (2010) Effect of flaxseed oil towards physicochemical and sensory characteristic of reduced fat ice creams and its stability in ice creams upon storage. *Int Food Res J* 17: 393-403.
- Shone H, Sidel H, Oliver S, Wood Sey A, Singlehon RC(1977). Sensory evaluation by quantitative descriptive analysis. *Food Tech* 28(1):24-26
- Tamime AY, Deeth HC (1980) Yoghurt: technology and biochemistry. *J Food Protc*, 43: 939-977.

**Table 1: Colour and appearance and body and texture of yoghurt prepared by incorporating flaxseed oil in different varieties of milk**

Flaxseed oil (%)	Colour and Appearance				Body and Texture			
	Milk				Milk			
	DTM	TM	STM	AVG*	DTM	TM	STM	AVG*
0(control)	7.89	7.95	8.00	7.95 <sup>a</sup>	7.83	7.88	7.90	7.87 <sup>a</sup>
1	7.85	7.83	7.70	7.79 <sup>ab</sup>	7.70	7.90	7.79	7.80 <sup>ab</sup>
2	7.77	7.70	7.60	7.69 <sup>b</sup>	7.66	7.85	7.71	7.74 <sup>b</sup>
AVG*	7.84 <sup>a</sup>	7.83 <sup>a</sup>	7.77 <sup>b</sup>		7.73 <sup>c</sup>	7.88 <sup>a</sup>	7.80 <sup>b</sup>	

DTM - Fat 1.5%, SNF 10%, TM - Fat 3.0 %, SNF 10% STM -Fat 4.5%, SNF 10% Mean values with different Superscript abc in a row/column differ significantly. (P≤0.05) Sugar level 8% \*Statistical Mean

**Table 2: Flavour and Over all acceptability of yoghurt prepared by incorporating flaxseed oil in different varieties of milk**

Flaxseed oil (%)	Flavour				Over all Acceptability			
	Milk				Milk			
	DTM	TM	STM	AVG*	DTM	TM	STM	AVG*
0(control)	7.83	7.95	8.00	7.93 <sup>a</sup>	7.83	7.96	8.00	7.93 <sup>a</sup>
1	7.75	7.87	7.80	7.81 <sup>ab</sup>	7.73	7.92	7.80	7.81 <sup>ab</sup>
2	7.60	7.77	7.65	7.68 <sup>b</sup>	7.69	7.89	7.75	7.78 <sup>b</sup>
AVG*	7.73 <sup>a</sup>	7.86 <sup>a</sup>	7.81 <sup>b</sup>		7.75 <sup>c</sup>	7.93 <sup>a</sup>	7.84 <sup>b</sup>	

DTM - Fat 1.5%, SNF 10%, TM - Fat 3.0 %, SNF 10% STM -Fat 4.5%, SNF 10% Mean values with different Superscript abc in a row/column differ significantly. (P≤0.05) Sugar level 8% \*Statistical Mean





**Sivakumar et al.**

**Table 3: Colour and appearance and body and texture of yoghurt prepared by incorporating flaxseed oil emulsion in different varieties of milk**

Flaxseed oil emulsion (%)	Colour and Appearance				Body and Texture			
	Milk				Milk			
	DTM	TM	STM	AVG*	DTM	TM	STM	AVG*
0(control)	7.83	7.88	7.90	7.87 <sup>a</sup>	7.81	7.91	8.00	7.91 <sup>a</sup>
2.5	7.88	7.81	7.77	7.82 <sup>b</sup>	7.75	7.85	7.70	7.77 <sup>b</sup>
5	7.64	7.58	7.54	7.59 <sup>c</sup>	7.53	7.63	7.33	7.50 <sup>c</sup>
7.5	7.23	7.17	7.13	7.18 <sup>d</sup>	7.00	7.22	6.70	6.97 <sup>d</sup>
AVG*	7.65 <sup>a</sup>	7.61 <sup>ab</sup>	7.57 <sup>b</sup>		7.52 <sup>b</sup>	7.65 <sup>a</sup>	7.43 <sup>c</sup>	

DTM - Fat 1.5%, SNF 10%, TM - Fat 3.0 %, SNF 10% STM -Fat 4.5%, SNF 10% Mean values with different Superscript <sup>abc</sup> in a row/column differ significantly. (P≤0.05) Sugar level 8% \*Statistical Mean

**Table 4: Flavour and Over all acceptability of yoghurt prepared by incorporating flaxseed oil emulsion in different varieties of milk**

Flaxseed oil (%)	Flavour				Over all Acceptability			
	Milk				Milk			
	DTM	TM	STM	AVG	DTM	TM	STM	AVG
0(control)	8.03	8.11	8.14	8.09 <sup>a</sup>	8.00	8.05	8.11	8.05 <sup>a</sup>
2.5	7.90	8.01	7.85	7.92 <sup>b</sup>	7.89	8.00	7.80	7.90 <sup>b</sup>
5	7.67	7.88	7.40	7.65 <sup>c</sup>	7.65	7.80	7.50	7.65 <sup>c</sup>
7.5	7.20	7.63	7.01	7.28 <sup>d</sup>	7.00	7.60	6.80	7.13 <sup>d</sup>
AVG*	7.70 <sup>b</sup>	7.91 <sup>a</sup>	7.60 <sup>c</sup>		7.64 <sup>b</sup>	7.86 <sup>a</sup>	7.55 <sup>c</sup>	

Mean values with different Superscript <sup>abc</sup> in a row/column differ significantly. (P≤0.05) DTM - Fat 1.5%, SNF 10%, TM - Fat 3.0 %, SNF 10% STM -Fat 4.5%, SNF 10% Sugar level 8% \*Statistical Mean





## Gas Sensing of ZnO:SnO<sub>2</sub> Thin Films Prepared by Spray Pyrolysis Technique

Noor Talib<sup>1</sup>, Mahdi HasanSuhail<sup>2\*</sup> and Suaadkhafory<sup>1</sup>

<sup>1</sup>Dept. of Physics, College of Science for Women, University of Baghdad- Iraq.

<sup>2</sup>Dept. of Physics, College of Science, University of Baghdad- Iraq.

Received: 8 July 2016

Revised: 21 Aug 2016

Accepted: 17 Sep 2016

### Address for correspondence

Mahdi HasanSuhail

Dept. of Physics, College of Science,

University of Baghdad- Iraq.

Email: mhsuhail@yahoo.com



This is an Open Access Journal / article distributed under the terms of the **Creative Commons Attribution License (CC BY-NC-ND 3.0)** which permits unrestricted use, distribution, and reproduction in any medium, provided the original work is properly cited. All rights reserved.

### ABSTRACT

Spray Pyrolysis of ZnO:SnO<sub>2</sub> thin films with different percentage (1:1,1:2,2:1) were deposited on a glass substrate at 400 °C temperature using solution of zinc acetate ,tin chloride and air as the carrier gas . The electrical measurements of pure and different ZnO:SnO<sub>2</sub> percentages (1:2,1:1and 2:1) films will be presented. These properties include the Hall effect which gives information about the type of conductivity and mobility of carriers, and also the d.c conductivity from which the transport mechanism of the charge carriers can be estimated. The prepared optimum condition of gas sensing measurements include determination of operation temperature of the sensor, gas sensing mechanism of pure and composition SnO<sub>2</sub>:ZnO thin films ,response time and recovery time.

**Keywords :** Metal-oxides , Dopant elements, Spray pyrolysis ,Gas sensing

### INTRODUCTION

Zinc stannite or zinc tin oxide (ZTO) is a class of ternary oxides that are known for their stable properties under extreme conditions, higher electron mobility compared to its binary counterparts and other interesting properties. These materials is thus ideal for applications from, gas detector, solar cells photocatalysts, light-emitting diodes, field effect transistors and heterojunction and homojunction diodes [1-5]. Among the various TCO's such as ZnO, In<sub>2</sub>O<sub>3</sub>, CdO, TiO<sub>2</sub> and SnO<sub>2</sub>[6], SnO<sub>2</sub> and ZnO is the most promising candidate for the development of transparent conductive material. ZnO in view of its high transmission over a wide spectral range including the useful UV-vis region and other interesting characteristics such as low toxicity, relatively low cost, and stability in reductive





### Mahdi HasanSuhail et al.

chemical environments. SnO<sub>2</sub> is an rutile tetragonal structure with wide band gap of 3.6 eV. Its high optical transparency and electrical conductivity leads to very appealing applications in spintronics device. ZnO and SnO<sub>2</sub> belong to the important family of semiconductor metal oxides that combines high electrical conductivity with optical transparency and thus constitutes an important component for optoelectronic applications [7]. Semiconductor metal oxide gas sensors have generated wide interest because of their various advantages, such as their small dimensions, low cost, fast response, and stable sensors in industry, environmental monitoring and biomedicine [8]. Common toxic and flammable gases which are measured by gas sensors include (NO<sub>x</sub>, NH<sub>3</sub>, O<sub>3</sub>, CO, CH<sub>4</sub>, H<sub>2</sub>, SO<sub>2</sub>, etc.) [9].

The sensitivity depends on many factors including the background gas composition, relative humidity level, sensor temperature, oxide microstructure, film thickness and gas exposure time [10]. Doping has long been used as a traditional mean to obtain new semiconductor metal oxide gas sensors that exhibit gas-sensing properties differentiated from the original ones. In the present work, ZnO:SnO<sub>2</sub> thin films were prepared using Spray Pyrolysis method. The influence of ZnO:SnO<sub>2</sub> content level on electrical and gas sensing in the composite had been studied.

## MATERIALS AND METHODS

The spraying apparatus was manufactured locally in the department laboratories. In this technique, the prepared aqueous solutions (tin Chloride SnCl<sub>2</sub>.2H<sub>2</sub>O and zinc acetate Zn(CH<sub>3</sub>COO)<sub>2</sub>.2H<sub>2</sub>O with purities 99.9% and concentration of 0.1M at (0,1:1,1:2,2:1,0) % ratios (by dissolving in distilled water and stirred with a magnetic stirrer for 15 minute) were atomized by a special nozzle glass sprayer at heated collector glass fixed at thermostatic controlled hot plate heater. Air was used as a carrier gas to atomize the spray solution with the help of an air compressor with pressure (7 Bar) air flow rate (8 cm<sup>3</sup>/sec) at room temperature. The glass substrate was maintained at 400 °C during spraying, distance between the collector and spray nozzle was kept at (30 ± 1 cm), number of spraying (100) and time between two spraying (10 sec). Coating thickness was about 1 μm tested by optical microscopy. The 10 – finger interdigitated electrode IDE metal mask which were utilized in this work is shown in figure 1. Interdigitated aluminum ohmic metal contacts were deposited on the thin films by using vacuum evaporation technique (Edward type E306A). A schematic cross sectional view of the gas sensor testing system is illustrated in Figure 2.

The unit consists of a vacuum tight stainless steel cylindrical test chamber of diameter 163 mm and of height 200 mm with a removable bottom base made removable and O- ring sealed. It has an inlet for allowing the test gas to flow in and an air admittance valve to allow atmospheric air in after evacuation. Another third port is provided for vacuum gauge connection. A multi – pin feed through at the base of the chamber allows for electrical connections to the heater assembly as well as to the sensor electrodes via spring loaded pins. The k – type thermo-couple senses of temperature at surface of the film exposed to the analyte gas. A PC – interface multi-meter, (type UNI-T UT81B) is used to register the variation of the sensor conductance exposed to predetermined air mixing ratio. The chamber can be evacuated using a rotary pump to a vacuum of 1 × 10<sup>-3</sup> bar. A gas mixing manifold is incorporated to control the mixing ratios of the test and carrier gases prior to being injected into the test chamber. The mixing gas manifold is fed by zero air and test gas through a flow meter and needle valve arrangement.

The sensitivity (S) is shown in equation [11]:

$$S = \left| \frac{R_{gas} - R_{air}}{R_{air}} \right| \times 100\%$$

where R is the electrical resistance and the subscript “air” indicates that background is the initial dry air state and the subscript “gas” indicates the analyte gas has been introduced.

The response time (τ<sub>res</sub>) of a gas sensor is defined as the time it takes the sensor to reach 90% of maximum/minimum value of conductance upon the introduction of the reducing/oxidizing gas. Similarly, the recovery time (τ<sub>rec</sub>) is defined as the time required to recover to within 10% of the original baseline when the flow of reducing or oxidizing gas is removed [12].





**Mahdi HasanSuhail et al.**

## RESULTS AND DISCUSSION

### Electrical measurement

The plot of  $\ln\sigma$  against  $10^3/T$  (the variation of conductivity in thermal range 283 – 473K) for the as deposited films were presented in figure 3. The figure showed in general two mechanisms from which the activation energies  $E_{a1}$  and  $E_{a2}$  have been calculated. The values of  $E_{a1}$  and  $E_{a2}$  and dc conductivity at room temperature were tabulated in Table 1. The data showed that the dc conductivity decrease as of SnO<sub>2</sub> percentage increases. Also it shows that the activation energy varies as the composition percentage increased. It should be noticed that the increases in conductivity accompanied by significant decrease in the thermal activation energy [13]. These value changed from (0.123 to 0.019 eV) for  $E_{a1}$  while for  $E_{a2}$  their magnitude changed from (0.44eV to 0.234 eV) The value of  $E_{a1}$  is always less than the value of  $E_{a2}$  which is in good agreement with the result obtained by [13,14]. The observed electrical conductivity at low temperature is explained based on hopping conduction mechanism (all the trap states are filled conduction occur through the variable range hopping of the electrons in localized states). Such change in the magnitude of the activation energy may attributed to the difference in the energy gap as the percentage of composition increased, and due to the change in conductivity.

The Hall measurements showed that the pure and composition ZnO:SnO<sub>2</sub> films which are deposited on glass substrate at temperature 400 ° C for different ZnO:SnO<sub>2</sub> percentages (1:2,1:1 and 2:1) are n- type semiconductors. This result is agree with several authors (Proceketal, 2014[13], Rahmani etal,2009[14] and Pustelny etal,2012[15]). The Hall parameters for the n- type films which include Hall coefficient  $R_H$ , carrier concentration  $n_H$ , and mobility  $\mu_H$  are shown in Table 2. The data show decreased carrier concentration and mobility  $\mu_H$  of the ZnO:SnO<sub>2</sub> films by increasing SnO<sub>2</sub> percentage in compositions. Thus, the conductivity decreases with increasing SnO<sub>2</sub> percentage in composition [16] and can be understood in terms of the position of SnO<sub>2</sub> in the ZnO lattice. A decrease in  $\mu_H$  at composition may be due to the interstitial occupancy of SnO<sub>2</sub> in the ZnO lattice. The presence of SnO<sub>2</sub> at interstitial sites and grain boundaries in the form of oxide, besides decreasing grain size, may act as scattering centers and result in a decrease in the observed mobility at composition. From this result, one may conclude that adding an amount of SnO<sub>2</sub> in ZnO material enhances the conductivity of the SnO<sub>2</sub> because the conductivity of the SnO<sub>2</sub> is higher than ZnO.

### Gas Sensing Measurement

The gas sensitivity tests were performed 3 % NO<sub>2</sub> air mixing ratio and the bias voltage 6 voltage was applied for all samples.

### Sensing characteristics of SnO<sub>2</sub> and ZnO thin film towards NO<sub>2</sub> gas

Figure 4 and figure 5 show the Conductance-time variation of the pure SnO<sub>2</sub> and ZnO thin film sensor at 50, 100, 150, 200, 250, 300, 350 and 400 °C testing temperatures upon exposure to 3% NO<sub>2</sub>:air gas mixing ratio. As it is apparent from the two Figures, the resistance increase linearly with increasing temperature for the range RT to 400 °C after which it began to drop with increasing temperature. It is well known that NO<sub>2</sub> gas is a Oxidative gas and ZnO and SnO<sub>2</sub> is a n-type semiconductor (electrons are the main charge carrier). When the sample of ZnO and SnO<sub>2</sub> is exposed to No<sub>2</sub> gas, electrons are transferred from ZnO and SnO<sub>2</sub> to NO<sub>2</sub>. ZnO and SnO<sub>2</sub> molecules donate electrons to the valence band of the NO<sub>2</sub>, thus decreasing the number of electrons. This forms a space charge region at the surface of the semiconducting ZnO and SnO<sub>2</sub> resulting in an increase of the electrical resistance [17].

### Sensing characteristics of ZnO:SnO<sub>2</sub> thin films for different percentages

Figures 6-8 shows the Conductance-time variation of ZnO:SnO<sub>2</sub> composition films sensor at 50, 100, 150, 200, 250, 300, 350 and 400 °C testing temperatures upon exposure to 3% NO<sub>2</sub>:air gas mixing ratio for different ratio composition.





### Mahdi HasanSuhail et al.

It is apparent from these Figures, the resistance and sensor sensitivity to NO<sub>2</sub> gas increase linearly with increasing temperature for the range R.T. to 400 °C. After which it began to drop with increasing temperature. The optimum operating temperature for the ZnO:SnO<sub>2</sub> thin films NO<sub>2</sub> gas sensor was found to be around 400 °C.

#### Determination of Operation Temperature of the Sensor

Figure 9 Show the responsivity as a function of operation temperature (is defined as the temperature when the sensor resistance reaches a constant value) at different time for pure ZnO films under 42 ppm NO<sub>2</sub> concentration. The changing of resistance is just only influenced by the presence of the amount of some interacted gases [18,19]. The variation of the responsivity with operation temperature showing a typical negative temperature coefficient of resistance (NTCR) due to the thermal excitation of the charge carriers in semiconductor. The variation of the responsivity with operation temperature show that 200°C is the best temperature of responsivity of gas. Figure 10 Show the responsivity as a functions of operation temperature at different time for pure SnO<sub>2</sub> films under 42 ppm NO<sub>2</sub> concentration. The variation of the responsivity with operation temperature show that 250°C is the best temperature of responsivity of gas.

Figure 11 Show the responsivity as a functions of operation temperature at different time for ZnO:SnO<sub>2</sub> with 1:2 composition films under 42 ppm NO<sub>2</sub> concentration. The variation of the responsivity with operation temperature increases as the temperature increases from room temperature to 250°C. Over 250°C, sensor responsivity decreases with the increasing temperature, The gas sensor has an the operation temperature at 260°C. Figure 12 show the variation of the responsivity of the tested films at 40 mA for ZnO:SnO<sub>2</sub> with 1:1 composition films. The films responsivity increases as the temperature increases from RT to 100°C and it is showing a typical negative temperature coefficient of resistance (NTCR) due to the thermal excitation of the charge carriers in semiconductor. When the temperature exceeds 100°C, the sensor film sensitivity is slowly decreased which led to positive temperature coefficient of resistance (PTCR), this can attributed to the saturation of the conduction band with electrons evaluate from shallow donor levels that caused by oxygen vacancies. At this point an increase in temperature leads to a decrease in the electron mobility and as subsequent an increase in the resistance. The peak responsivity may be attributed to the optimum surface roughness, porosity, large surface area and large rate of oxidation. The gas sensor has an the operation temperature at 100 °C.

Figure 13 show the responsivity as a function of operating temperature of ZnO:SnO<sub>2</sub> with 2:1 for different etching time on glass for NO<sub>2</sub> gas. The films responsivity decreases as the temperature increases from RT to 100°C and when the temperature exceeds 100°C, the sensor film responsivity is slowly increased, this can attributed to the saturation of the conduction band with electrons evaluate from shallow donor levels that caused by oxygen vacancies. The gas sensor has an the operation temperature at 300 °C.

#### Response Time and Recovery Time:

Figure 14 show the response \recovery and recovery time as a function of operation temperature for pure ZnO, the reveals that the decrease of response \recovery time with increasing of operation temperature. The figure show that the (10 min) etching time sample exhibits a fast response speed of (29.82s) and recovery time (10.72s) at 200°C operation temperature. This revealed that a (10min) etching time is the best one to achieve fast response sensor. Figure 15 shows the relation between the response time and the Recovery time as a function of operation temperature of pure SnO<sub>2</sub>. The figure show that the (10min) etching time sample exhibits a fast response speed (25.964s) and recovery time (26.315s) at 250°C operation temperature, the reveals that the decrease of response \recovery time with increasing of operation temperature. Figure 16 show the relation between the response time and the Recovery time as a function of operation temperature of the ZnO:SnO<sub>2</sub> with 1:2.

The figure shows that the (10min) etching time sample exhibits a fast response speed (25.155s) and recovery time (11.956s) at 250°C operation temperature. This figure shows that the decrease of response and recovery time with







### Mahdi HasanSuhail et al.

increasing operation temperature. Figure 17 shows the relation between the response time and recovery time of ZnO:SnO<sub>2</sub> with 1:1. The figure shows that the fast response (28.88s) and recovery time (72.90s). This revealed that a quick response sensor may be found enough amount of gas for reaction. This can be attributed to faster oxidation of gas which particularly reduces the work function and the activation energy of surface reaction, may be associated with an increase in oxygen vacancies created upon ZnO:SnO<sub>2</sub> lattice. In real situations a fast response time is usually required, but a fast recovery time is not so important, and recovery time decreases above optimal time with increasing temperature. Figure 18 shows the relation between the response time and the Recovery time as a function of operation temperature of ZnO:SnO<sub>2</sub> with 2:1. The figure shows that the (10min) etching time sample exhibits a fast response speed (53.282s) and recovery time (16.335s) at 300°C operation temperature. In general the response time decreased when increased the ZnO percentage in composition.

## CONCLUSION

ZnO/SnO<sub>2</sub> composite films have been obtained on glass substrates by Spray Pyrolysis under a substrate temperature of 400°C. The physical properties of these films have been studied in detail as a function of different content. All prepared films had two activation energies ( $E_{a1}$  and  $E_{a2}$ ). Gas sensor measurement of pure ZnO and doped have high resistivity for NO<sub>2</sub>. In general the response time decreased when increased the ZnO percentage in composition and decrease in response and recovery time with increasing operation temperature.

## REFERENCES

1. Li Y Q, Yong K, Xiao H M, Ma W J, Zhang G L and Fu SY. Preparation and electrical properties of Ga-doped ZnO nanoparticles by a polymer pyrolysis method. *Mater. Lett.*, 2010; 64: 1735-1737.
2. Z. K. Tang, G. K. L. Wong, P. Yu, M. Kawasaki, A. Ohtomo, H. Koinuma and Y. Segawa. Room-Temperature Ultraviolet Laser Emission from Self-Assembled ZnO Microcrystallite Thin Films. *Applied Physics Letters*, 1998; 72 (25): 3270-3272.
3. Y. B. Li, Y. Bando and D. Golberg. ZnO Nanoneedles with Tip Surface Perturbations: Excellent Field Emitters. *Applied Physics Letters*, 2004 ; 84 (18): 3603-3605.
4. Lee, S. H., Lee, S. S., Choi, J. J., Jeon, J. U. and Ro, K.. Fabrication of a ZnO Piezoelectric Micro Cantilever with a High-Aspect-Ratio Nano Tip, *Microsystem Technologies*, 2005; 11(6): 416-423.
5. Xu, J. Q., Pan, Q. Y., Shun, Y. A. and Tian, Z. Z. Grain Size Control and Gas Sensing Properties of ZnO Gas Sensor. *Sensors and Actuators B: Chemical*, 2007; 66(1-3): 277-279.
6. Cathleen A., Hoel T. and Thomas O. Mason. Transparent conducting oxides in the ZnO-In<sub>2</sub>O<sub>3</sub>-SnO<sub>2</sub> system. *Chem. Matter.*, 2010; 22: 3569-3579.
7. Buosciolo, A., 2007. Tin Oxide Thin Films in Opto-Chemical Sensing: Preparation, Surface Morphology, Near Field, Optical Properties and Testing, Ph.D. thesis, University of Naples "Federico II."
8. Bagga, S., 2007. Gas sensor-studies on sensor film deposition, ASIC design and testing, M.Sc. Thesis, Indian institute of science, Bangalore, India.
9. C. Wang, L. Yin, L. Zhang, D. Xiang and R. Gao. Metal Oxide Gas Sensors: Sensitivity and Influencing Factors, *Sensors*, 2010; 10: 2088.
10. Taguchi, N.. A metal oxide gas sensor, Japan Patent, 1962; No. 45-38200.
11. Barsan, N. and Weimar, U.. Understanding the fundamental principles of metal oxide based gas sensors; the example of CO sensing with SnO<sub>2</sub> sensors in the presence of humidity. *J. Phys.: Condens. Matter*, 2003; 15: 813.
12. Capone, S., A. Forleo, L. Francioso, R. Rella, P. Siciliano, J. Spadavecchia, D. S. Presicce and A. M. Taurino. Solid state gas sensors: state of the art and future activities. *Journal of Optoelectronics and Advanced Materials*, 2003; 5: 1335.





**Mahdi HasanSuhail et al.**

13. Procek, M., T. Pustelny, A. Stolarczyk, and E. Macoak. Studies of changes in electrical resistance of zinc oxidenanostructures under the influence of variable gaseous environments. Bulletin of the polish academy of sciences technical sciences, 2014; 62(4): 635-639.
14. Rahmani, M. B., S. H. Keshmiri, M. Shafiei, K. Latham and K. K.-Z. J. du Plessis. Transition from n- to p- type of spray pyrolysis deposited Cu doped ZnO thin films for NO<sub>2</sub> sensing. Sensor letters, 2009; 7(4): 1-8.
15. Pustelny, T., M. Procek, E. Maciak, A. Stolarczyk, S. Drewniak, M. Urbanczyki, M. Setkiewicz, K. Gut, and Z. Opilski. Gas sensors based on nanostructures of semiconductors ZnO and TiO<sub>2</sub>. Bulletin of the Polish Academy of Sciences Technical Sciences. 2012; 60(4): 853-859.
16. Masamichi Ippommatsu, Hirokazu Sasaki, Hiroaki Yanagida. Sensing mechanism of SnO<sub>2</sub> gas sensors. Journal of Materials Science, 1990; 25(1): 259-262.
17. Halek, P., H. Teterycz, G. Halek, P. Suchorska, K. Wiśniewski. Sensing performance of heterojunction gas sensors based on SnO<sub>2</sub>, WO<sub>3</sub> and ZnO metal oxides. IMCS 2012 – The 14th International Meeting on Chemical Sensors, 1297-1300, DOI 10.5162/IMCS2012/P2.0.12
18. Struka, P., T. Pustelny, K. Goaszewskab, M.A. Borysiewicz and A. Piotrowska. Gas Sensors Based on ZnO Structures. Acta Physica Polonica, 2013; A 124: 567-569.
19. MokhtarHjiri, Lassaad El Mir, Salvatore GianlucaLeonardi Nicola Donato and Giovanni Neri. CO and NO<sub>2</sub> Selective Monitoring by ZnO-Based Sensors. Nanomaterials, 2013; 3: 357-369.

**Table 1: E<sub>a1</sub> and E<sub>a2</sub> and dc conductivity for all samples under investigations.**

Sample	Percentages	E <sub>a1</sub> (eV)	Range (K)	E <sub>a2</sub> (eV)	Range (K)	σ <sub>RT</sub> (Ω.cm) <sup>-1</sup>
SnO <sub>2</sub>	pure	0.123	283-363	0.440	363-473	0.336 x 10 <sup>-4</sup>
ZnO	pure	0.264	283-363	0.486	363-473	4.10 x 10 <sup>-4</sup>
SnO <sub>2</sub> :ZnO	1:1	0.131	283-363	0.206	363-473	0.725 x 10 <sup>-4</sup>
SnO <sub>2</sub> :ZnO	1:2	0.031	283-363	0.374	363-473	2.23 x 10 <sup>-4</sup>
SnO <sub>2</sub> :ZnO	2:1	0.019	283-363	0.234	363-473	0.25 x 10 <sup>-4</sup>

**Table 2: Hall coefficient R<sub>H</sub>, carrier concentration n<sub>H</sub>, and mobility μ<sub>H</sub>.**

Sample	Percentage	R <sub>H</sub> (cm <sup>2</sup> /C) x 10 <sup>3</sup>	n <sub>H</sub> (cm <sup>-3</sup> ) x 10 <sup>15</sup>	μ <sub>H</sub> (cm <sup>2</sup> /v.sec)
ZnO	pure	-3.201	1.950	77.78
SnO <sub>2</sub>	pure	-1.720	3.629	287.4
SnO <sub>2</sub> :ZnO	1:2	-0.5455	11.44	2.425 x 10 <sup>-5</sup>
SnO <sub>2</sub> :ZnO	1:1	-2888	0.002161	29.97
SnO <sub>2</sub> :ZnO	2:1	-2.287	2.729	89.02





Mahdi HasanSuhail et al.

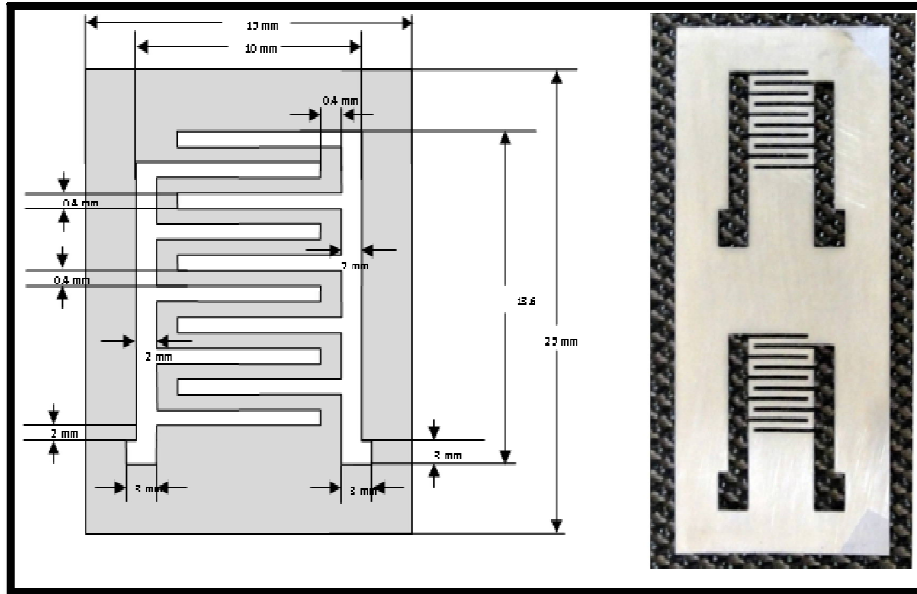


Figure 1: A schematic diagram of the IDE mask utilized in this work.

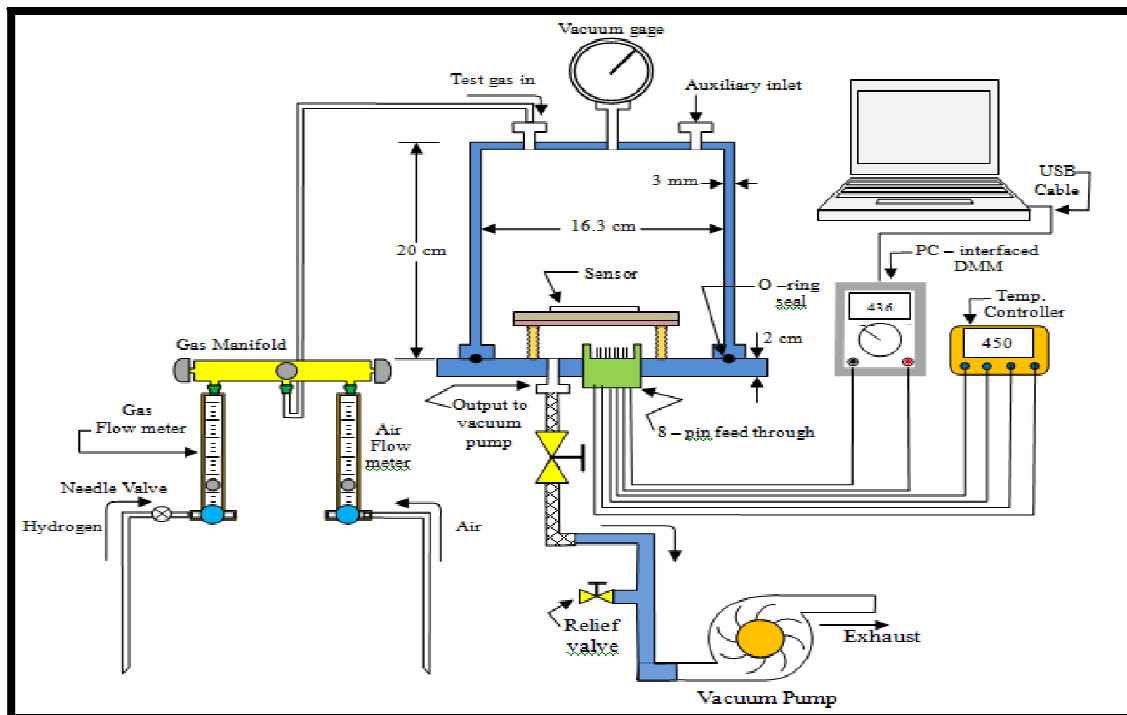


Figure 2: Gas sensor testing system.





Mahdi HasanSuhail et al.

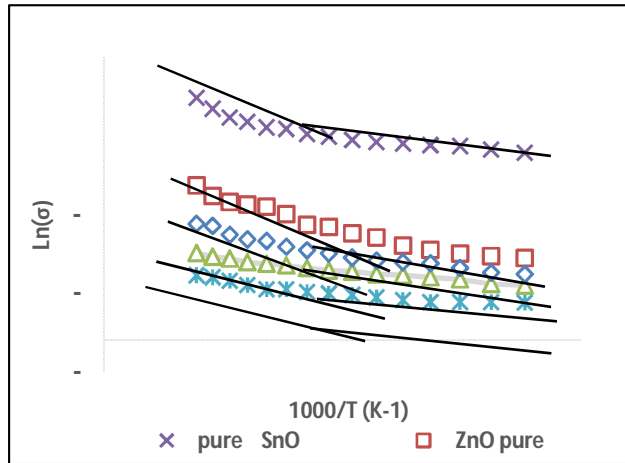


Figure 3:  $\text{Ln}\sigma$  against  $10^3/T$  for pure and composition  $\text{ZnO}:\text{SnO}_2$  thin films with different percentage.

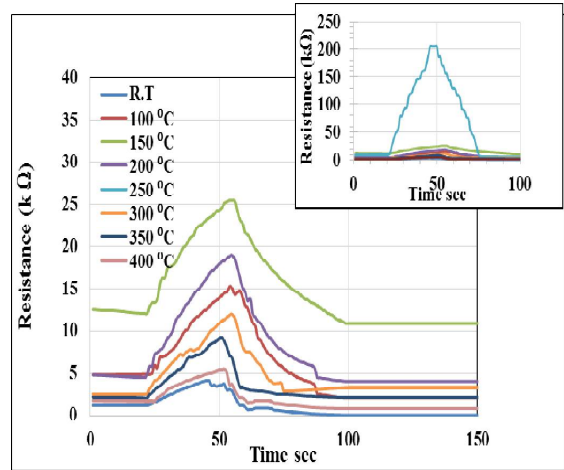


Figure 4:  $\text{NO}_2$  gas sensing behavior of the pure  $\text{SnO}_2$  thin film at different temperatures.

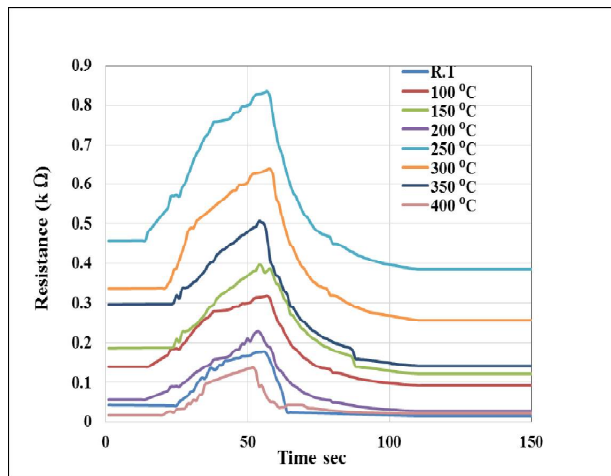


Figure 5:  $\text{NO}_2$  gas sensing behavior of the pure  $\text{ZnO}$  thin film at different temperatures.

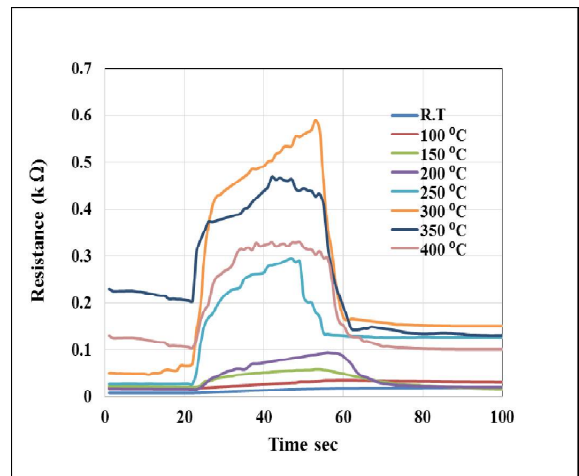


Figure 6:  $\text{NO}_2$  gas sensing behavior of the  $\text{ZnO}:\text{SnO}_2$  composition thin film with 1:2 at different temperatures





Mahdi HasanSuhail et al.

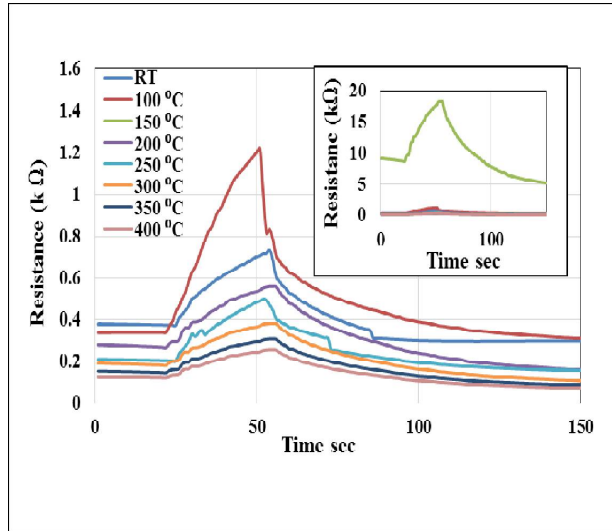


Figure 7: NO<sub>2</sub> gas sensing behavior of the ZnO:SnO<sub>2</sub> composition thin film with 1:1 at different temperatures.

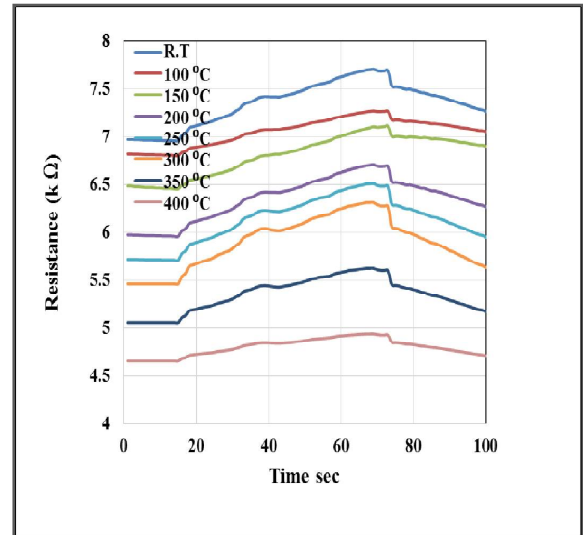


Figure 8: NO<sub>2</sub> gas sensing behavior of the ZnO:SnO<sub>2</sub> composition thin film with 2:1 at different temperatures

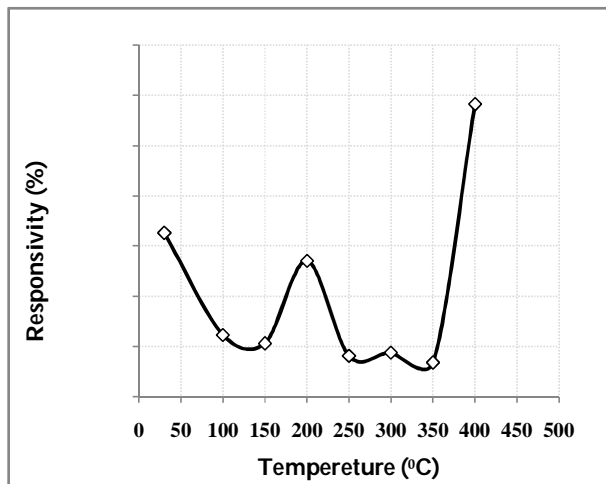


Figure 9: Variation of responsivity with the operating temperature of pure ZnO for different etching time.

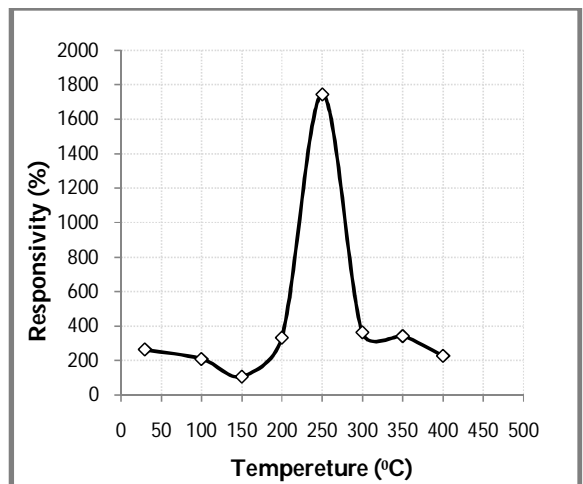


Figure 10: Variation of responsivity with the operating temperature of pure SnO<sub>2</sub> for different etching time.





Mahdi HasanSuhail et al.

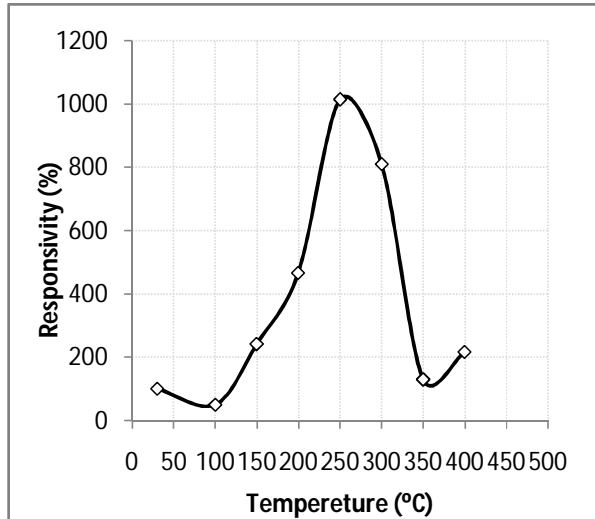


Figure 11: Variation of responsivity with the operating temperature of ZnO:SnO<sub>2</sub> with 1:2 composition for different etching time.

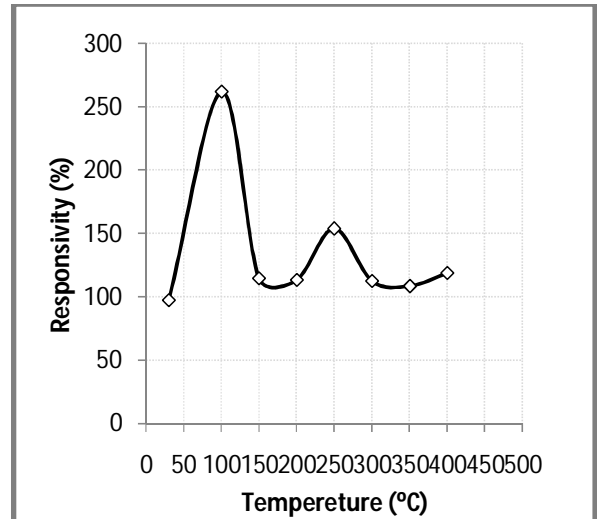


Figure 12: Variation of responsivity with the operating temperature of ZnO:SnO<sub>2</sub> with 1:1 composition for different etching time .

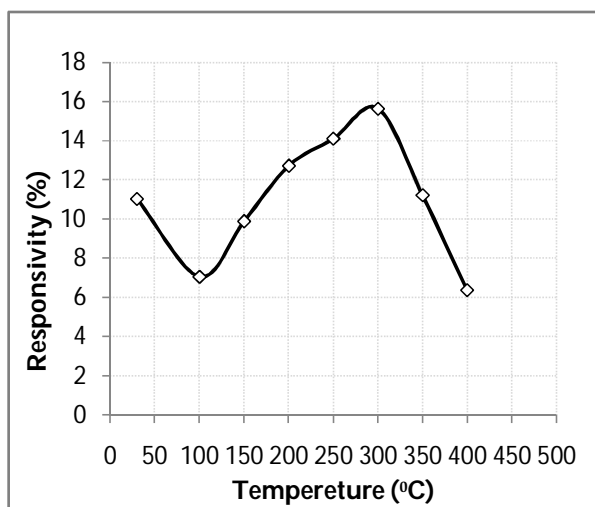


Figure 13: Variation of responsivity with the operating temperature of ZnO:SnO<sub>2</sub> with 2:1 composition for different etching time

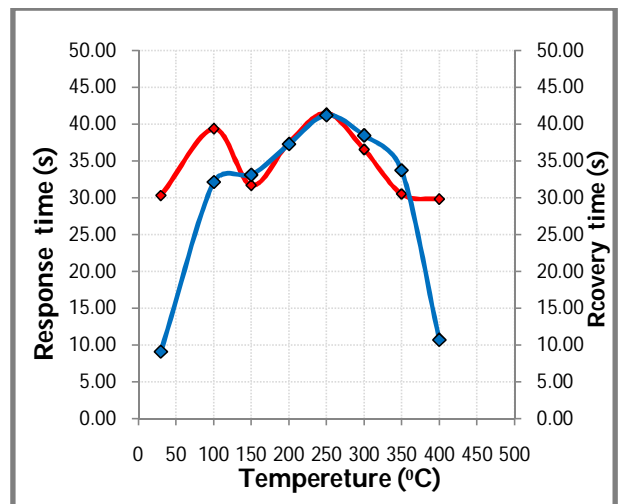


Figure 14: The variation of Response time and Recovery time with operating temperature of pure ZnO for NO<sub>2</sub> gas





Mahdi HasanSuhail et al.

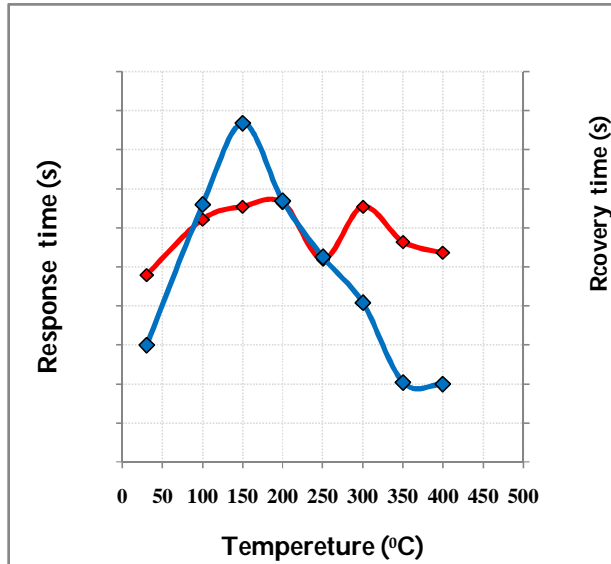


Figure 15: variation of Response time and Recovery time with operating temperature of pure SnO<sub>2</sub> for NO<sub>2</sub> gas.

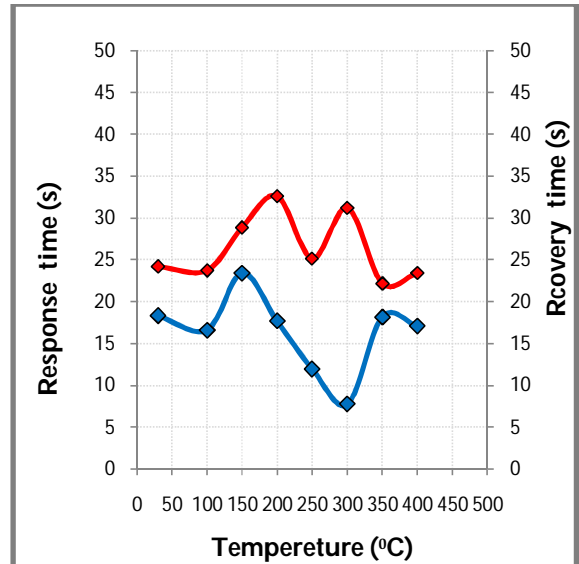


Figure 16: variation of Response time and Recovery time with operating temperature of ZnO:SnO<sub>2</sub> with 1:2 for NO<sub>2</sub> gas

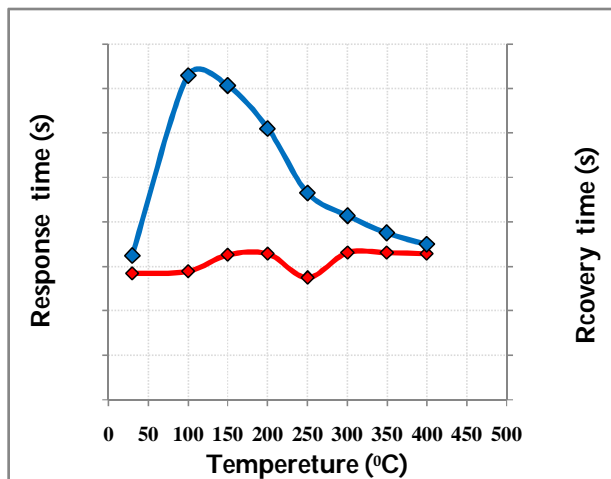


Figure 17: The variation of Response time and Recovery time with operating temperature of ZnO:SnO<sub>2</sub> with 1:1 for NO<sub>2</sub> gas.

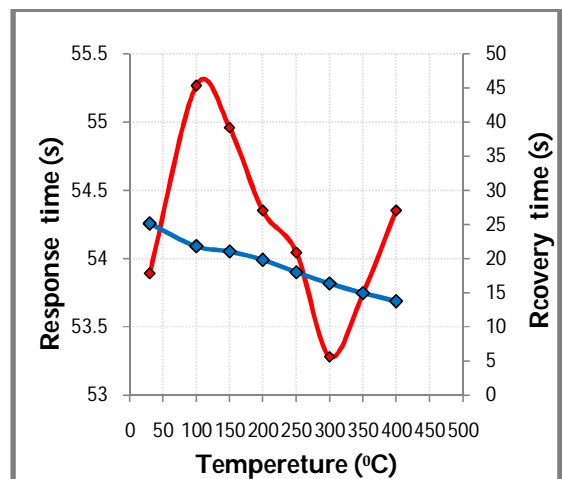


Figure 18: Variation of Response time and Recovery time with operating temperature of ZnO:SnO<sub>2</sub> with 2:1 for NO<sub>2</sub> gas





## Electrical Properties of PVA:PEG/MnCl<sub>2</sub> Thin Film Composites

Abeer Mohammed<sup>2</sup>, Mohammed Ghazi<sup>2</sup> and Mahdi Hasan suhail<sup>1\*</sup>

<sup>1</sup>Dept. of Physics, College of science, University of Baghdad-Iraq.

<sup>2</sup>Dept. of Physics, College of science, University of Anbar-Iraq.

Received: 24 July 2016

Revised: 19 Aug 2016

Accepted: 18 Sep 2016

### Address for correspondence

Mahdi HasanSuhail

Dept. of Physics, College of Science,

University of Baghdad- Iraq.

Email: mhsuhail@yahoo.com



This is an Open Access Journal / article distributed under the terms of the **Creative Commons Attribution License (CC BY-NC-ND 3.0)** which permits unrestricted use, distribution, and reproduction in any medium, provided the original work is properly cited. All rights reserved.

### ABSTRACT

PVA:PEG/MnCl<sub>2</sub>Composites have been prepared by adding (MnCl<sub>2</sub>) to the mixture of the poly vinyl alcohol(PVA) and poly ethyleneglycol(PEG) with different weightpercentages (0,2,4,6,8 and 10)wt.% by using casting method.The type of charge carriers, concentration ( $n_H$ )and Hall mobility ( $\mu_H$ ) have been estimated from Hall measurements and show that the films of all concentration have a negative Hall coefficient . In D.C measurement increase temperature leads to decrease the electrical resistance.The D.C conductivity for the composites increases with the increasing of the concentration of additive particles and temperature.The activation energy decreases for all composites with increasing the concentration of the additive particles. The A.C conductivity increases with increasing ofthe frequency and the concentration of MnCl<sub>2</sub> particles. The A.C electrical properties show that the dielectric constant and dielectric loss of thecomposites decrease with increasing of the frequency.

**Keywords :** Electrical properties; PEG matrix; MnCl<sub>2</sub> filler; Composite; Field frequency; Dielectric constant; AC-Conductivity; Polarization.

### INTRODUCTION

Polymeric materials were given a great interest, such as the ease of fabrication, low cost, light weight, ease of chemical modification and excellent insulation or good conduct ion properties,in many industrial application sowing to their desirable characteristics and properties which made them favorable compared to other commercial materials[1,2]. Considerable efforts focused on an applied research in the field of polymer compositesto turn these materials into useful products for electronic industry. This is mainly because they possess interesting properties which can be utilized to develop a lot of related potentials. Recently, many reports have appeared in literature dealing with the







**Mahdi HasanSuhail et al.**

effects of the filler concentration, frequency of the applied field and temperature on the physical properties of the conductive polymer composite such as impedance, dielectric behavior and electrical conduction [3-5]. Many studies showed that physical properties of polymers clearly depended on many factors concerning their preparation methods and chemical structure[6]. The thermal stabilities of crystalline PEG-MnCl<sub>2</sub> system depend on the salt molar ratio, the PEG molecular weight, the choice of the solvent and the concentration, and the thermal history. The melting temperatures also depend on the nature of the complex salts[7].

The poly vinyl alcohol (PVA) is a polymer with exceptional properties such as water solubility, biodegradability, biocompatibility, non-toxicity, and non-carcinogenic that possesses the capability to form hydrogels by chemical or physical methods [8]. PVA has high enough tensile strength and satisfactory flexibility. The PEG polymer has a wide range of application including the use as pharmaceutical recipients, food additives and plasticizers[9]. Studies were centered on the enhancement of its ionic conductivity with the aim of developing the material to have the promising electrical application[9,10]. In the present study, the electrical properties of PVA:PEG/MnCl<sub>2</sub> composites is investigated as a function of applied frequency and concentration to use this Polymeric materials in many industrial application showing their desirable characteristics and properties which made them favorable compared to other commercial materials.

## MATERIALS AND METHODS

The materials used in the present work were Poly-vinyl alcohol (PVA) and Poly-ethylene glycol (PEG) with addition of different concentrations from (MnCl<sub>2</sub>). All the polymer composite films were prepared by casting from solution. Equal weights of PVA and PEG with ratio (50:50)wt.% for one gm of PVA and one gm of PEG was first dissolved in the common solvent (30 mL of distilled water) and then both the polymers were homogeneously mixed using a magnetic stirrer at the constant temperature at (50)°C for (12)hours. Complete homogeneous solution was casted on Teflon petri-dishes and left for the evaporation of the solvent. The resulting PVA:PEG films were dried up to (4)days at room temperature in the desiccators to remove the traces of solvent, and then lifted out of the petri-dish for further analysis. On the other hand, MnCl<sub>2</sub> was dissolved in double distilled water in the same condition. The resulting solution of MnCl<sub>2</sub> particles were added to the polymer blend PVA:PEG solution with mass fraction (0, 2, 4, 6, 8, 10)wt.%. mixed using a magnetic stirrer at the constant temperature at 100°C for 12hours until a homogenous solution is obtained. The resulting solution was then casted on glass slides and leave over it for about 72hr. After drying, the films were kept in vacuum desiccators until use. The thickness of films were in ranging from 0.15 to 0.2 μm.

## RESULTS AND DISCUSSION

### Hall Effect

The type of charge carriers, concentration ( $n_H$ ) and Hall mobility ( $\mu_H$ ), have been estimated from Hall measurements. The films of all concentration have a negative Hall coefficient ( $n$ -type charge carriers). Table (1) illustrates electrical parameters for (PVA:PEG/MnCl<sub>2</sub>) films at different concentration of MnCl<sub>2</sub> (2, 4, 6, 8 and 10)wt.%. It is noted from Table 1 that the carriers concentration ( $n_H$ ) increases while Hall mobility ( $\mu_H$ ) decreases with the increase of the concentration.

### D.C conductivity

The variation of D.C electrical conductivity of PVA:PEG as a function of (MnCl<sub>2</sub>) particles concentrations is shown in figure 1. From this figure, the electrical conductivity increases with the increase of the concentration of (MnCl<sub>2</sub>) particles. The increase in D.C electrical conductivity of composite is a result to the rearrangement of (MnCl<sub>2</sub>) particles throughout the polymer matrix[11]. The electrical conductivity could be increased as a result of increasing of electronic charge carriers which can be increased due to increasing filler content [12].





**Mahdi HasanSuhail et al.**

### The Activation Energy of (PVA:PEG/MnCl<sub>2</sub>) composites

The relation between  $\ln(\sigma)$  and the inverse absolute temperature for (PVA:PEG/MnCl<sub>2</sub>) composites shown in Figure 2A and 2B.

The activation energy was calculated by using equation [13] :

$$\sigma = \sigma_0 \exp\left(-E_{act} / K_B T\right)$$

where:

$\sigma$ : electrical conductivity at temperature T

$\sigma_0$ : electrical conductivity at absolute zero temperature

$K_B$ : Boltzmann constant

$E_{act}$ : Activation Energy

The high values existence for activation energy in state pure polymer.

When adding MnCl<sub>2</sub> particles, the values of the activation energy decrease for all (PVA:PEG/MnCl<sub>2</sub>) composites as a result of the impact of space charge. The addition of MnCl<sub>2</sub> creates local energy levels in the forbidden energy gap which act as traps for charge carriers, which move by hopping among these levels. When increasing MnCl<sub>2</sub> particles concentrations, the activation energy decreases as a result of the increase of local centers, as shown in Table 2.

### The A.C electrical properties of the Composite

Figure 3A shows the variation of the dielectric constant of (PVA, PEG and PVA:PEG) composites with frequency. Figure 3B shows the variation of the dielectric constant of (PVA:PEG-MnCl<sub>2</sub>%) composites with frequency. This figure shows that the dielectric constant decrease when increasing the frequency. This is attributed to decreasing of space charge polarization with respect to the total polarization. The space charge polarization becomes more contributing type of polarization at low frequencies, and less contributing with the increase of frequency [14]. The other types of polarizations appear at subsequent frequencies. The ionic polarization reacts slightly to the variation in the field frequencies compared with electronic polarization; this is because the mass of ion is greater than that of the electron. The electrons respond even to the high frequencies of the field vibrations. The low mass of electron makes the electronic polarization was the only type of polarization at higher frequencies, this makes the dielectric constant approximately constant for all samples at high frequencies [15].

Figure 4A show the dielectric loss of (PVA, PEG and PVA:PEG) as a function of frequency. The effect of adding MnCl<sub>2</sub> particles on the dielectric loss at room temperature (30°C) is shown in Figure 4B. It is clear from the figures that dielectric loss decreases with frequency. The larger value of dielectric loss at low frequency could be due to the mobile charges within the polymer backbone. This is attributed to the decrease of the space charge polarization contribution when increasing the frequency [16]. From the behavior the dielectric constant ( $\epsilon_1$ ) and the dielectric loss ( $\epsilon_2$ ), one can observe a strong frequency dependence especially at low frequencies, which reflects the behavior of the polar materials. It is clearly seen that both ( $\epsilon_1$ ) and ( $\epsilon_2$ ), increase with salt concentration and decrease with the frequency of the electric field and they have a high value at low frequencies and a low value at high frequencies. These results suggest that polar entities of the composite are effectively operating under the electric field. This behavior can be understood as follows: at low frequencies, the time interval required for the molecular dipoles of the polymer to response to the applied electric field is sufficient.

This enables these dipoles to follow the oscillating field, i.e., the orientation polarization is high, which leads to enhance the dielectric constant values. While at high frequencies, the time interval needed for the dipoles to response to the applied electric field is insufficient. Hence, the dipoles are unable to follow the rapid alternation of the oscillating field, i.e., the orientation polarization drops down greatly and leads to very small value of ( $\epsilon_1$ ) and ( $\epsilon_2$ ) at high frequencies. [16] which is similar to the behaviour for polar polymer and materials [17]. This dielectric behaviour





**Mahdi HasanSuhail et al.**

explains the increasing in the AC conductivity at high concentration [18]. The variation of the conductivity for (PVA, PEG and PVA:PEG) composites with frequency is shown in Figure 5A and the variation of the conductivity for (PVA:PEG-MnCl<sub>2</sub>) composites with frequency shown in Figure 5B. The conductivity is increasing when increasing the frequency for all different concentration of MnCl<sub>2</sub> nanoparticles for (PVA:PEG/MnCl<sub>2</sub>) composites. These figures show that A.C electrical conductivity increases with the increase of frequency, this is attributed to the space charge polarization that occurs at low frequencies, and also to the motion of charge carriers by hopping process. The increasing of the conductivity is small at high frequencies; this is attributed to the electronic polarization and the charge carriers which travel by hopping process [19].

## CONCLUSION

The research work presented in this paper deals with the electrical properties of PVA:PEG/MnCl<sub>2</sub> composite. The electrical conductivity, dielectric behavior of these polymeric membranes was studied as a function of MnCl<sub>2</sub> concentration and the applied frequency. Frequency and MnCl<sub>2</sub> concentration affect on the electrical and dielectric behavior of the composite and explained on the basis of the interfacial (space charge) polarization, dipolar polarization and on the decrease of the hindrance of the polymer matrix. Activation energy for all composites decreased with increasing of concentration. Dielectric constant and dielectric loss decreased with increasing of frequency and increase with increasing of concentration but A.C electrical conductivity  $\sigma_{a.c}$  increased with increasing of frequency and MnCl<sub>2</sub> concentration due to enhancement of ionic conduction in the membrane bulk for all samples.

## REFERENCES

1. Mort J, Electrical properties of polymer (John Wiley & Sons) New York; 1982.
2. Kohlman RS, Joo J, Epstein AJ. Conducting Polymers: Electrical Conductivity, Physical Properties of Polymers Hand book, in Physical Properties of Polymers Handbook (J.E. Mark, Ed., AIP) New York; 1996, vol. 453.
3. Newton DC, Craig Hill JRJ. Materials Science New York; 1993.
4. Wright VJ. Macromolecular Science Chemistry 1989; A26:519.
5. Albinssi, Mellandar B. on Polymer, New York; 1991.
6. Perepechko I. An Introduction to polymer physics, Mir Publisher, Moscow; 1981
7. Herman F, Donald F., Charles G. Encyclopedia of chemical technology (3<sup>rd</sup> Edition. John Wiley & Sons. inc., New York 1982, vol.18.
8. Patachia S. Blends based on poly(vinyl alcohol), the products based on this polymer, in Vasile C AKulshreshtha, K. Eds, in Handbook of polymer blends and composites, (Rapra Technology) Shawbury; 2003.
9. Abusamra MM, Impedance dielectric properties of ions selective PVC membrane electrodes. M.Sc thesis, university of Jordan, Amman Jordan; 1982.
10. Salih A, Ramadin A, Zihlif Y, A electrical properties of poly(Ethylene Oxide) Polymer doped by MnCl<sub>2</sub>, IBN AL-HAITHAM, J. for pure & Appl. sci. 2010; 23:1.
11. Abu Hijleh M, The electrical behaviour of mica-polystyrene composite, M.Sc. thesis, university of Jordan, Amman Jordan; 1996.
12. Nagham Adel Al-Buissam, study the Effect of MgO on the electrical and optical properties of (PVA-PEG), MSc. thesis, university of Babylon; 2014.
13. Ahmed M.S, Zinlif A.M, The electrical conductivity of Polypropylene and Nickel-Coated Carbon Fiber composite, J. mater. sc; 1992:25:15.
14. Indris S, Heitjans P, Ulrich M, Bunde A. AC and DC conductivity in Nano Crystalline Li<sub>2</sub>O:B<sub>2</sub>O<sub>3</sub> composites: Experimental Results and Theoretical Models, Z. Phy. Chem. 2005; 219:89.
15. Chiteme C, Lowther S, Harrison S. Science of polymer 2005; 219:89.
16. Streetman B.G. Bonerjee S. Solid state electronic devices, 5<sup>th</sup> Edition Engle Wood cliffs, Ni prentice illall; 2000.
17. VaValek L.H. Materials science for Engineering, 3<sup>rd</sup> edition, Amsterdam; 1975.





**Mahdi HasanSuhail et al.**

18. M.Abu Samra,M.R,Bitar,A.Zihlif,A.M,Jaber,A.M.Applied Physics Communications 1983;3:225

19. Shahin M.AL,Haj-Abdullah,Zihlifn,M.Farris,A.R,Journal of Polymer materials.2005;12:1995.

**Table 1: Illustraes electrical parameters for (PVA:PEG/MnCl<sub>2</sub>)**

Sample	$\sigma_{RT} \times 10^{-6}$ ( $\Omega^{-1} \cdot \text{cm}^{-1}$ )	$R_H \times 10^5$	$n$ ( $\text{cm}^{-3}$ ) $\times 10^{13}$	type	$\mu_H$ ( $\text{cm}^2/\text{v} \cdot \text{sec}$ )
PVA	7.73	140	0.045	p	108.22
PEG	5.74	-225	0.028	n	129.16
PVA:PEG	4.46	-30.5	0.205	n	13.62
<b>PVA:PEG With MnCl<sub>2</sub></b>					
2%	5.43	-20.5	0.305	n	11.14
4%	6.94	-3.80	1.643	n	2.64
6%	8.80	-0.924	6.764	n	0.81
8%	0.123	-0.323	19.344	n	0.40
10%	0.173	-0.083	75.211	n	0.14

**Table 2 : Activation energy for(PVA:PEG/MnCl<sub>2</sub>)composites**

Sample	$E_{a1}$ (eV)	Range (K)	$E_{a2}$ (eV)	Range (K)	$\sigma_{RT} \times 10^{-6}$ ( $\Omega^{-1} \cdot \text{cm}^{-1}$ )
PVA	0.026	303-353	0.367	353-433	7.73
PEG	0.034	303-353	0.395	353-433	5.74
PEG:PVA(0%)	0.047	303-353	0.492	353-433	4.46
2 %	0.045	303-353	0.474	353-433	5.43
4 %	0.044	303-353	0.450	353-433	6.94
6 %	0.037	303-353	0.428	353-433	8.80
8 %	0.022	303-353	0.396	353-433	0.123
10 %	0.022	303-353	0.345	353-433	0.173





Mahdi HasanSuhail et al.

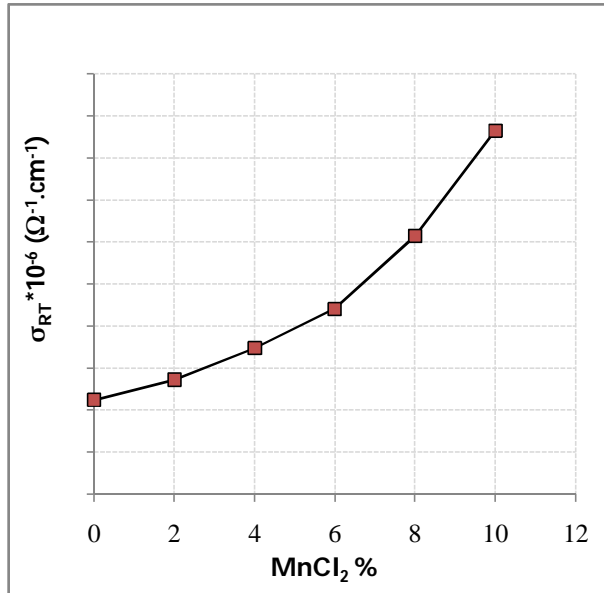


Figure (1): D.C conductivity with different concentration of MnCl<sub>2</sub> particles.

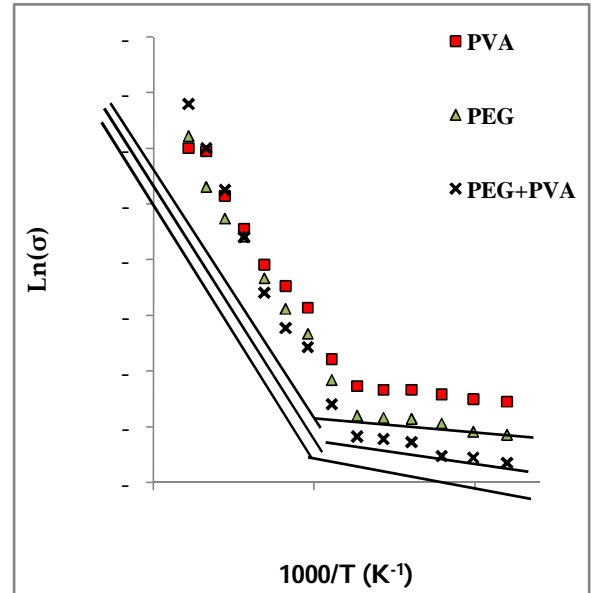


Fig.2(A): The relation between ln(σ) and the inverse absolute temperature for (PVA, PEG and PVA:PEG) composites.

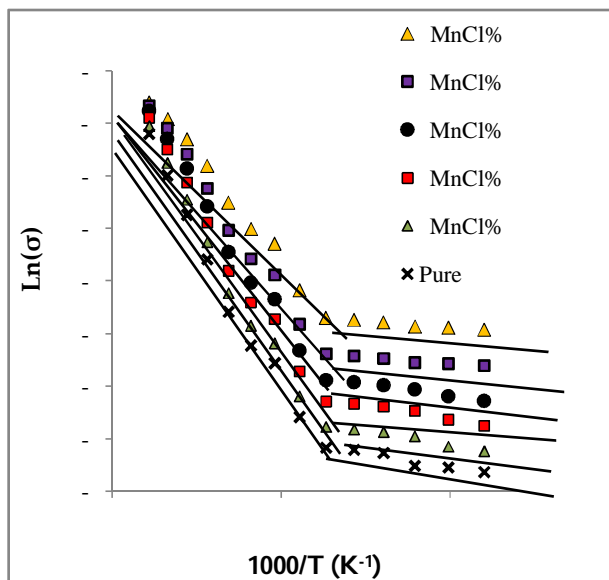
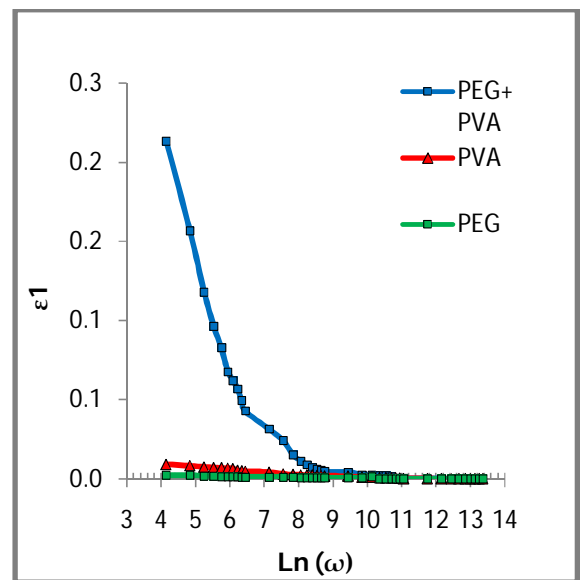


Fig.2(B): The relation between ln(σ) and the inverse absolute temperature for (PVA:PEG/MnCl<sub>2</sub>) composites.

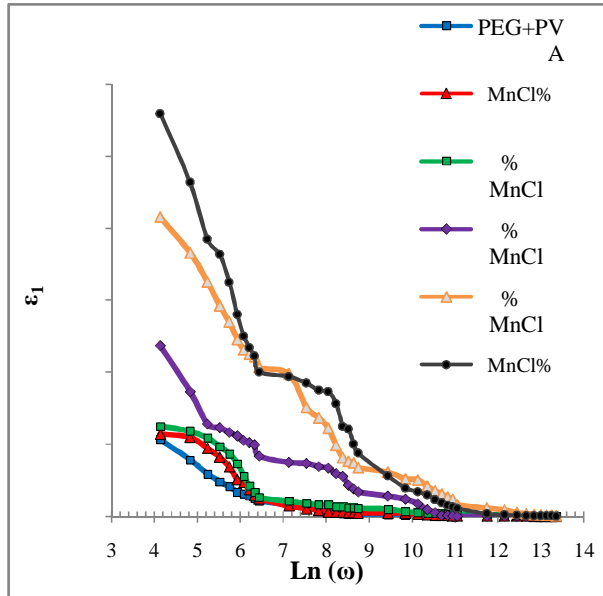


Figure(3A): The variation of the dielectric constant with frequency.





Mahdi HasanSuhail et al.



Figure(3B): The variation of the dielectric constant of (PVA:PEG- (MnCl<sub>2</sub>%)) with frequency.

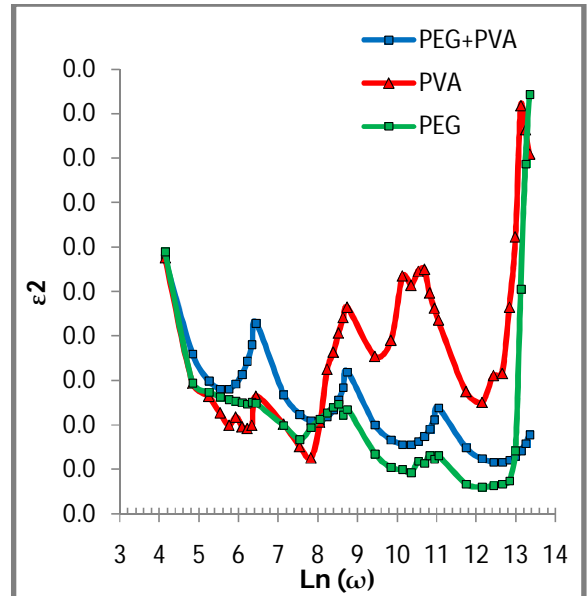


Figure (4A): Variation of the dielectric loss with frequency for(PVA,PEG and PVA:PEG) composites.

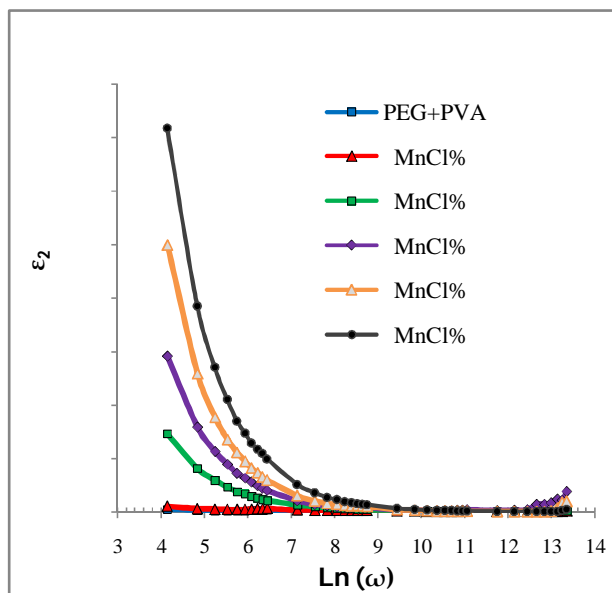


Figure (4B): Variation of the dielectric loss with frequency for(PVA:PEG-MnCl<sub>2</sub>) composites.

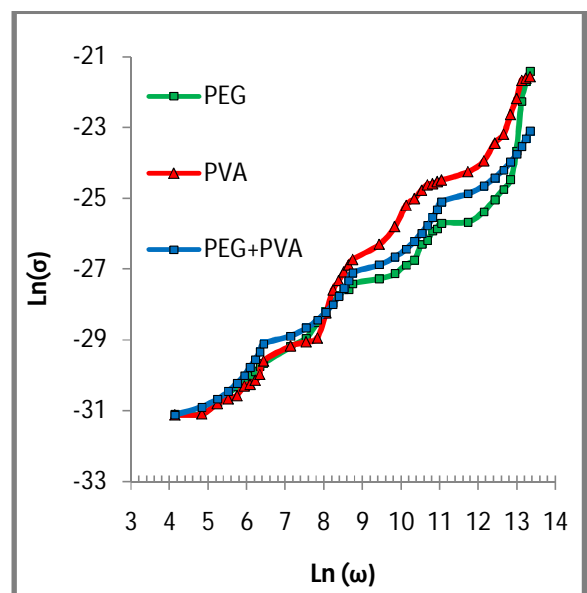


Figure (5A): The variation of the conductivity for (PVA-PEG-PVA:PEG) composites with frequency.





Mahdi HasanSuhail et al.

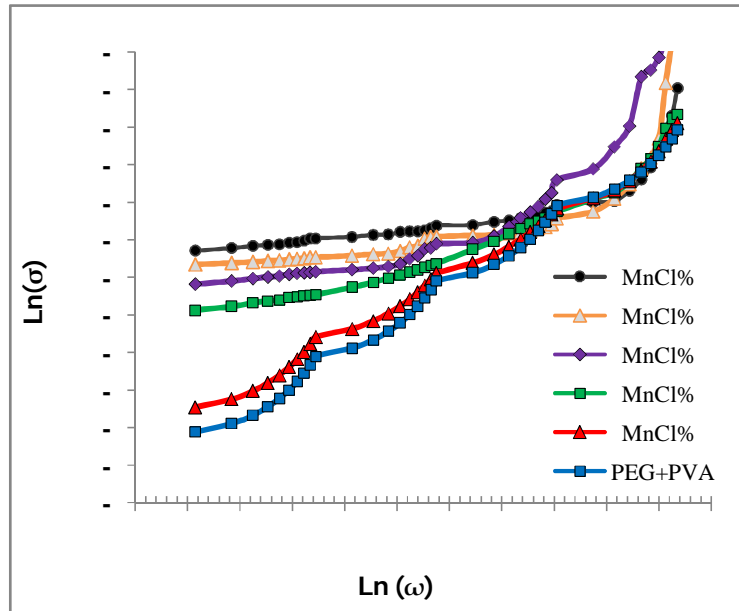


Figure (5B): The variation of the conductivity for (PVA-PEG-PVA:PEG) composites with frequency





RESEARCH ARTICLE

## Monitoring of Iron Concentration in Ground Water of Lucknow City, Uttar Pradesh

Aisha siddiqui<sup>1\*</sup>, Zulfiquar Ali<sup>2</sup> and S.Malhotra<sup>3</sup>

<sup>1</sup>Research Scholar, Department of Chemistry, Integral University, Kursi road, Lucknow,India

<sup>2</sup>Assistance Professor, Department of Chemistry, Integral University, Kursi road, Lucknow,India.

<sup>3</sup>Ex Scientist, Phytochemistry Division, National Botanical Research Institute, India

Received: 9 July 2016

Revised: 18 Aug 2016

Accepted: 19 Sep 2016

### Address for correspondence

Aisha Siddiqui  
Research Scholar,  
Department of Chemistry,  
Integral University, Dashauli, Kursi Road, Lucknow.  
Uttar Pradesh,226021,India.  
Email: aishawali994@gmail.com



This is an Open Access Journal / article distributed under the terms of the **Creative Commons Attribution License (CC BY-NC-ND 3.0)** which permits unrestricted use, distribution, and reproduction in any medium, provided the original work is properly cited. All rights reserved.

### ABSTRACT

In this study an attempt is made to analyze the concentration of heavy metal in ground water samples collected from different areas (commercial, residential, agriculture, industrial) of Lucknow. Samples were collected and analyzed for Cr, Cu, Fe, Ni, and Zn by atomic absorption spectrophotometer. The results were compared with BIS and WHO limits. The result shows that iron concentration was found higher than the acceptable limits set by BIS in S<sub>1</sub>, S<sub>2</sub>, S<sub>6</sub>, S<sub>8</sub>, S<sub>11</sub>, S<sub>12</sub>, S<sub>14</sub>, S<sub>15</sub>, ground water samples which indicate the deterioration of ground water quality. Mean concentration of iron was found higher in commercial area. Whereas concentration of other heavy metals analyzed in ground water samples were found within the acceptable limit of drinking water set by WHO and BIS.

**Keywords :** Ground water, Heavy metal, Iron concentration, Lucknow city,

### INTRODUCTION

Water is one of the basic amenity and universal solvent without which existence of life cannot be imagined on earth [19,20,21]. Among the two main sources of drinking water i.e. ground water and surface water, ground water is the major source of water supply for domestic purposes in the urban and rural parts of India. Ground water was taken as the safest form of water for drinking as it is not in direct contact of surface activities. Natural impurities of rainwater





**Aisha Siddiqui et al.**

get removed through soil strata when in restore ground water system, that's why ground water is less susceptible to contamination when compared to surface water. But with passage of time level of contamination in ground water is increasing with increase in pollution level of surface [1,2,3]. In our country groundwater is used intensively for irrigation and industrial purposes, and variety of land and water-based human activities are polluting it. Excess use of fertilizers and pesticides not only increase productivity, but it also increases pollution level in the groundwater on a large scale[11,12,13]. Groundwater quality deteriorate due to diffusion of contaminant such as chemicals from the agricultural fields, septic tanks, dumping areas etc., from surface which covers it [8,9,10]. Landfills are also responsible for deterioration of groundwater quality not only in India but throughout the world [16,17,18].

Iron is the natural occurring element and makes up five percent of earth crust. Iron enters in ground water by dissolving from the rocks and minerals that form aquifers. Internal corrosion of metallic pipes is one of the factors responsible for concentration of iron in drinking water [6,7]. Ferrous and ferric are the two main form of iron, present in water. Ferric form is insoluble whereas ferrous form of iron is soluble. In ground water iron is generally present in ferrous form and ferric form is generally present in surface water as it is oxidized by oxygen of atmosphere. Iron enters in human body through contaminated water. Iron is one of the components of human blood. For healthy body iron is necessary but excess of iron concentration is fatal for life. In many studies it is found that High concentration of iron in human body is linked with most types of neurodegenerative disorders such as Alzheimer's, Parkinson's, and Huntington's diseases [4]. Higher concentration of redox active metal can disturb normal functioning of cell [14,15].

Many tube wells of Lucknow city record elevated  $\text{NO}_3^-$  concentrations and in other cases dissolved Fe and Mn problems were reported[5]. This paper is based on the investigation of concentration of iron along with some heavy metal in groundwater of Lucknow city .

**MATERIALS AND METHODS**

Fifteen different areas were selected form Lucknow city capital of Uttar Pradesh for collection of ground water (bore well, hand pump) samples. Samples were collected in month of September-october 2014. Although Lucknow city is not industrial city yet for convenience areas were divided into four type such as agricultural, commercial, residential and industrial area on basis of their use; Concentration of metal were analysed through atomic absorption spectrophotometer (variance 240 FS) following standard methods of analysis of water and waste water.

**RESULTS AND DISCUSSION**

The variation in concentration of heavy metal in ground water samples are shown in Table -2 to 5. To know the distribution pattern of metal concentration in ground water statistical analysis has been done. The variations of different metal in ground water are graphically represented figure 1-5.

Minimum iron concentration was found in S<sub>9</sub> which is 0.012 mg/l.

Maximum iron concentration was found in S<sub>8</sub> which is 4.44 mg/l.

The result of analysis of water samples revealed that the concentration of all the heavy metal analyzed in the ground water sample of Lucknow city were within the permissible limit of drinking water set by WHO and BIS. It can be concluded from above study that all the heavy metals which were analyze found within the permissible limit, but in some samples concentration of iron was found above the desirable limit. Clean water is basic need for healthy life. So, it becomes important to check the quality of water regularly to get safe drinking water.

**ACKNOWLEDGEMENTS**

The author is thankful to The Head Department of Chemistry, Integral University, Kursi Road Lucknow Uttar Pradesh, India, for support and providing opportunity to carry out study.





**Aisha Siddiqui et al.**

## REFERENCES

1. WHO 2004, Guidelines for drinking water quality, v1 WHO, Geneva.
2. US EPA (1985) Drinking water criteria document on fluoride. Washington, DC, US Environmental Protection Agency, Office of Drinking Water (TR-823-5).
3. Bishnoi Mukul and Malik Ravinder, Ground water quality in environmentally degraded localities of Panipat city ,India, *Journal of Environmental Biology*, 29(6), 881-886(2008) jeb.co.in/journal issues/2008 11\_nov08/paper\_14.pdf.
4. Dobson Jon ,Magnetic Iron Compounds in Neurological Disorders , *Annals of the New York Academy of Sciences Volume 1012, Redox-Active Metals in Neurological Disorders pages 183–192, March 2004.* onlinelibrary.wiley.com.
5. Foster Stephen and Choudhary N. K., 2009, Lucknow City – India: *Groundwater Resource Use & Strategic Planning Needs, Sustainable Groundwater.* siteresources.worldbank.org/INTWAT/Resources/GWMATE\_CP23Lucknow.pdf
6. Yang Fan, Shi Baoyou, Gu Junnong , Wang Dongsheng, Yang Min, Morphological and physicochemical characteristics of iron corrosion scales formed under different water source histories in a drinking water distribution system , *water research 46 (2012)* www.ncbi.nlm.nih.gov/pubmed/22882957
7. Singh A, Singh J. and Shikha, Status of Ground Water and Municipal Water Supply of Lucknow Region – U.P., *IJPAES*, 2012, 2(4), 139-142. www.ijpaes.com/ admin/ php/ uploads/ 246\_pdf.pdf
8. B.K .Sharma, Environmental Chemistry, 2012, ISBN 81-8283-119-9, p 36
9. Khan A. Arbab and Khan Mohd Nawaz , Physico-Chemical Study of Groundwater at Shahjahanpur city, Uttar Pradesh, India, *Research Journal of Chemical Sciences*, Vol. 5(1), 55-59, January (2015) www.isca.in/rjcs/Archives/v5/i1/9.ISCA-RJCS-2014-219.pdf
10. Annapoorna H., Janardhana M.R., Assessment of Groundwater Quality for Drinking Purpose in Rural Areas Surrounding a Defunct Copper Mine, *Aquatic Procedia, Volume 4, 2015, Pages 685-692.* doi:10.1016/ j.aqpro. 2015.02.088
11. Teikeu William Assatse , Meli'i Jorelle Larissa , Philippe Njandjock et al, Assessment of groundwater quality in Yaoundé area, Cameroon, using geostatistical and statistical approaches, *Environmental Earth Sciences*, January 2016, 75:21. doi:10.1007/s12665-015-4779-7
12. Janardhana N. Raju, Hydrogeochemical parameters for assessment of groundwater quality in the upper Gunjanaeru River basin, Cuddapah District, Andhra Pradesh, South India, *Environmental Geology*, June 2007, Volume 52, Issue 6, pp 1067–1074, doi:10.1007/s00254-006-0546-0
13. Hariprasad N. V., Dayananda H.S.. Environmental impact due to agricultural runoff containing heavy metals-a review, *International Journal of Scientific and Research Publications*, Volume 3, Issue 5, May 2013 www.ijsrp.org/research-paper-0513/ijsrp-p171116.pdf
14. Mudgal Varsha , Madaan Nidhi , Mudgal Anurag , Singh R.B. and Mishra Sanjay, Effect of Toxic Metals on Human Health , *The Open Nutraceuticals Journal*, 2010, 3, 94-99 benthamopen.com/ contents/ pdf/ TONUTRAJ/ TONUTRAJ-3-94.pdf
15. Janardhana Raju Nandimandalam , U. K. Shukla,, Prahlad Ram, Hydrogeochemistry for the assessment of groundwater quality in Varanasi: a fast-urbanizing center in Uttar Pradesh, India,, *Environmental Monitoring and Assessment* ,February 2011, Volume 173, Issue 1, pp 279-300 . Doi 10.1007/s10661-010-1387-6
16. Srinivasa Gowd S. , Ramakrishna Reddy M., Govil P.K., Assessment of heavy metal contamination in soils at Jajmau (Kanpur) and Unnao industrial areas of the Ganga Plain, Uttar Pradesh, India, *Journal of Hazardous Materials Volume 174, Issues 1–3*, 15 february 2010, Pages 113–121 .doi:10.1016/j.jhazmat.2009.09.024
17. Archana and Dutta V. , Seasonal Variation on Physico-Chemical Characteristics of Leachate in Active and Closed Municipal Solid Waste Landfill Site in Lucknow, India , *G- Journal of Environmental Science and Technology 1(4): (2014)* gjestenv.com/Current\_Issue/vol\_1/Gjest\_1008.pdf
18. Khan Mohammad Muqtada Ali, Umar Rashid and Lateh Habibah, Study of trace elements in groundwater of Western Uttar Pradesh, India, *Scientific Research and Essays Vol. 5(20)*, pp. 3175-3182, 18 October, 2010 .http://www.academicjournals.org/SRE ISSN 1992-2248





**Aisha Siddiqui et al.**

19. APHA 2005., Standard methods for the examination of Water and Wastewater, 21st edition, APHA, AWWA & WPCF, Washington, D.C.
20. Indian Standard for Drinking Water – Specification IS 10500 : 2012
21. Prakash K. L. and Somashekar R. K., Groundwater quality - Assessment on Anekal Taluk, Bangalore Urban district, India, *Journal of Environmental Biology*, October 2006, 27(4) 633-637  
jeb.co.in/journal\_issues/200610\_oct06/paper\_05.pdf

**Table 1 -Showing Drinking water limits set by BIS and WHO**

PARAMETER	BIS limit IS 10500-2012		WHO limits(WHO's 2004)	
	Acceptable limit	Permissible limit in the Absence of Alternate Source	Highest desirable limit	Maximum permissible limit
Fe	0.3 mg/l	No relaxation	0.1 mg/l	1mg/l
Cu	0.05 mg/l	1.5 mg/l	0.05 mg/l	1.5mg/l
Cr (Cr <sup>+3</sup> , Cr <sup>+6</sup> )	0.05 mg/l	No relaxation		
Zn	5 mg/l	15 mg/l	5mg/l	15mg/l
Ni	0.02 mg/l	No relaxation		

**Table-2 Residential Area**

Parameter	Fe <sup>2+</sup>	Cr <sup>2+</sup>	Cu <sup>2+</sup>	Zn <sup>2+</sup>	Ni <sup>2+</sup>
Location	mg/l	mg/l	mg/l	mg/l	mg/l
S <sub>1</sub>	0.423	0.007	0.1	0.3	0.01
S <sub>2</sub>	0.712	0.015	0.1	0.2	0.01
S <sub>3</sub>	0.115	0.003	0.11	0.1	0.02
S <sub>4</sub>	0.039	0.019	0.1	0.1	0.02
Mean	0.039	0.011	0.1025	0.175	0.015
SD	0.308	0.007	0.005	0.095	0.005
SE	0.154	0.003	0.0025	0.047	0.002





**Aisha Siddiqui et al.**

**Table-3 Commercial Area**

Parameter	Fe <sup>2+</sup>	Cr <sup>2+</sup>	Cu <sup>2+</sup>	Zn <sup>2+</sup>	Ni <sup>2+</sup>
Location	mg/l	mg/l	mg/l	mg/l	Mg/l
S <sub>5</sub>	0.094	0.012	0.1	0.1	0.01
S <sub>6</sub>	0.85	0.015	0.1	0.2	0.01
S <sub>7</sub>	0.054	0.016	0.11	0.3	0.02
S <sub>8</sub>	4.44	0.014	0.1	0.1	0.03
Mean	1.359	0.014	0.1025	0.175	0.017
SD	2.086	0.001	0.005	0.095	0.009
SE	1.043	0.0005	0.0025	0.047	0.004

**Table-4 Agriculture Area**

Parameter	Fe <sup>2+</sup>	Cr <sup>2+</sup>	Cu <sup>2+</sup>	Zn <sup>2+</sup>	Ni <sup>2+</sup>
Location	mg/l	mg/l	mg/l	mg/l	Mg/l
S <sub>9</sub>	0.012	0.008	0.1	0.1	0.01
S <sub>10</sub>	0.35	0.017	0.1	0.2	0.02
S <sub>11</sub>	0.715	0.018	0.11	0.1	0.01
S <sub>12</sub>	0.929	0.019	0.1	0.2	0.01
Mean	0.501	0.015	0.1	0.15	0.012
SD	0.404	0.005	0.005	0.057	0.005
SE	0.202	0.002	0.0025	0.028	0.005

**Table -5 Industrial area**

Parameter	Fe <sup>2+</sup>	Cr <sup>2+</sup>	Cu <sup>2+</sup>	Zn <sup>2+</sup>	Ni <sup>2+</sup>
Location	mg/l	mg/l	mg/l	mg/l	Mg/l
S <sub>13</sub>	0.039	0.009	>0.1	0.2	0.02
S <sub>14</sub>	0.875	0.012	0.1	0.1	0.02
S <sub>15</sub>	0.65	0.02	0.2	0.5	0.2
Mean	0.521	0.013	0.15	0.266	0.08
SD	0.432	0.005	0.07	0.208	0.103
SE	0.249	0.002	0.04	0.12	0.059





**Aisha Siddiqui et al.**

**Table 6-Correlation table for residential area**

	Fe <sup>2+</sup>	Cr <sup>2+</sup>	Cu <sup>2+</sup>	Zn <sup>2+</sup>	Ni <sup>2+</sup>
Fe <sup>2+</sup>	1				
Cr <sup>2+</sup>	0.081118	1			
Cu <sup>2+</sup>	-0.44808	-0.7303	1		
Zn <sup>2+</sup>	0.667576	-0.19069	-0.52223	1	
Ni <sup>2+</sup>	-0.91841	-5.4E-17	0.57735	-0.90453	1

**Table 7-Correlation table for commercial area**

	Fe <sup>2+</sup>	Cr <sup>2+</sup>	Cu <sup>2+</sup>	Zn <sup>2+</sup>	Ni <sup>2+</sup>
Fe <sup>2+</sup>	1				
Cr <sup>2+</sup>	-0.05516	1			
Cu <sup>2+</sup>	-0.41721	0.68313	1		
Zn <sup>2+</sup>	-0.5208	0.8664	0.870388	1	
Ni <sup>2+</sup>	0.810366	0.254824	0.174078	-0.09091	1

**Table 8-Correlation table for agriculture area**

	Fe <sup>2+</sup>	Cr <sup>2+</sup>	Cu <sup>2+</sup>	Zn <sup>2+</sup>	Ni <sup>2+</sup>
Fe <sup>2+</sup>	1				
Cr <sup>2+</sup>	0.890354	1			
Cu <sup>2+</sup>	0.35186	0.328976	1		
Zn <sup>2+</sup>	0.393924	0.569803	-0.57735	1	
Ni <sup>2+</sup>	-0.24968	0.197386	-0.33333	0.57735	1

**Table 9-Correlation table for industrial area**

	Fe <sup>2+</sup>	Cr <sup>2+</sup>	Cu <sup>2+</sup>	Zn <sup>2+</sup>	Ni <sup>2+</sup>
Fe <sup>2+</sup>	1				
Cr <sup>2+</sup>	0.50335	1			
Cu <sup>2+</sup>	0.257581	0.964579	1		
Zn <sup>2+</sup>	0.017953	0.87298	0.970725	1	
Ni <sup>2+</sup>	0.257581	0.964579	1	0.970725	1





**Aisha Siddiqui et al.**

**Table-10 - Areas selected for samples were as follows**

S.No.	Source	Sampling site
S <sub>1</sub>	Hand Pump	Vikas nagar
S <sub>2</sub>	Hand Pump	Indira nagar
S <sub>3</sub>	Hand Pump	Nishatganj
S <sub>4</sub>	Bore Well	Hussainganj
S <sub>5</sub>	Bore Well	Hazratganj
S <sub>6</sub>	Bore Well	Aminabad
S <sub>7</sub>	Bore Well	Chowk
S <sub>8</sub>	Bore Well	Alambagh
S <sub>9</sub>	Hand Pump	Rasoolpur
S <sub>10</sub>	Hand Pump	Behta
S <sub>11</sub>	Hand Pump	Bakshi ka talab
S <sub>12</sub>	Hand Pump	Malesemau
S <sub>13</sub>	Hand Pump	Sarogni nagar
S <sub>14</sub>	Hand Pump	Chinhat
S <sub>15</sub>	Hand Pump	Talkatora

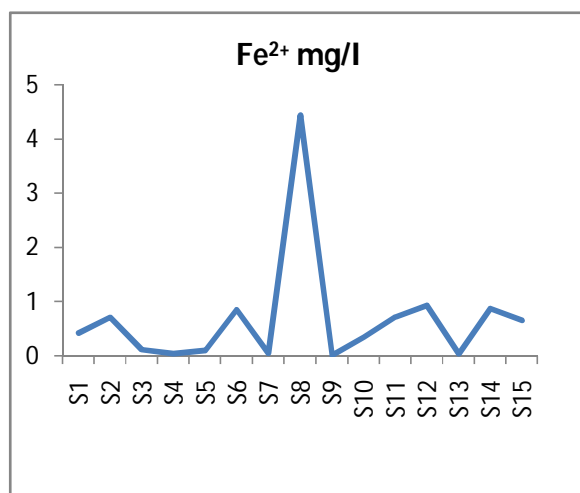


**Figure-1 variation in con of iron**

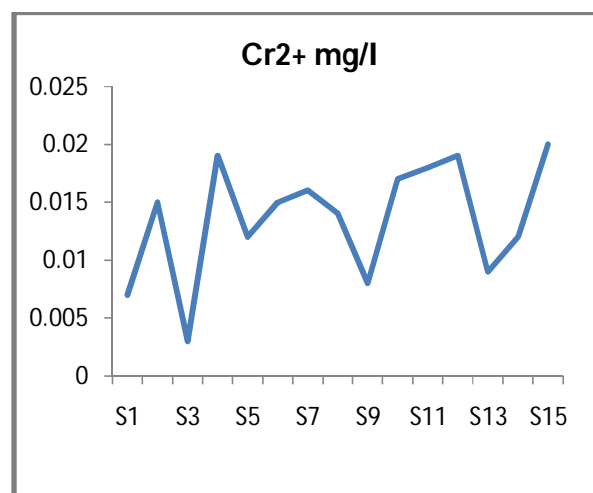


**Figure-2 variation in con of Chromium**





**Aisha Siddiqui et al.**

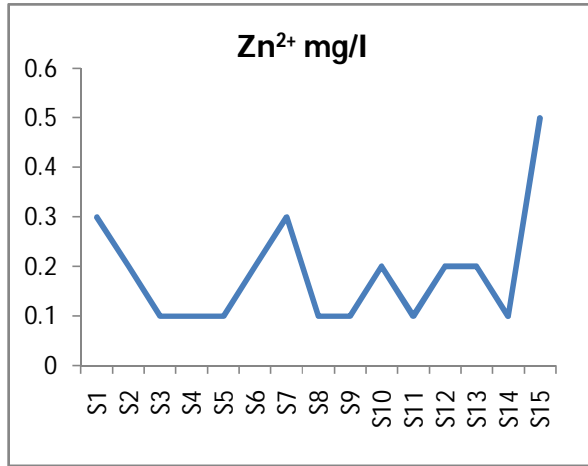


Figure-3 variation in con of Zinc

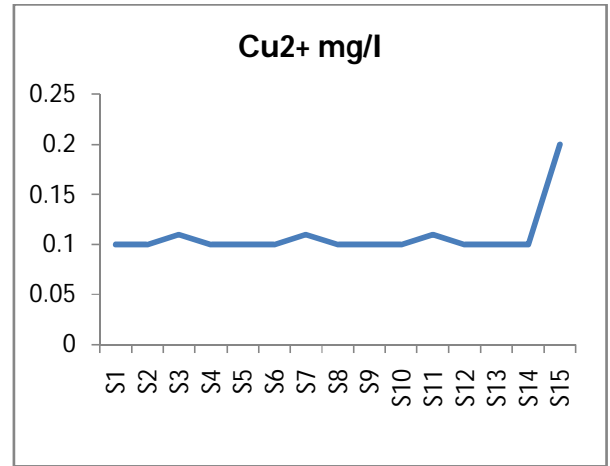


Figure-4 variation in con of Copper

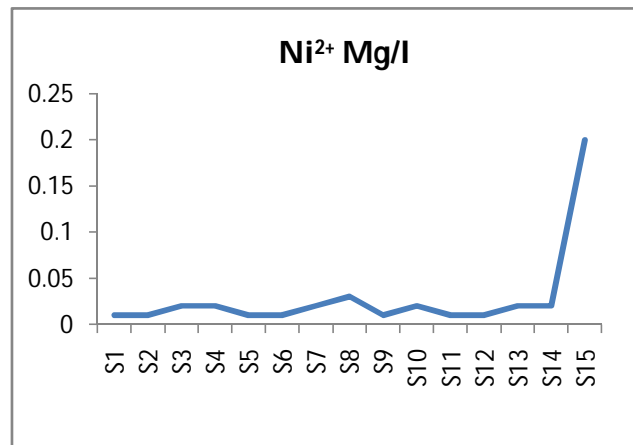


Figure-5 variation in con of Nickel





## RESEARCH ARTICLE

## Aerosol Optical Properties Estimation over Iraq and Surrounding Regions using Best GIS Spatial Interpolation Method

Saadiyah H. Halos<sup>1\*</sup>, Mounim H. Al-Jiboori<sup>2</sup> and Osama T. Al-Taai<sup>2</sup>

<sup>1</sup>Atmosphere and Space Sciences Center, Directorate of Space Technology & Communication, Ministry of Sciences and Technology, Iraq.

<sup>2</sup>Department of Atmospheric Science, Collage of Science, AL-Mustansiriyah University, Iraq.

Received: 5 July 2016

Revised: 16 Aug 2016

Accepted: 27 Sep 2016

### Address for correspondence

SaadiyahHasan Halos

Ministry of Sciences and Technology

Directorate of Space Technology & Communication

Atmosphere and Space Science Center

Baghdad, Iraq.

E mail ID: sadia\_alhassan@yahoo.com



This is an Open Access Journal / article distributed under the terms of the **Creative Commons Attribution License (CC BY-NC-ND 3.0)** which permits unrestricted use, distribution, and reproduction in any medium, provided the original work is properly cited. All rights reserved.

### ABSTRACT

Dust storm is a significant environmental problem and plays an influential role in climatology over Iraq by suffering a significant increase in dust storms in the last decade. Spatial and temporal variance of aerosol optical properties (AOP) over Iraq and surrounding regions is of significant importance to find out the dust aerosol hot spots sources. Aerosol absorption optical depth (AAOD), aerosol extinction optical depth (AOD) and aerosol single scattering albedo (SSA) at wavelength 500 nm were used. These products are derived from the Ozone Monitoring Instrument (OMI) on board Aura satellite with spatial resolution 1°x1°. The used data is for Iraq and surrounding regions with latitude (26.5°N-39.5°N) and longitude (36.5°E-51.5°E) at the past decade (January 2005-December 2014). Different Spatial Interpolation GIS methods were applied on annual mean of AOP, namely Inverse Distance Weighting (IDW), Radial Basis Functions (RBF) with 3 sub-types (Spline completely regularized, Spline with tension, Spline with thin plate) and Kriging with 3 sub-types (Ordinary, Simple, Universal). The best spatial interpolation method of lowest root mean squared error (RMSE) values concluded for estimate AOP over Iraq and surrounding regions was spline completely regularized method. Spatial distributions of annual mean of AAOD, AOD (SSA) over study area have high (low) values located at northwest and south of Iraq extend to Kuwait and northeast of Arabia Saudi. This indicates to abundance of dust absorbing aerosols and the absorbing process is more active than scattering and responsible for increasing aerosol extinction.

**Keywords :** Aerosol optical properties, Ozone Monitoring Instrument, Spatial interpolation methods, GIS, Iraq





**Saadiyah Hasan Halos et al.**

## INTRODUCTION

Iraq is one of the most affected countries in the Middle East concerning the occurrences of sand and dust storms. The frequency of the occurrence has increased drastically in the last decade. The events of sand and dust storms are either regional or local. The regional event, generally extends outside the Iraqi territory, into different directions, but usually covers part of Syria, crossing the Iraqi territory towards Kuwait and Saudi Arabia, and/or towards the Arabian Gulf, and less frequently extends to Iran [1]. Aerosols affect the climate of earth both directly by absorption and scattering and indirectly by altering the cloud properties. The attenuation due to aerosol is called aerosol extinction. Aerosol optical properties (AOP) are used to measure the aerosol load in the atmosphere. The aerosol extinction optical depth (AOD) is a vertical integral of the aerosol extinction coefficient from the earth surface (SFC) to the top of the atmosphere (TOA) [2]. The aerosol single scattering albedo (SSA) is a measure of the effectiveness of scattering relative to extinction for the light encountering the atmospheric aerosol particles [3]. Extinction is the sum of scattering and absorption.

The aerosol absorption optical depth (AAOD) is measure of concentration of near-UV absorbing aerosol particles such as smoke and mineral dust. These properties are useful for monitoring the sources and sinks of aerosols, and important parameters in radiative transfer model, air quality, health environment and earth radiation budget [4]. The present study is aimed to choice the best spatial interpolation method for mapping AOP at the past decade (January 2005- December 2014) over Iraq and surrounding regions. To choice the best spatial interpolation method, three well-known spatial interpolation techniques, namely Inverse Distance Weighting (IDW), Radial Basis Functions (RBF) with 3 sub-types, and Kriging with 3 sub-types were examined in ARCGIS software.

### Spatial Interpolation Methods

Spatial interpolation methods are used to determine phenomena over a continuous space. There are two main groupings of interpolation techniques in ARCGIS (Ver. 10.2.2): deterministic and geostatistical. Deterministic interpolation techniques create surfaces from measured points, based on either the extent of similarity (IDW) or the degree of smoothing (RBFs). Geostatistical interpolation techniques (Kriging) utilize the statistical properties of the measured points [5]. Geostatistical techniques quantify the spatial autocorrelation among measured points and account for the spatial configuration of the sample points around the prediction location [6, 7]. A deterministic interpolation can either force the resulting surface to pass through the data values or not. An interpolation technique that predicts a value that is identical to the measured value at a sampled location is known as an exact interpolator. An inexact interpolator predicts a value that is different from the measured value. The latter can be used to avoid sharp peaks or troughs in the output surface. IDW and RBF are considered as exact interpolators [8,9]. The performance of each interpolator will depend on the arrangement, density and variability of the point data [10]. Spatial interpolation is used to convert point data of aerosol properties into continuous surfaces in this study. These surfaces will be later used to find out the distribution patterns of AOP and the dust aerosols hotspots sites over Iraq and surrounding regions.

## MATERIALS AND METHODS

Field measurements of aerosol properties are often carried out by remote sensing using satellite or ground based instruments. Ozone Monitoring Instrument (OMI) on board NASA's Aura satellite provides aerosol information on a global scale at a daily basis, passing over a certain location once or twice a day [11, 12]. A detailed description of the characteristics of the OMI instrument is given by [13]. AAOD, SSA, AOD at wavelength 500 nm products on daily basis are used in this study. These data is averaged for ten years (January 2005 – December 2014) over Iraq and surrounding regions with grid of latitude (26.5° N-39.5°N) and longitude (36.5° E-51.5°E) with spatial resolution 1°X1°. These data are available at Giovanni web tool: <http://giovanni.sci.gsfc.nasa.gov/giovanni/>.





**Saadiyah Hasan Halos et al.**

### Choice the Best Interpolation Method by using ARCGIS Software

ESRI (Environmental Systems Research Institute) offers multiple Geographic Information System (GIS) products that can be utilized in performing spatial interpolation. Aeronautical Reconnaissance Coverage Geographic Information System (ARCGIS) Spatial Analyst software provides various tools to perform spatial data analysis including some limited interpolation functionality [14]. ARCGIS Geostatistical Analyst provides a full set of tools for performing both spatial data analysis and interpolation [15]. To choose the optimum interpolation method for estimating AOP, two main groupings of interpolation techniques in ARCGIS are examined: deterministic and geostatistical. Deterministic interpolation techniques like IDW and RBF and geostatistical interpolation techniques like Kriging. The selected methods in this study for estimate AOP by using ARCGIS (version 10.2.2) are three spatial interpolation techniques i.e. IDW, RBF with 3 sub-types (Spline completely regularized, Spline with tension, Spline with thin plate) and Kriging with 3 sub-types (Ordinary, Simple, Universal). The most often used measure of interpolation quality is cross-validation.

This approach is empirical and objective [16]. The cross-validation method computes the spatial interpolation for each measured point using all the available information except from that one point, i.e. it withholds one data point and then makes a prediction at the spatial location of that point. The predicted and measured values are then compared and the procedure is repeated for all points. The most common indicator in cross-validation method is Root Mean Squared Error (RMSE):

$$RMSE = \sqrt{\frac{1}{N} \sum_{i=1}^N (Z(s_i) - \hat{Z}(s_i))^2}$$

Where  $Z(s_i)$  is the measured aerosol optical property value in the  $i$ -th point,  $\hat{Z}(s_i)$  is the estimated aerosol optical property value in the  $i$ -th point using other points,  $(s)$  is Location and  $(N)$  is the size of samples. A smaller RMSE generally means a better estimation. Other cross-validation summary statistics is Mean Prediction Error (MPE), which is the same as average bias:

$$MPE = \frac{1}{N} \sum_{i=1}^N (Z(s_i) - \hat{Z}(s_i))$$

MPE should be the nearest to zero [6].

## RESULTS AND DISCUSSION

The choice of the best interpolation method was decided from many criteria obtained by cross validation procedure for three spatial interpolation techniques. Figure 1 show the summary of choosing the best interpolation method for spatial prediction and comparative evaluation of the methods used for estimate AOP. These were evaluated based on RMSE and MPE values, the predicted values are compared with the measured data. The statistical details of the errors produced by the adopted interpolation methods for the annual AOP at last decade are given in Table 1 and Table 2. It is obvious in these two Tables the spline completely regularized method produce lowest RMSE values and is good for estimate AOP over study area. IDW interpolation method produced the worse results (i.e. highest RMSE) and unsuitable for AOP. The Kriging methods gave poor RMSE results, where ordinary and universal Kriging methods generally gave roughly similar results and then they can't also be recommended when applied to estimate AOP. Therefore the prediction maps for AOP in this study have been generated by using the best method (spline completely regularized) due to its best results as shown in Figure 2.

High, moderate and low AOP regions indicate that different regions in study area have various features of aerosol load where the high value of AAOD located at northwest and the south of Iraq extend to Kuwait and the northeast of Arabia Saudi as shown in (Figure 2a). The highest annual mean AAOD is reached to value ( $>0.09$ ) in study area at Arabia Saudi and Kuwait. The low annual mean of AAOD is found over western parts of Iraq with value ( $0.019 \pm 0.003$ ). From (Figure 2b) AOD pattern was similar to that of AAOD. The highest AOD located in northwest





### Saadiyah Hasan Halos et al.

and south of Iraq with AOD range over Iraq is (0.20-0.73) extended to Kuwait and northeast of Arabia Saudi with value (>0.94). The range of SSA over Iraq noticed to be (0.93-0.98) as illustrated in (Figure 2c). SSA pattern is opposite to AOD and AOD patterns where the region of AOD and AOD is high, SSA is low that indicate to abundance of dust absorbing aerosols and absorbing process is more active than scattering and responsible of increasing aerosol extinction. This occurred in the region of sources of dust storm in the sedimentary plain of Iraq's *Tigris* and *Euphrates* rivers as a consequence of Shamal wind which transport aerosols particles from their sources to the south regions towards the Arabian Gulf.

## CONCLUSION

Three well-known spatial interpolation techniques, IDW, RBF with 3 sub-types, and Kriging with 3 sub-types were examined in ARCGIS software. The best interpolation method of lowest RMSE values concluded for OMI/Aura AOP data over Iraq and surrounding regions was spline completely regularized method. Spatial distributions of annual mean of AOD, AOD (SSA) over study area have high (low) values located at northwest and south of Iraq extend to Kuwait and northeast of Arabia Saudi. That indicates to abundance of dust absorbing aerosols and the absorbing process is more active than scattering and responsible to increase aerosol extinction.

## ACKNOWLEDGEMENTS

The author would like to thank NASA Giovanni, GES DISC User Service staff for their valuable help and support online data.

## REFERENCES

1. Varoujan K, Nadhir A. Sven K. Sand and dust storm events in Iraq. *Natural Science* 2013; 5: 1084-1094. doi: 10.4236/ns.2013.510133.
2. Chung, C. E., Aerosol direct radiative forcing: a review. In: Hayder A. Razzak, editors. *Atmospheric Aerosols Regional Characteristics Chemistry and Physics*. ISBN 978-953-51-0728-6: Publisher: InTech; 2012.
3. Pradeep Khatri, Tamio Takamura, Atsushi Shimizu, Nobuo Sugimoto, Observation of low single scattering albedo of aerosols in the downwind of the East Asian desert and urban areas during the inflow of dust aerosols. *Journal of Geophysical Research: Atmospheres* 2014; DOI: 10.1002/2013JD019961.
4. Giovanni-3 GES-DISC Interactive Online Visualization and Analysis, Online User's Manual: Data Parameter Appendix." GES DISC. NASA (Accessed Web. 1 July 2016).
5. Tiberiu, A. Research Activity on Statistical Downscaling for Precipitation. CMCC Research Paper 2009; 57.
6. ArcGIS, E. S. R. I. 9.2 Desktop help. ESRI, Redlands, CA. ArcGIS 2008; 9.
7. Gasmelseid, T. M. Handbook of Research on Hydroinformatics: technologies, Theories and applications. King Faisal University, Saudi Arabia. Hershey, New York: Information Science Reference; 2011.
8. Zandi, S., Ghobakhlou, A. and Sallis, P. A comparison of spatial interpolation methods for mapping soil pH. 19<sup>th</sup> International Congress on Modelling and Simulation, Perth, Australia, 12-16 December 2011.
9. Kamińska, A., and Grzywna. Comparison of deterministic interpolation methods for the estimation of groundwater level. *Journal of Ecological Engineering* 2014; 15: 55-60.
10. Sterling, D. L. A comparison of spatial interpolation techniques for determining shoaling rates of the Atlantic Ocean Channel, (M.S., thesis) 2003; Science in Geography, Virginia Polytechnic Institute and State University.
11. Veeffkind P., Van Oss, Eskes H., Borowiak A., Dentner F., Wilson J. The Applicability of Remote Sensing in the Field of Air Pollution. Institute for Environment and Sustainability, Italy; 2007. p. 59.
12. Schepanski, K., Tegen, I., and Macke, A. Satellite based Observations of Saharan Dust Source Areas-Comparison and Variability. In EGU General Assembly Conference Abstracts 2012; 14: p. 4565.
13. Levelt, P. F., van den Oord, G. H. J., Dobber, M. R., Mäkelä, A., Visser, H., de Vries, J., Stammes, P., Lundell, J., and Saari, H. The Ozone Monitoring Instrument, *IEEE Trans. Geo. Rem. Sens.* 2006; 44: 1093–1101.





**Saadiyah Hasan Halos et al.**

14. McCoy, J., Johnston, K., Using ArcGIS spatial analyst. Redlands, California: ESRI Press; 2001.
15. Johnston, K., VerHoef, J. M., Krivoruchko, K., & Lucas, N., Using ArcGIS geostatistical analyst. Redlands, California: ESRI Press; 2001.
16. Denby, B., Horálek, J., Walker, S. E., Eben, K., & Fiala, J. Interpolation and assimilation methods for European scale air quality assessment and mapping. Part I: Review and Recommendations. European Topic Centre on Air and Climate Change Technical Paper: 2005: 7.

**Table1: Statistical errors obtained by using interpolation methods for AAOD, AOD, the lowest RMSE are in bold.**

Interpolation Method	No. of Point	AAOD		AOD	
		MPE	RMSE	MPE	RMSE
IDW	224	0.0000781	0.00422	0.0005044	0.06302
Spline completely regularized	224	0.0000091	<b>0.00396</b>	0.0001994	<b>0.05381</b>
Spline with tention	224	0.0000065	0.003961	-0.0000390	0.05395
Spline with thin plate	224	0.0000003	0.00417	-0.0000272	0.05464
Ordinary Kriging	224	-0.0000467	0.00400	-0.0002019	0.05500
Simple Kriging	224	-0.0000173	0.00398	-0.0004131	0.05885
Universal Kriging	224	-4.67E-05	0.00400	-0.000202	0.05500

**Table2: Statistical errors obtained by using interpolation methods for SSA, the lowest RMSE is in bold.**

Interpolation Method	No. of Point	SSA	
		MPE	RMSE
IDW	224	-0.0001532	0.00679
Spline completely regularized	224	-0.0000279	<b>0.00677</b>
Spline with tention	224	-0.0000560	0.006771
Spline with thin plate	224	0.0000211	0.00769
Ordinary Kriging	224	0.0001049	0.00682
Simple Kriging	224	-0.0000044	0.00680
Universal Kriging	224	0.0001049	0.00682





Saadiyah Hasan Halos et al.

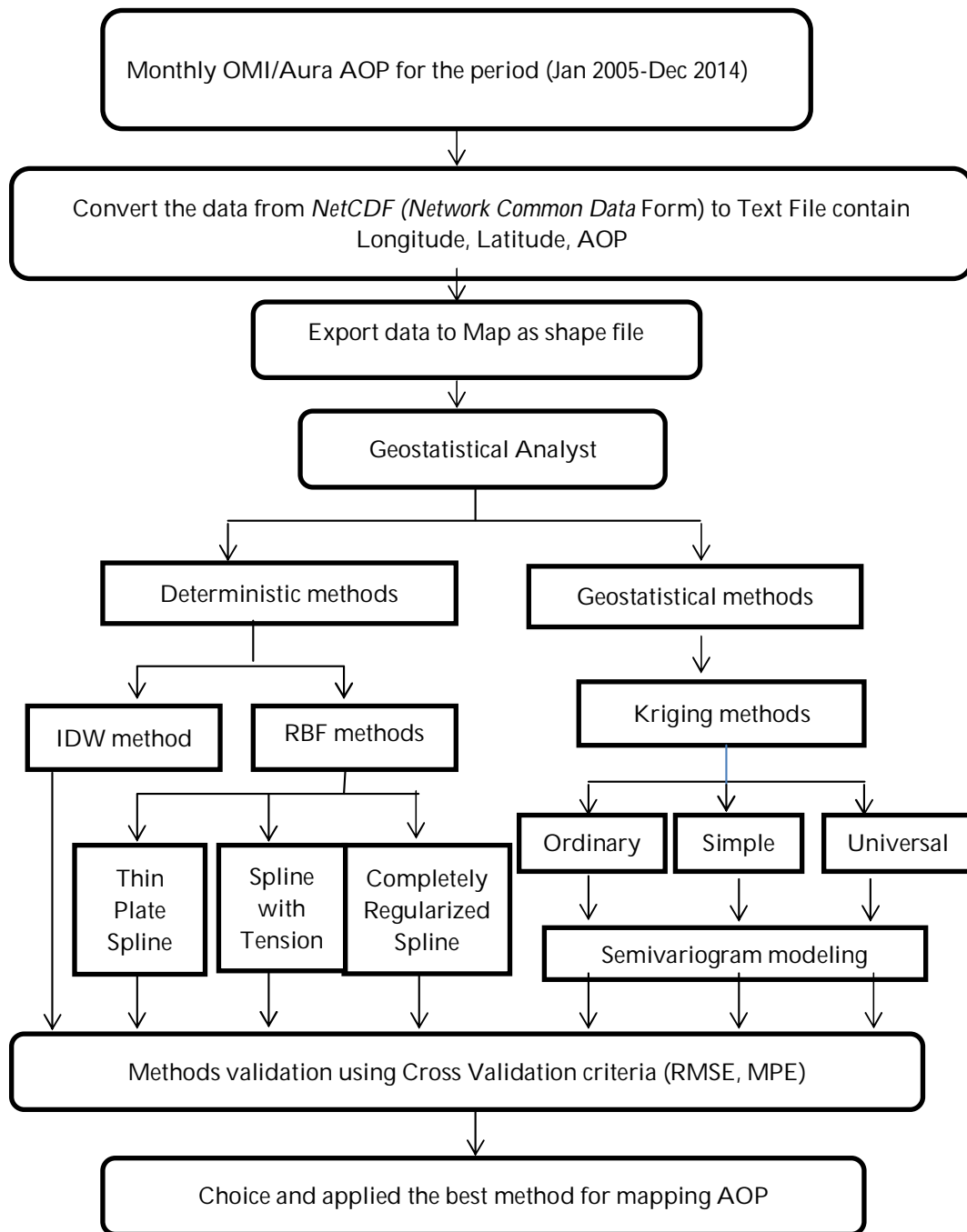


Figure1: Flow chart for the processes of choosing the best interpolation method for mapping AOP





Saadiyah Hasan Halos et al.

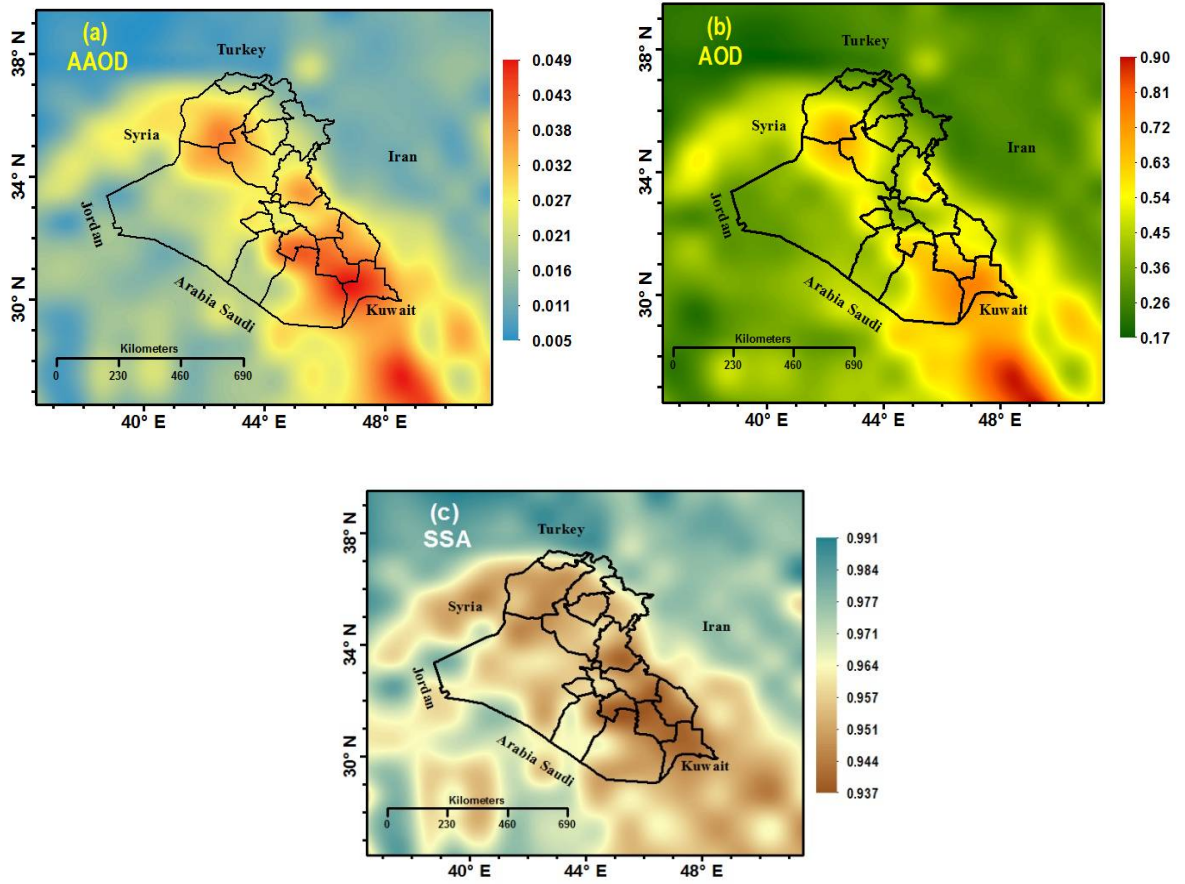


Figure2: Spatial distribution of annual mean of (a) AAOD(b) AOD (c) SSAfor ten years (2005-2014)





## Synthesis, Characterization and Biological Studies of Transition Metal Complexes with Coumarin Derivatives

S. Radha<sup>1</sup>, K.K Mothilal<sup>2\*</sup> and A .Thamarai chelvan<sup>3</sup>

<sup>1</sup>Department of Chemistry, Saiva BhanuKshatriya College, Aruppukottai-626101, Tamilnadu, India

<sup>2</sup>Department of Chemistry, Saraswathi Narayanan College, Madurai-625002, Tamilnadu, India

<sup>3</sup>Chettinad Hospital and Research Institute, Chettinad Academy of Research and Education Chennai- 603 103,India.

Received: 3 July 2016

Revised: 12 Aug 2016

Accepted: 28 Sep 2016

### \*Address for correspondence

Dr.K.K.Mothilal

Associate Professor,

Department of Chemistry,

Saraswathi Narayanan College, Madurai

E-mail address: mothi63@yahoo.com



This is an Open Access Journal / article distributed under the terms of the **Creative Commons Attribution License (CC BY-NC-ND 3.0)** which permits unrestricted use, distribution, and reproduction in any medium, provided the original work is properly cited. All rights reserved.

### ABSTRACT

The metal complexes of 7-Diethylamino-3-thenoylcoumarin (L1), 5, 7-Dimethoxy-3-(1-naphthoyl) coumarin (L2) have gained considerable importance due to their exerted biological activity. A series of metal complexes of the above ligands have been synthesized and characterized by elemental analysis, molar conductance, FT-IR, thermogravimetric analysis, proton NMR, powder XRD and cyclic voltammetry techniques. The IR spectra of the ligands and their complexes show that both ligands behave as bidentate and confirm the presence of nitrate ions in the coordination sphere. Thermal stability of the complexes has been studied by thermo gravimetric and differential thermo gravimetric which support the presence of nitrate ions and ligand molecules in complexes. All complexes exhibited an octahedral geometry around metal centre. The redox property of metal complexes has been characterized by cyclic voltammetry which showed that all the complexes exhibit semi reversible, quasi-reversible one electron transfer redox and irreversible process respectively. The antimicrobial studies of synthesized metal complexes and ligands (L1& L2) were screened for antibacterial activity against bacteria such as *Escherchia coli*, *Staphylococcus aureus*, *Pseudomonousaureginosa* and antifungal activity against *P. Aeruginosa* and *Candida albicans* species and it was found to have greater effect on the antimicrobial activities. The DNA binding studies were performed by electronic spectroscopy and cleavage studies are investigated by Agarose gel electrophoresis technique. The experimental results indicate that all complexes have marked effect on the binding affinity to CT-DNA.

**Keywords :** Metal complex, Thermogravimetry, Cyclic voltammetry, Antimicrobial;



**Mothilal et al.**

## INTRODUCTION

Coumarins are naturally occurring organic compounds found throughout the plant kingdom [1, 2]. Coumarins are classified into four types. They are simple coumarins, furanocoumarins, pyranocoumarins and the pyrone-substituted coumarins. Different substituted coumarins are associated with diverse pharmacological activities such as antibacterial, antifungal, antihelminthic and carcinogens [3]. Furanocoumarins consist of a five-membered furan ring attached to the coumarin nucleus, divided into linear or angular types with substitution at one or both of the remaining benzoid positions [4]. Pyranocoumarin members are analogous to the furanocoumarins, but contain a six-membered ring. Coumarins substituted in the pyrone ring include 4-hydroxycoumarin [5, 6]. Natural coumarins are known to have antidiabetic activity, anabolic antioxidant and hepato protective activities [7, 8]. Synthetic coumarins have stimulated their antibiotic [9], anti-coagulant [10], anticancer [11], anti-inflammatory [12], and anti-HIV [13] properties. A number of synthetic derivatives of coumarin have found pharmaceutical applications [14]. Coumarins are nowadays an important group of organic compounds that are used as additives to food and cosmetics [15], optical brightening agents [16] and dispersed uorescent and laser dyes [17]. Substituted coumarin derivatives have been reported to have variety of biological activities. Coumarin derivatives are involved in photo generation of ROS (reactive oxygen species) from ketocoumarins.

Coumarin derivatives can be synthesized by one of such methods as the Claisen rearrangement [18], Perkin reaction [19], Beckmann reaction [20], Wittig reaction [21], as well as the Knoevnagel condensation [22, 23]. Coordination compounds of coumarin derivatives are important due to their role in biological and chemical systems in various ways. It has been observed that metal complexes with appropriate ligands are chemically more significant and specific than the metal ions and original [24-27]. A number of coumarins have been investigated for complexing ability [28]. The investigation of the binding properties of coumarin derivatives to different metal ions could help in understanding its isomer isocoumarin binding properties and factors controlling their biological activity [29]. Coumarins are also used as ligands and they involves in the synthesis of coordination compounds [30]. The coumarin ring can participate in mono dentate, bidentate or  $\pi$ -arene binding sites to a metal centre. Transition metal complexes of coumarins are found in biological and medical application. Drzewiecka et al have reported the synthesis and structural studies of novel Cu (II) complexes with coumarin derivatives [31]. A new series of Ruthenium complexes with Coumarin derivative are reported [32]. This consideration prompted us to synthesis a new series of metal complexes of 7-substituted coumarins to investigate their antimicrobial and DNA cleavage activities. Hence, we report here the synthesis and spectral characterization of Ni (II), Cu (II) and Zn(II) complexes of L1 and L2 ligands.

## MATERIALS AND METHODS

Ligands (L1 & L2) and metal salts were purchased from Sigma Chemicals Co. (USA) and used as such. All solvents and chemicals used for antimicrobial and DNA studies were reagent grade and used without further purification.

### Physical measurements

Elemental analyses (C, H, and N) of the complexes were performed at SAIF, Cochin University, Cochin, and Kerala. IR spectra were recorded on FT-IRJASCO 460 PLUS spectrophotometer with samples prepared as KBr pellets. Electron paramagnetic resonance spectra were recorded on JOEL-FA200EPR spectrometer. UV-Vis spectra were recorded on a Shimadzu UV-3101PC spectrophotometer using cuvettes of 1 cm path length and conductivity measurements were carried out in aqueous solutions of the complexes with an Elico conductivity bridge type CM 82 and a dip-type cell with a cell constant of 1.0. Cyclic voltammetry measurements were made on Princeton EG and G-PARC model potentiostat. The thermal analyses were performed with a Perkin Elmer Diamond instrument at heating of 5 °C/min under a dynamic air atmosphere (150 ml/min). All complexes were investigated in the temperature range 20-800 °C. The antibacterial and antifungal activities were done at 50 ppm concentration in DMSO solvent by using





**Mothilal et al.**

bacteria (*P. aeruginosa*, *E. coli*, *S.cocci species*) and fungi such as *Aspergillusniger*, *Candida albicans* by a modified disc diffusion method.

**Synthesis of Complexes 1(a), 1(b) and1(c)**

To a solution of 7-diethylamino-3-thenoylcoumarin (L1)  $C_{18}H_{17}NO_3S$  (0.655g, 2mmol) in 23 ml of methanol was treated with a methanolic solution of Nickel (II) nitrate (0.290 g, 1 mmol). The reaction mixture was stirred on magnetic stirrer. Green crystalline product formed after 7-8 hrs was collected by filtration. The solid was washed several times with methanol (50 mL), then with diethyl ether (30 mL) and finally dried in vacuum. The obtained complex (1a) was recrystallized from dry methanol. Mol. Formula (complex 1(a)),  $NiC_{36}H_{34}N_4S_2O_{12}$ : Mol. Wt. 837.473, M.P. 210° C, Yield: 0.572g. Colour-Pale Green. The metal complexes 1(b), 1(c) were synthesized from the respective precursor ligand by adopting similar procedure used (with slight modifications) for the synthesis of the above mentioned complexes. Mol. Formula (complex 1(b)),  $Cu C_{36}H_{34}N_4S_2O_{12}$ : Mol. Wt. 842.35, Yield: 0.687 g, Colour-pale brown; Mol. Formula (complex 1(c)),  $Zn C_{36}H_{34}N_4S_2O_{12}$ : Mol. Wt. 844.18, Yield: 0.676 g, Colour -White;

**Synthesis of Complexes 2(a), 2(b) and2(c)**

To a solution of 5, 7-dimethoxy-3-(1-naphthoyl)coumarin(L2)  $C_{22}H_{16}O_5$  (0.721g, 2mmol) in 20 ml of methanol was treated with a methanolic solution of Nickel(II) nitrate (0.290 g, 1 mmol). The reaction mixture was stirred on magnetic stirrer. Bluish Green crystalline product formed after 6-7hrs was collected by filtration. The solid was washed several times with methanol (25 mL), then with diethyl ether (10 mL) and finally dried in vacuum. The obtained complex 2(a) was recrystallized from dry methanol. Mol. Formula complex 2(a),  $NiC_{44}H_{32}N_2O_{16}$ : Mol. Wt. 837.493, Yield: 0.772g. Colour-bluish Green. The metal complexes 2(b), 2(c) were synthesized from the respective precursor ligand by adopting similar procedure used (with slight modifications) for the synthesis of the above mentioned complexes. Mol. Formula complex 2(b),  $Cu C_{44}H_{32} N_2O_{16}$ : Mol. Wt. 908.27, Yield: 0.716 g, Colour- brown; Mol. Formula complex 2(c),  $Zn C_{44}H_{32} N_2O_{16}$ : Mol. Wt. 910.10, Yield: 0.658 g, Colour -white;

**DNA binding experiment**

A solution of Calf thymus DNA samples (CT-DNA; ~ 200 base pairs in length) in the aqueous buffer solution (50mM NaCl- 5Mm Tris-HCl, Ph 7.1) gave UV absorption in the range 260 and 280nm indicating that the DNA was sufficiently free of protein [33, 34] Milli-Qwater was used to prepare the solutions. The DNA binding experiments were performed at 30°C. DNA absorbs at 260-280 nm in the UV region with molar extinction coefficient value  $6600cm^{-1}$  which indicates its purity. The electronic absorption spectra of the complexes have been carried out at the fixed concentration of the complexes (15 $\mu$ M) in DMSO at 25° C, with the concentration of DNA as 5 $\mu$ M which incubate 15-20 min before the absorption.

**DNA cleavage study**

The DNA cleavage activity of ligands and their metal complexes was monitored by agarose gel electrophoresis on Human serum proteins by using Ready- to- use- precast Gel(8 $\times$ 5cm). Each reaction mixture contained 30  $\mu$ M of serum and 40  $\mu$ M of each complex in DMF in 50mM Tris-HCl buffer (pH 7.2). The reaction was incubated at 37°C for 2hrs. The sample was electrophoresed for 30 minutes at 100V on a Biotech recast Agarose gel (8 $\times$ 5cm). The gel was stained with methylene blue in 0.1X TAE) and photographed under UV light.

**RESULTS AND DISCUSSION****Conductance and Elemental analysis**

The complexes were colored, insoluble in water as well as stable in air. The analytical data of these complexes showed that the solids are stable and can be stored for months without any significant change in their formulae. The purity of the complexes were derived from C, H, N analysis, and the results were found to be in good agreement





### Mothilal et al.

with the calculated values given as follows: complex 1(a) Found: C, 50.33%; H, 4.07%; N, 5.94%; Ni, 6.21%;  $C_{36}H_{34}NiN_4S_2O_{12}$  calcd: C, 51.58%; H, 4.06%; N, 6.69%; Ni, 7.00%; O, 22.93; complex 1(b) Found: C, 49.99%; H, 3.98%; N, 6.46%; Cu, 7.15%;  $C_{36}H_{34}CuN_4S_2O_{12}$  calcd: C, 51.29%; H, 4.03%; N, 6.65%; Cu, 7.54%; O, 22.79; complex 1(c) Found: C, 51.03%; H, 3.99%; N, 6.26%; Zn, 7.08%;  $C_{36}H_{34}ZnN_4S_2O_{12}$  calcd: C, 54.17%; H, 3.02%; N, 6.63%; Zn, 7.74%; complex 2(a) Found: C, 55.52%; H, 3.40%; N, 2.99%; Ni, 5.85%;  $NiC_{44}H_{32}N_2O_{16}$  calcd: C, 58.44%; H, 3.50%; O, 28.33%; N, 3.09%; Ni, 6.49%; complex 2(b) Found: C, 54.72%; H, 3.14%; N, 2.88%; Cu, 6.08%;  $CuC_{44}H_{32}N_2O_{16}$  calcd: C, 58.13%; H, 3.52%; N, 3.08%; O, 28.19%; Cu, 6.99%; complex 2(c) Found: C, 57.28%; H, 3.44%; N, 3.08%; Zn, 6.98%;  $ZnC_{44}H_{32}N_2O_{16}$  calcd: C, 58.02%; H, 3.51%; N, 3.07%; O, 28.13%; Zn, 7.18%;

### FT-IR Spectra

The analysis of the FT-IR spectra of ligands and complexes were measured in the region 400-4500  $cm^{-1}$  provided information on the coordination mode between the ligands and the metal ion. IR spectral data of all complexes were summarized in Table 1. The IR spectra of complexes in Fig. 1, 2 showed sharp band at around 1350  $cm^{-1}$  - 1410  $cm^{-1}$  and 1343  $cm^{-1}$  - 1399  $cm^{-1}$  in L1, L2 complexes respectively. These bands may probably be due to the vibrations of nitrate ions coordinated through oxygen to metal, which are not observed in ligand L1 indicates the absence of coordinated nitrate ion. The  $\nu_{(C=O)}$  stretching vibration band appeared at  $\approx 1718 cm^{-1}$  in the spectra of L1, and its complexes showed this band at  $\approx 1600-1620 cm^{-1}$ ; this band shifted towards lower energy, suggesting that coordination occurs through the carbonyl oxygen atom in lactone ring. The most notable change observed upon complex formation is a shift of the C=O stretch to lower frequency. The C=O band at 1726  $cm^{-1}$  exhibits a shift of 30-45  $cm^{-1}$  to lower wave number values on complexation which may be taken as evidence for the participation of the C=O group in coordination. The bands at 460 - 550  $cm^{-1}$  for complexes of L1 and L2 were assigned  $\nu_{(M-O)}$  stretching vibrations.

### Electronic Spectra

The  $n \rightarrow \pi^*$  characteristic band in the UV spectra assigned to the C=O bond appear at 271 nm for carbonyl and is shifted toward higher wave lengths with 6 nm, 9 nm and 2 nm for complex 1(a), 1(b) and 1(c) respectively confirming the presence of the ligand in the complex and the covalent nature of the metal-ligand bond. In the visible domain, d-d transition appears between at 620 nm in the copper complex. In the visible domain, Nickel complex 1(a) spectrum shows a band at 512 nm attributed to the d-d transition of electrons attributed to  ${}^3A_{2g}(F) \rightarrow {}^3T_{1g}(F)$ ,  ${}^3A_{2g} \rightarrow {}^3T_{2g}$ ,  ${}^3A_{2g} \rightarrow {}^3T_{1g}(P)$ . Complex 2(b) is assigned to  ${}^2E_g \rightarrow {}^2T_{2g}$ ,  $4T_{1g}(P) \rightarrow 4T_{1g}(F)$  which is conformity in octahedral geometry. Zn(II) complex 2(c) attributed to LMCT transition, which is compatible with this complex having an octahedral symmetry of zinc ion [35].

### Thermo gravimetric Analysis of Complexes

The thermo gravimetric curves of the complexes are shown in Fig. 3. TGA shows presence of two nitrate ions per metal ion which are lost in one step process at relatively high temperature (240°C - 300°C). This confirms that the two nitrate ions are coordinatively bonded through oxygen to the metal ions. The dry compound which is stable in small temperature range was the oxides of the metal ion, which were not further decomposed. The TGA of ligand (L1) showed 72% of ash content, the residue in complexes 1(a), 1(b), 1(c) is equal to 28%, 16%, 39% of metal oxide content respectively after complete decomposition corresponds to the theoretical value. With the above discussion we propose the structure for all complexes are consisting mononuclear molecule in which one copper atom is joined with two carbonyl group of the 7-Diethylamino-3-Thenoylcoumarin ligand (L1) and is also bonded to two nitrate ions. Thus, in all complexes four oxygen atoms lying on its plane and the two oxygen atoms on its apex. Hydrogen bonded network could account for insolubility of complex.

In all complexes, metal atom is coordinated by aryl carbonyl group and carbonyl of lactone ring and bonded with two nitrate ions. From TGA of complexes 2(a), 2(b), 2(c) carbonyl group and carbonyl of benzopyrone ring in 5, 7-dimethoxy-3-(1-naphthoyl)coumarin ligand (L2) bonded to metal atom which also bonded to two nitrate ions in all



**Mothilal et al.**

complexes. The TGA of ligand(L2) showed 72% of ash content, the residue in complexes 2(a), 2(b), 2(c) is equal to 25%, 18%, 10% of metal oxide content respectively after complete decomposition corresponds to the theoretical value.

**<sup>1</sup>HNMR Spectra**

Proton spectra of the compounds recorded at 250MHz in DMSO-d<sub>6</sub> confirm the formation of the complex; typical chemical shifts of the <sup>1</sup>HNMR spectra in DMSO-d<sub>6</sub> are represented in Fig.4. Different chemical shifts of complexes were attributed to coordination occurred. Comparison of the <sup>1</sup>HNMR spectra of the complex with the ligands L1, L2 reveals that the resonances are considerably broadened and also shifted on complexation. A well resolved multiplets at 7.41δ–7.76δ corresponding to five aromatic protons in L1. In their complexes, these signals were shifted to lower field were observed at 7.20-7.48 δ due to complexation. In the ligand L1 we observe the signals at 3.64-4.20δ (ppm) assigned to the protons of CH<sub>2</sub> - group. These signals are shifted to down field 3.51-3.64 (ppm) because of coordination through oxygen of C=O (lactone). The <sup>1</sup>HNMR spectrum of the ligand L1 shows a singlet at 2.4, 7.48 ppm due to –CH<sub>3</sub> group, phenyl ring respectively, which also shifted to lower field in all their complexes. In the <sup>1</sup>HNMR spectrum of complex 1(c) the –CH<sub>3</sub> is at 2.23 ppm is not significantly changed and aromatic protons signals lowers at 6.4–6.8 ppm due to complexation. In complexes of L2, the peaks shifted to lower field in the range 8.38 ppm(2(a)) and 8.40 ppm(2(b)) which indicates the lactone C=O involved in coordination. In the complex 2(a), the peak shifted at 8.02 ppm shows, the coordination through 1-naphthalene C=O group.

**Cyclic voltammetry**

Cyclic voltammetry has been used to study a variety of redox processes, stability of reaction products, the presence of intermediates in oxidation-reduction reactions, reaction and electron transfer kinetics and the reversibility of a reaction. Cyclic voltammetric behaviour of complexes was recorded in the range from +1.2V to -2.0V at a scan rate of 0.1Vs<sup>-1</sup>. Complexes of L1 showed oxidation at the potential range 0.3V to 0.8V, reduction at the potential range of -0.3V to -1.5 V and, the reduction process is found to be quasireversible in nature (Fig.5) With the increasing scan rates, ΔE<sub>p</sub> value also increases and there is a negative shift of the cathodic peak potential with increasing sweep rate giving further evidence for the quasi-reversible Cu (II)/Cu(I) couple.

**Powder X-ray diffraction**

X-ray patterns of the copper (II) complex 1(b) & 2(b) recorded at 2θ= 0–70 range. Powder XRD pattern at 2θ value indicates the characteristic peaks of metal such as Ni (II), Cu (II), Zn (II) present in complexes were shown. Attempts to prepare single crystals were unsuccessful. All the complexes are nano sized powder solids (amorphous). Well defined peaks indicate the arrangements of atoms in lattices are regular. The resulted complexes are soluble in DMF and DMSO and are decomposed in diluted solutions of all strong acids.

**Antimicrobial Studies**

The *in vitro* antimicrobial activity of coumarin derivatives and their metal complexes were evaluated against gram positive, gram negative bacteria and fungi. The activity of complexes was measured by measuring inhibition zone observed around the tested material (Fig.6(a & b), Fig7(a & b)). All the metal complexes showed increased zone of inhibition compared with their respective coumarin derivatives against bacteria and fungi under study. Complexes 1(b) and 1(c) were active against both gram positive (*staphylococci*) and gram negative (*E.coli* and *pseudomonas aeruginosa*) bacteria, whereas Complexes 1 (a) showed lesser activity against both gram negative and gram positive bacteria. The antifungal activities test of the coumarins and their metal complexes are studied against two fungi species: *C.albicans* and *Aspergillus niger*. In both coumarin metal complexes Copper(II) and Zinc(II) complexes showed higher activities against two fungi species. Hence, the result of these studies showed that all the metal-coumarin complexes are more effective antibacterial-antifungal against tested species. The increased inhibition activity of the metal complexes can be explained on the basis of Tweedy's Chelation theory (Tweedy, 1964).



**Mothilal et al.**

### Gel electrophoresis-DNA cleavage study

The cleavage reaction on Human serum proteins by using Ready-to-use-precast Gel by complexes were performed with the agarose gel electrophoresis method and the results were represented in Fig.8 The ability of metal complexes to mediate DNA cleavage is well documented. In control experiment using DNA alone, Lane(C) does not show any significant cleavage of DNA even after long exposure time. Both ligands (L1 and L2) have slight effect on the cleavage of DNA at concentrations up to 40µM. except 1c, all other complexes show significant effect on cleavage of DNA. From the observed results, it is concluded that Ni (II) and Cu (II) complexes (1b and 2b) cleave the DNA significantly as compared to the other complexes as shown in Fig.8. DNA cleavage effect of different complexes is due to binding efficiency of the complexes to DNA

### DNA binding study

UV-Vis absorption spectroscopy is very suitable for interaction studies related to DNA. However, when DNA and metal complexes are interacting, a clear change in DNA spectrum absorbance is observed. The intercalation reactions caused the hypochromism and /or hyperchromism, red and/or blue shifts of the band. Hypochromism is due to the contraction of DNA in the helix axis and changes in the conformation of DNA, while hyperchromism results from the damage of the DNA double helix structure. Metal complexes contain labile ligands that can be easily replaced by covalent binding to nitrogenous basis of DNA. Complex binds to DNA through covalent binding generally results in hyperchromism (increase in absorption intensity).From the Fig.9, it is clearly understood that all metal complexes bind to DNA through covalent binding. Hyperchromism results from breakage of secondary structure of DNA due to the fact that phosphate group can provide the suitable anchors for coordination with complexes.

### CONCLUSION

The present work focuses on the synthesis, characterization and biological studies of transition metal complexes of coumarin derivatives as ligand. The ligands, coumarins act as bidentate, coordinating through carbonyl oxygen. The complexes were studied by melting point, conductivity measurements, IR, UV-visible, NMR and ESR spectroscopy. The IR and thermal studies confirmed the presence of nitrate ions in the coordination sphere of  $[M(L1)_2(NO_3)_2]$ ,  $[M(L2)_2(NO_3)_2]$ . All the complexes have octahedral coordination in which the metal ions are coordinated to ligand molecule as bidentate and nitrate ions. Cyclic voltammetry studies of the metal complexes revealed the semi reversible and quasi-reversible one electron transfer redox processes respectively. Antibacterial and antifungal activity of these metal complexes reveals that they show better activity when compared to that of the coumarin ligands. Antimicrobial study reveals that copper complexes of L1 and L2 have more biological activity than the other complexes. DNA binding and cleavage studies showed that all metal complexes have significant activities than the coumarin ligand.

### ACKNOWLEDGEMENTS

One of the authors S.Radha is grateful to the Management of SaivaBhanuKshatriya College, Aruppukottai, Tamilnadu, India for providing facilities and granting permission to carry out this research work.

### REFERENCES

1. S. D. Nachiket, R. P. Shashikant, S. S. Dengale, D. S. Musmade, M. Shelar, V. Tambe, M. Hole, *Der PharmaChemica*, 2010, 2(2): 65-71.
2. Lake B. Synthesis & pharmacological investigation of 4-hydroxycoumarin derivatives & shown as anti-coagulant. *Food ChemTox.*1999; 3: 412-423.
3. P. K. Jain and Himanshu Joshi Coumarin: Chemical and Pharmacological Profile



**Mothilal et al.**

4. Journal of Applied Pharmaceutical Science 02 (06); 2012: 236-240
5. Ojala T. PhD Thesis, University of Helsinki, Helsinki, Finland.2001; 95-106.
6. Keating G., O' Kennedy R. coumarin cytotoxicity activity on albino rats. John Wiley & Sons.1997; 2: 54-66.
7. Murray RDH., Mendez J., Brown SA. Coumarin activity in plants and bioorganism aspects. John Wiley.1982; 2: 45-55.
8. A.Karaliota, O.Kratsi, C.Tzouqraki, *Journal of Inorganic Biochemistry*, 2001, 84, 33.
9. Lewis, R.J., Singh, O.M.P., Smith, C.V., Karzynski, T.S., Maxwell, A., Wonacott, A.J. and Wingley, D.B., *EMBO J.*, 15, 1412 (1996). 9. Chen, Y.L., Wang, T.C., Lee, K.H., Chang, Y.L., Teng, C.M. and Tzeng, H.C., *Chim. Acta.*, 79, 651 (1996) Kam, C.M., Kerrigan, J.E., Plaskon, R.R., Daffy, E.J., Lollar, P., Suddath, F.L. and Powers, J.C., *J. Med. Chem.*, 37, 1298 (1996).
10. Manfredini, S., Baraldi, P.G., Bazzanini, R., Guarneri, M., Simoni, D., Balzarini, J. and Clercq, E.D., *J. Med. Chem.*, 37, 2401 (1994).
11. Pochet, L., Doucet, C., Schynts, M., Thierry, N., Boggeto, N., Pirotte, B., Liang, K.Y., Masereel, B., Detulio, P., Delarge, J. and Reboud-Ravaux, M., *J. Med. Chem.*, 39, 2579 (1996).
12. Fuller, R. W. and Gustafson, K. R. *Bioorg. Med. Chem. Lett.*, 4, 1961 (1994).
13. (a) Masche, U.P., Rentsch, K.M., Von Felten, A., Meier, P.J. and Fattinger, K.E., *Eur. J. Clin. Pharmacol.*, 54, 865 (1999); (b) Parrish, J., Fitzpatrick, T., Tannenbaum, L. and Patak, M., *New Eng. J. Med.*, 291, 1207 (1974).
14. R. O'Kennedy and R. D. Thornes, *Coumarins: Biology, Applications and Mode of Action*, Wiley & Sons, Chichester, 1997.
15. M. Zahradnik, *The Production and Application of Fluorescent Brightening Agents*, Wiley & Sons, Chichester, 1992.
16. M. Maeda, *Laser Dyes*, Academic Press, New York, 1984.
17. R. D. H. Murrey, D. Medez, S. A. Brown, *The natural coumarins occurrences, chemistry and biochemistry*, John Wiley Interscience, New York 1982.
18. S. R. Ghantwal, S. D. Samant, *Ind. J. chem.* 1999, 38(B): 1242-1247.
19. P. L. Majumder, S. Majumder, *Eur. J. Med. Chem.* 1993, 28:572-578.
20. K. K. Upadhyay, R. K. Mishra, A. Kumar, *Catal. Lett.* 2008, 121:118-120.
21. T. Harayama, K. Nakatsuka, H. Nishioka, K. Murakami, N. Hayashida, H. Ishii, *Chem. Pharm. Bull.* 1994, 42(10): 2170-2173.
22. A. Shaabani, R. Ghadari, A. Rahmati, A. H. Rezayan, *J. Iran chem. Soc.* 2009, 6(4):710-14.
23. J.J. Inbary, R. Gandhdosan, S. Subramanian, R. Murugesan, J. Photochem. Photobiol. A: Chemistry 117,(1998).21-25
24. Mildvan AS (1970). *The Enzyme*: 3rd ed: Boy PD: New York, Academic-Press. 11: p. 445.
25. Steinhardt J, Beychok S (1964). *The Proteins*, 2nd ed. New York, Academic Press. pp. 261-276.
26. M.C.Ganortar. and L.Nalada, *IND.t.chem.* (1988), 27(6),542.
27. Sulekh Chandra, Smriti Raizada, Monika Tyagi, and Archana Gautam, *Synthesis, Spectroscopic, and Antimicrobial Studies on Bivalent Nickel and Copper Complexes of Bis(thiosemicarbazone)*, *Bioinorganic Chemistry and Applications Volume 2007*, Article ID 51483.
28. H.B. Singh, Some studies on the complexation reactions of biologically active coumarins with iron (III), *Acta Cienc. Indica, Ser. Chem.* 6 (1980) 88.
29. I. Kostova, G. Momekov, P. Stancheva, *Met Based Drugs*, 2007, 15925.
30. S. Sandari, Y. Mari, K. Horita, R.G. Micetch, S. Nishibe, M. Danesh talah *Bio org. Med. Chem.* 1997; 7, 1933-1940.
31. A Drzewiecka, A.E. Koziol.etal *Polyhedron*, 2012; 43, 71-80
32. M.J.Li, K.M.C.Wong, C.Yi, U.W.W.Yam *Chem.: Eur J* 2008, 14, 8724-8730.
33. R.S. Kumar, S. Arunachalam, V.S.Periyasamy, C.P.Preethy, A.Riyasdeen, M.A. Akbarsha, *polyhedron* 27(2008) 1111-1120
34. R.Senthilkumar, S.Arunachalam, *European journal of medicinal chemistry* (2009) 44.
35. D.H.More, P.P. Mahulikar, *Indian journal of chemistry*, 2011, 50(B):745-747





Mothilal et al.

Table 1. IR Spectral frequencies ( $\text{cm}^{-1}$ ) of Coumarins and their metal complexes.

Ligand/Complex	$\nu_{\text{(C=O)}}$	$\nu_{\text{(C=C)}}$	$\nu_{\text{(C-O)}}$	$\nu_{\text{(C-O-C)}}$	$\nu_{\text{(M-O)}}$
$\text{C}_{18}\text{H}_{17}\text{NO}_3\text{S}$ (L1)	1718	1234	1197	1078	-----
$\text{C}_{36}\text{H}_{34}\text{NiN}_4\text{S}_2\text{O}_{12}$ 1(a)	1620	1234	1196	1075	468
$\text{C}_{36}\text{H}_{34}\text{CuN}_4\text{S}_2\text{O}_{12}$ 1(b)	1618	1232	1194	1074	445
$\text{C}_{36}\text{H}_{34}\text{ZnN}_4\text{S}_2\text{O}_{12}$ 1(c)	1619	1230	1197	1076	446
$\text{C}_{22}\text{H}_{16}\text{O}_5$ (L2)	1730	1225	1200	1045	-----
$\text{NiC}_{44}\text{H}_{32}\text{N}_2\text{O}_{16}$ 2(a)	1652	1236	1199	1044	526
$\text{CuC}_{44}\text{H}_{32}\text{N}_2\text{O}_{16}$ 2(b)	1649	1234	1199	1043	451
$\text{ZnC}_{44}\text{H}_{32}\text{N}_2\text{O}_{16}$ 2(c)	1618	1236	1197	1041	451

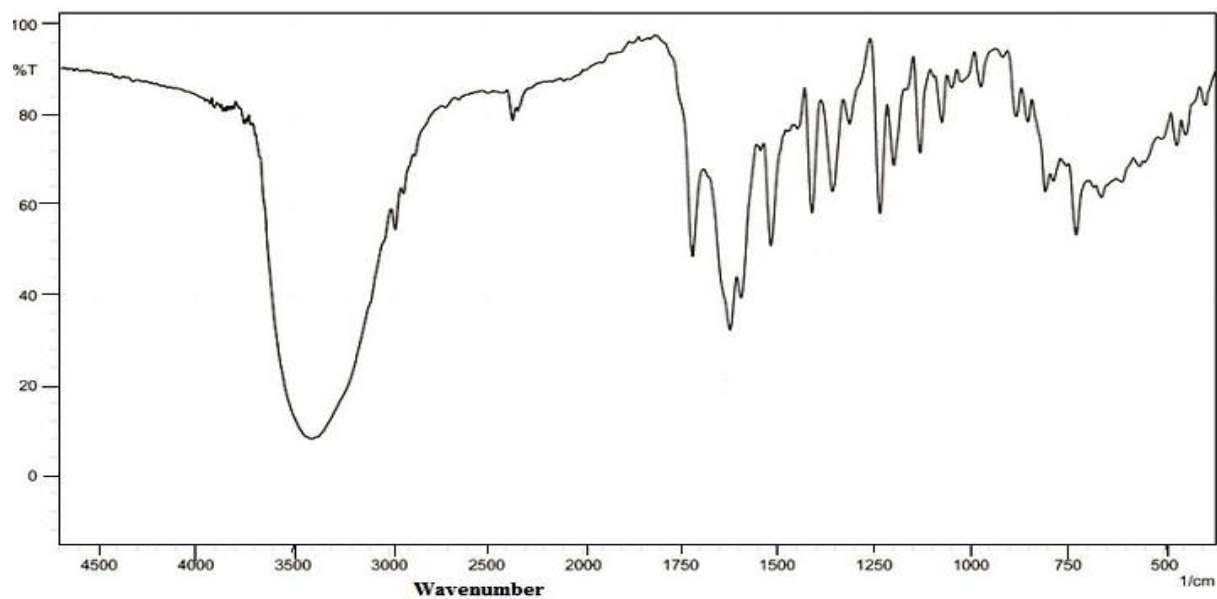


Fig. 1. IR spectrum of Nicomplex, 1(a)





Mothilal et al.

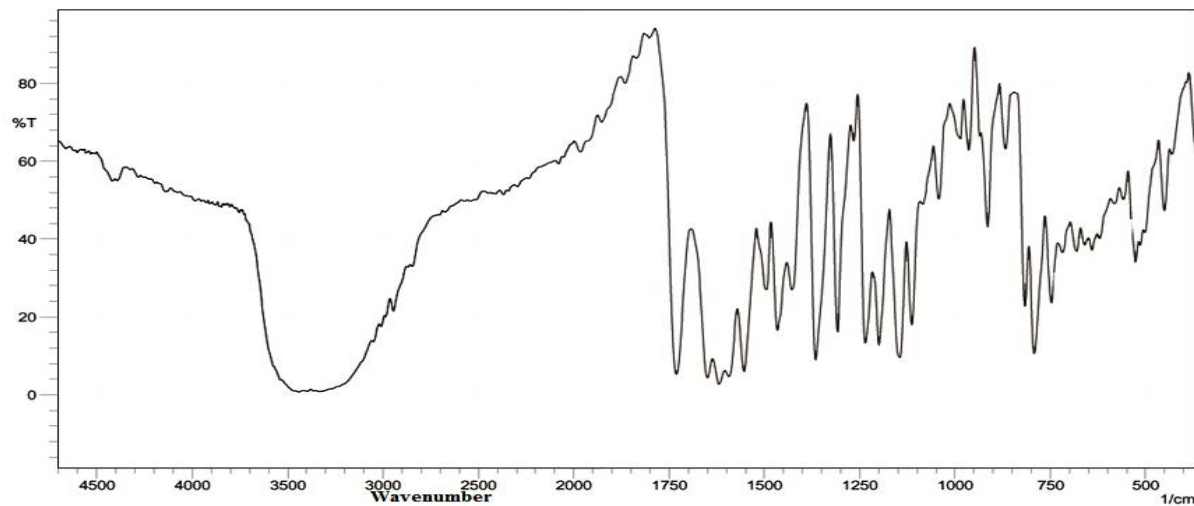


Fig. 2. IR pectrum of Cu complex, 1(b)

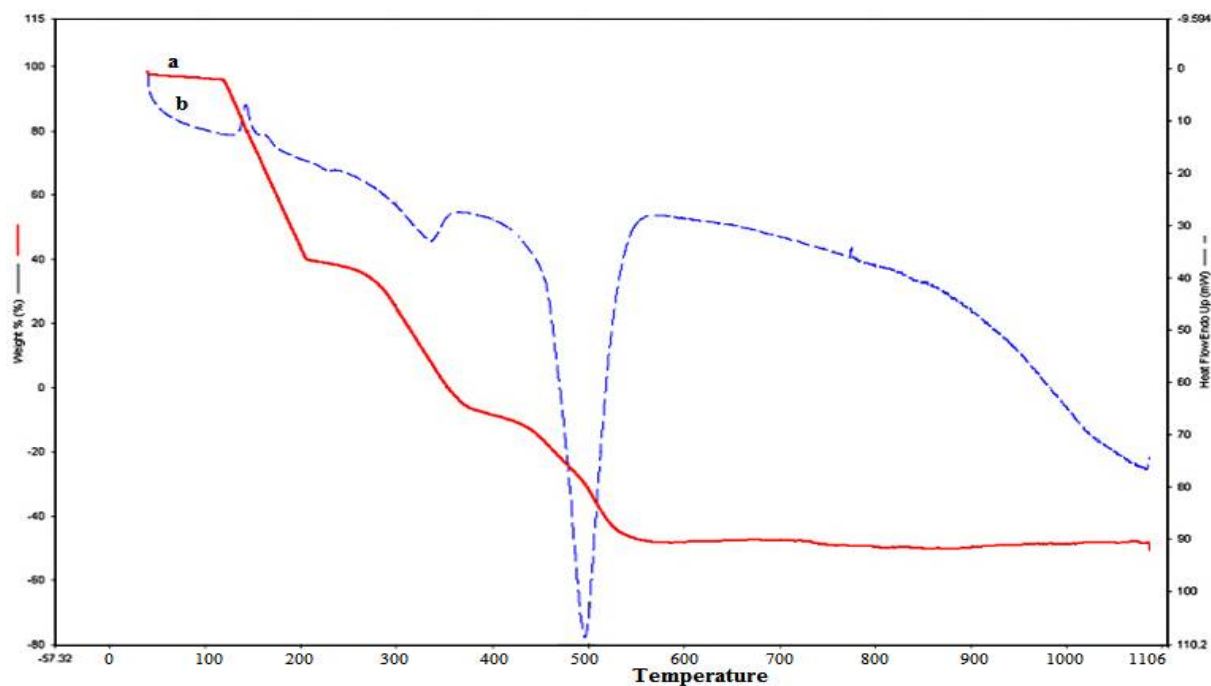


Fig. 3. Superimposed thermogravimetric (TG), differential thermogravimetric (DTG) curves for Nicomplex, 1(a) under N<sub>2</sub> atmosphere; heating rate: 10°C/min.





**Mothilal et al.**

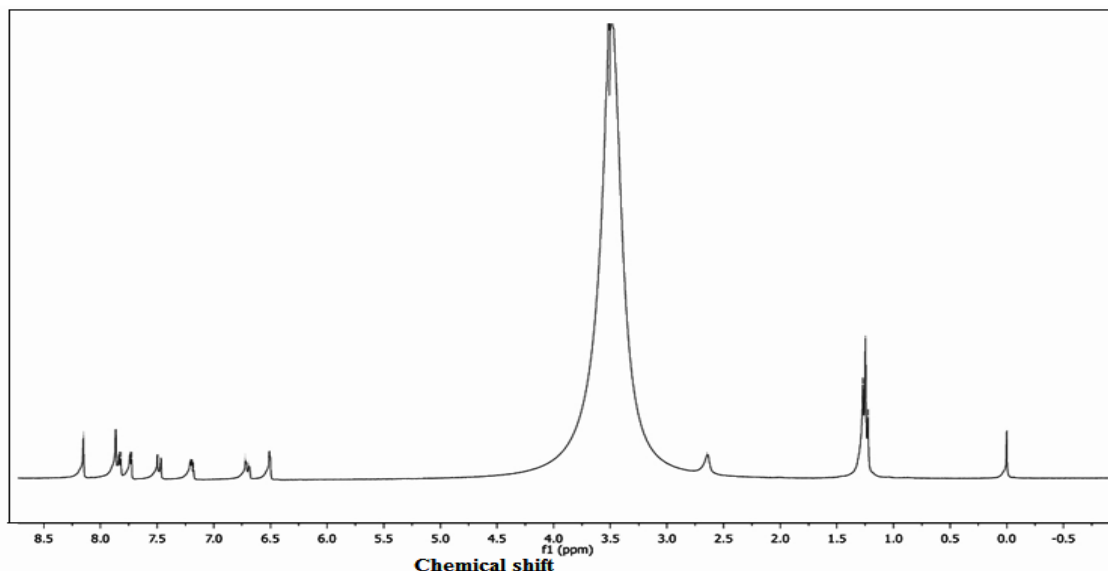


Fig. 4. <sup>1</sup>H NMR spectrum of Zn complex, 1(a)

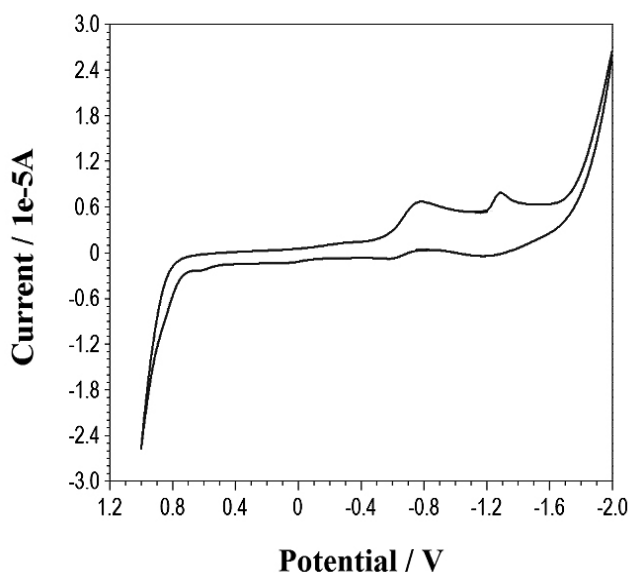


Fig. 5. Cyclic voltammogram of Ni complex 1(c) in DMSO with 0.5 M NBu<sub>4</sub>ClO<sub>4</sub> as supporting electrolyte and scan rate of 50mVs<sup>-1</sup>

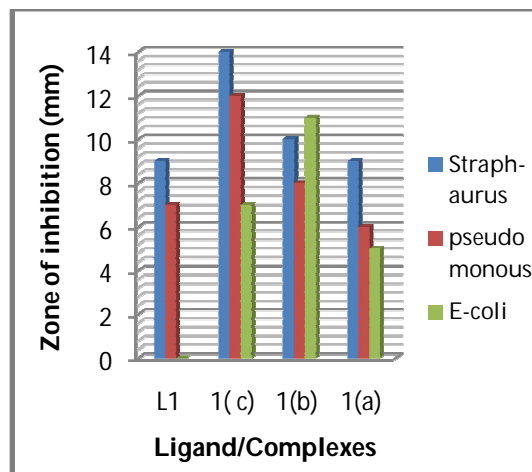


Fig.6 a. Antibacterial activity of Ligand(L1) and Complexes







Mothilal et al.

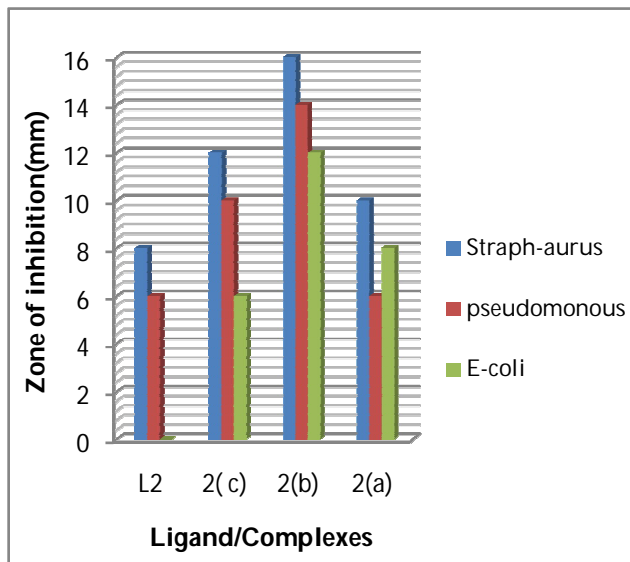


Fig.6 b. Antibacterial activity of Ligand (L2) and complexes

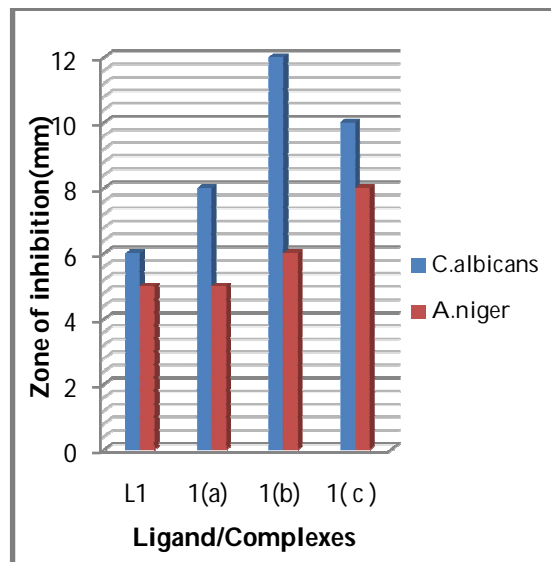


Fig.7 a. Antifungal activity of ligand(L1) and complexes

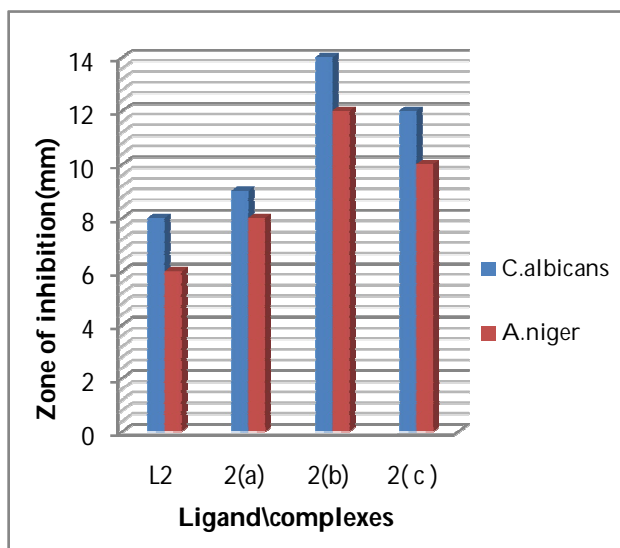


Fig.7 b. Antifungal activity of ligand(L2) and complexes

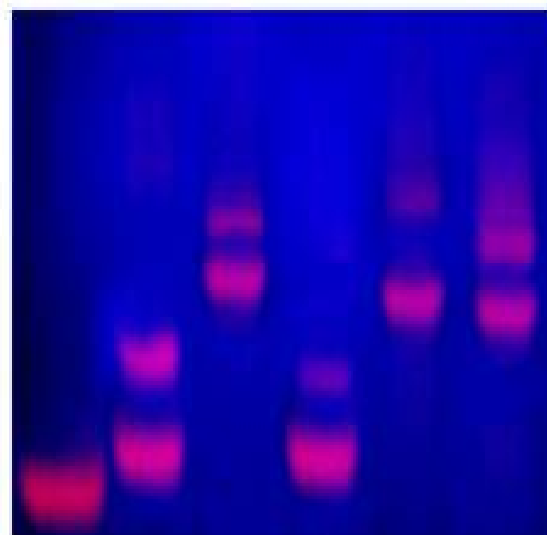


Fig.8 DNA Cleavage of serum proteins (30  $\mu$ M) by the metal complexes (40  $\mu$ M). From left to right, Lane C. Control; Lane 1. DNA + 1(a); Lane 2. DNA + 1(b); Lane 3. DNA + 2(c) ; Lane 4. DNA + 2(a); Lane 5. DNA + 2(b).





Mothilal et al.

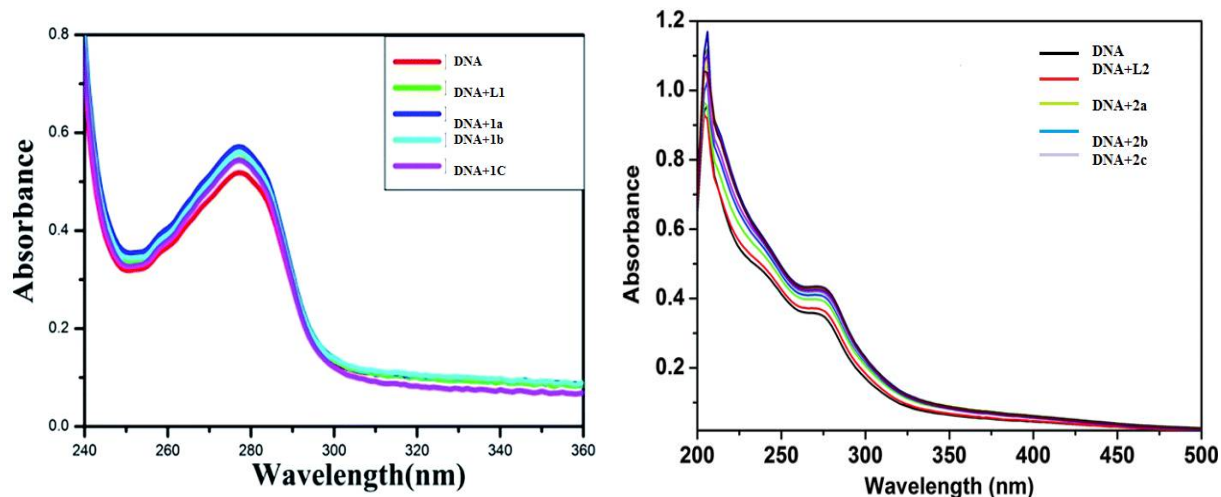


Fig.9 Electronic Absorption spectra of Coumarins (L1 and L2) and metal complexes (1a – 1c and 2a- 2c) of fixed concentration (15µM) in DMSO at 25°C, with the concentration of DNA as 5µM after incubating 15-20 min before the absorption.





RESEARCH ARTICLE

## Analysis of Seismic Torsional Pounding Effect in Adjacent Buildings Evaluating by Indian Standard Codes

Kheti Huseni<sup>1\*</sup>, Panaskar Sourabh Vilasrao<sup>2</sup>, Tashi Dorji Tamang<sup>3</sup> and Abdul Rahim. A<sup>4</sup>

Structural Engineering, VIT University, Vellore-632014 (Pursuing),TamilNadu,India.

Received: 20 June 2016

Revised: 12 July 2016

Accepted: 26 Aug 2016

### Address for correspondence

Kheti Huseni  
M. Tech Scholar, Structural Engineering,  
VIT University, Vellore-632014.  
TamilNadu,India.  
Email: husenikheti@yahoo.in



This is an Open Access Journal / article distributed under the terms of the **Creative Commons Attribution License (CC BY-NC-ND 3.0)** which permits unrestricted use, distribution, and reproduction in any medium, provided the original work is properly cited. All rights reserved.

### ABSTRACT

The past histories have shown that the buildings are susceptible to severe damage during an earthquake. The buildings move out of phase and collide with each other during strong earthquake motions which in turn lead to collapse of structure causing great human loss and economical loss. Thus to prevent the collapse due to colliding of building Indian standards suggests that the minimum separation gap should be provided to prevent collision of adjacent buildings. This colliding of two or more adjacent buildings with each other during strong earthquake motion is termed as pounding. Adopting of required safe separation distance is unrealistic in metropolitan zones because of high land esteem and constrained accessibility of area space. Among the possible structural damages the seismic induced pounding is quite obvious one. This paper examines the computational study of pounding phenomenon of buildings using with dissimilar heights using response spectrum analysis and time history analysis as well as damage caused due the pounding. Further pounding was mitigated by adopting shear wall and bracing system and analysis was carried out in ETABS software. Proper separation distance was proposed to prevent the linear pounding and torsional pounding.

**Keywords :** Safe separation distance, Pounding, Response spectrum analysis, Time history analysis

### INTRODUCTION

In metropolitan cities buildings are constructed close to each other due to high land esteem and lack of space availability. The two adjacent buildings can be used for different operational purposes like one may be used for residential purpose and the other may be used for commercial purpose. Two adjacent buildings will never have same



**Kheti Huseni et al.**

dynamic properties due to different loading conditions, different masses, different heights and many other various reasons. Due to different dynamic properties adjacent buildings collides with each other during strong earthquake motion or any other strong vibrations and causes collapse which in turn causes economical and human loss. To prevent the colliding of adjacent building Indian standard code of building practices suggests separation distance should be adopted. This colliding of adjacent buildings during strong earthquake motions caused due to insufficient separation gap is termed as pounding. For long span buildings expansion joints are implemented at proper intervals to connect the different units of same building, if the joint provided is improper building may have chance to pound.

Pounding is most commonly observed effect during a seismic activity. Pounding damage was observed in El Centro earthquake (1944), Mexico City Earthquake (1985), Sequenay earthquake (1988), Loma Prieta Earthquake (1989), Cairo Earthquake (1992), Kobe earthquake (1999). Mexico City earthquake (1985) that struck Mexico City causing an unusually large number of building failures, in some of which pounding appeared to have played a primary role. In chi-chi earthquake (1999) Structural pounding damages caused in central Taiwan (4 Jeng-Hsiang Lin et.al. 2002). In Christchurch earthquake (2011) around 6% of building were damaged due to pounding which was surveyed by Central Business District (CBD) (5 G.L. Cole et.al., 2012).

Many researches have been carried out on pounding due to past earthquakes. Because of insufficient gap between adjacent buildings pounding could have worst damage in earthquake (6 Shehata E. Abdel Raheem 2006). Impact force decreases with the increment of separation gap (7 Bipin Shrestha 2013). Buildings with different floor levels, different dynamic properties, and raw buildings damage more due to pounding (8 Chandra Sekhara Reddy et. al. 2014). The simplest way to mitigate pounding is to provide proper separation gap between adjacent buildings. But it is unrealistic to provide sufficient gap due to high land value. Most of the word regulations do not take pounding into account. Argentina, Australia, Canada, France, India, Indonesia, Mexico, Taiwan and USA codes specify the minimum distance between adjacent buildings. Among all countries codal provision safe separation distance is higher in FEMA: 273-1997 and NBC PeruE030-2003 (9 Chenna Rajaram et. al., 2012).

Different mitigation practices like constructing new reinforced concrete (RC) walls, Cross bracing system, Combined RC walls and bracing, Dampers, Combined system of RC walls and dampers, Combined system of bracing and dampers can be used in practice to reduce pounding effects. In mitigation techniques X cross bracing system is more effective in reducing the lateral displacement in all bracing systems. (10 Ravindranatha et.al. 2016). Mitigation of pounding in existing structure was done in two adjacent six story R/C frame buildings sited in Pordenone using a pressurized fluid viscous (FV) dampers as protective devices (11 S. Sorace et. al. 2013). Collision shear wall is also beneficial technique deliberated for pounding mitigation (12 S.A. Anagnostopoulos et.al. 2008). Displacement of building can be greatly reduced by adopting shear walls (13 Khaja Afroz Jamal et. al., 2013).

**Required Seismic Separation Distance to avoid Pounding**

As per the bureau of Indian standards, IS 4326,1993, "Indian code of practice for earthquake resistant design and construction of buildings" states that the safe separation distance of adjoining structures or parts of same structure is required for structures having different total heights and different dynamic characteristics. This is to avoid collision during an earthquake. The codes mentioned the gap width as shown in the Table No.1.(3 IS 4326, 1993). As per IS 1893-2002, "Indian standard criteria for earthquake resistant design of structures, part 1 general provision and building", it states that the two adjacent buildings or two adjacent units of the same building with separation joint in be between shall separate by a distance equal to the amount  $R$  times the sum of the calculated storey displacements, to avoid damaging contact storey's when the two units deflect towards each other. When floor levels of same adjacent or similar building are at the same elevation levels, factor  $R$  in this requirement may be replaced by  $R/2$  (1 IS 1893-2002).



**Kheti Huseni et al.****Occurrence of pounding damage**

Seismic pounding between two adjacent buildings occur due inadequate separation gap to which high intensity of earthquake strike and due to different dynamic characteristic loading and structural pattern of adjacent buildings, building vibrate out of phase. Pounding led to non-structural damage to the buildings like cracks to masonry walls to severe damages till collapse of the building.

**Objective**

The fundamental scope of this paper is to examine pounding effect, to find out the pounding force between the building of different heights, to evaluate the separation distance to prevent torsional pounding and to analyze the structure by adopting RC shear wall and steel bracing system. The pounding force is evaluated when the floors of adjacent buildings are at same level but buildings with different height. Response spectrum analyses and time history analyses was carried out using ETABS software.

**MATERIALS AND METHODS**

This paper examines the behavior of reinforced concrete structure under linear static analysis, response spectrum analysis and time history analysis using ETABS software. Seismic pounding of G + 6 and G + 8 buildings are analyzed for displacement and pounding force aspects. Besides structure response with addition of shear wall and bracing system are also studied. For time history function El-centro earthquake data is considered for Table No.2.

**Gap element Model**

With a specific end goal to watch pounding between adjoining structures, buildings are connected by clear gap of different distance by gap element link. The principle reason to adopt gap element is to assess the impact force of pounding between two adjacent buildings. This gap element becomes active when two adjacent building approach each other. The stiffness of the gap element is generally adopted as  $10^2$  to  $10^4$  times the stiffness of the adjacent connected element.

**Details of structure**

Response spectrum analysis and time history analysis were carried out for following cases-

Combined 3D model has been created of G + 6 and G + 8 building using ETABS. Building 1 is 8 storey building having 3 numbers of bays in X and Y direction. Width of bays in X direction are 5m, 4m, 5m respectively and in Y direction are 4m, 5m, 4m respectively. Building 2 is 6 storey building having 3 numbers of bays in X and Y direction. Width of bays in X direction are 4m, 3m, 4m respectively and in Y direction are 4m, 5m, 4m respectively. Height of each storey in both the building is 3.2m and with slab thickness of 150mm. Grade of concrete used is M25 and grade of steel is FE415. Gap elements are between two buildings at floor levels shown in Figure No.1.

**Case no.1- Structure with gap elements only****Case no.2- Structure with gap elements and bracing system**

In this case X cross bracing are adopted along X direction in the 1<sup>st</sup> and 3<sup>rd</sup> bay of size 250mm x 250mm RC bracing of M25 grade as shown in Figure No.2 .

**Case no.3- Structure with gap elements and shear wall**

In this case 230 mm shear wall is adopted in the middle core of both the buildings as shown in Figure No.3.





### Kheti Huseni et al.

#### Loads assigned and load combinations

TABS software auto assigns the self-weight of the structural elements and the various load combinations. Table No.3 shows the loads assigned on the G + 6 and G + 8.

#### Response Spectrum Analysis

Due to the different dynamic property of the two buildings, the structures will have out of phase movement and the two buildings will collide with each other if the separation distance is inadequate than as per specified in the code (1 IS 1893-2002). Response spectrum analysis of three models is carried for zone V is specified as;

Zone factor (Z) = 0.36

Importance factor (I) = 1

Response reduction factor (R) = 3

$S_a/g = 1.62$

## RESULTS AND DISCUSSION

#### Safe separation distance to prevent linear pounding

As per IS 1893-2002 the safe separation gap between two adjacent building units to be provided to prevent pounding effect is 350mm. Initially the building are modeled and analyzed using ETABS software and by adopting a gap of 100mm. The results in terms of displacement are shown Table No 4 and displacement graphs for different models shown in Figure No 4,5,6.

As per SRSS (square root of sum of squares) method the safe separation gap should be

$$S = \sqrt{U_a^2 + U_b^2} \text{ (SRSS)}$$

where,

$U_a, U_b$  = Maximum displacement of each of adjacent buildings.

#### Safe separation gap

- i. for bare frame=160mm
- ii. for bracing system=108mm
- iii. for shear wall model=101mm

#### Safe separation distance to prevent torsional pounding

Even though the separation gap was provided as per the IS 1893-2002 i.e. 350 mm it is observed that it could prevent linear pounding but torsional pounding could occur. The 3D view and plan view representing the torsional collision phenomenon for all three model for different modes are shown in figure No 7,8,9.

In order to prevent the torsional pounding effect in all the three models the separation distance was increased and a safe separation distance to prevent torsional pounding was found out and is mentioned in Table No.5

#### Axial force in gap element link

The force in the gap elements for the 6th, 5th and 4th floor were found out for each of the model and are shown with the help of graph in figure No.10.





**Kheti Huseni et al.**

## CONCLUSION

This study concludes that pounding would occur for a separation distance of 100 mm. So by adopting proper safe separation distance as per IS 1893-2002 linear pounding was prevented but it could not prevent torsional pounding. To reduce the displacement of bare frame bracing system and shear wall is installed. Further to account for the torsional pounding, the separation distance was increased subsequently and various safe separation distance for each of three models i.e. bare frame, bracing system, shear wall are stated. The best system to prevent torsional pounding is providing bracing system than providing shear wall in the middle core of the building since the gap required for bracing system is less than that of required for shear wall.

## ACKNOWLEDGEMENTS

We wish to express our thanks to Professor Visu Vasam (VIT University Vellore) for sharing his knowledge and pearls of wisdom with us during the course of this research.

## REFERENCES

1. IS 1893 (part 1):2002 "Indian standard Criteria for Earthquake Resistant Design of Structures, part 1 General Provisions and buildings, (Fifth Revision)".
2. IS 456:2000 "Indian Standard Plain and Reinforced Concrete Code of Practice".
3. IS 4326:1993 "Indian Standard Code of Practice for Earthquake Resistant Design and Construction of Buildings (Second Revision)".
4. Jeng-Hsiang Lin and Cheng-Chiang Weng, "A study on seismic pounding probability of buildings in taipei metropolitan area", Journal of the Chinese Institute of Engineers, Vol. 25, No. 2 (2002).
5. G.L. Cole, R.P. Dhakal and N. Chouh, "Building Pounding Damage observed in the 2011 Christchurch earthquake", (15 WCEE-2012).
6. Shehata E. Abdel Raheem "Seismic Pounding between Adjacent Building Structure", Electronic Journal of Structural Engineering, 6 (2006).
7. Bipin Shrestha "Effects of separation distance and nonlinearity on pounding response of adjacent structures", International journal of civil and structural engineering Volume 3, No 3, 2013.
8. Chandra Sekhara Reddy T, Kiran Kumar Reddy K and Pradeep Kumar R, "Pounding problems in urban areas", IJRET International Journal of Research in Engineering and Technology, vol. 3, issue 09, Sep 2014.
9. Chenna Rajaram and Ramancharla Pradeep Kumar "Study on Impact between Adjacent Buildings Comparison of Codal Provisions" 15 WCEE LISBOA 2012.
10. Ravindranatha, Pradeep Karanth, Shivananda S.M and H.L Suresh, "A study of seismic pounding effect between adjacent buildings and its mitigation by using different type of bracing systems", International Journal of Research in Engineering and Technology (IJRET), eissn: 2319-1163, pissn: 2321-7308, 2016.
11. S. Sorace and G. Terenzi, "Damped Interconnection Based Mitigation of Seismic Pounding between adjacent R/C Buildings", IACSIT International Journal of Engineering and Technology, vol. 5, No. 3, June 2013.
12. S.A. Anagnostopoulos and C.E. Karamaneas "Collision shear walls to mitigate seismic pounding of Adjacent buildings", The 14<sup>th</sup> World Conference on Earthquake Engineering (14 WCEE-2008)
13. Khaja afroze jamal and H.S. Vidyadhara, "Seismic pounding of multistoried building", IJRET International Journal of Research in Engineering and Technology, eissn: 2319-1163 pissn: 2321-7308 Nov 2013.
14. S. Efraimiadou, G. D. Hatzigeorgiou and D. E. Beskos, "Structural pounding between adjacent buildings: The effects of different structures configurations and multiple earthquakes", 15 WCEE LISBOA 2012.
15. M. E. Ruiz Sandoval, L.B. Ugarte and B.F. Spencer, "Study of Structural Control in Coupled Buildings", 15 WCEE LISBOA 2012.





**Kheti Huseni et al.**

**Table1. Pounding Gap for Various Structures**

Sr. No.	Type of construction	Gap width/storey in mm for design seismic coefficient ( $\alpha_h=0.12$ )
1	Box system or frames with shear walls	15
2	Moment resistant reinforced concrete frame	20
3	Moment resistant steel frame	30

Note: minimum total gap shall be 25mm for any other values of  $\alpha_h$ , the gap element width shall be determined proportionately.

**Table2. Dimensions of Structural Component of Two Building Structure**

Building	G + 8	G + 6
Beam dimension	300 mm x 500 mm	300 mm x 450 mm
Inner column dimension	500 mm x 500 mm	450 mm x 450 mm
Outer column dimension	450 mm x 450 mm	400 mm x 400 mm

**Table 3. Various Loads Assigned on the Structural Model**

Building	G + 8	G + 6
Live load	3 KN/m <sup>2</sup>	2.5 KN/m <sup>2</sup>
Roof floor	1.5 KN/m <sup>2</sup>	1.5 KN/m <sup>2</sup>
Floor finish	1 KN/m <sup>2</sup>	1 KN/m <sup>2</sup>
Weathering course on roof	1 KN/m <sup>2</sup>	1 KN/m <sup>2</sup>
Load due to 230 mm thick wall	14 KN/m <sup>2</sup>	14 KN/m <sup>2</sup>

**Table 4. Maximum Positive And Negative Displacement Of G + 6 And G + 8 Structure With Different Types Of Models**

Building	Displacement (mm)	G + 6	G + 8
Bare Frame	+ve	105 mm	120 mm
	-ve	100 mm	100 mm
Bracing system	+ve	42 mm	85 mm
	-ve	50 mm	95 mm
Shear wall	+ve	43 mm	79 mm
	-ve	45 mm	90 mm







**Kheti Huseni et al.**

**Table No 5. Safe separation gap to prevent torsional pounding**

Sr No.	Model type	Safe separation gap (mm)
1	Bare frame model	800
2	Braced system model	540
3	Shear wall model	650

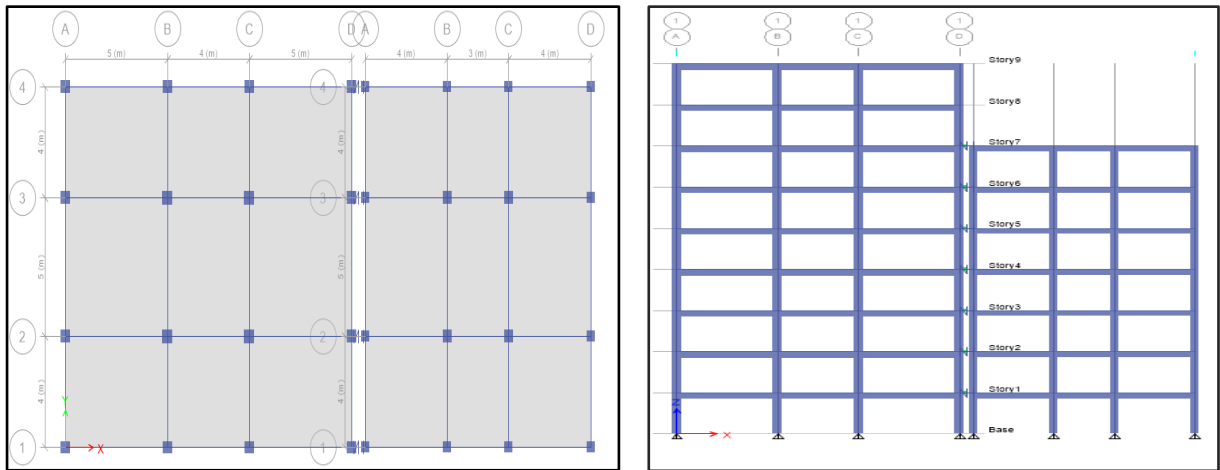


**Figure 1. Plan view and elevation view of bare frame with gap element in between them**

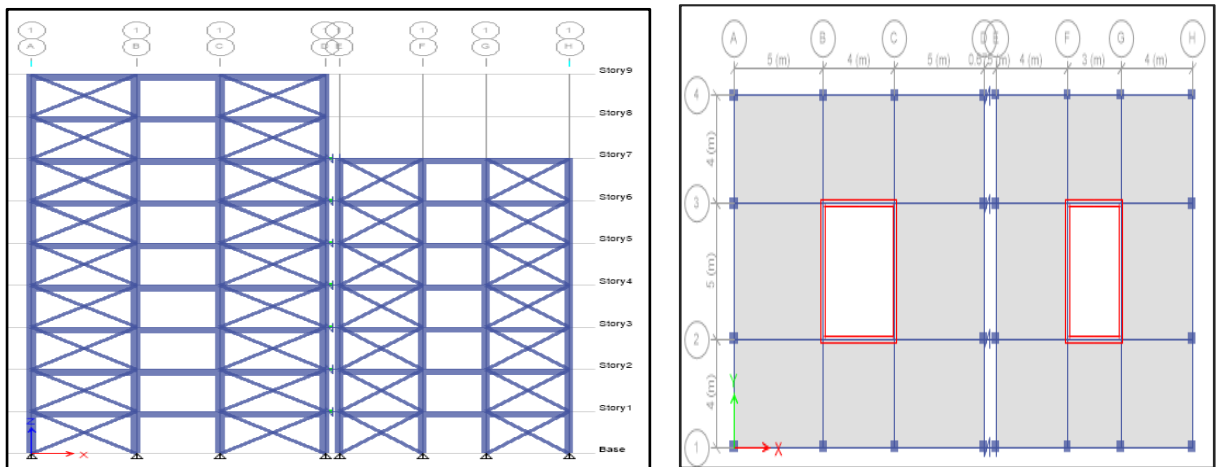


**Figure 2. Elevation view of bracing model**

**Figure 3. Plan view of shear wall model**





**Kheti Huseni et al.**

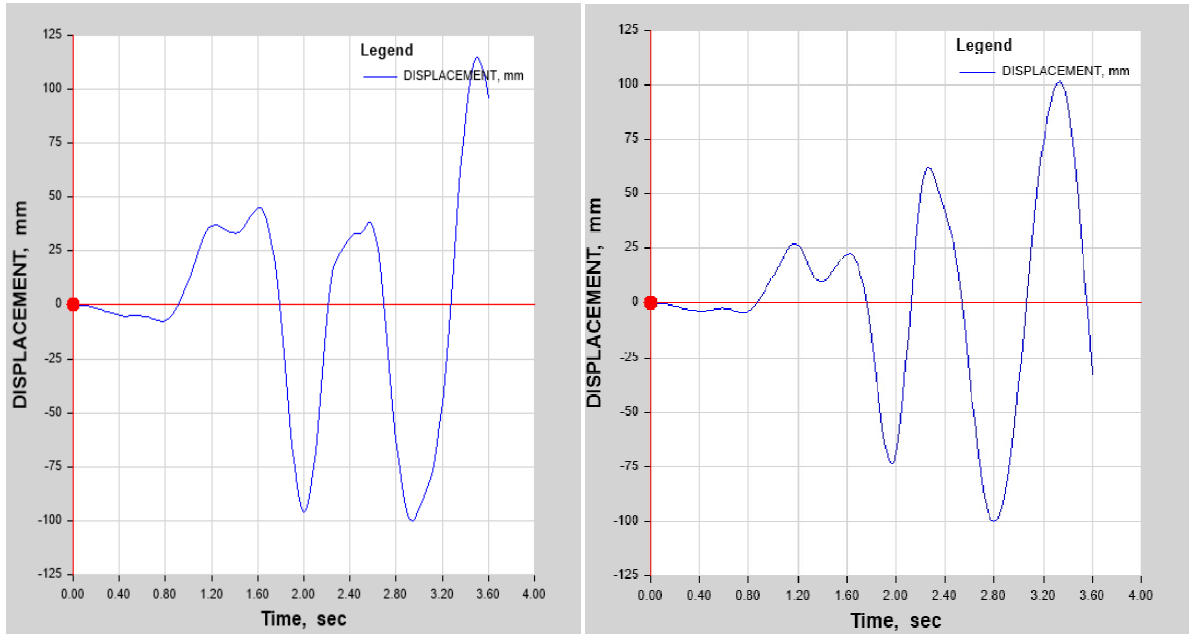


**Figure 4. Displacement graph of G + 6 and G + 8 bare frame model**

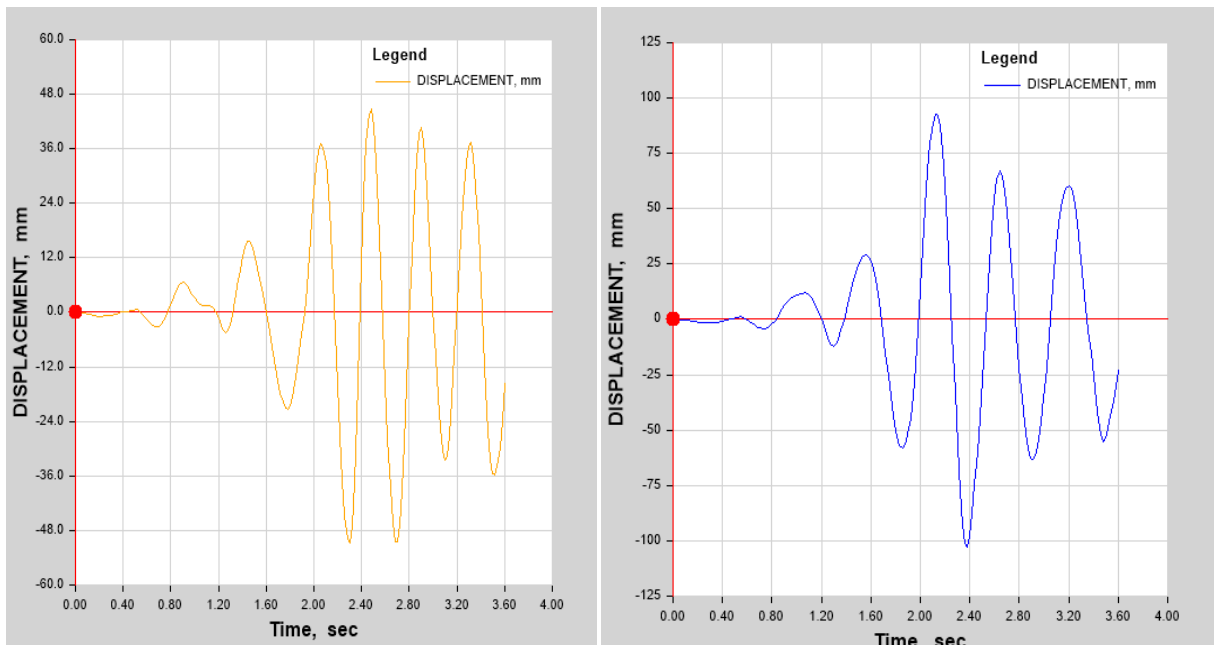


**Figure 5. Displacement graph of G + 6 and G + 8 braced model**





**Kheti Huseni et al.**

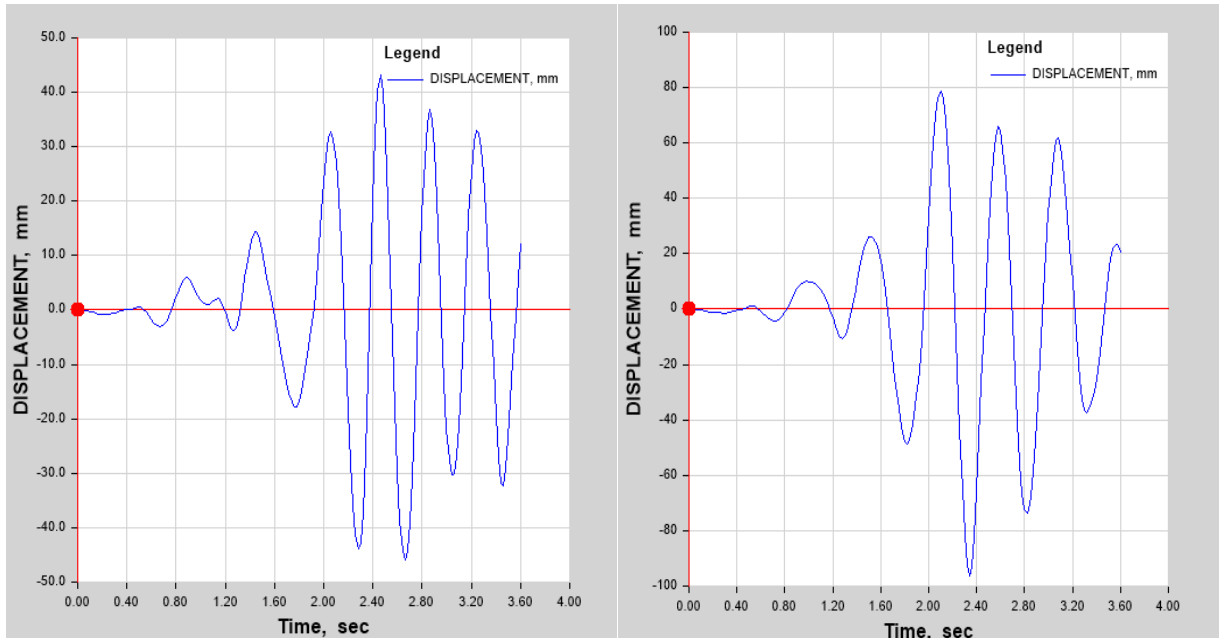


Figure 6. Displacement graph of G + 6 and G + 8 shear wall mode

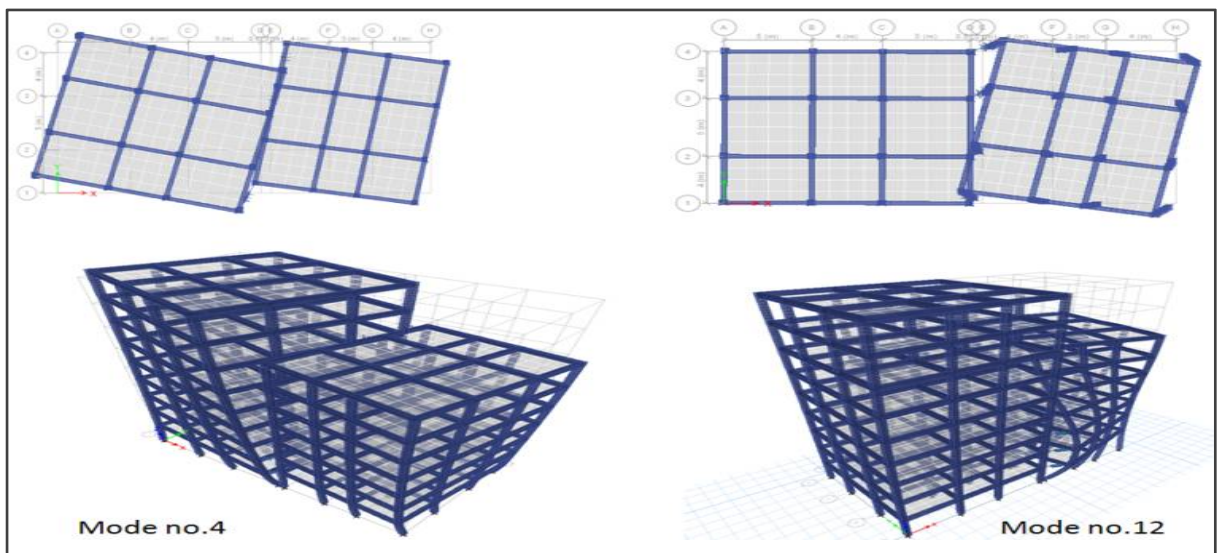
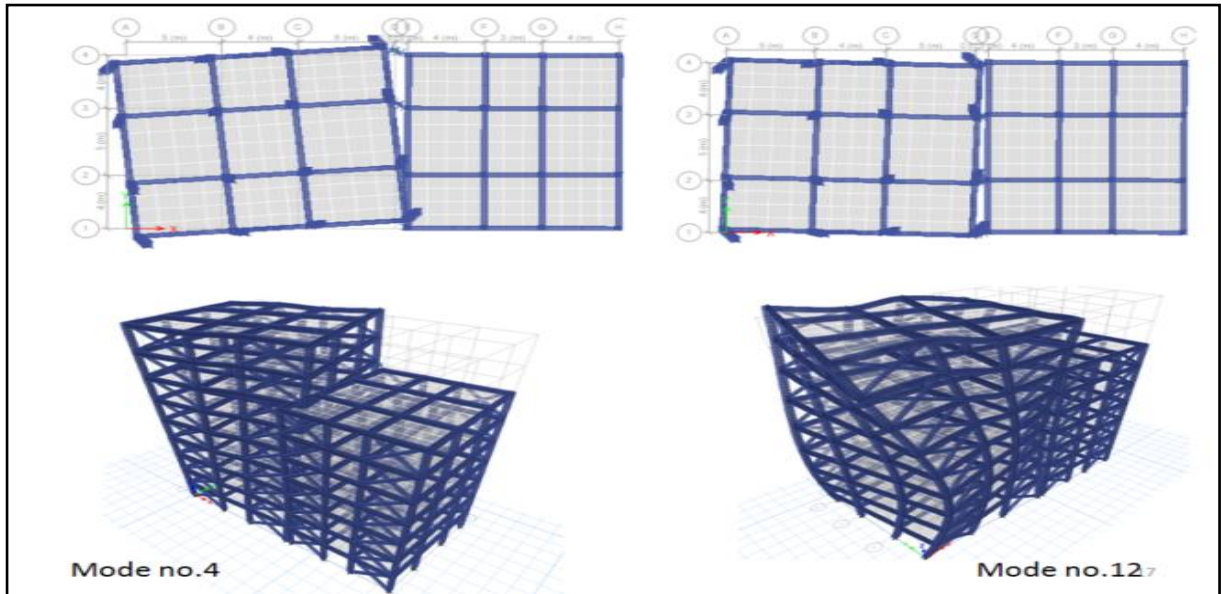


Figure 7. Plan view and 3D view showing torsional pounding of bare frame system





**Kheti Huseni et al.**



**Figure 8. Plan view and 3D view showing torsional pounding of braced system model**

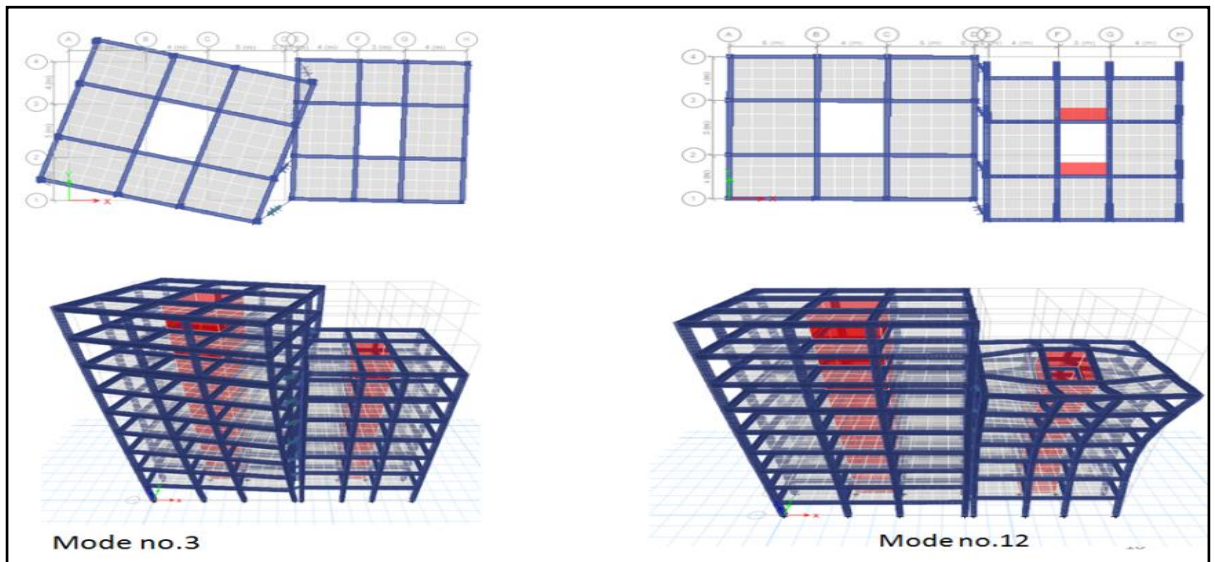


**Figure 9. Plan view and 3D view showing torsional pounding of shear wall model**





**Kheti Huseni et al.**

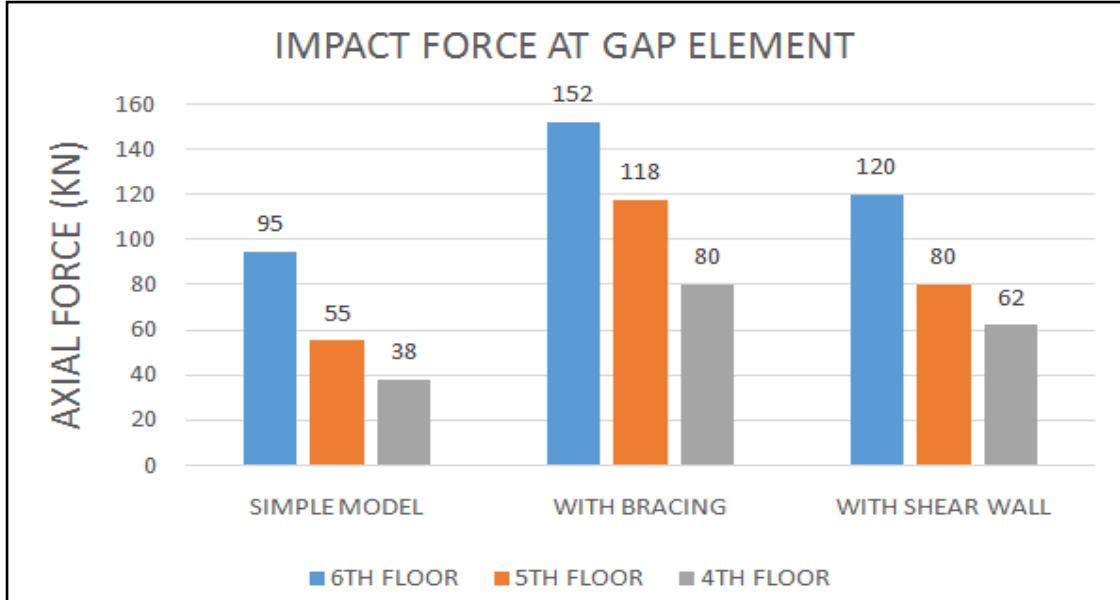


**Figure No 10. Axial force in the gap element**





RESEARCH ARTICLE

## Does Literature help EFL Learners to Improve Language?

S.Vijaylakshmi and Parveen Bala\*

Department of English, JECRC University, Jaipur, India.

Received: 9 July 2016

Revised: 18 Aug 2016

Accepted: 29 Sep 2016

### Address for correspondence

Dr. Parveen Bala

Department of English,

Assistant Professor,

JECRC University, Jaipur, India.

Email: vijaylakshmi.somra@gmail.com



This is an Open Access Journal / article distributed under the terms of the **Creative Commons Attribution License (CC BY-NC-ND 3.0)** which permits unrestricted use, distribution, and reproduction in any medium, provided the original work is properly cited. All rights reserved.

### ABSTRACT

The study intends first to investigate that after giving a proper input of literature, does the performance of the students change (in terms of improving LSRW skills and developing an interest in literature?) For this the students had a regular class of one hour daily including literary texts and BEC handbooks. Students were examined at the initial level before these classes and assessed again after a period of six months to find out if there is a significant difference in their performance. Students were assessed through certified exams like BEC and iTEP. The investigator, being a certified and trained Cambridge Examiner, assessed the students at the initial level on her own abiding by the set norms of these examinations and conducted the standard exams of BEC and iTEP again after a period of six months to find out the differences. The study is primarily focused on the students of Jaipur, Rajasthan who belong to different colleges of Jaipur i.e. JECRC college, Sitapura, UDML, Kukas and JECRC University, Jaipur.

**Keywords :** EFL, Pedagogy, experimenting, English language teaching, BEC, iTEP, literature

### INTRODUCTION

Teaching and learning are two different theories which are conjoined on the grounds of pedagogy as the theory of teaching comes from the theory of learning. That is why these two terms build up a cross-way, but each way is supposedly approached differently by its respective practitioner; learning part by learners but teaching part by teachers. Such interdependence of these different perspectives might be the source of pedagogical achievements and thereby the major motive behind the conduct of this study. Felder and Brent claim that "Learning begins when you, the teacher, learn from the learner. Put yourself in his place so that you may understand what he learns and the way he understands it" [1]. The statement asserts that learners have different skills, strategies, and styles from those of their teachers. Some of them are visually-oriented, some learn by experimenting, while others prefer to learn by working in groups. Similarly, the teaching style of teachers is supposed to be different. Some teachers are excellent, some teach

11678



**Parveen Bala and Vijayalakshmi**

mainly through demonstration; others are more comfortable with theories and abstractions, while some others may resort to their own specific styles of various types in their career.

Felder and Henriques (1995) define learning styles as "The ways in which an individual characteristically acquires, retains, and retrieves information"[2]. They are durable ways of approaching a learning situation which are not usually amenable to change. On the contrary, the term teaching style, according to Conti[3](2004), refers to the distinct qualities displayed by a teacher that are consistent from situation to situation regardless of the subject matter. Felder[4](1993) argues that teachers' teaching style reflects either their own learning styles or the way they were taught in college classes given these points, the major challenge would be what happens when the learners are confronted with a teaching process which is in contrast with their preferred learning style?

The pedagogy needs to be altered with time keeping in mind the level, language skills and mindsets of students. As it has been an incessant and continuous tradition in the Asian countries, especially North India, of communicating in the National language whether the context is official or unofficial and that has been the reason of keeping less interest in communicating in English. Thus to improve their efficiency in the foreign language, English, it was thought of as an experimental task to teach English Literature to EFL students of non-literature background so as to assess whether the students actually develop interest in literature and learn the language in a better way.

**Purpose and settings of the study**

The study intends first to investigate that after giving a proper input of literature, does the performance of the students change (in terms of improving LSRW skills and developing an interest in literature?). The study was performed to find out whether the literary competence of students assist them to acquire more positive response to the literary texts and also to find out if the students have developed the skills of experiencing the world created by and within the literary texts. Also it was intended to find out whether there is an impact of literature on the growth and development of students in terms of applying the LSRW skills in real life situations. For this the students had a regular class of one hour daily including literary texts and BEC handbooks. Students were examined at the initial level before these classes and assessed again after a period of six months to find out if there is a significant difference in their performance. Students were assessed through certified exams like BEC and iTEP. The investigator, being a certified and trained Cambridge Examiner, assessed the students at the initial level on her own abiding by the set norms of these examinations and conducted the standard exams of BEC and iTEP again after a period of six months to find out the differences. The study is primarily focused on the students of Jaipur, Rajasthan who belong to different colleges of Jaipur i.e. JECRC college, Sitapura, UDML, Kukas and JECRC University, Jaipur.

**Participants**

The participants of this study consisted of 230 college students and their ages ranged from 18 to 22 with the average of 20. The heterogeneous groups or participants of this research consisted of girls and boys from all sorts of academic backgrounds. New methods and the activities related to ELT with the use of literature were applied. At the time of data collection, they had studied English as a foreign language and their English level was lower, and during the data collection period they had one hour of sessions every day.

**MATERIALS AND METHODS****Instruments**

In order to collect data, the instruments used in this study were some literary texts, BEC Handbook (Business English Certificate by Cambridge University), BEC Examinations and ITEP examinations which are a qualification at intermediate and pre-intermediate levels recognized by educational institutions as well as other sectors, and shows that a person can deal with everyday English at these levels. BEC helps students to find out their strength and





### Parveen Bala and Vijayalakshmi

weakness in listening, speaking, reading and writing. It provides real situations in which students can use English. Reading skills, such as skimming and scanning are tested. Students are expected to understand different kinds of texts such as public notices and signs, packaging information, communicative messages (e.g. notes, emails, postcards); read texts (e.g. from journals, websites, leaflets, newspapers and magazines) of a factual nature and show understanding of the structure of the language, as it is used to express notions of relative time, space, possession, etc.; scan factual material for information in order to perform relevant tasks, disregarding redundant or irrelevant material; read texts of an imaginative or emotional character and appreciate the central sense of the text, the attitude of the writer to the material and the effect the text is intended to have on the reader.

#### Details about BEC and ITEP examinations

Define abbreviations and acronyms the first time they are used in the text, even after they have been defined in the abstract. Abbreviations such as IEEE, SI, MKS, CGS, sc, dc, and rms do not have to be defined. Do not use abbreviations in the title or heads unless they are unavoidable.

- Business English

Cambridge English Language Assessment is the part of the University of Cambridge and has been providing English Language assessments and qualifications for over 100 years. The exams referred to in are BEC exams which are of three different levels, B1, B2 and C1 with the names, BEC Preliminary, BEC Vantage and BEC Higher.

- CEFR (Common European Framework of Reference)

The CEFR describes language ability on a scale of levels from A1 for beginners up to C2 for those who have mastered a language. This makes it easy for anyone involved in language teaching and testing (learners, teachers, teacher trainers, etc.) to see the level of different qualifications. It also means that employers and educational institutions can easily compare qualifications and see how they relate to exams they already know in their own country

iTEP, one of the globally recognized English certification, is a USA based company established in 2007, specialized in online English language proficiency assessment & on demand training.

iTEP is an English certification accredited by Ministry of HRD, Govt. of India, the Academic Credentials Evaluation Institute (ACEI) & Accrediting Council for Continuing Education & Training (ACCET) & Teachers of English to Speakers of Other Languages (TESOL).

#### There are four iTEP exams[5]

**iTEP Academic** is used by colleges, universities for admissions purposes.

**iTEP SLATE** evaluates high school, secondary school, and middle school students, and is used by boarding schools and academies[6].

**iTEP Business** measures the English skills needed for a work environment. It is used by companies to screen new hires, make decisions about promotions and assignments, and evaluate English training programs[7].

**iTEP Hospitality** measures the English skills necessary to work at restaurants, hotels, resorts, and cruise lines that serve English speakers. The test lasts 30 minutes and evaluates speaking and listening. It is typically administered onsite by an employer for hiring and promotional decisions[8].

iTEP Academic, SLATE, and Business each have a "core" version and a "plus" version. The "core" versions are Internet-based, last 60 minutes, and test reading, grammar and listening. The "plus" versions last 90 minutes in total





**Parveen Bala and Vijayalakshmi**

and also test writing and speaking, requiring the test taker to submit writing and speaking samples via computer. Results are available instantly on the multiple-choice "core" sections, and the speaking and writing results are graded in 5 business days. The "plus" exams retail for \$99USD and can be scheduled within 3 days, making iTEP one of the most flexible and least expensive options among its competitors, which include TOEFL and IELTS. Institutions and businesses administering iTEP exams on-site receive discounted rates[9].

**Procedures**

The materials were given to students during their classes. The aim of this was to motivate them for individual reading of literary texts, and towards independent self-reading[10]. These full-length texts are: "Pied Beauty" and "To Christ our Lord" by G. M. Hopkins; "Success is Counted Sweetest" by Emily Dickinson and "The Gift of Magi" by O. Henry. A pre-experimental reading and writing paper format of a BEC and iTEP test was given to them. During the experimental study poems and short stories were introduced because short stories are often ideal ways of introducing students to the literature in the foreign language classroom and poems direct the students to think in their own unique ways.

During reading comprehension exercises such as pre-reading questions, true or false questions, who said what questions, and what-comes-next questions were included in reading activities. In short, the characters, the plot, language, and topic issues were dealt with reading activities. After reading, types of activities were differed. For writing, activities such as writing a summary or a recommendation, re-writing the story from a character's point of view or a letter to a character were included; for speaking, activities such as role-plays, dramatization or interviewing with the characters were included. Also students were asked to analyze the given poems stylistically so as to generate interest in literature[11]. Also projects such as drawing illustrations, preparing a series of pictures for comics, or posters were included.

**RESULTS AND DISCUSSION**

According to the data obtained and showed in various Tables 1,2 below, the results were better than expected. It is shown that experimental application has contributed better to academic success of the students in the examinations held by iTEP and BEC. It can, therefore, be claimed that the experimental application has affected the academic success of the students positively, at a significant level. In the Figures 1,2 below, findings about the differences in academic success of the students after the experiments are summarized. Our results suggest that the use of literature[12] in ELT increases the motivation of students at university level. We have identified that the performance of students studying English[13] through literature was better than studying English without literature[14]. Also the use of literature[15] in ELT improved students' writing performance and positively affected their attitude[16] to both reading and language learning.

We observed that literature should be included in ELT classrooms[17] as a complement to curriculum because it provides comprehensible input[18] necessary for the English language acquisition and develops the students' abilities[19], as students may build new vocabulary as well as they expand their understanding[20] of words they already know (Ono, Day & Harsch, 2004). In summary, our study reveals that the use of literature[21] in ELT classrooms may motivate[22] students better than abridged and simplified reading passages in students' course books. The results show the motivational effects[23] of the use of literature in ELT, so literature can be used as a positive stimulation to motivate students, and a good means to improve reading and writing skills[24]. In our study it is also proved that especially short stories are ideal[25] literary means for classroom usage[26]. Our results imply the importance of the use of literature in ELT[27], and that literature should be part of teaching-learning process. We had this study in Jaipur, Rajasthan and got positive results about motivation, and reading-writing[28,29] in ELT; however, further research should explore the issue in a different country, and with students at different levels.





### Parveen Bala and Vijayalakshmi

## REFERENCES

1. Felder RM, Brent R (2005). Understanding student differences. *J Engr. Ed.*, 94 (1):57-72.
2. Felder RM, Henriques ER (1995). Learning and teaching styles in foreign and second language education. *Foreign Language Annals*. 28:21–31.
3. Conti GJ (2004). Identifying your teaching style. In Galbraith, Michael W. (Ed) Pp. 76-91. Malabar, FL: Krieger Publishing Company.
4. Felder R(1993). Reaching the second tier: Learning and teaching styles in college science Education. *J. College Science Teaching*. 23(5):286- 290.
5. Ashwill, Mark A. "iTEP Arrives in Vietnam!". *International Educator*. Retrieved 31 August 2012.
6. Thomas, Daniel. "iTEP SLATE exam climbs 300%, USA". *Professionals in International Education*. Retrieved 28 June 2013.
7. "Programs & Activities / Current". United States-Mexico Chamber of Commerce. Retrieved 31 August 2012.
8. "iTEP Hospitality Exam Tests English Proficiency". *qsr magazine.com*. QSR Magazine. Retrieved 7 January 2015.
9. "International Test of English Proficiency ( iTEP)". Cleveland State University. Retrieved 4 September 2012.
10. Bamford, J. and Day R. R. (2004). *Extensive Reading Activities for Teaching Language* Cambridge, UK: Cambridge University Press.
11. Benton, M. and Fox G. (1985). *Teaching Literature. Nine to Fourteen*. Oxford: Oxford University Press.
12. Brown, R. (2000). Extensive Reading in the EFL Class. *Extensive Reading*, 3 Nov. Brumfit, C. (1981). Reading skills and the study of literature in a foreign language. *System* 9 (1): 243–8.
13. Brumfit, C.J. and Carter R.A. (1991). *Literature and Language Teaching*. Oxford:Oxford University Press.
14. Carroli, P., Pavone A. and Tudini, V. (2003). *Face Value: teaching Italian verbal and social-cultural interaction*. Melbourne, Australia.
15. Carter, R. (1999). Common language: corpus, creativity and cognition. *Language and Literature* 8 (3): 195–216. and *Literature* 8 (3): 195–216.
16. Carter, R. A. and Long, M. N. (1991). *Teaching Literature*. London: Longman.
17. Clandfield, L. and Duncan F. (2006). "Teaching Materials: Using Literature in the EFL/ESL Classroom".
18. Collie, J. and Slater S. (1990). *Literature in the Language Classroom: A Resource Book of Ideas and Activities*. UK: Cambridge University Press.
19. Dawson, N. (2005). *Penguin Readers Teacher's Guide to Using Graded Readers*. Essex, UK: Pearson.
20. Deci, E. L. and Ryan, R. M. (1985). *Intrinsic motivation and self-determination in human behavior*. New York, USA: Plenum Press.
21. Deci, E. L., Koestner, R. and Ryan, R. M. (1999). A meta-analytic review of experiments examining the effects of extrinsic rewards on intrinsic motivation. *Psychological Bulletin*, 125, 627-338.
22. Duff, A. and Maley, A. (2007). *Literature*. (Second edition). Oxford: Oxford University Press. Ellis, G. (2002).
23. Learning English through Children's Literature. *Teaching English*, 18 Dec.
24. Gredler, M. E., Broussard, S. C. and Garrison, M. E. B. (2004). The relationship between classroom motivation and academic achievement in elementary school aged children. *Family and Consumer Sciences Research Journal*, 33(2), 106–120.
25. Guay, F., Chanal, J., Ratelle, C.F., Marsh, H. W., Larose, S. and Boivin, M. (2010). Intrinsic identified and controlled types of motivation for school subjects in young elementary school children. *British Journal of Educational Psychology*, 80, 711-735.
26. Hall, G. (2001). The poetics of everyday language in J. McRae (ed.) *Reading beyond Text: Processes and Skills*. CAUCE. 24. Sevilla: Universidad de Sevilla.
27. Hall, G. (2003). Poetry, pleasure and second language classrooms. *Applied Linguistics* 24 (3): 295–9.
28. Hedge, T. (1985). *Using Readers in English Teaching*. London, UK: Macmillan. Kramsch, C. and Kramsch, O. (2000). The avatars of literature in language study. *Modern Language Journal* 84: 553–73.
29. Larsen-Freeman, D. (1986). *Techniques and principles in language teaching*. Oxford: Oxford University Press.





**Parveen Bala and Vijayalakshmi**

**Table 1: iTEP**

There were a total of 230 students who appeared for iTEP tests and the results are as follows:

	Before	After
Advanced	5	17
Upper Intermediate	17	70
Intermediate	33	37
Elementary	116	64
Beginner	59	42

**Table 2: BEC (Business English Certificate)**

The students also appeared for BEC and the results are:

	Before	After
Vantage A	0	2
Vantage B	3	5
Vantage C	8	11
Preliminary B1	12	5

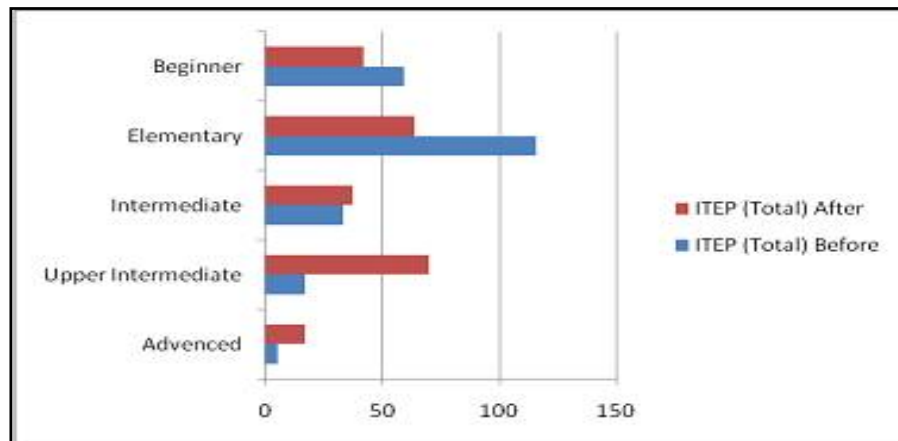


**Figure 1. Findings about the differences in academic success of the students ( iTEP tests and the results)**





**Parveen Bala and Vijayalakshmi**

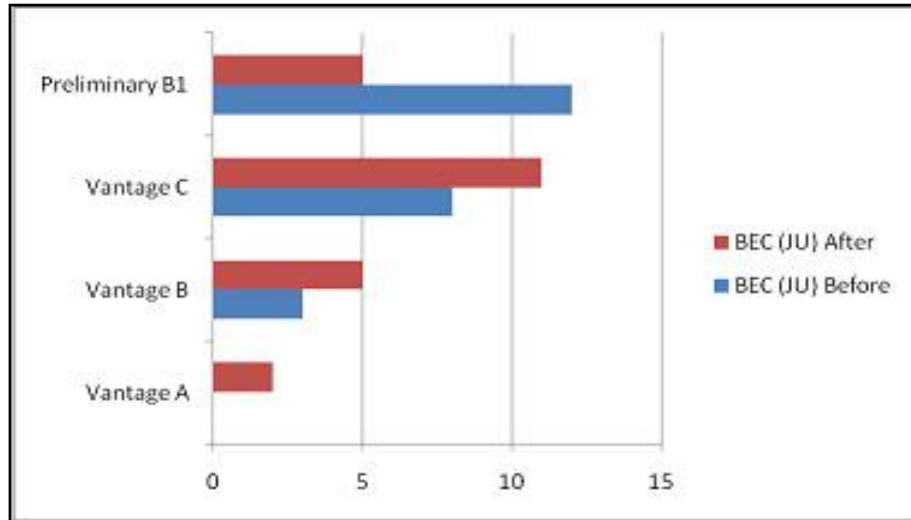


Figure 2. Students also appeared for BEC





RESEARCH ARTICLE

## Extraction Quantity Estimation of Gallic Acid in Fruits of Indian Medicinal Plants Amla Haritaki and Vibitaki

Arvind Varchaswi, K Ramakanth Reddy, M Ravi Kumar Reddy, A Anuradha, K Gnananath and MachaVijay\*

Source Natural Foods and Herbal Supplements Limited, Plot No 22 & 23, SVCIE, Bachupally, Outhbullapur, RR District, Hyderabad, India.

Received: 7 May 2016

Revised: 10 June 2016

Accepted: 02 July 2016

### Address for correspondence

Macha Vijay  
Quality Control,  
Source Natural Foods and Herbal Supplements Limited  
Plot No 22 & 23, SVCIE, Bachupally,  
Outhbullapur Mandal, RR District,  
Hyderabad-50009, India.  
Email: vijaymachares@gmail.com



This is an Open Access Journal / article distributed under the terms of the **Creative Commons Attribution License (CC BY-NC-ND 3.0)** which permits unrestricted use, distribution, and reproduction in any medium, provided the original work is properly cited. All rights reserved.

### ABSTRACT

Now-a-days people are widely using herbal medicines. Triphala is a traditional Ayurvedic herbal formulation (medicine) for this preparation we are using three plant fruits namely Amla, Haritaki and Vibitaki in equal proportions, before using this materials for formulation we have evaluated Physicochemical parameters. Preliminary phytochemical analysis and quantitative estimation of Active Marker. In physicochemical parameters we observed total ash content of Amla (6.13) was high, in Vibitaki acid insoluble ash (3.9) and alcohol soluble extracts (9.76) are very low. In Preliminary phytochemical analysis Haritaki showed higher presence of secondary metabolites. The aim of present investigation Gallic acid was taken as Active marker because this compound is unique in three fruits. by using validated in house Thin Layer Chromatographic method we concluded that retention factor value of Gallic acid was 0.27 and quantity estimation of Gallic acid was evaluated by validated High pressure liquid chromatographic method in this method we are used C-18 column Photo diode array detector, the quantity of Gallic acid was high in Amla (3.40%) compared with other two fruits in Haritaki (0.80%) contain low quantity of Gallic acid compared with Amla and Vibitaki (1%)

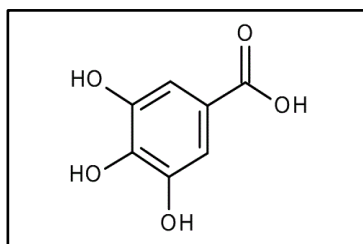
**Keywords :** Gallic acid, Amla, Haritaki, Vibitaki, Thin Layer Chromatography, High pressure liquid chromatography



**Macha Vijay et al.**

## INTRODUCTION

Gallic acid is a poly phenolic compound and it is more active constituent of Indian medicinal plant fruits of Amla Haritaki and Vibitaki Gallic acid (3, 4, and 5 - Trihydroxy benzoic acid) is a poly phenolic compound and possesses an antioxidant property. Gallic acid content is more in fruits of Amla, Haritaki and Vibhitaki and it acts as a marker for controlling the quality of the product [1].Gallic acid and its derivatives have neuroprotective effects with free radical scavenging effects [2].



Structure of Gallic acid

The fruits of Amla, Vibhitaki and Haritaki are used widely in the Ayurvedic herbal formulations. These are rich sources of vitamin-C, vitamin-A and vitamin-B complex. They are used as laxative, digestive and expectorant. The mixture of Amla (*Phyllanthus emblica* Linn.), Haritaki (*Terminalia chebula*) and Vibitaki (*Terminalia bellerica*) three fruits of medicinal herbs in equal proportions is termed as 'Triphala'[3].The fruit of Amla is rich in nutrition and contains minerals and vitamins. Amla protects cell against free radical damage and provides antioxidants protection [4]. Triphala has been integral cornerstone of Ayurvedic medicine before 16<sup>th</sup> century A.D. Triphala is the most widely revered herbal formula for supporting gastrointestinal wellness, cures diabetes, leprosy, Laxative, good for eyes, improves taste and cures intermittent fevers [5].Amla contains hepatoprotective and antiatherosclerotic property[6].Vibhitaki was traditionally used to clear excess fat and bile from the system, as well as to enhance the appetite[7]. The effect of Vibhitaki is partly due to Gallic acid which exhibits antioxidant effects. [8].Haritaki is used as intestinal cleansers and it is used both for occasional constipation and diarrhea, its action is due to the astringent properties of its tannic and Gallic acid[9].

The aim of the present investigation was isolation and quantity estimation of Gallic acid content in fruits of Indian Medicinal plants was determined by using Thin Layer Chromatography (TLC) and High Performance Liquid Chromatography (HPLC).

## MATERIALS AND METHODS

Amla(*Phyllanthus emblica* Linn.), Haritaki(*Terminalia chebula*) and Vibitaki (*Terminalia bellerica*)collected from commercially, All solvents and reagents are AR and HPLC grade obtained from SLR, Standard Gallic acid compound purchased from Natural remedies From India.

### Sample and standard preparation

For TLC system, Take 4g of plant material individually in three conical flasks, add 40 ml methanol and keep aside it for 24hrs at room temperature, after concentrate remove the mark and fractionate with chloroform then take chloroform fraction made up to 10 ml. For Reference standard, Take 1 mg of Gallic acid in 1 ml Analytical grade methanol this solution becomes 1000 ppm. For HPLC Weigh accurately about 1g of Amla powder in 100mL volumetric flask. Add 40mL of Hot HPLC Grade water then sonicate for 10 minutes and cool, and make up the volume to 100mL with HPLC Grade Water. Mix well and filter the solution through 0.45µ membrane filter paper. Reference preparation is take 0.1mg/ml of Gallic acid in HPLC Grade Water.



**Macha Vijay et al.****Physicochemical parameters**

Physicochemical properties of plant materials like moisture, water soluble extract, Total Ash, Acid insoluble ash, and Alcohol soluble extract were determined as per the Ayurveda Pharmacopeia guidelines[10].

**Phytochemical parameters**

Preliminary phytochemical analysis of selected three Plant fruits performed their methanolic extract. We carried out presence of alkaloids, sugars, flavonoids, phenols, saponins, steroids, and terpenoid. By using various(selected) testing methods [11,12].

**TLC Method for Gallic acid**

The sample solution 20 $\mu$ l and reference Gallic acid was applied on TLC Aluminum plate precoated with silica gel 60 F254 of 0.2 mm thickness. The plate was developed in Methanol: Chloroform (6: 4 v/v). After drying the plate there was no absorbance in UV 254 and 366 nm. After the plate was dipped in Vanillin – Sulphuric acid and heated on hot plate at 105 $^{\circ}$ C till the spots appeared.

**HPLC method for Gallic acid**

Chromatographic condition:

**Column:** Hibar, Prepacked column, LiChrospher 100, RP-18e (5 $\mu$ m) (Merck)

Phenomenex-Luna 5 $\mu$  C-18(2) Size: 250 $\times$ 4.60mm,

**Detector:** Photo diode array detector

**Wave length:** 270 nm

**Flow rate:**1.5ml/min

**Injection volume:** 20 $\mu$ l

**Mobile phase**

In mobile phase system solvent-A was dissolved in 0.136 g of anhydrous potassium dihydrogen orthophosphate (KH<sub>2</sub>PO<sub>4</sub>) in 900 mL of HPLC grade water and then add 0.5mL of orthophosphoric acid. Make up to 1000 mL with water, filter through 0.45  $\mu$  membrane and sonicate it for 3 minutes and Solvent-B was Acetonitrile, Gradient Programming of the solvent system was initially at 95%A. Changed to 55% at 18.0 min maintained 2.0 min, changed to 95% A at 25.0 min.

**RESULTS AND DISCUSSION****Physicochemical properties**

Physicochemical parameters of Amla Haritaki and Vibitaki are tabulated in Tabel No 1. All results are under limits which are taken from Ayurveda Pharmacopeia. The loss on drying at 105 $^{\circ}$ c three plant materials not showed much variation, total ash content which indicate the purity of material, in Amla dried Fruits moisture (6.13) is more than other two plant materials, Acid insoluble ash was evaluated siliceous matter in plant material and alcohol soluble extract shows active constituents of secondary metabolite, in Vibitaki acid insoluble ash and alcohol soluble extracts are very low Compared with Amla and Haritaki as well as Haritaki shown higher value and water soluble extract indicate presence of mineral content the yield of water extract was high in Haritaki.

**Phytochemical properties**

Preliminary Phytoconstituents are described in Tabel No 2. The methanolic extract of haritaki shown rich source of phytochemicals compared to Amla and Vibitaki, In Amla Steroid, Terpenoid and Saponin are not present, in methanolic extract of Vibitaki shown Presence of Alkaloid, Flavonoids and Tannin.



**Macha Vijay et al.****Quantitative estimation of Gallic acid**

The fruits of Amla, Haritaki and Vibitaki was Isolated by TLC are tabulated in Table No. 3. The isolation of Gallic Acid was determined by Validated In house process method. The Rf value of the three different fruits i.e. Amla, Haritaki and Vibitaki was 0.27 which is an unique value. The quantity estimation of Gallic Acid was determined by Validated In house process method. The quantity estimation of Gallic Acid in Amla was more 3.40% compare to Haritaki and Vibitaki, whereas, in Haritaki the quantity of Gallic Acid was less 0.80% compare to Amla and Vibitaki and the quantity estimation of Gallic Acid in Vibitaki was 1%.

**CONCLUSION**

In present investigation we evaluated Physicochemical, Phytochemical and Gallic acid in three different Indian medicinal plant fruits Amla, Haritaki and Vibitaki, The Results of Physicochemical Parameters are within in the limits as per Ayurvedic Pharmacopoeia so this three plant fruits are used for herbal formulation. In Phytochemical analysis for this three fruits we performed Alkaloids, Flavonoids, Steroid, Tannin, Sugar, Terpenoid and Saponin Tests and we observed presence and absences of this secondary metabolites, by using thin layer chromatography we conclude that Gallic acid was present in Amla, Haritaki and Vibitaki and the Rf value of Gallic acid was 0.27, Gallic acid was evaluated by using High pressure liquid chromatography and respective quantity of Gallic acid in Amla(3.40), Haritaki(0.80), and Vibitaki(1)

**ACKNOWLEDGEMENTS**

We are thankful to Mr.Arvind Varchaswi, Trustee, Sri Sri Ayurveda for providing support to carry out this work.

**REFERENCES**

1. Evans WC. Trease and Evans' Pharmacognosy. 14th ed. London: WB Saunders Company; 1996. pp. 224–228).
2. Zhongbing et al, 2006 & Kubo et al 2010
3. Biradar YS, Jagatap Sh, Khandelwal KR, Singhania SS. Exploring of antimicrobial activity of Triphala Mashi- an ayurvedic formulation. Evid. Based Complement. Alternat. Med. 2008; 5:107–113.
4. Kroes BH, Van Den Berg JJ, Quarles Van Ufford HC, Van Dijk H and Labadie RP: Anti-inflammatory activity of Gallic Acid. *Planta Medica* 1992; 58: 499-5.
5. S.R.R. Srikanth Murthy, Volume I, Bhavaprakasha, Chowkhamba Krishnadas Academy, 2008, p, 159-65
6. Jose JK and Kuttan R: Antioxidant Activity of *Emblica Officinalis*. *Journal of Clinical Biochemistry and Nutrition* 1995; 19:63-70.
7. Charaka Samhita. 1996. Translated by: Kaviratna AC, Sharma P, Sigdell JE. *Indian Medical Science Series No. 41*. India: Sri Satguru Publications. 1503 p.
8. (Jagetia GC, Baliga MS, Malagi KJ and Kamath KS. The evaluation of the radioprotective effect of Triphala (an Ayurvedic rejuvenating drug) in the mice exposed to radiation. *Phytomedicine*. 2002, 9:99-108. 4. Singh DP.)
9. Dixit D, Dixit AK, Lad H, Gupta D, Bhatnagar D. 2013. Radioprotective effect of *Terminalia chebula* Retzius extract against  $\gamma$ -irradiation-induced oxidative stress. *Biomedicine & Aging Pathology* 3:83-8.
10. Anonymous, The Ayurvedic Pharmacopoeia of India, Part-I, New Delhi, Govt. of India, Ministry of Health & FW, Dept. of ISM and H 1999; 1-4:213-14.
11. Shukla VJ, Bhatt UB. Methods of Qualitative Testing of some Ayurvedic Formulations. Jamnagar, Gujarat Ayurved University, 2001, 5-10.
12. Khandelwal KR. Practical Pharmacognosy – Techniques and Experiments. 9th ed.: Nirali Prakashan, Pune, 2002, 149-153







**Macha Vijay et al.**

**Table 1: Physicochemical Properties**

Physicochemical Parameters				
S.No.	Test	Amla	Haritaki	Vibitaki
1	Loss on Drying (%) w/w	5.6	5.2	5.96
2	Total Ash Value (%)w/w	6.13	3.4	3.9
3	Acid insoluble ash(%) w/w	1.03	3.9	0.83
4	Alcohol soluble extractive(%) w/w	42.5	46.5	9.76
5	Water soluble extractive(%) w/w	52.7	62	39.6

**Table 2: Phytochemical Properties**

Phytochemical parameters					
S.No.	Natural Product	Test performed	Amla	Haritaki	Vibitaki
1	Alkaloid	Dragendorff's test	+ Ve	+ Ve	+ Ve
2	Flavone	Shinoda test	+Ve	+ Ve	+ Ve
3	Steroid	Liebermann-Burchard reagent	-Ve	+ Ve	-Ve
4	Tannin	Neutral FeCl <sub>3</sub>	+Ve	+ Ve	+ Ve
5	Sugar	Molisch's test	+Ve	+ Ve	-Ve
6	Terpenoid	Noller's tes	-Ve	+ Ve	-Ve
7	Saponin	NaOH solution	-Ve	+ Ve	-Ve

**Table 3: Isolation and Quantity Estimation of Gallic Acid**

S.No.	Plant name	Quantity	TLC Rf Value
1	Amla	3.40%	0.27
2	Haritaki	0.80%	0.27
3	Vibitaki	1%	0.27





**Macha Vijay et al.**

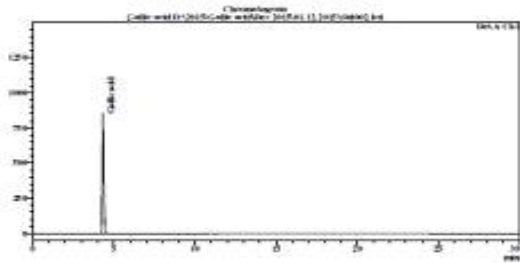


**Fig: Gallic acid standard**

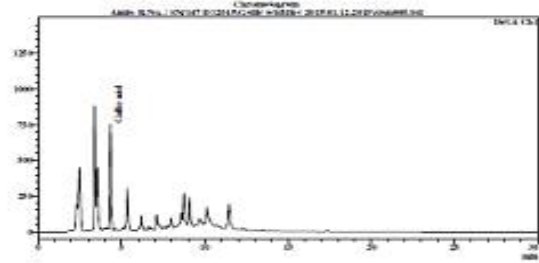


**Fig: Gallic acid in Amla**

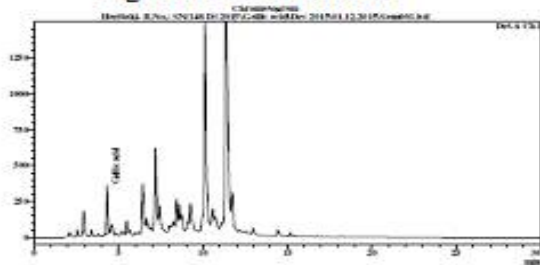


**Fig: Gallic acid in Haritaki**

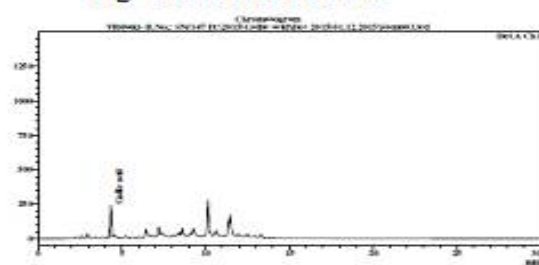


**Fig: Gallic acid in Vibitaki**

**Fig 1: Chromatograms of Gallic acid in Amla, Haritaki and Vibitaki Fruit's**

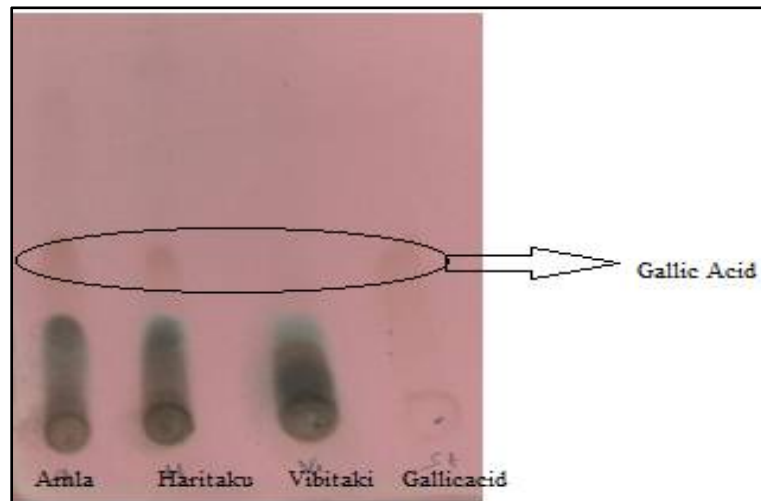


**Fig 2: TLC for Gallic acid**





## Transition Period and its Successful Management in Dairy Cows

P.Ravi Kanth Reddy<sup>1\*</sup>, Jakkula Raju<sup>2</sup>, A. Nagarjuna Redy<sup>3</sup>, P.Pandu Ranga Reddy<sup>4</sup> and Iqbal Hyder<sup>5</sup>

<sup>1</sup>Dept. of Animal Nutrition, NTR CVSc, Gannavaram, A.P.India.

<sup>2</sup>Dept. of Animal Nutrition, PVNR Telangana state university for veterinary, Hyderabad, Telangana.

<sup>3</sup>Dept. of LPM, NTRCVSc, Gannavaram, India.

<sup>4</sup>Scientist and Head, Livestock Research Station, Mahanandi, India.

<sup>5</sup>Dept. of Veterinary Physiology, NTR CVSc, Gannavaram, A.P.India.

Received: 8 July 2016

Revised: 14 Aug 2016

Accepted: 27 Sep 2016

### Address for correspondence

P. Ravi Kanth Reddy  
Ph.D Scholar, Dept. of Animal Nutrition,  
NTR CVSc, Gannavaram, A.P.,India.  
Email: ravi.nutrition001@gmail.com



This is an Open Access Journal / article distributed under the terms of the **Creative Commons Attribution License (CC BY-NC-ND 3.0)** which permits unrestricted use, distribution, and reproduction in any medium, provided the original work is properly cited. All rights reserved.

### ABSTRACT

Cows that fail to transition successfully into lactation are vulnerable to a host number of problems which occur just after the calving. Further consequences in the early lactation period include, lowered milk production, Immunodepression and compromised reproductive performance. Dry matter intake (DMI) starts to decrease a few weeks before parturition with the lowest level occurring at calving. During the dry period, energy and protein requirements are lower, as there are no needs by the udder for milk production. Generally, dairy cows require around two times more energy for milk production than maintenance with a progress in the lactation period. Cattle have the ability to compensate for deficits of food energy through the mobilization of adipose reserves. Most of the fat soluble antioxidant vitamins such as retinol,  $\alpha$ -tocopherol and  $\beta$ -carotene decrease at the time of parturition are reported to be associated with several health problems. The optimal body condition score for a dry cow is 3.0-3.25 and the cows that were conditioned at BCS-3 had higher feed intake coupled with peak milk yield. Lymphocytes play an important role in the mammary gland defense through secretion of lymphokines and antibodies, which facilitate the destruction of microorganisms. Dry cow therapy is the treatment of cows at the end of lactation with a long acting antibiotic preparation with or without a teat sealant.

**Keywords :** Dry matter intake,  $\alpha$ -tocopherol,  $\beta$ -carotene, Dry cow therapy, antioxidant.



**Ravi Kanth Reddy et al.**

## INTRODUCTION

The transition period, 3 weeks before to 3 weeks after parturition (Grummer, 1995) is considered as a critical determinant of productivity and profitability in dairy farming. This includes Close up dry cows (3 weeks prepartum to calving), maternity cows (2-3 days around calving) and fresh cows (calving to 3 weeks postpartum). During this span, animal enters from a pregnant non-lactating to lactating non-pregnant state, which is accompanied with several physiological and biochemical changes exerting stress to animals and thus making them more susceptible to various metabolic and infectious diseases (Goff and Horst, 1997, Mallard *et al.*, 1998) resulting in monetary losses to dairy farmers. These economic losses, associated with poor peripartum management are reflected in suboptimal milk production, diminished reproductive performance, increased morbidity, mortality, treatment cost and involuntary culling. Therefore, periparturient management is a critical determinant of productivity and profitability of dairy farming.

### Why Transition period - A challenging phase?

Cows that fail to transition successfully into lactation are vulnerable to a host number of problems which occur just after the calving. Further consequences in the early lactation period include, lowered milk production, Immunodepression and compromised reproductive performance. Therefore, it is important for the animal's productivity and welfare so that, it do not succumb to production diseases. The variations that occur in animals during the transition period include:

### Inadequate feed intake during transition period

Dry matter intake (DMI) starts to decrease a few weeks before parturition with the lowest level occurring at calving. During the dry period, energy and protein requirements are lower, as there are no needs by the udder for milk production. In the last trimester of pregnancy, the fetus grows enormously exerting pressure on the rumen and sending negative signals to the satiety centre of hypothalamus on voluntary feed intake. The reduction of feed intake at the end of pregnancy may also be due to the decreased plasma estradiol concentration (Grummer, 1995) and presence of clinical or subclinical diseases. As the parturition approaches the dry matter intake of the animal reduces, thus it provides the possibility for getting into negative energy balance (NEB) which may occur already before calving. Generally, dairy cows require around two times more energy for milk production than maintenance with a progress in the lactation period. But, as per the NRC (2001) recommendations the dry matter intake and nutrient requirements are constant for the entire non-lactating period. It unveils that the cows are in negative energy balance during the final week of prepartum (Roy *et al.*, 2014).

### Reduced Body weight and Body condition score

Cows experience negative energy balance so often, due to restricted nutrient supply and consequently becomes metabolically stressed. Cattle have the ability to compensate for deficits of food energy through the mobilization of adipose reserves. This situation leads to the  $\beta$ -oxidation of body fat reserves, declining the fat depots and so the body weight along with Body Condition Score (BCS). The optimal body condition score for a dry cow is 3.0-3.25 and the cows that were conditioned at BCS-3 had higher feed intake coupled with peak milk yield (Sharad *et al.*, 2016). Further, a few adaptations occur in the animal's body include increased hepatic gluconeogenesis, reduced use of glucose by peripheral tissues, increased mobilization of non-esterified fatty acids (NEFA) from adipose and increased use of NEFAs by peripheral tissues (Bell, 1995). The imbalance in energy status results in most dairy animals experiencing a period of negative energy balance (NEB) after calving, which increases the risk of both metabolic and infectious diseases (Duffield, 2000).



**Ravi Kanth Reddy et al.****Diminished plasma concentrations of fat soluble vitamins**

Most of the fat soluble antioxidant vitamins such as retinol,  $\alpha$ -tocopherol and  $\beta$ -carotene decrease at the time of parturition are reported to be associated with several health problems (Weiss, 1998). The concentration of  $\alpha$ -tocopherol will be dropped by 50% at parturition and remains low until 20 to 30 days (Weiss *et al.*, 1990). Low plasma concentration of  $\alpha$ -tocopherol at parturition is a significant risk factor for intramammary infection and mastitis during the first week of lactation (Weiss *et al.*, 1997). Both  $\beta$ -carotene and its precursor (Retinol) are indispensable for the proper stratification and integration of epithelium. Their deficiency will result in hyperkeratinization which leads to break in the integrity of epithelium thereby making it prone for the entrance of various pathogens.

**Immuno suppression**

Immune status of animals depress markedly in and around parturition due to interaction of several factors. During the peripartum period, both humoral and cell mediated immunity get depressed due to the increased blood cortisol concentration (Manak, 1986). Phagocytic and bactericidal ability of blood polymorphonuclear cells (PMNs) get decreased during first week of lactation (Kehrli *et al.*, 1989). Parturition in dairy cows temporarily alters the gene expression patterns in circulating neutrophils, which disables their maturation, adhesion, apoptosis and other immune mediated roles (Crookenden *et al.*, 2016). Lymphocytes play an important role in the mammary gland defense through secretion of lymphokines and antibodies, which facilitate the destruction of microorganisms. Lymphocyte proliferation is higher at one week pre- and postpartum than at calving but antibody production ability in response to mitogens decreased significantly around parturition (Smith *et al.*, 1985). The serum concentration of immune system components such as immunoglobulin, conglutinin and complement factors of immune system are also decreased at parturition in dairy cows (Stable *et al.*, 1991). Although cortisol concentration is only transitionally elevated but changes in estrogen and progesterone at the time of parturition might contribute to immunosuppression for several days around calving (Preisler *et al.*, 2000). Moreover,  $\beta$ -oxidation of body fat reserves terminates with the production of  $\beta$ -hydroxybutyrate, other ketone bodies as end products which have negative effect on immune function of animals, thus enhancing the susceptibility of animals to infections in and around parturition (Ingvarsen and Moyes, 2013; Sordillo and Mavangira, 2014).

**Mastitis and Metritis**

The keratin plug sealing of teats break down about 7 to 10 days before parturition, permitting easy access to bacteria in the mammary gland (Smith *et al.*, 1985). Around parturition, as the mammary secretions change over to colostrums, the level of lactoferrin declines, which increases the amount of iron available for bacterial growth (Goff, 2000). At parturition, most of the cows become hypocalcemic, which is suspected to impair smooth muscle contraction, vital for the perfect closure of teat sphincter after milking, which contributes towards increased incidence of mastitis during periparturient period. Further, impaired PMN function may leads to the peripartum metritis and mastitis (Cai *et al.*, 1994).

**Enhanced chances for the occurrence of Metabolic diseases**

All aforesaid cascading changes increase the incidence of periparturient diseases. Dairy animals often fail to adapt to the metabolic and management changes, resulting in 75% of dairy animal disease incidence during the first month after calving (Singh *et al.*, 2015). The fundamental productive and reproductive disorders during the transition period are divided into three principle axes:

- A) Disorders related to energy metabolism (Ketosis, Fatty liver, Acidosis and Displaced abomasum)
- B) Disorders related to mineral metabolism (Milk fever, Hypophosphatemia, Hypomagnesimia & Udder edema) and
- C) Problems related to the immune system (Mastitis, Metritis/Endometritis, Pyometra and Retention of foetal membrane).



**Ravi Kanth Reddy et al.****Managemental interventions**

For safe and efficient transition period and to prevent the above said disorders, special managemental interventions in and around parturition should aim at:

- i. Protection against infectious agents,
- ii. Improvement of feed intake,
- iii. Prevention of over conditioning of animal,
- iv. Prevention of lipid metabolism,
- v. Supply of specific nutrient factors and
- vi. Protection against environmental and managemental stress.

To achieve these objectives following managemental practices need to be followed.

**Drying off the dairy animals**

Animals should be given a sufficient time to rest and regenerate mammary tissue, which can be attained by providing a dry period of 45 to 60 days duration (Rastani *et al.*, 2005). The method of complete cessation of milking is a common practice in the low producing cows (<6 kg). In case of high yielders, incomplete milking or alternate day milking for 1-2 weeks followed by complete cessation is an effective method to dry off the animals.

**Dry cow therapy**

Dry cow therapy is the treatment of cows at the end of lactation with a long acting antibiotic preparation with or without a teat sealant. This is to treat for any intra-mammary infections contracted during lactation and provides protection against new infections during the dry period. Recently, dry cow therapy is being practiced via two different techniques i.e. use of intra mammary and systemic administration of antibiotics prior to calving. Systemic administration of antibiotics at drying off or some weeks before parturition looks to be nominal accompanying treatment for intra-mammary therapy, which may be advisable for practice (Ahmad *et al.*, 2015).

**Feeding Management**

A decrease in DMI occurs due to the rapid growth of the fetus taking up abdominal space and displacing rumen volume. This decrease ranges from 2% of body weight in the first weeks of the dry period to 1.4% of body weight in the 7-10 days period before calving. This 30% decrease in DMI appears to occur very rapidly in the transition period (Bertics *et al.*, 1992). During the 3 weeks post calving, DMI increases at the rate of 1.5 to 2.5 kg per week, which is more rapid in multiparous cows than primiparous cows. The optimum DMI during prepartum and postpartum should be 1.7% and 2-3% of body weight, respectively. Optimum nutrient and dry matter intake can be supplied by augmenting nutrient density of feed. Therefore, peripartum diet of animal should contain high concentrate and high quality low roughage. Sudden shift to high concentrate diet predisposes the animal to ruminal impaction and metabolic acidosis.

The practice of gradual increase in peripartum diet quantity and quality will acclimatize the ruminal microflora to high concentrate ration without disturbing ruminal ecology. Some experts have suggested that when prepartum nutrient restriction is followed by increased postpartum nutrient intake, the negative effect of prepartum nutrient restriction may be overcome partially. However, the effectiveness of elevated postpartum nutrient intake may depend on the severity of prepartum nutrient restriction (Lalman *et al.*, 1997). Moreover, feed additives such as Propionate production promoters; Propionate enhancers like fumarate (Remling *et al.*, 2014) and malate; Antioxidants (Osorio *et al.*, 2014a); Ketosis controlling agents; Methyl donors like Methionine (Osorio *et al.*, 2014b) and Choline (Grummer, 2011); Monensin (Duffield *et al.*, 2008); Rumen inert fats (Sharma *et al.*, 2016); Rumen bypass protein (Gang *et al.*, 2016); Direct fed microbials (Alzahal *et al.*, 2014); Niacin (Karkoodi and Tamizrad, 2009); Folic acid and



**Ravi Kanth Reddy et al.**

Vitamin B<sub>12</sub> (Duplessis *et al.*, 2012); Pantothenic acid and Riboflavin (Evans and Mair, 2013) are very much effective in managing the transition stress in dairy animals.

**Housing management**

For better feeding and care, the animals in dry period should be separated from lactating animals, at least 60 days before expected date of calving. This practice will protect the pregnant animals from injuries due to infighting and hence abortion, torsion, dystocia and other complications. Housing of periparturient animals will require the following structures.

**Dry Animal Shed**

Preferably 10 to 15 days before parturition, the animal must be transferred to loose housing type shed. Shifting the animals to confined housing on the day of calving instead of earlier, and use of restraint measures at milking increases the somatic cell count, indicates the incidence of mastitis (Svensson *et al.*, 2006). The shed may consist of centrally placed manger with curbs of 0.6 meter length and width per animal under a roof in paddock. The manger should be surrounded by a 2.2 meter wide paved platform with drains. The roofed portion should be 5.6 meter wide and may be gabled. Ties should be provided on the outside of the manger curb at 1.5 meter approximately for occasional use, if required.

**Down – Calver Shed**

The down-calver sheds should have calving boxes for housing those animals very close to calving and standings adjacent to boxes for accommodating those animals heavy-in-calf. A plentiful supply of clean, dry and fresh bedding material on a well-designed comfortable lying surface is a prerequisite in close-up pens (Nigel *et al.*, 2004). The dimension of each calving box should be 3X4 meters with partition of at least 1.2 meter high between the two calving boxes. A manger and water trough, each 0.5 meter wide should be constructed at the rear end of calving box. A single leaved door 2 meter high and 1.2 meter wide should be provided for each calving box. The lower half portion of angle iron frame of the door leaf may be of galvanized steel sheet and upper half of the same may be covered with wire netting the floor of the calving box should be sloped towards the drains.

**Standings**

The standing of the down-calver shed should be constructed with a continuous manger along the wall and provided with tying arrangements so that the animals are tethered facing the wall. The length and width of each standing should be 2.0 and 1.6 meters, respectively. There should be a drain laid on other side of the standing.

**CONCLUSION**

The transition period constitutes a turning point in the productive cycle of the cow since it imposes a number of abrupt changes on the cow which are in 'physiological transit' from one lactation to the subsequent lactations and hence it requires proper management for successful dairy farming. All the concepts of sound nutrition that are important in the pre-calving transition period are equally important in the post-calving transition period. Continued ruminal adaptation to high concentrate diets is critical to control the risk of ruminal acidosis, careful attention to mineral metabolism, as well as energy and protein metabolism, is essential for a successful lactation. Again, the concepts of homeostatic and homeorhetic changes are crucial. Failure to adequately support one area of metabolism will inevitably impact negatively on other metabolic processes. Careful attention to minimise the depth and length of negative energy and protein balance are equally as important as the provision of adequate calcium, magnesium and phosphorus. Apart from the nutritional aspects, housing is also very important for effective management of transition cows especially to reduce the incidence of the probable complications arising out of metabolic disturbances.





**Ravi Kanth Reddy et al.**

**Table 1. Additional Recommendations to be followed during the common transition stress disorders**

Common metabolic disease	Dietary Prevention
<b>Milk Fever</b>	Supplementation of calcium gel- 3 doses each 300 gms. Feeding negative Dietary Cation Anion Diets (DCAD) in late gestation period and high DCAD in early lactation (Razzaghi <i>et al.</i> , al., 2012), Maintain proper Ca and P (2:1) ration in the diet and Prepartum administration of vitamin-D (Thilsing-Hansen <i>et al.</i> , 2002).
<b>Udder oedema</b>	Excess feeding of Na and K should be avoided. Supplementation of Vitamin-E @1000 IU/day during early lactation is effective in prevention of udder oedema (Mueller <i>et al.</i> , 1989).
<b>Retention of foetal Membrane</b>	Daily supplementation of 100,000 IU of vitamin A and 400 IU of vitamin E with 3 mg/day of selenium or injections of Se and Vit E (Twice: 30 and 15 days prior to calving). Further, antioxidant supplementation during dry period can prevent the condition (Weiss <i>et al.</i> , 1990).
<b>Fatty liver and Ketosis</b>	Starvation of the pregnant animal should be avoided. Supplementation of Niacin @ 3 to 12 gm/day reduces the NEFA mobilization from adipose tissues (Dufva <i>et al.</i> , 1983). Intravenous administration of glucose may decrease blood ketones (Hamada <i>et al.</i> , 1982). Oral drenching of propylene glycol (Sauer <i>et al.</i> , 1973) & Monensin hydrochloride @2.5 mg/day; and salts of Propionic acid (Schultz, 1958) may be effective in lowering the blood ketones.
<b>Ruminal acidosis</b>	Provide the ration containing more than 32% NDF, with greater than 80% being from long forage and avoid sudden dietary shifts (Grant and Albright, 1996). Use neutralizing agents such as sodium carbonate, potassium carbonate, magnesium oxide, sodium hydroxide and calcium hydroxide @ 2 to 4% (Staples and Lough, 1989); Ionophore rumen modifiers like Monensin, lasalocid, narasin and salinomycin (Duffield <i>et al.</i> , 2008); Yeast culture (Dawson, 1995); Virginiamycin (Al Jassim and Rowe, 1999); and Tylosin (Nagaraja <i>et al.</i> , 1987).
<b>Displacement of abomasum</b>	Over feeding of cows should be avoided during dry period (Mann <i>et al.</i> , 2016). Diet should constitute about 50% forage and fed long and/or coarsely chopped good quality forage during the dry period and early lactation. Minimize stress due to other periparturient diseases like milk fever and ketosis.





**Ravi Kanth Reddy et al.****REFERENCES**

1. Ahmad T, Nadeem A, Saleem MI, Nadeem M, Saqib M. Control of Mastitis through Dry Cow Therapy: A Review. *Sch Adv Anim Vet Res* 2015; 2 Suppl 3:128-135.
2. Al Jassim RAM, Rowe JB. Better understanding of acidosis and its control. *Rec adv Anim Nutr Austr* 1999; 12:91-97.
3. AlZahal O, McGill H, Kleinberg A, Holliday JI, Hindrichsen IK, Duffield TF, McBride BW. Use of a direct-fed microbial product as a supplement during the transition period in dairy cattle. *J Dairy Sci* 2014; 97:7102–7114.
4. Bell AW. Regulation of organic nutrient metabolism during transition from late pregnancy to early lactation. *J Anim Sci* 1995; 73:2804-2819.
5. Bertics SJ, Grummer RR, Cardorniga-Valino C, Stoddard EE. Effect of prepartum dry matter intake on liver triglyceride concentration and early lactation. *J. Dairy Sci* 1992; 75:1914.
6. Cai T, Weston PG, Lund LA, Brodie B, McKenna DJ, Wagner WC. Association between neutrophil functions and periparturient disorders in cows. *Am J Vet Res* 1994; 55:934-943.
7. Crookenden MA, Heiser A, Murray A, Murray VSR, Dukkupati JK, Kay JJ, Loor S, Meier MD, Mitchell KM, Moyes CG, Walker JR, Roche. Parturition in dairy cows temporarily alters the expression of genes in circulating neutrophils. *J Dairy Sci* 2016; 99 Suppl 8:6470-6483.
8. Dawson KA. The use of yeast strain 8417 in manipulating ruminant high concentrate diets. In *proc. 56<sup>th</sup> Minnesota Nutrition Conference & Alltech, Inc. Technical Symposium, Minn. Ext. Serv., St. Paul, MN; 1995. p. 25-36.*
9. Duffield T. Subclinical ketosis in lactating dairy cattle. *Vet Clin North Am Food Anim Pract* 2000; 16:231-253.
10. Duffield TF, Rabiee AR, Lean IJ. A Meta-Analysis of the Impact of Monensin in Lactating Dairy Cattle. Part 1. Metabolic Effects. *J Dairy Sci* 2008; 91:1334–1346.
11. Dufva GS, Bartley EE, Dayton AD, Riddell DO. Effect of niacin supplementation on milk production and ketosis of dairy cattle. *J Dairy Sci* 1983; 66:2329-36.
12. Duplessis M, Girard CL, Santschi DE, Lefebvre DM, Pellerin D. Folic acid and vitamin B<sub>12</sub> supplement enhances energy metabolism of dairy cows in early lactation. *J Dairy Sci* 2012; 95:118.
13. Evans E, Mair DT. Effects of a rumen protected B vitamin blend upon milk production and component yield in lactating dairy cows. *Open J. Anim. Sci.* 2013; 3 Suppl 1:76-82.
14. Gang L, Zhi M, Anshan S, Lin W, Zhongpeng Bi. Effects of dietary rumen-protected lysine on milk yield and composition in lactating cows fed diets containing double-low rapeseed meal. *Inter. J. Dairy Tech* 2016; 69 Suppl 3:380–385.
15. Goff JP. Mastitis and retained placenta relationship to bovine immunology and nutrition. USDA, Metabolic Diseases and Immunology Research Unir, Ames IA5001-0-0070, USA; 2000.
16. Goff JP, Horst RL. Effects of the addition of potassium or sodium, but not calcium, to prepartum rations on milk fever in dairy cows. *J Dairy Sci* 1997; 80:176-186.
17. Grant RJ, Albright JL. Feeding behaviour and management factors during the transition period in dairy cattle. *J Anim Sci* 1996; 73:2791-2803.
18. Grummer RR. Impact of changes in organic nutrient metabolism on feeding the transition dairy cow. *J Anim Sci* 1995; 73:2820-2833.
19. Grummer RR. Controlling Energy Metabolism Through the Use of Feed Additives. *Proc. 2011 Seminar Vetryny Jenikov, Czech Republic.*
20. Hamada T, Ishii T, Taguchi S. Blood changes of spontaneously ketotic cows before and four hours after administration of glucose, xylitol, 1,2-propanediol, or magnesium propionate. *J Dairy Sci* 1982; 65:1509.–1513.
21. Ingvarstsen KL, Moyes K. Nutrition, immune function and health of dairy cattle. *Animal* 2013; 7:112–122.
22. Karkoodi K, Tamizrad K. Effect of niacin supplementation on performance and blood parameters of Holstein cows. *South Af J Anim Sci* 2009; 39(4):349-354.



**Ravi Kanth Reddy et al.**

23. Kehrli ME Jr, Nonecke BJ, Roth JA. Alterations in bovine lymphocyte function during the periparturient period. *Amer J Vet Res* 1989; 50:215.
24. Lalman DL, Keisler DH, Williams JE, Scholljegerdes EJ, Mallet DM. Influence of postpartum weight and body condition change on duration of anestrus by undernourished suckled beef heifers. *J. Anim. Sci.* 1997; 75:2003-2008.
25. Mallard BA, Dekkers JC, Ireland MJ, Leslie KE, Sharif S, Lacey C, Wagter VL, Wilkie BN. Alteration in immune responsiveness during the peripartum period and its ramification on dairy cow and calf health. *J Dairy Sci* 1998; 81:585-595.
26. Manak RC. Neonatal calf serum immunoregulation of lymphocyte function during the periparturient period. *Amer J Vet Res* 1986; 50:215.
27. Mann S, Abuelo A, Nydam DV, Leal Yepes FA, Overton TR, Wakshlag JJ. Insulin signaling and skeletal muscle atrophy and autophagy in transition dairy cows either overfed energy or fed a controlled energy diet prepartum. *J Comp Physiol B* 2016; 186(4):513-525.
28. Mueller FJ, Miller JK, Ramsey N, DeLost RC, Madsen FC. Reduced udder edema in heifers fed vitamin E prepartum. *J Dairy Sci* 1989; 72:2211.
29. Nagaraja TG, Taylor MB, Harmon DL, Boyer JE. *In vitro* lactic acid inhibition and alterations in volatile fatty acid production by antimicrobial feed additives. *J Anim Sci* 1987; 65:1064-1076.
30. Nigel B, Cook, Kenneth V, Nordlund V. Behavioral needs of the transition cow and considerations for special needs facility design. *Vet Clin Food Anim* 2004; 20:495-520.
31. NRC, 2001. Nutrient Requirements of Dairy Cattle. 7th rev. ed. Natl. Acad. Sci., Washington, DC.
32. Osorio JS, Trevisi E, Drackley Ji P, Luchini D, Looor JJ. Smartamine M and MetaSmart supplementation during the peripartal period alter hepatic expression of gene networks in 1-carbon metabolism, inflammation, oxidative stress, and the growth hormone-insulin-like growth factor 1 axis pathways. *J. Dairy Sci* 2014b; 97: 7451–7464.
33. Osorio JS, Trevisi E, Drackley JiP, Luchini JK, Bertoni DG, Looor JJ. Biomarkers of inflammation, metabolism, and oxidative stress in blood, liver, and milk reveal a better immunometabolic status in peripartal cows supplemented with Smartamine M or MetaSmart. *J Dairy Sci* 2014a; 97:7437–7450.
34. Preisler MT, Weber PS, Temelman RJ, Erskine HH, Burton. Glucocorticoid receptor down-regulation in neutrophils of periparturient cows. *Am J Vet Res* 2000; 61:14-19.
35. Rastani RR, Grummer SJ. Reducing Dry Period Length to Simplify Feeding Transition Cows: Milk Production, Energy Balance, and Metabolic Profiles. *J Dairy Sci* 2005; 88:1004–1014.
36. Razzaghi H, Aliarabi MM, Tabatabaei AA, Saki R, Valizadeh, Zamani P. Effect of Dietary Cation-Anion Difference during Prepartum and Postpartum Periods on Performance, Blood and Urine Minerals Status of Holstein Dairy Cow. *Asian-Australas J Anim Sci* 2012; 25(4):486–495.
37. Remling N, Riede S, Lebzien P, Meyer U, Höltershinken M, Kersten S, Breves G, Flachowsky G, Dänicke S. Effects of fumaric acid on rumen fermentation, milk composition and metabolic parameters in lactating cows. *J Anim Physiol Anim Nutr* 2014; 98(5): 968–981.
38. Roy AK, Singh M, Sehgal JP. Significance of energy metabolism during Transition period in Dairy Cows. *Livestock Tech.* 2014; 3(12):28-30.
39. Sauer FD, Erfle JD, Fisher LJ. Propylene-glycol and glycerol as a feed additive for lactating dairy-cows - evaluation of blood metabolite parameters. *Canadian J. Anim. Sci., Ottawa,* 1973; 53(2):265-271.
40. Schultz LH. Use of sodium propionate in the prevention of ketosis in dairy cattle. *J Dairy Sci* 1958; 4:160-167.
41. Sharad M, Kiran Kumari, Ashutosh Dubey. Body Condition Scoring of Dairy Cattle: A Review. *Research and Reviews: J Vet Sci* 2016; 2 Suppl 1:58-65.
42. Sharma S, Singh M, Kumar Roy A, Thakur S. Effect of pre-partum prilled fat supplementation on feed intake, energy balance and milk production in Murrah buffaloes. *Vet World* 2016; 9(3):256–259.
43. Singh A, Meena BS, Wani SA. Transition period and related challenges for good health and production. *Livestock Tech* 2015; 5(2):10-11.
44. Smith KL, Todhunter DA, Schoenberger PS. Environmental mastitis: Cause, prevalence, prevention. *J Dairy Sci* 1985; 68:1531-1553.





**Ravi Kanth Reddy et al.**

45. Sordillo LM, Mavangira V. The nexus between nutrient metabolism, oxidative stress and inflammation in transition cows. *Anim Prod Sci* 2014; 54:1204-1214.
46. Stable JR, Kehrl MEJ, Thurston JR, Goff JP, Boone TC. Granulocyte colony-stimulating factor effects on lymphocytes and immunoglobulin concentrations in periparturient cows. *J Dairy Sci* 1991; 75:2190-2198.
47. Staples CR, Lough DS. Efficacy of supplemental dietary neutralizing agents for lactating dairy cows. A Review. *Anim Feed Sci Technol* 1989; 23:277-303.
48. Svensson C, Nyman AK, Persson Waller K, Emanuelson U. Effect of housing, management and health of dairy heifers on first-lactation udder health in southwest Sweden. *J Dairy Sci* 2006; 89 Suppl 6:1990 – 1999.
49. Thilising-Hansen T, Jorgensen RJ, Ostergaard S. Milk Fever Control Principles: A Review. *Acta Veterinaria Scandinavica* 2002; 43 Suppl 1:1 -19.
50. Weiss WP. Requirement of fat soluble vitamins for dairy cows: A review. *J Dairy Sci* 1998; 77:1422-1429.
51. Weiss, W.P., Hogan, J.S., Todhunter, D.A. and Smith, K.L. (1997). Effect of vitamin E supplementation in diets with a low concentration of selenium on mammary gland health of dairy cows. *J Dairy Sci* 80 Suppl 8:1728-37.
52. Weiss WP, Horgan JS, Smith LK, Hoblet. Relationships among selenium, vitamin E and mammary gland health in commercial dairy herds. *J Dairy Sci* 1990; 73:381-390.





## Recent Trends in Supplementation of Exogenous Fibrolytic Enzymes in Ruminant Nutrition – A Review

P.Ravi Kanth Reddy<sup>1</sup>, J.Raju<sup>2\*</sup>, A. Nagarjuna Reddy<sup>1</sup>, A.Ramadevi<sup>1</sup> and P.Pandu Ranga Reddy<sup>1</sup>

<sup>1</sup>College of Veterinary Science, Gannavaram, SVVU, Tirupati, A.P.

<sup>2</sup>College of Veterinary Science, Rajendranagar, PVNR TVU, Hyderabad, India.

Received: 4 July 2016

Revised: 18 Aug 2016

Accepted: 28 Sep 2016

### Address for correspondence

Dr.J.Raju,  
Ph.D. Scholar & ICAR-SRF,  
Dept. of Animal Nutrition, College of Veterinary Science,  
P. V. Narsimha Rao Telangana Veterinary University,  
Hyderabad, India - 500030.  
Email: drrajuj@gmail.com



This is an Open Access Journal / article distributed under the terms of the **Creative Commons Attribution License (CC BY-NC-ND 3.0)** which permits unrestricted use, distribution, and reproduction in any medium, provided the original work is properly cited. All rights reserved.

### ABSTRACT

In the recent past, increasing consumer concern about the use of feed additives such as growth promoters and antibiotics in livestock production, has forced the animal nutritionists to increase the safe enzyme usage for improving the productivity of the animals. The concept of supplementation of exogenous enzymes can be traced back to 1990s. The enzyme utilization in ruminant industries have sustained by virtue of the widest range of exogenous enzyme products availability, better developed methods to evaluate enzyme activity, revised knowledge on rumen functions and recent advances of biotechnology. Up to date numerous researches have been done with ruminants like cattle (both dairy and beef), goat, sheep and less with buffalo. The results seem to be inconsistent but positive results on feed intake, nutrient digestibility, growth performance, other production parameters, manure nutrient excretion etc., have been obtained. The conflicting results can be attributed to experimental conditions in which energy is not the limiting nutrient, as well as to the activities and characteristics of the enzymes supplied, under or over supplementation of enzyme activity, and inappropriate method of providing the enzyme product to the animal. Therefore more calibrated research efforts are needed for the generalization of exogenous enzyme usage in ruminant nutrition. The research conducted by using exogenous fibrolytic enzymes (EFE) in ruminants, sources, different methods of application and the possible modes of action are reviewed here.

**Keywords :** Exogenous fibrolytic enzyme, Direct fed microbials, digestibilities, production.



**Raju et al.**

## INTRODUCTION

The efficiency by which ruminants obtain energy from structural plant polysaccharides and, in turn, produce high quality meat and milk protein is increasingly important if the demands of an expanding human population are to be met (Mealeet *et al.*, 2014). Various strategies have been attempted to improve forage quality for ruminant livestock including treatment with physical agents such as heat, steam, and pressure; with chemicals such as acids, alkalis, and NH<sub>3</sub>; with biological agents such as white rot fungi; via natural selection, breeding, or molecular engineering and enzyme technology (Adesoganet *et al.*, 2014). However, none of these methods is widely used for improving forage quality and ruminant animal performance.

This is due to the capital and energy intensive nature of physical methods such as steam or pressure explosion, the potential of pelleting, chopping, or grinding to limit salivary buffering of ruminal acids and retention time in the rumen (decreasing digestibility), the cost and corrosive and/or hazardous nature of chemicals such as ammonia and sodium hydroxide, the potential for extreme DM losses following hydrolysis by white rot fungi, and the prolonged nature of breeding approaches (Adesoganet *et al.*, 2014). In recent years, exogenous fibrolytic enzymes are increasingly considered as cost-effective means of improving feed efficiency (Krause *et al.*, 2003), and their use in forage processing may be desirable as they are not corrosive and/or hazardous, unlike chemical treatments. It has been demonstrated that EFE work in synergy with the endogenous rumen microbial enzymes to enhance the digestibility and nutritive value of high fibrous diet (Morgaviet *et al.*, 2000), thereby increasing the economic benefits for the farmer.

### Enzyme Source

Commercial ruminant enzyme additives contain concentrated enzymatic activities that are involved in degrading fiber. They are derived primarily from four bacterial (*Bacillus subtilis*, *Lactobacillus acidophilus*, *Lactobacillus plantarum*, and *Streptococcus faecium*) and three fungal (*Aspergillus oryzae*, *Trichoderma reesei*, and *Saccharomyces cerevisiae*) species (McAllister *et al.*, 2001). Solid State Fermentation and Submerged Fermentation are the major methods for enzyme extraction which have combined with several other biotechnological aspects (Sujani and Seresinhe, 2015). Although the microorganisms from which the enzymes derived only constitute a very limited group, the types and activity of enzymes produced can be diverse depending on the strain selected, the substrate they are grown on, and the culture conditions used (Gashe, 1992; Lee *et al.*, 1998; Mealeet *et al.*, 2014).

### Methods of Application of Enzymes

Studies conducted by various authors indicated that enzymes can be applied to total mixed rations (TMR), hay, ensiled forages, concentrate, supplement or premix. Beaucheminet *et al.* (2003) reported that exogenous enzymes are more effective when applied to high moisture feeds (such as silages) compared to dry feeds due to higher moisture content. The requirement for water in the hydrolysis of complex polymers to soluble sugars is a fundamental biochemical principle. Furthermore, silage pH values are usually at, or around, the optimal pH for most fungal enzymes. However, in practice, some exogenous enzymes are more effective when applied in a liquid form to dry forage as compared to wet forage.

Feng *et al.* (1996) applied an enzyme solution directly to grass and observed no effect when added to fresh or wilted forage. However, when it was applied to dried grass, enzymes increased DM and fibre digestibility. In contrast, Yang *et al.* (1999) observed no difference between applying an enzyme product to dry forage or to both dry forage and concentrate. Studies conducted by Lewis *et al.* (1996) and McAllister *et al.* (1999) demonstrated that infusion of enzymes into the rumen has not been effective. Similarly, Hristovet *et al.* (2008) reported that supplementation of EFE combinations at low doses @ 10 g/Holstein cow/day intra-ruminally had no effect on nutrient digestibility and rumen fermentation pattern. In contrast to above findings, Giraldoet *et al.* (2008) indicated that supplementing a fibrolytic enzyme @ 12 g/d directly into the rumen increased the fibrolytic activity in ruminal fluid, without pre-feeding feed-enzyme interaction, when sheep were fed on grass hay: concentrate (70:30; DM basis) diet.



**Raju et al.**

Further, applying fibrolytic exogenous enzymes in a liquid form to the feeds prior to consumption can have a positive effect on animal performance (Kung *et al.*, 2000; Yang *et al.*, 2000). It may therefore be inferred that association of enzymes with feed may enable some form of pre-ingestive attack of the enzymes upon the plant fibre and/or enhance binding of the enzymes to proteolysis in the rumen. As stated by Beauchemin *et al.* (2003), inconsistencies in animal responses with added enzymes are multifactorial, and can possibly be attributed to four main factors: enzyme characteristics (e.g., differences in enzyme preparations, enzyme activities, units of activity added, pH and temperature effects on activity), forage (e.g., type, maturity), animal (e.g., species, age) and management (e.g., diet, mode of enzyme application, application rate, interaction time of enzymes applied to feed). Kung *et al.* (2000) suggests that overdose of enzymes causes decreased chewing due to an increase in the digestibility of the feed; which further decreases the production of saliva, ruminal pH and thus generates less fiber digestion, resulting in less amount of milk yield produced. Meanwhile Treacher *et al.* (1996) suggests that excessive doses of enzymes affect the ruminal micro-organisms adhering to the substrate and also promote the release of anti-nutritional factors as secondary compounds, thereby reducing the microbial digestion.

**Modes of Action of Exogenous Fibrolytic Enzymes****Pre Consumption Effects**

The EFE are most effective when applied in liquid form onto dry feed prior to ingestion (Kung *et al.*, 2000; Beauchemin *et al.*, 2003). This may partially digest feed or weaken cell wall barriers that limit microbial digestion in the rumen. The EFE releases reducing sugars from the feedstuffs before feed consumption (Hristov *et al.*, 1996) which arises at least partially from the solubilisation of NDF and ADF (Hristov *et al.*, 1996; Krause *et al.*, 1998; Gwayumba and Christensen, 1997). This may therefore increase available carbohydrates in the rumen (Yang *et al.*, 2000) and also enhance the rapid microbial attachment and growth (Forsberg *et al.*, 2000).

**Ruminal Effects**

McAllister *et al.* (2001) reported that in the rumen, the EFE may hydrolyse feed directly or work synergistically with ruminal microbes to enhance feed digestion. EFE are actively stable to continue hydrolysis of feed in the rumen fluid (Hristov *et al.*, 1998 and Wallace *et al.*, 2001). In sub rumen conditions (pH  $\leq$  5.9) resulted from using high fermentable diet, EFE effectiveness was considered to be reduced compared to its effectiveness at higher rumen pH conditions (Beauchemin *et al.*, 2004). Another benefit of EFE application in ruminants is the indirect increase of attachment and numbers of cellobiose- and glucose- utilizing bacteria in the rumen (Nsereko *et al.*, 2002).

**Post Ruminal Effects**

It is also reported that EFE work synergistically with microbes even in the large intestine (Beauchemin *et al.*, 2004). In the small intestine, EFE appear to survive for a sufficient period of time with sufficient effects on substrate particles when applied to wet feeds and concentrate premix (Morgaviet *et al.*, 2001).

**The Research Conducted using Efe in Ruminants**

The noticeable facts about these researches are that numerous enzyme products have applied at various dose rates to different forage types to different animals in various stages of production and mostly the results shown were with higher variability. In spite of conducting an enormous number of studies, generating a precise conclusion or protocol on enzyme utilization has become a challenge due to several reasons, especially the lack of information on enzyme activity and concentrations.

**In Cattle**

Mohamed *et al.* (2013) confirmed that, even though supplementation of fibrolytic enzymes to the early lactating dairy cow diets did not cause any significant changes in dry matter intake, it improved ( $P < 0.05$ ) the milk yield and feed



**Raju et al.**

efficiency when compared to untreated dairy cows. These results are in collaboration with the outcome of Bassiouniet al. (2010) where they observed enhanced milk production and nutrient digestibility with fibrozyme supplementation to either corn silage or berseem hay. In contrast to these results Peters et al. (2015) revealed that the supplementation of enzyme product contained primarily cellulose and xylanase did not improve *invivo* digestibility of lactating cows, therefore, both milk quantity and quality was not significantly affected.

Dileret al. (2014) revealed an increased ( $P < 0.05$ ) total daily milk yields in the Holstein Friesian cows group fed with direct fed microbials (DFM) plus enzymes. Likewise, Ramsinget al. (2009), Phondbaet al. (2009) and HeidariKhormiziet al. (2010) reported that feeding DFM and feed enzymes or both increased significantly daily milk yield. On the other hand, results of the several studies (Rihmaet al., 2007 and Oetzelet al., 2007) demonstrated that supplemental DFM and/or exogenous enzymes had beneficial effect on milk yield in lactating dairy cows, but they were not statistically significant. Similarly, Romero et al. (2016) revealed that the application of EFE to the Bermuda grass based TMR in dairy cattle increased DM intake and milk production without affecting the ruminal DM degradation kinetics or ruminal pH, ammonia-N and volatile fatty acid concentration.

Elwakeelet al. (2007) observed that dry matter intake, milk production, milk efficiency, production of milk and milk compositions were not affected by the addition of fibrolytic enzymes. But they hypothesized that slight differences of milk production might be due to repartitioning of energy between milk and body reserves for cows receiving enzymes. Likewise, Ortiz-Rodeaet al. (2013) observed that the addition of enzyme has no effect on the increment in milk yield production, fat content, lactose or protein. However, Klingermanet al. (2009) reported a significant increment of milk production with unaltered milk fat and milk protein in the enzyme supplemented group.

Vargas et al. (2013) conducted a study in beef steers to determine the impact of dietary enzyme levels @ 0, 2, 4 and 6 ppm in a finishing diet on the steer's performance and carcass characteristics. They concluded that fibrolytic enzymes do not affect steer performance but improve carcass yield and tenderness. Later, Salem et al. (2011) reported that enzyme addition did not affect DM intake, whereas it increased total tract apparent digestibility of nutrients including NDF and ADF, concentrations of rumen ammonia N and total short chain fatty acids (SCFA) and live weight gain.

**In Buffaloes**

Malik and Bandla (2010) evaluated the optimum doses of enzymes and probiotics, selected through *in vitro* experiments on male buffalo calves' performance. Calves exhibited higher ADG and feed efficiency when fed with mixture of probiotics and enzyme. The OM, NDF and ADF digestibility were improved significantly. Rajamma et al. (2014) conducted a work to know the influence of supplementation of EFE in TMRs fed to buffalo bulls. They found that the EFE supplementation increased ( $P < 0.01$ ) the digestibility of CP, EE and CF, while there was no effect on digestibility of other nutrients. Another study conducted by Ravikanthet al. (2016) to investigate the effect of TMR supplemented with EFE and/or live yeast culture in buffalo bulls, revealed no effect on the digestibility of nutrients, fibre fractions, DCP and TDN content of rations. On the contrary, Reddy et al. (2016) reported a linear increase in the *invitro* digestibility of DM, CP, ADF and NDF in the EFE supplemented group.

Rajamma et al. (2014b) conducted a research work in buffalo bulls fed TMRs with roughage: concentrate ratios of 60:40 and 70:30 with/without EFE. Supplementation of EFE in TMRs irrespective of R: C ratio decreased ( $P < 0.01$ ) rumen pH and increased ( $P < 0.01$ ) the concentrations of TVFA,  $\text{NH}_3\text{-N}$  and N fractions. Similar results of increased ( $P < 0.05$ ) pH value with a decline in TVFA and  $\text{NH}_3\text{-N}$  concentration were noticed by Gaafaret al. (2010). Later, Poonooruet al. (2015) reported that supplementation of EFE to buffalo bulls fed TMR had no effect ( $P < 0.05$ ) on rumen pH and food and protozoal N concentration, while it influenced to increase ( $P < 0.01$ ) the concentration of TVFA,  $\text{NH}_3\text{-N}$  and other N fractions as compared to the control. According the experiment conducted by El-Kadyet al. (2006), feed intake was not affected by enzyme supplementation but caused a significant ( $P < 0.05$ ) increase in average daily gain, total body weight gain, feed conversion and Total digestible nutrients.



**Raju et al.**

Chandra Sekharet *et al.* (2010) concluded that supplementation of cellulase and xylanase mixture at 1.5 g/kg of DM of TMR containing Roughage: concentrate @ 60: 40 on DM basis significantly increased ( $P < 0.05$ ) the average daily milk yield and FCM yield in Murrah buffaloes due to improved dietary fiber digestion. Later, Gaafaret *et al.* (2010) confirmed a significant decrease ( $P < 0.05$ ) in Feed cost/kg 7% FCM with an increase ( $P < 0.05$ ) in output of 7% FCM and economic efficiency in the fibrolytic enzyme supplemented group.

**In Sheep**

Bhaskeret *et al.* (2013) conducted a trial on 12 rams by feeding 50 % maize stover based TMR supplemented with or without enzyme (cellulase-xylanase, 12,800-12,800 IU/g) to study the effect on rumen fermentation pattern. Results indicated that TVFA ( $P < 0.01$ ) and  $\text{NH}_3\text{-N}$  ( $P < 0.05$ ) concentration was higher in enzyme supplemented group while no effect was observed on pH and total N concentration. The invitro study conducted by Ganaietal. (2011) by using complete feed containing bajra straw supplemented with EFE revealed a significant increase ( $P < 0.01$ ) in TVFA and an unaltered rumen pH, total nitrogen and ammonia N compared to control. In another study, twenty Pelibuey lambs were randomly assigned to control or to one of three enzyme treatments to evaluate their effects on rumen fermentation and reported that fibrolytic enzyme extracts supplementation had no effect on pH,  $\text{NH}_3\text{-N}$  and TVFA concentration in lambs (Torres *et al.*, 2013). Similar results were obtained by Giraldoet *et al.* (2008) in Merino sheep fed with mixed grass hay and concentrate in 70: 30 ratios with or without direct fed EFE @ 12 g/d.

Bueno *et al.* (2013) evaluated the effect of high doses of EFE (@0, 5 or 10 gms per 1 kg oat straw) on lamb performance. A linear decrease ( $P < 0.05$ ) in intake with increasing enzyme doses were noticed without changing the weight gain, feed conversion, digestibility and ruminal fermentation variables. Similar results of unchanged weight gain and dry matter intake were also evident in the study by Torres *et al.* (2013) and Isaac Almarazet *et al.* (2010). Titi and Lubbadeh (2004) found that the EFE treatment significantly increased ( $P < 0.05$ ) the milk production, total solids, milk, fat and protein percentage with no effect on feed intake. On the contrary, Flores *et al.* (2008) reported no effects on lactation when the fibrolytic enzyme product was added to the concentrate of dairy ewes. Another study conducted by Van de Vyver and Useni (2012) reported a significant increase in the *in situ* microbial protein synthesis and an unaltered *in situ* disappearances of DM, NDF and CP of the roughage mixture.

Meat quality of growing lambs was evaluated with the addition of *Salix babylonica* L. extracts and exogenous enzymes in combination or individually. They found that only the combination of *Salix babylonica* extract and enzyme had a significant effect on meat quality parameters but not with the enzyme addition alone (Cayetanoet *et al.*, 2013). However, Riveroet *et al.* (2012) reported the effect of *Salix babylonica* extracts and exogenous enzymes separately and as a combination on hematological parameters in growing lambs, where no effect with any treatment observed. Lara *et al.* (2013) evaluated the effects of high doses of EFE (@0, 5 or 10 gms) on lamb performance and *in situ* digestibility using a ration with 60% oat straw. They found that intake decreased linearly ( $P < 0.05$ ) with increasing doses of EFE, without changing the weight gain, feed conversion, digestibility and ruminal fermentation variables. It indicated that using high doses of EFE in oat straw based diets did not improve the growth performance and nutrient digestibility in finishing lambs.

**In Goats**

Wahyuniet *et al.* (2012) studied the effect of supplementing the TMR containing oil palm frond (OPF) silage with different levels of enzyme on feed intake in goats. They revealed that the supplementation of enzyme to TMR did not affect the DMI, apparent digestibilities of nutrients. On the contrary, Balaet *et al.* (2009) reported an increase ( $P < 0.05$ ) in the diet digestibility of DM, OM, CP, NDF, ADF and total carbohydrates in the enzyme supplemented group. Titi and Lubbadeh (2004) observed a significant increment ( $P < 0.05$ ) in the weaning weight, milk production and milk composition in the enzyme treated groups compared to untreated ones. A study by Hussain *et al.* (2014) witnessed that the enzyme supplementation with the TMR resulted in 31.25% increase in net profit by improving ( $P < 0.05$ ) the average daily weight gain without any effect on feed intake.







### Raju et al.

Khaderet *et al.* (2015) conducted a study in Baladi lactating goats fed with TMR with or without enzyme (Asperozym) supplementation and found an increased ( $P<0.05$ ) milk yield without any change in milk composition in the treatment group. Another study was conducted to investigate the effects of adding cellulolytic enzyme "Asperozym" or Tomoko® to the diets on the performance of goats. The diets supplemented with either enzymes showed significantly ( $P<0.05$ ) increased digestibility of all nutrients compared to the control diet (Kholif and Aziz, 2014).

## CONCLUSION

Adding exogenous fibrolytic enzymes to dairy cow and feedlot cattle diets can potentially improve cell wall digestion and the efficiency of feed utilization by ruminants. Positive responses in milk production and growth rate have been observed for cattle fed some enzyme products, although results have been inconsistent. Some of the variation can be attributed to product formulation, under or over supplementation of enzyme activity, inappropriate method of providing the enzyme product to the animal, and the level of productivity of the test animal. Research is needed to understand the mode of action of these products so that on farm efficacy of ruminant enzyme technology can be assured. With increasing consumer concern about the use of growth promoters and antibiotics in ruminant production, and the magnitude of increased animal performance obtainable using feed enzymes, these products could play an important role in future ruminant production systems.

## REFERENCES

1. Adesogan, A.T., Ma, Z.X., Romero, J.J., Arriola, K.G., 2014. Improving cell wall digestion and animal performance with fibrolytic enzymes. *Journal of Animal Science*, 92, 1317–1330.
2. Bala, P., R. Malik and B. Srinivas, 2009. Effect of fortifying concentrate supplement with fibrolytic enzymes on nutrient utilization, milk yield and composition in lactating goats. *J. Anim. Sci.*, 80: 265-272.
3. Bassiouni M I, Gaafar H M A, Mohi El-Din A M A, Metwally A M and Elshora M A H. 2010. Evaluation of rations supplemented with fibrolytic enzyme on dairy cows performance 3. Productive performance of lactating Friesian cows. *Livestock Research for Rural Development* 22(6).
4. Beauchemin K A, Colombatto D, Morgavi D P and Yang W Z 2003 Use of exogenous fibrolytic enzymes to improve feed utilization by ruminants. *Journal of Animal Science* 81(2): 37-47.
5. Beauchemin K A, Colombatto D, Morgavi D P, Yang W Z and Rode L M 2004 Mode of action of exogenous cell wall degrading enzymes for ruminants. *Canadian Journal of Animal Sciences* 84: 13-22.
6. Bhasker T V, Nagalakshmi D and Srinivasa Rao D 2013. Development of appropriate fibrolytic enzyme combination for maize stover and its effect on rumen fermentation in sheep. *Asian Australasian Journal of Animal Science* 26(7): 945-951.
7. Bueno, A.L., G.M. Martinez, P.H. Garcia, J.M. Garcia and F.P. Perez, 2013. Evaluation of high doses of exogenous fibrolytic enzymes in lambs fed an oat straw based ration. *Anim. Nutr. Feed Technol.*, 13: 355-362.
8. Cayetano, J.A., A.Z.M. Salem, B.M.A. Mariezcurrena, R. Rojo, M.A. Cerrillo-Soto, H. Gado and L.M. Camacho, 2013. Effect of adding *Salix babylonica* extracts and exogenous enzymes to basal diets on the meat quality of growing Suffolk lambs. *Anim. Nutr. Feed Technol.*, 13: 373-380.
9. Chandra Sekhar, Thakur S S, Sachin K S. 2010. Effect of exogenous fibrolytic enzymes supplementation on milk production and nutrient utilization in Murrah buffaloes. *Tropical Animal Health and Production* 42 (7): 1465-70.
10. Diler, A., R. Kocyigit, M. Yanar and R. Aydin, 2014. Effect of feeding direct-fed microbials plus exogenous feed enzymes on milk yield and milk composition of Holstein Friesian cows. *Veterinarija Zootecnika*, 65: 11-16.
11. El-Kady, R.I., I.M. Awadalla, M.I. Mohamed, M. Fadel and H.A. El-Rahman, 2006. Effect of exogenous enzymes on the growth performance and digestibility of growing buffalo calves. *Int. J. Agric. Biol.*, 8: 354-359.
12. Elwakeel, E.A., E.C. Titgemeyer, B.J. Johnson, C.K. Armendariz and J.E. Shirley, 2007. Fibrolytic enzymes to increase the nutritive value of dairy feedstuffs. *J. Dairy Sci.*, 90: 5226-5236.





## Raju et al.

13. Feng P Hunt C W, Pritchard G T and Julien W E 1996 Effect of enzyme preparations on *in situ* and *in vitro* degradation and *in vivo* digestive characteristics of mature cool-season grass forage in beef steers. Journal of Animal Sciences 74: 1349-1357.
14. Flores, C., G. Caja, R. Casals, E. Albanell and X. Such, 2008. Performance of dairy ewes fed diets with a fibrolytic enzyme product included in the concentrate during the suckling period. Animal, 2: 962-968. Animal, 2: 962-968.
15. Forsberg C, Forano E and Chesson A 2000 Microbial adherence to the plant cell wall and enzymatic hydrolysis. In: P.B. Cronje (ed) Ruminant Physiology: Digestion, Metabolism, Growth and Reproduction. CABI Publishing, Wallingford, UK. Pp 79-97.
16. Gaafar H M A, Abdel-Raouf E M and El-Reidy K F A 2010 Effect of fibrolytic enzyme supplementation and fiber content of total mixed ration on productive performance of lactating buffaloes. Slovak Journal of Animal Science 43: 147-153.
17. Ganai A M, Sharma T and Dhuria R K 2011 Influence of exogenous fibrolytic enzymes on *in vitro* fermentation of bajra straw in goats. Veterinary Practitioner 12 (2): 138-141.
18. Gashe, B.A., 1992. Cellulase production and activity by Trichoderma sp. A-001. Journal of Applied Bacteriology, 73, 79-82.
19. Giraldo L A, Tejido M L, Ranilla M A, Ramos S and Carro M D 2008. Influence of direct-fed fibrolytic enzymes on diet digestibility and ruminal activity in sheep fed a grass hay-based diet. Journal of Animal Sciences 86: 1617-1623.
20. Gwayumba W and Christensen D A 1997 The effect of fibrolytic enzymes on protein and carbohydrate degradation fractions in forages. Canadian Journal of Animal Science 77: 541-542.
21. HeidariKhormizi, S.R., DehghanBanadaky, M., Rezayazdi, K., Zali, A. Effects of live yeast and Aspergillus niger meal extracted supplementation on milk yield, feed efficiency and nutrients digestibility in Holstein lactating cows. Journal of Animal and Veterinary Advances. 2010. 9. P. 1934-1939.
22. Hristov A N, Basel C E, Melgar A, Foley A E, Ropp J K, Hunt C W and Tricarico J M 2008 Effect of exogenous polysaccharide-degrading enzyme preparations on ruminal fermentation and digestibility of nutrients in dairy cows. Animal Feed Science and Technology 145: 182-193.
23. Hristov A N, Rode L M, Beauchemin K A and Wuerfel 1996 Effect of commercial enzyme preparation on barley silage *in vitro* and *in sacco* dry matter degradability. Journal of Animal Science 74(1): 273.
24. Hristov A N, McAllister T A and Cheng K J 1998 Stability of exogenous polysaccharide-degrading enzymes in the rumen. Animal Feed Science and Technology 76: 165-172.
25. Hussain, H.N., S.A. Khanum, M. Hussain, A. Shakur and F. Latif, 2014. Effect of fibrolytic enzymes produced from an improved mutant of *Chaetomium thermophile* DG-76 on the performance of beetal-dwarf crossbred goat. Pak. Vet. J., 34: 394-394.
26. Isaac Almaraz, Sergio Segundo Gonzalez, Juan Manuel Pinos-Rodriguez and Luis Alberto Miranda. 2010. Effects of exogenous fibrolytic enzymes on *in sacco* and *in vitro* degradation of diets and on growth performance of lambs. Italian Journal of Animal Science., 9(1).
27. Kader A. E, Kholif M, Mahmoud Abd El-Aziz, Mahmoud H. El-Senaity, Mona A. Ad El-Gawad, Ahmed F.Sayed. 2015. Effect of Diet Supplemented with Cellulase Enzymes on Lactating Goats Performance, and Milk and Cheese Properties. Life Science Journal. 2015; 12 (2S): 16-22.
28. Kholif, A.M. and Aziz, H.A. 2014. Influence of feeding cellulolytic enzymes on performance, digestibility and ruminal fermentation in goats. Animal Nutrition and Feed Technology, 14: 121-136.
29. Klingerman, C.M., W. Hu, E.E. McDonell, M.C. DerBedrosian and L. Kung Jr., 2009. Anevaluation of exogenous enzymes with amylolytic activity for dairy cows. J. Dairy Sci., 92: 1050-1059.
30. Krause M, Beauchemin K A, Rode L M, Farr B I and Norgaard P., 1998. Fibrolytic enzyme treatment of barley grain and source of forage in high grain diets fed to growing cattle. Journal of Animal Science. 76: 2912-2920.
31. Krause, D.O., Denman, S.T., Mackie, R.I., Morrison, M., Rae, A.L., Attwood, G.T., McSweeney, C.S., 2003. Opportunities to improve fiber degradation in the rumen: Microbiology, ecology, and genomics. FEMS Microbiology Review, 27, 663-693.





**Raju et al.**

32. Kung L Jr, Treacher R J, Nouman G A, Smagala A M, Endres K M, and Cohen M A 2000 The effect of treating forages with fibrolytic enzymes on its nutritive value and lactation performance of dairy cows. *Journal of Dairy Science* 83: 115-112.
33. Lara B, German D Mendoza, P A Hernandez and F X Plata P (2013). Evaluation of high doses of exogenous fibrolytic enzymes in lambs fed an oat straw based ration. *Animal Nutrition and Feed Technology* 13(3): 355.
34. Lee, B., Pometto, A.L., Demici, A., Hinz, P.N., 1998. Media evaluation for the production of microbial enzymes. *Journal of Agricultural and Food Chemistry*, 46, 4775–4778.
35. Lewis G E, Hunt C W, Sanchez W K, Treacher R, Pritchard G T and Feng P 1996 Effect of direct fed fibrolytic enzymes on the digestive characteristics of a forage-based diet fed to beef steers. *Journal of Animal Science* 74: 3020-3028.
36. Malik, R. and S. Bandla, 2010. Effect of source and dose of probiotics and Exogenous Fibrolytic Enzymes (EFE) on intake, feed efficiency and growth of male buffalo (*Bubalus bubalis*) calves. *Trop. Anim. Health Prod.*, 42: 1263-1269.
37. McAllister T A, Oosting S J, Popp J D, Mir Z, Yanke L J, Hristov A N, Treacher R J and Cheng K-J 1999 Effect of exogenous enzymes on digestibility of barley silage and growth performance of feedlot cattle. *Canadian Journal of Animal Science* 79: 353-360.
38. McAllister T.A., Hristov, A.N., Beauchemin, K.A., Rode, L.M., Cheng, K-J., 2001. Enzymes in ruminants diets. In: Bedford, M.R., Partridge, G.G. (Eds.), *Enzymes in farm animal nutrition*. CABI, Wiltshire, UK, pp. 273–298.
39. Meale, S.J., Beauchemin, K.A., Hristov, A.N., Chaves, A.V., McAllister, T.A., 2014. BoardInvited Review: Opportunities and challenges in using exogenous enzymes to improve ruminant production. *Journal of Animal Science*, 92, 427–442.
40. Morgavi D P, Beauchemin K A, Nsereko V L and Rode L M 2000 Synergy between ruminal fibrolytic enzymes and enzymes from *Trichoderma longibrachiatum* in degrading fibre substrates. *Journal of Dairy Science* 83: 1310-1321.
41. Morgavi D P, Beauchemin K A, Nsereko V L, Rode L M, McAllister T A, Iwaasa A D, Wang Y and Yang W Z 2001 Resistance of feed enzymes to proteolytic inactivation by rumen microorganisms and gastrointestinal proteases. *Journal of Animal Science* 79: 1621-1630.
42. Nsereko V L, Beauchemin K A, Morgavi D P, Rode L M, Furtado A F, McAllister T A, Iwaasa A D, Yang W Z and Wang Y 2002 Effect of fibrolytic enzyme preparation from *Trichoderma Longibrachiatum* on the rumen microbial population of dairy cows. *Canadian Journal of Microbiology* 48: 14-20.
43. Oetzel, G. R., Emery, K. M., Kautz, W. P., Nocek, J. E. Direct-fed microbial supplementation and health and performance of pre- and postpartum dairy cattle: A field trial. *Journal of Dairy Science*. 2007. 90. P. 2058–2068.
44. Ortiz-Rodea, A., A. Noriega-Carrillo, A.Z.M. Salem, O.C. Ortega and M. Gonzalez-Ronquillo, 2013. The use of exogenous enzymes in dairy cattle on milk production and their chemical composition: A meta-analysis. *Anim. Nutr. Feed Technol.*, 13: 399-409.
45. Peters A, Meyer U, Danicke S. 2015. Effect of exogenous fibrolytic enzymes on performance and blood profile in early and mid-lactation Holstein cows. *Animal Nutrition*. 1(3) – 229-238.
46. Phondba, B.T., Kank, V.D., Patil, M.B., Gadegaonkar, G.M., Jagadale, S.D., Bade, R.N. Effect of feeding probiotic feed supplement on yield and composition of milk in crossbred cows. *Animal Nutrition and Feed Technology*. 2009. 9. P. 245–252.
47. Poonooru R.K.R, Sreenivas Kumar. D, Raghava Rao. D and Ananda Rao. K (2015). Rumen fermentation pattern in Buffalo Bulls Fed Total Mixed Rations Supplemented with Exogenous Fibrolytic Enzymes and / or Live Yeast Culture. *Journal of Advanced Veterinary and Animal Research* 2(3): 310-315.
48. Rajamma K, Srinivas Kumar D, Raghava Rao E and Narendra Nath D 2014b effect of fibrolytic enzymes supplementation on rumen fermentation of buffalo bulls fed total mixed rations. *International Journal of Agricultural Sciences and Veterinary Medicine* 2(3): 106-113.
49. Rajamma K, Srinivas Kumar D, Raghava Rao E and Narendranath D. 2014. Nutrient utilisation in Buffalo Bulls fed Total mixed rations supplemented with Exogenous Fibrolytic Enzymes. *Indian Journal of Animal Nutrition* 2014. 31(3): 213-217.





**Raju et al.**

50. Ramsing, E. M., Davidson, J. A., French, P. D., Yoon, I., Keller, M., Peters-Fleckenstein, H. Effects of yeast culture on peripartum intake and milk production of primiparous and multiparous Holstein cows. The Professional Animal Scientist. 2009. 25. P. 487–495.
51. Ravikanth Reddy P, Srinivas Kumar D, Raghava Rao E and Ananda Rao K. 2016. Nutritional evaluation of Total mixed rations supplemented with Exogenous fibrolytic enzymes and/or Live yeast culture in Buffalo Bulls. Indian Journal of Animal Nutrition. 2016. 33 (1): 54-58.
52. Reddy PR, DS Kumar, ER Rao and KA Rao, 2016. *In vitro* evaluation of total mixed rations supplemented with exogenous fibrolytic enzymes and live yeast culture. Inter J Vet Sci, 5(1): 34-37.
53. Rihma, E., Kart, O., Mihhejev, K., Henno, M., Joudu, I., Kaart, T. Effect of dietary live yeast on milk yield, composition and coagulation properties in early lactation of Estonia Holstein cows. Agraarteadus., 2007. 18. P. 37–41 (Abst).
54. Rivero, N., A.Z.M. Salem, H.M. Gado, M. Gonzalez-Ronquillo, A.B. Pliego, C.P.C. Penuelas and N.E. Odongo, 2012. Effect of exogenous enzymes and *Salix babylonica* extract or their combination on haematological parameters in growing lambs. J. Anim. Feed Sci., 21: 577-586.
55. Romero J J, Macias E G, Ma Z X, Martins R M, Staples C R, Beauchemin K A and Adesogan A T, 2016. Improving the performance of dairy cattle with a xylanase-rich exogenous enzyme preparation.
56. Salem, A.Z.M., M. El-Adawy, H. Gado, L.M. Camacho, M. Gonzalez-Ronquillo, H. Alsersy and B. Borhami, 2011. Effects of exogenous enzymes on nutrients digestibility and growth performance in sheep and goats. Trop. Subtrop. Agroecosyst., 14: 867-874.
57. Sujani S and Seresinhe R. T (2015). Exogenous Enzymes in Ruminant Nutrition: A Review. Asian Journal of Animal Sciences 9 (3): 85-99.
58. Titi, H.H. and W.F. Lubbadeh, 2004. Effect of feeding cellulase enzyme on productive responses of pregnant and lactating ewes and goats. Small Rumin. Res., 52: 137-143.
59. Torres N, Mendoza G D, Barcena R, Loera O, Gonzalez S, Aranda E, Hernandez P A and Crosby M 2013 Effect of various fibrolytic enzyme extracts on digestibility and productive performance of lambs fed a forage-based diet. Animal Nutrition and Feed Technology (2013) 13: 381-389.
60. Treacher, R. J. and C. W. Hunt. 1996. Recent developments in feed enzymes for ruminants. Proc. Pacific Northwest Nutrition Conference. Seattle, WA.
61. Van de Vyver, W.F.J. and B.A. Useni, 2012. Digestion and microbial protein synthesis in sheep as affected by exogenous fibrolytic enzymes. S. Afr. J. Anim. Sci., 42: 488-492.
62. Vargas, J.M., G.D. Mendoza, M.D.S. Rubio-Lozano and F.A. Castrejon, 2013. Effect of exogenous fibrolytic enzymes on the carcass characteristics and performance of grain finished steers. Anim. Nutr. Feed Technol., 13: 435-439.
63. Wahyuni, R.D., W. Ngampongsai, C. Wattanachant, W. Visessanguan and S. Boonpayung, 2012. Effects of enzyme levels in total mixed ration containing oil palm frond silage on intake, rumen fermentation and growth performance of male goat. Songklanakarin J. Sci. Technol., 34: 353-360.
64. Wallace R J, Wallace S J ,McKain N, Nsereko V L and Hartnell G F 2001 Influence of supplementary fibrolytic enzymes on the fermentation of corn and grass silages by mixed ruminal microorganisms *in vitro*. Journal of Animal Science 79: 1905-1916.
65. Yang W Z, Beauchemin K A and Rode L M 2000 A comparison of methods of adding fibrolytic enzymes to lactating cow diets. Journal of Dairy Science 83: 2512-2520.
66. Yang W Z, Beauchemin K A and Rode L M 1999 Effects of an enzyme feed additive on extent of digestion and milk production of lactating dairy cows. Journal of Dairy Science 82: 391-403.
67. Mohamed, D.E.D.A., Borhami, B.E., El-Shazly, K.A. and Sallam, S.M.A. 2013. Effect of dietary supplementation with fibrolytic enzymes on the productive performance of early lactating dairy cows. J. Agric. Sci., 5: 146-155

